



CRANFIELD UNIVERSITY

AIDAN F. O'DONOGHUE

**On the Steady State Motion of Conventional
Pipeline Pigs using Incompressible Drive Media**

SCHOOL OF MECHANICAL ENGINEERING

PhD THESIS



**On the Steady State Motion of Conventional
Pipeline Pigs using Incompressible Drive Media**

**by Aidan F. O'Donoghue
April 1996**

**A thesis submitted for the
Degree of Doctor of Philosophy**

**School of Mechanical Engineering,
Cranfield University, Bedfordshire, England**

ABSTRACT

A pig is a maintenance tool used in the Oil and Gas Industry, chiefly to remove solids or liquids from pipelines. It is in essence a sliding seal, which moves due to the action of the fluid pushing it. The aim of this work is to describe the steady state motion of the pipeline pig in terms of several key characteristics.

An analytical model of the pig motion has been prepared to calculate these parameters. The model also shows how these characteristics vary with velocity and distance due to wear. All assumptions and limitations are listed. The model has been verified by tests performed on a 10" carbon steel pipeline.

The model works by firstly calculating the force exerted by the pig seal on the pipe wall. A generalisation of the seal shape allows calculation of the contact parameters. A simplified lubrication analysis ensues, enabling calculation of the seal film profile. Knowledge of film thickness allows estimation of friction, differential pressure and leakage rates. Varying pig velocity affects the film shape and thickness, which in turn affects seal friction and therefore alters the program output. Changes in pig characteristics due to abrasive wear are accounted for using a wear coefficient and estimating the volume of material removed over successive distance increments.

The model compares well with the experimental results for characteristics such as differential pressure and friction. For this reason the wall force, contact and surface roughness models (i.e. the mechanical side of the problem) are considered to be accurate. However, agreement between leakage test results and the model was less well defined and it is apparent that the hydrodynamic analysis requires further study.

ACKNOWLEDGEMENTS

I would like to express my thanks to many friends and colleagues who have been directly or indirectly connected with the work in this thesis. First of all my support panel, Dr. Simon Leefe for his invaluable help in the technical aspects of the work, Dr. Hoi Yeung for his help in getting the dissertation right and Mr Jim Cordell for keeping it all relevant to what the industry requires today. To Luke Mathews, Mark Kennard and Safa Ash-Kuri and all our endless chats about pigs!

I would also like to thank Inpipe Products for their help and to Mr Ernst Klaus, formerly of SIPM, for his support and excellent contribution to the research work and to CALTEC for facilities, time, funding and the opportunity to carry out this work.

I'd like to thank all my family and friends who helped me along the way, even if they didn't realise it. If I didn't realise it, then a belated thanks!

NOMENCLATURE

Model variables:

a	Half footprint length, (m)
a^-	Negative extreme of footprint (m)
a^+	Positive extreme of footprint (m)
A	Location of pig seal clamp
$A, B, ..$	Unknowns or finite difference constants
A_N	Nominal area of contact (m ²)
A_R	Real area of contact (m ²)
A_{wear}	Volume of material removed due to wear per unit circumference (m ²)
C	Value of constant for Winklers foundation, $C = K/h_w$ (m ⁻¹)
C_d	Discharge coefficient (-)
C_o	Coefficient for Neo-Hookean model (Pa)
d	Internal diameter of pipeline (m)
$d\theta$	Small segment of sealing disc viewed axially (rad)
D	Diameter of sealing disc (m)
E	Youngs modulus (Pa)
E_c	Compressive Modulus (Pa)
E_t	Tensile Modulus (Pa)
f	Frictional force per unit length (N/m)
f_o	Frictional coefficient (-)
F	Friction or force (N)
g	Acceleration due to gravity (m/s ²)
G	Duty parameter (-)
h	Film thickness, $h = h_s + h^*$ (m)
h_o	Original seal shape or h_{orig} (m)
h_s	Film thickness when pig is stopped, support due to roughness alone (m)
h_w	Depth of Winklers foundation (m)
h^*	IHL flow criterion (m)

H	Dimensionless film thickness, h/σ_s
k_{wear}	Coefficient of wear (m^2/N)
K	Spring constant for Winklers foundation
K_s	Dimensionless surface parameter, $K_s = R_s^{1/2} \eta_s \sigma_s^{3/2}$
K_{bulk}	Bulk seal spring constant (N/m)
K_{local}	Local seal spring constant (N/m)
l	Length of pipe (m)
l	Characteristic seal length, $l = (D - \phi)/2$
l'	Characteristic seal length, $l' = (d - \phi)/2$
m	Entry slope into the seal (-)
M	Moment about a point (Nm)
M	Total mass of pig (kg)
n	Number of seals on pig (-)
n_s	Number of asperities in contact with disc seal (-)
N	Number of asperity summits in nominal area of contact (-)
P	Pressure (Pa)
P_a	Load support due to asperities (Pa)
P_f	Load support due to fluid pressure generation (Pa)
P_o	Pressure at $x = 0$ in seal (Pa)
P_t	Total load to be supported, or contact load (Pa)
P^+	Pressure behind a seal (Pa)
P^-	Pressure in front of seal (Pa)
P_{int}	Pressure between seals (Pa)
ΔP	Differential pressure across the pig (Pa)
q	Flow or leakage per unit length (m^2/s)
Q	Total flow or leakage (m^3/s)
r	Radial coordinate (m)
r_i	Radius of pig seal clamp or hub, $r_i = \phi/2$ (m)
r_o	Internal radius of pipe, $r_o = d/2$ (m)
R	Radius of curvature of stressed seal (m)

R	Parabola tip radius of curvature for Winkler/Hertz comparison (m)
R_s	Mean radius of curvature of roughness asperities (m)
s	Fraction of load supported by fluid (-)
t	Thickness of seal (m)
u	Velocity of fluid in seal at a point (m/s)
V_p	Velocity of Pig (m/s)
V_{wear}	Volume of material removed due to wear (m ³)
w	Wall force per unit length (N/m)
W	Total wall force (N)
x	Local seal coordinate in axial direction (m)
x'	Chamfer length moulded or worn on edge of seal (m)
x'_o	Initial chamfer length moulded or worn on edge of seal (m)
x'_{new}	New chamfer length after wear over distance increment (m)
X	Pipe or global x-coordinate, or distance travelled (m)
y	Circumferential coordinate (m)
z	z-direction coordinate for small scale radial directions (m)
z_o	Mid film height at which $u = V_p$ (m/s)
z_s	Summit height in rough surface (m)
α	Small section of seal angle, β taken during wall force calculations (rad)
ϵ	Strain (-)
β	Contained angle in seal (rad)
Δ	Real oversize of seal based on radius (m)
δ	Local deformation at the seal/pipe wall contact (m)
δ_o	Maximum local deformation (m)
δ_{wear}	reduction in oversize due to wear (m)
η	Viscosity of fluid (Pa.s)
η_s	Number of asperity summit peaks per unit area (m ⁻²)
μ	Coefficient of dynamic friction (-)
ν	Poissons ratio (-)
σ	Stress due to radial or hoop strain in seal (Pa)

- σ_s Standard deviation of asperity summit heights (m)
 ϕ Diameter of pig body hub or spacer discs (m)
 $\phi(z_s)$ Distribution of roughness summit heights (m⁻¹)

Subscripts and superscripts:

- a* Asperity
c Compressive
f Fluid
for Forward
i Node number for central difference
int Internal
o Static or maximum
new New
r Radial
rev Reverse
s Summit
t Tensile
tot Total
wear Wear
 * Fluid component
 θ Hoop component

GLOSSARY OF TERMS

Abrasion	A sharp texture in the base surface causes wear and tearing of the sliding elastomer. Micro-cutting and longitudinal scratches are observed on the abraded elastomer surface.
Bidirectional Pig	Pig with the ability to travel in either direction, usually with two guide discs for support and at least 4 sealing discs for drive.
Finite difference	Numerical method for solving differential equations using approximations for differentials.
Characteristics	Parameters of interest during the steady state motion of the pig in a clean pipeline which can be linked by experiment to how the pig will perform its function.
Coulette flow	Flow through a gap due to relative motion between the gap boundaries.
EHL	Elastohydrodynamic Lubrication, or the mechanism that describes the separation by a lubrication film of two deformable elastic elements, loaded against each other, and in relative motion.
FEA	Finite Element Analysis, or stress analysis of structures and their deformation by splitting up the structure into small elements.
Function	The maintenance task to be performed by the pig in the pipeline, for example cleaning debris from the line.
Guide disc	Thick disc of diameter less than that of the pipeline, used to support the bidirectional pig.
Hertzian Analysis	Analysis of the stresses at the contact of two elastic solids as first described by Hertz in the 19th Century.
IHL	IHL, or Inverse Hydrodynamic Lubrication is a simplified method for calculating the fluid film height during motion.
Poissons ratio	Relationship between longitudinal extension and lateral contraction in an extension test indicating the degree of incompressibility of the

	material.
Poiseuille flow	Flow through a gap due to the pressure drop across that gap.
QuickBASIC	Programming environment available on most IBM compatible PC's, integrated with the BASIC programming language.
Sealing disc	Disc of diameter greater than that of the pipeline used to seal against fluids and debris.
Swabbing	Removal of liquids from pipelines using conventional pipeline pigs.
Youngs Modulus	The constant of proportionality between uniaxial stress and strain in a solid.
Wall force	Force exerted on the pipe wall due to the oversize of the sealing disc.
Winkler foundation	Modelling of the solid contact problem using a simple "spring mattress" rather than an elastic half space in order to avoid integral equations.
10" Flow loop	CALtec's 10" Carbon steel, schedule 40, pipeline for testing pigs, measuring their characteristics and assessing their function at the Aberdeen Offshore Technology Park, Aberdeen.

CONTENTS

	Page
Abstract	iii
Acknowledgements	iv
Nomenclature	v
Glossary of terms	ix
Contents	xi
CHAPTER 1 INTRODUCTION TO PIPELINE PIGGING	1
1.1 Conventional pipeline pigging	3
1.2 Objectives of this work	6
CHAPTER 2 REVIEW OF RELEVANT LITERATURE	10
<i>Introduction</i>	
2.1 Review of pigging literature	11
2.2 Review of relevant tribological considerations	26
CHAPTER 3 SELECTION OF LUBRICATION TECHNIQUES	39
<i>Introduction</i>	
3.1 Model of the pig sealing disc	41
3.2 Calculation of wall force	42
3.3 Comparison with Finite Element Analysis, FEA	45
3.4 Contact analysis - calculation of P_t	47
3.5 Statistical method for surface roughness	
- calculation of P_a	51
3.6 Comparison between IHL and iterative EHL	54
scheme - calculation of P_f	
3.7 Summary	60
CHAPTER 4 STEADY STATE MOTION MODEL	75
<i>Introduction</i>	
4.1 Overall model of the pig	76
4.2 Estimation of wall force	80
4.3 Contact analysis	81
4.4 Rough surface model	84
4.5 Calculation of film thickness	85
4.6 Friction and differential pressure	87
4.7 Leakage past the seal	90
4.8 Pig disc wear	90

CHAPTER 5	PIGPlus, COMPUTER PROGRAMME	96
	<i>Introduction</i>	
5.1	PIGPlus, the core programme	98
5.2	The MAINS and WEARS routines	102
5.3	Examples of input and output	104
CHAPTER 6	VERIFICATION OF THE MODEL	111
	<i>Introduction</i>	
6.1	The test facility	113
6.2	Description of test pig	117
6.3	Inputs into PIGPlus model for verification against experiment	118
6.4	Validation of PIGPlus using the wear trials	122
6.5	Verification using the swabbing trials	123
6.6	Verification using the cleaning trials	124
6.6	Further validation	124
CHAPTER 7	DISCUSSION AND CONCLUSION	145
	<i>Introduction</i>	
7.1	Discussion	146
7.2	Conclusions	151
CHAPTER 8	RECOMMENDATIONS	156
	<i>Introduction</i>	
REFERENCES		160
APPENDICES		
A	Derivation of equilibrium wall force model	
B	Finite Element Analysis of pig seal	
C	Winklers foundation and Hertzian analysis of parabolic line contact	
D	Derivation of asperity contact pressure	
E	EHLPROG.BAS, iterative EHL program	
F	PIGPlus, model of pig motion program listing	

CHAPTER 1

INTRODUCTION TO PIPELINE PIGGING

1. INTRODUCTION

A pig is a tool used for various maintenance tasks in pipelines. It is defined as "a projectile, forced through the inside of a pipe using either hydraulic or pneumatic pressure, while maintaining a positive seal with the pipe wall". Maintenance tasks include functions such as cleaning the line, swabbing (removal of liquid hold-up or condensate from gas pipelines) and inspection (using on-board instrumentation and data acquisition to assess the integrity of the pipe wall).

Pipeline operators lack information about the actual internal condition of the line. Only indirect measurement can be used along with experience and engineering judgement. For example, an increase in pipeline pressure drop may indicate a build-up of debris. When a pig is launched the same problem occurs - i.e. it is impossible for the operator to know exactly what the pig is doing. As a result, a pig launched and received without problems is often viewed as a successful pig run. However, it is difficult to know what the pig has actually achieved.

A starting point to understanding the way a pig operates is to understand its motion characteristics such as differential pressure, film profile and leakage rates, and then to attempt to link these characteristics to how the pig performs its function. Such characteristics can be affected by velocity and distance. For example, the differential pressure across a pig drops with increasing velocity. It also drops with distance, due to wear. This has been established by experimental testing and the model detailed in this work also indicates this trend. Such knowledge is vital, for instance, in predicting the motion of pigs in *gas* pipelines due to compressibility effects.

The model is based on stress analysis of the sealing disc and a lubrication analysis of the contact with the pipe wall. It is this which allows the principle characteristics of the pig to be determined. Although this work concentrates on one particular type of pig, the methods used can, in principle, be applied to the analysis of other pig designs or seal shapes.

1.1 Background to conventional pipeline pigging

Pipelines are the most efficient method of transporting fluids. In the Oil and Gas industry they are used to transport gas and crude oil to the terminal and processed fluids from there to the users. In 1989, in the British sector of the north sea alone, there was 2500 miles of various diameter hydrocarbon pipeline (Tiratsoo J., (1989)). Building a pipeline requires a huge capital expenditure, CAPEX. The payback is great however, in terms of revenue for the operator.

Given the uncertainty of oil prices, it is essential to keep OPEX, or operating expenditure, as low as possible. Hence the pipeline must be operated as efficiently as possible. The efficiency of these pipelines depends upon (Landes M., (1983)):-

- Continuous throughput
- Keeping corrosion to a minimum
- Keeping pumping costs to a minimum

Steps must therefore be taken to maintain the line as close as possible to the as-built condition. For, example, any build up of solid debris (e.g. sand produced from the well) in the line will cause an increase in the pressure drop along the pipeline and hence increase pumping costs. The need for maintenance is clear.

The pig is one aid to maintenance. Landes (1983), defined a pig as "a projectile, forced through the inside of a pipe using either hydraulic or pneumatic pressure, while still maintaining some sort of positive seal with the pipe wall". Figure 1.1 shows examples of some pipeline pigs in common usage. The bidirectional pig is most commonly used for heavy duty pigging jobs - cleaning, swabbing and batching. It is a very effective cleaning pig with guide discs and sealing discs for general cleaning purposes. Large amounts of solid debris are removed and only soft debris such as paraffins are bypassed (Rosen H., (1995)). This pig can operate either direction, which is an advantage but not essential. The main advantage is its flat

face, and relatively good seals which make it superior at cleaning and maintenance tasks (O'Donoghue A., (Sept/Oct 1993)).

It is apparent that the pig seal and overall front shape are important in understanding how the pig performs. The shape can influence what is forced into the seal area, with a flat fronted pig operating most efficiently, fig 1.2 (Rosen, (1995)). The seal is key to understanding friction (due to its contact with the pipe wall), differential pressure, and leakage - similar to any seal in other applications. The seal is generally a self-acting seal due to the oversize of the disc. Therefore as pressure is applied behind it, it is forced harder against the pipe wall. Such a seal takes care by itself that the maximum contact pressures against the wall always exceed the sealed pressure, so that no leakage occurs under static conditions (Kanters A., (1990)).

The other two pigs shown, the conical cupped pig and the sphere, are less effective than the bidirectional pig (bidi). This is sometimes necessary if the operator does not require removal of all the debris from a pipeline due to reduced handling capacity at the receiving station. Note that the sphere does not have a self-acting seal, and any build-up of pressure behind it tends to deform it, and destroy the seal.

Conventional pigs are used in all stages of pipeline life. They are differentiated from intelligent tools in that the intelligent pigs are used to gather data on the condition of the pipe using on-board sensors and data acquisition. The following list shows how conventional pigs are used for more physical functions (The main physical attributes and seal characteristics affecting this function are in *italics*):-

- Removal of construction debris - *Pig shape, bypass*
- Acceptance testing (Water fill, dewatering) - *Forward/reverse leakage*
- Pipeline cleaning - *Pig shape, forward leakage, bypass and differential pressure*
- Application of internal coating - *film profile and seal shape*

-
- Condensate removal, or swabbing of gas lines - *reverse leakage*
 - Product separation or batching - *forward and reverse leakage*
 - Pipeline isolation or plugging - *Self acting seal*
 - Line gauging - *Pig shape, configuration*
 - Velocity control of intelligent tools - *Seal friction* (Landes M., (1983), Cordell J., (1992))

Unfortunately, there is very little design or operation guidance available to enable the user to determine the efficiency of the seal, and only qualitative guides to the best type of pig to employ in a given situation. This is apparent from the literature, and although pigging has come a long way in the last 100 years, it has done so in a very haphazard fashion. The general philosophy appears to be that if nothing is obviously wrong then it must be right. If an operator launches and receives a pig without problems then it is viewed as a successful run. Due to the operator's inability to actually see what has occurred in the line, it is difficult to assess the performance of the pig (Cordell J., (1991)).

Pigging a line costs money, chiefly in manhours given the relatively low cost of the conventional pigs. However, Lochte and Kozel (1995), have shown that CAPEX costs are increasing due to the emergence of new deep water fields and the possible need for subsea pig launchers. Due to the risk of getting the pig stuck and the inability to determine its performance, many operators are reluctant to pig the line at all. This low level of confidence is further demonstrated when pre-online inspection devices are sent down a pipeline to clean it prior to the use of an intelligent tool. Intelligent pigs, utilising on-board magnetic flux systems or ultrasonics to check for cracks and corrosion, can only operate successfully if the line has been cleaned effectively. Debris can damage sensors and falsify results.

However, it has been reported by Cordell and Gorzeman (1991) that, even after as many as 7 conventional pigs have been sent down to clean, an intelligent tool was

received having much debris in front of it. It is clear then, that quite often, conventional pigs do not perform adequately.

The challenge is to understand and improve pig performance. If this can be achieved, then major savings can be obtained by increasing and maintaining a higher through-put from the line.

1.2 Objectives of this work

In 1990, a major project was launched by CALTEC to investigate the conventional pipeline pig. The overall aim of this work at CALTEC was to improve the industries understanding of the tools. A number of different approaches were taken:-

- A comprehensive literature review was undertaken to determine the state-of-the-art in pigging and what aspects required further research.
- An experimental programme aimed at investigating areas that were not well understood.
- A theoretical study to investigate the motion of the pig in both compressible and incompressible drive media.

The theoretical studies focused on clean and ideal pipelines due to the inherent difficulty in accounting for pipeline defects such as weld-beads as well as, for example, non-Newtonian effects from wax accumulations. However, close ties between the experimental and the theoretical programmes has been maintained. The following philosophy underlines this relationship:-

"A Pipeline pig, like other equipment, has certain characteristics which influence how it performs its function (i.e. cleaning, swabbing etc). These characteristics should be listed, then measured and calculated for a clean pipeline. Finally, through experiment and observation, a link established between these pig characteristics and the ability of the pig to perform its function"

The experimental programme commenced after the completion of the 10" carbon steel flow loop. Meanwhile, the theoretical work was designed to produce engineering models for calculation of pig characteristics in both compressible and incompressible flow. Such models must address the real aspects of the problem such as rough walled pipe and wear on the seals. The characteristics of interest are:-

- Wall force on the pipewall, w
- Contact footprint length and total contact pressure, P_t
- Seal entry slope, m
- Film profile in the seal, $h(x)$
- Friction and differential pressure, ΔP
- Leakage rates through the seal, Q
- Internal pressure between seals, P_{int}
- *Accelerations, velocity excursions and motion under compressible flow*

All the above listed characteristics, except the last one in italics, are the subject of this thesis. The work considers the estimation of the characteristics and how they vary with both distance travelled (due to wear) and the velocity of the pig. This is the main objective of the work pursued in this thesis. Further work is on-going in order to understand pig functions such as cleaning, swabbing or inhibitor laydown using the characteristics as a basis. This is beyond the scope of this thesis.

To calculate the parameters of interest, a model is built up using a lubrication analysis of the seal. This is due to the sliding nature of the problem. Only the most commonly used pig, the bidirectional pig has been modelled. However, the approach adopted could be extended to any other type of pig encountered. Like seals found in other industries, pig seals slide, generate friction and suffer leakage in both the forward and reverse directions. For this reason a review of sealing and lubrication methods considered relevant to the problem is given in the following chapter along with a review of current practices in the pigging industry itself.

The subsequent chapters are laid out in the following logical order:-

- Chapter 3 Selection of techniques to be used in the model
- Chapter 4 Development of the pig motion model
- Chapter 5 Details of *PIGPlus*, a computer program based on the model
- Chapter 6 Verification of *PIGPlus* output using experiments conducted in the
Pigging Technology Project
- Chapter 7 Discussion of the results and conclusions based on these results
- Chapter 8 Recommendations for future work given the limitations of the model

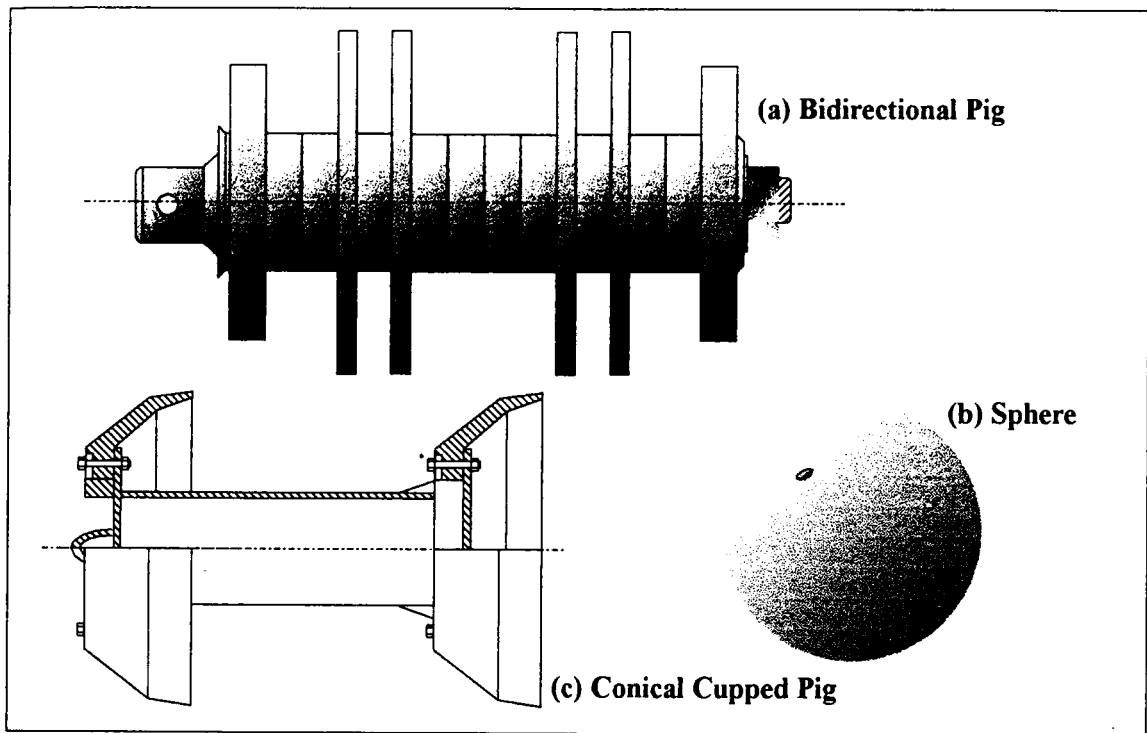


Figure 1.1 Examples of convention pipeline pigs

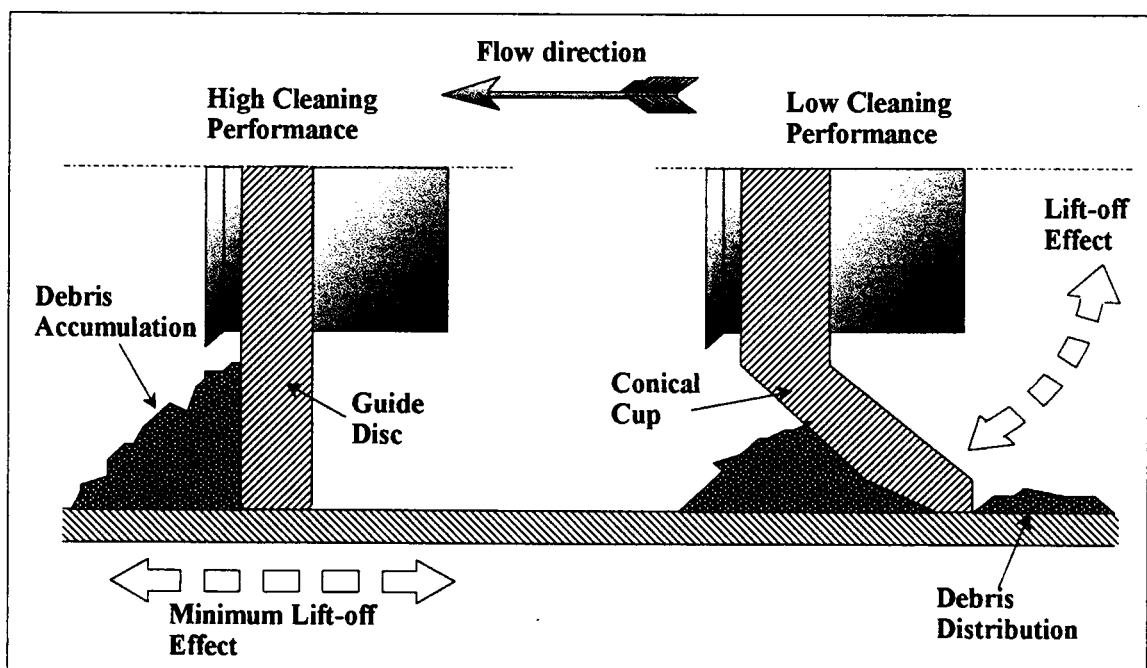


Figure 1.2 Influence of pig shape on function

CHAPTER 2

REVIEW OF RELEVANT LITERATURE

2. REVIEW OF RELEVANT LITERATURE

This chapter introduces a review of pigging literature and relevant sealing analysis techniques. The pigging review aims to discover what is already known in the industry regarding the motion of pipeline pigs. Additionally, evidence is provided that a lubrication analysis is the correct way forward in modelling the motion characteristics. The sealing and lubrication review shows the simple, yet effective techniques available to analyse the rough walled sliding contact problem.

In fact, there is very little hard data available on the steady state motion of pigs in the literature. Indeed, as reported by Cordell, Russell and Short (1991), it appears to be regarded as a superficial problem! On the other hand, lubrication theory presents a huge volume of data, techniques and views. The literature search focused on simplified techniques which could be easily incorporated into a model of the pig. Since detailed information regarding the pipeline and pigs themselves is very limited, the inputs into the model are kept as simple as possible. However, the validity of the model used cannot be compromised.

2.1 Review of conventional pigging literature

A review of the literature available regarding pipeline pigs shows that most of the information concerning pigs and their selection has evolved over the years, as people learn from their mistakes. Many difficulties have been overcome, often in ingenious ways, and many successful operations have taken place.

Fig 2.1 shows the complexity of the problem, given the number of variables involved (O'Donoghue, (1993), and Kanters, (1990)). Due to the absence of design information, it is apparent that even the most basic questions regarding pig differential pressure, leakage and other parameters can only be guessed at. The ability of the pig to perform its function effectively is an even greater challenge. This section considers the current state of the art in conventional pipeline pigging in terms

of:-

- Basic pig types, especially the bidi pig
- Common pig seal materials
- Operational experiences
- Parameters and variables
- Pig disc stress analysis
- Current pig models

Basic pig types and the bidi

A wide range of commercially available conventional pigs (almost 300 in all) are available from many different suppliers and manufacturers (in the region of 30 world wide), as indicated by Cordell (1992). However, out of these different makes and models, three main types can be singled out. These are the sphere, the conical cupped pig and the bidirectional or bidi pig. Fig 1.1 in the previous chapter introduced these tools.

The sphere generally has an outer polyurethane skin and is inflated using water and/or glycol. However, at smaller diameters, say 3" and below, they are usually solid cast. Spheres are used in instances where tight bends cause problems for the other longer and more rigid types. They are frequently used in automated systems. Due to their geometry, they can be launched into the line at right angles to the flow, through a 3-way valve for instance.

Conically cupped pigs utilise cone shaped cups, with the outer diameter sized to the line outer diameter, and the inner diameter at the lines nominal bore (TD Williamsons (1993)). This type of pig is useful in that it can conform easily to any ovality in the pipe due to its shape, and the seal is always self-acting. However, if they do get stuck then this shape tends to inflate with pressure build-up behind the

seal. This can initiate tearing at the bolt holes.

The bidi was first introduced in the 1980's by Kopp, and consists of flat oversized drive or sealing discs and guide-discs for support (Cordell J., (1988)). The configuration can be changed by adding more drive discs or swapping guide and seal locations, for example. A typical bidi has four sealing discs usually, but six is not uncommon (M^cNulty G., Short G., Russell D., (1992)). The bidi can be manufactured in either the mandrel form or solid cast. The mandrel is made up from a number of different components such as the body, discs, nuts and bolts etc. This allows ease of change of discs and/or the pig configuration. The solid cast pig is completely moulded from one material, and as such it is easier to clean and handle. It also avoids the problem of leakage through the bolt holes.

Over the years variations on the bidi have been developed usually for once-off jobs. Inclusion of brushes and scrapers is now almost standard for removal of wax and scale on pipeline internal surfaces. However, it is not uncommon to find the brushes between seals, which means that the trailing seal smears the wax back onto the line. Induced bypass is considered very important in the transport of loose debris from the pipeline. M^cNulty, Short and Russell (1992) show that this is achieved by opening bypass ports on the pig and allowing about 8% of the flow to be directed at the debris, and effectively jetting it along in front of the pig.

Magnetic cleaning pigs are now available, using on board magnets to collect ferrous debris. Kershaw (1991) provided details of the pressure bypass pig, developed by British Gas/Kershaw (BG/Kershaw) which uses a pressure relief valve in front of the pig. This is set to go off at a pre-determined pressure. Therefore, if the pig gets stuck, pressure builds up and the relief valve jets the obstacle out of the way. Talks with the manufacturer indicate that the jet actually pulsates, resulting in a more effective action (Cordell J., Kershaw C., (1990)). Other BG/Kershaw innovations

include the pin-wheel pig for removal of wax from the pipe wall and multidiameter pigs with over lapping butterfly disks for flexibility and spring steel for support. Diameter steps from 20" to 26" were achieved using this technique.

The success of the bidi appears to be mainly due to the shape of the front of the pig and the relatively high efficiency of the seal. O'Donoghue (1993) outlined three mechanisms for transportation of substances from a pipeline using pigs. These are listed here in order of effectiveness:-

- (i) Jetting action due to leakage of Induced and Directed Bypass jets
- (ii) The "Bulldozer" mechanism due to the front shape of the pig
- (iii) The seal

Due to the high differential pressure across the bidi, strong bypass jets can be used to move the substance along ahead of the pig. The high differential is due to the high seal wall force. Unfortunately, as Kennard (1993) has demonstrated, this leads to wear causing rapid reduction in differential pressure. The "bulldozer" mechanism is next effective for transporting functions. The flat face of the bidi means that substances radially inward from the pipe wall are directed in an axial direction. Figure 1.2 in the previous chapter showed how the conical cup pig directed the debris towards the wall.

Finally, the seal is not considered to be very effective for moving debris. Once a particle enters this area it is pressed into the wall and ridden over. However, this is true for all types of pig and for transporting fluids (for example a glycol batch linking fluid for an ultrasonic intelligent pig) the bidi seal is the "least worst".

Seal materials

Originally Nitrile or Neoprene were used for the pig cups or drive disks, and Nitrile

is still used in some low temperature application, at extremes of -45° Celsius, although it has a very high wear rate (Cordell J., Saunders P., (1991)). Now Polyurethane, or PU, is most commonly used as it has high abrasion resistance, tear strength, and resistance to hydrocarbons. However it is not suitable at elevated temperatures or high humidity as indicated in the BRMA handbook¹.

There is a wide range of different grades of PU and in many cases the material used for pig cups seals is selected on the basis of cost, i.e. the cheapest material to adequately perform the job in hand. In this case the material is usually relatively unsophisticated, off-the-shelf PU. However, many manufacturers are capable of producing urethane with improved wear characteristics and reduced friction coefficients (using powder lubricant inclusions) while retaining tear resistance, % elongation and resistance to chemical attack (Cordell J., Short G., Russell D., (1991)). It is important that quality control is to a high standard, and that a specification is published. Pig manufacturers, TDWilliamson are amongst those who have implemented such a system (TDWilliamson (1993)).

Fillers or reinforcers are sometimes included also. Fillers are used to increase abrasion resistance and reinforcement is used to increase tear resistance. Tearing and abrasion are the two most common methods of failure in this application of polyurethane. BG/Kershaw for example use a nylon scrim, beneath the surface of the pig seal/disc to reduce tearing at the bolt holes. Care must be taken however, since the reinforcement and filler must be compatible with PU, as it has been suggested that reinforcing can sometimes initiate tearing rather than preventing it (Cordell J., Short G., Russell D., (1991)).

1

PU is a non-linear material as the load/extension curve supplied by Peppiat (1985) for 85 IRHD hardness urethane shows, see fig 2.2. However, for low extensions or low strains, i.e. at the very beginning of this stress/strain curve the material can be considered linear. Care must be taken therefore in any linear stress analysis to check that the maximum strain levels do actually fall into this region.

Operational experiences

Having selected the correct pig type and cup material for the particular pigging problem under consideration, it is then necessary to operate this tool in the most effective manner. This involves consideration of the following:-

- Configuring the pig effectively
- Operating at the correct velocity
- Pressure considerations
- Effect of the pipeline condition

These will influence the effectiveness of the pig in service, but may have been considered in the selection process too. Pigging in the oil industry to maintain throughput involves consideration of the optimum frequency of pigging. This varies between 1 day and 1 month, but seldom outside these extremes (Cordell J., Short G., Russell D., (1991)). Initially, when a pipeline is new, tentative steps must be taken when pigging, since despite much planning and detailed selection and engineering to ensure trouble free pigging, as Cordell (1992) states, the engineer would do well to observe the rule - "Expect the Unexpected". Much of the experience obtained from operators in pigging never gets reported, and it is only when something goes wrong that the manufacturer gets any real feedback. For this reason much of the operational experiences reported are of a very general nature. However, they do give many clues about the nature of the pig in motion.

Configuration of the pig is important before it is launched. It is important to decide on either front or rear drive. Front cup drive can be achieved by using ports in the rear cup so that the drive pressure acts on the front cup. This has the seeming advantage of pulling the pig rather than pushing it and is therefore more stable. However, all the pressure is dropped across this front cup possibly increasing wear. The counter argument for this is that due to the increased stability, the pig does not nose down as much and therefore wear is reduced. It is difficult to tell which will apply under any given set of circumstances without experimentation and modelling (TDWilliamsons (1993)).

Another configuration problem is to decide if induced bypass is required and if so how much. A number of ports for bypass can usually be opened in cleaning pigs, allowing for a bypass percentage in the region of 8 to 10%. It is probable that the direction and the flow of bypass can be optimised. However, care must be taken that the bypass is not excessive or else it will be impossible to drive the pig. If this occurs a foam pig could be launched behind the pig to block the bypass (InPipe Products (1995)).

Velocity considerations are very important in gas lines and the avoidance of speed excursions (large initial accelerations and subsequent large amplitude start-stop motions) is important. This is also very important with intelligent tools as they usually have an upper speed limit beyond which they are less effective. However, Smith (1992) states that in liquid lines the velocity of the pig is usually that of the product, unless bypass or leakage is present. For crude lines in the North Sea this is usually in the region of 1 to 5 m/s. An optimum pig velocity is required for most applications, and if the flowrate cannot be regulated then perhaps the bypass could be adjusted in order that the pig can achieve this velocity (Cordell J., (1991)).

Velocity certainly affects the effectiveness of the seal. In inhibitor laydown, the film thickness of inhibitor depends to a large extent upon the pig velocity (Cordell J., (1991)). Little work has been done on leakage past pigs, but Barrett (1959) shows that at low velocities there is a higher forward leakage than backwards, with the opposite true at increased velocities. This work was performed using spheres however, where leakage would be expected to be high due to the possibility of deformation due to pressure drop across it, and therefore possibly easier to measure.

Absolute pressure is given little attention in relation to pipeline pigging, besides insuring that adequate pressure exists to drive the pig. However it is important for other reasons too. In pipelines with elevations, as Cordell, Short and Russell (1991) have pointed out, gas locks can occur causing the multiple heads to become additive. This is especially true when a pig is removing liquid from a gas line. Hence, increased drive pressure is required and this may be beyond the capability of the supply.

More attention is generally paid to the differential pressure across the pig. Again, it is probable that this can be optimised for a given application. Pig cleaning efficiency for example, according to McNulty, Short and Russell (1992), is reported to be higher at higher differential pressures. Swabbing efficiency - related to reverse leakage past the seal is also reported to be higher at larger differential pressures across the pig (Kennard M., (1995)).

It is also reported that the individual differential pressures of each pig on its own are not directly additive in a pig train. A pig train consists of several pigs pushed along together in the pipe one after the other. This has been reported by Cordell (1991) in the case of spheres. It was found that the differential across each of two similar spheres was 10% less than that across a single sphere. In the case of a self acting

seal, such as in the conically cup pig, it is probably more than the sum of the individual differential pressures since it is the actual pressure acting on the self acting seal that will increase the force against the wall and hence friction, especially in the static case. Finally, on the question of pressure, it has been shown by Barrett (1959) that differential pressure decreases with increasing velocity, again for the spheres. Out (1993) has explained this as a lubrication effect.

The state of the pipe's internal wall will affect friction. The wall of a typical process plant stainless steel pipe is normally very smooth. However, the Oil industry usually deals with rougher surfaced pipe unless it is lined. These lines are usually Carbon steel construction and have a shot blasted finish. The resulting roughness can be in the region of 40 to 150 microns peak-to-peak.

Wear affects the motion of pigs as they travel through pipelines. Fig 2.3 shows the motion of a bypass pig in a two-phase pipeline, reported by Wu et al (1995). Use of a typical pig in this application would result in all of the liquid being pushed from the line at once. This could potentially flood the slug-catcher at the processing facilities. To avoid overloading the slug-catcher separator, a bypass pig was used. This is a pig which allows a certain amount of the flow to pass through the pig via holes in the body. This has the effect of aerating the slug of liquid in front and slowing down the pig velocity. Hence, liquid arrives at the slug-catcher at a much reduced rate and the separator can handle the smaller liquid flowrate.

The bypass flow through the body is driven by the differential pressure across the pig. Due to wear on the seals, the differential pressure reduces. Hence the bypass flow reduces and the pig velocity increases as it offers less and less resistance to motion, tending towards the gas velocity. The pig used was a standard bidirectional pig with a hole in the body which allows a percentage of the gas driving flow to

bypass through the pig. The reason for this was to aerate the slug of liquid condensate in front of the pig and also to slow the pig down. This avoided the problem of overloading the slug catcher with a sudden volume of liquid and since it was aerated, the gas supply to the processing plant was un-interrupted. Due to the wear on the seal discs, the velocity increases however, as it offers less and less resistance to motion. The figure shows an initial sharp rise in velocity and subsequent levelling out, which suggests run-in and steady state wear. The authors indicated that they believed that wear and lubrication could be used to explain the rise in velocity. Also, the better the lubricant - in this case condensate, the less wear recorded.

Mathews and Rendle (1994) investigated the wear on multidiameter pigs in CALTEC's 10" flow loop facility. They concluded that wear was affected by velocity insofar as less wear was recorded at higher velocities. This is again probably a lubrication effect. In addition, polyurethane as expected wore less than nitrile. An "run-in" period was also indicated. That is, an initial high rate of wear for the first five kilometers approximately.

Parameters

Fig 2.1 shows the many different parameters associated with conventional pipeline pigs. These variables can be grouped into a number of different categories:-

- Material
- Operational
- Geometry
- Physical
- Pipeline

The material, normally polyurethane, has been discussed already. Fig 2.1 assumes

linear material properties for the pig cup material expressed in terms of Young's Modulus, E and Poisson's Ratio. This is only valid at low strain levels as discussed before. For greater deformations, a Mooney-Rivlin or Neo-Hookean analysis would be required.

Operational variables include the velocity of the pig in the pipeline and the pipe's inlet and outlet pressure for example. These parameters are controlled by the operator to some extent. However there are cases where the operator has control over neither, for instance in some gas lines where the pressure is dictated by the condition of the well and pig velocity is determined by the gas flow rate.

The geometry of the pig can be selected by the operator so long as the desired pig is commercially available. If not, one-off designs may be produced to suit. In the field, for example, the thickness and hardness of the drive disks can be changed and this will have an effect on the operation of the pig. This is possibly one area where the user is more in control. However, it is not really known how geometry affects the pig steady state motion, especially small changes from disc to disc, although the effect is expected to be substantial, according to O'Donoghue (1993). This is also true regarding physical properties such as the mass of the pig. Again this is something that the operator can control to some extent but it is not known how to exploit this. In fact there are two contrary trains of thought on the subject of pig mass. One argument is that the heavier the pig, the less likely the pig will ride over debris, and this leads to better cleaning efficiency. The other argument states that the lighter the pig, then there is less likelihood of wear, and hence a more effective seal will be maintained (TDWilliamsons, (1993)).

The pipeline will also influence the motion of the pig. The actual diameter affects the differential pressure since the force can be obtained in large diameter pipelines

with a smaller pressure, as in small diameter lines with large pressures, due to reduced area, (e.g. FORCE ACTING ON THE PIG = DIFFERENTIAL PRESSURE X AREA). Hence the required differential pressure to drive the pig is inversely proportional to diameter. Obviously, other factors come into account such as the cup material, the pig mass and pipe surface roughness. Cordell (1992) offers a guide to differential pressures across the pig in different pipelines, and this is shown in Fig 2.4. For the bidi in the 10" line, differential pressures in the order of 1 to 1.5 bars are expected. It puts forward the argument that differential pressure across the pig is inversely proportional to the pipe diameter. However, this rough guide does not consider factors such as cup oversize or material hardness, pig mass, and it is unclear as to whether it is steady state differential pressure (as friction depends on velocity) or the pressure to initiate the pig in the first place.

Obviously, the problem is more complicated than this simple model suggests (This chart does seem useful when comparing restart differential in the same pipeline, but the sphere is difficult to place). In addition the author has found the drive pressure for criss-cross foam pig to be greater than that of a bidi for one particular application (O'Donoghue A., Russell D., (1992)). Tests on the 10" line reveal this to be misleading. However, this is only intended as a rough guide. A more rigorous approach would be to firstly estimate the force exerted on the pipe by the pig and then relate this to differential pressure. A number of investigations along these lines have been undertaken. These tend to concentrate on cup stress analysis using Finite Element Methods (FEM) (Romagnoli and Varelli (1991) and Saevick and Soreide (1988)).

Stress Analysis

Literature regarding pig cup or disc stress analysis concentrates on an FEM analysis of the conically cupped pig. Romagnoli and Varvelli (1991) aimed to define and

characterise the deformation behaviour of the cup in an effort to predict the overflow and drive pressure. The overflow pressure can be defined as the pressure required to flip the pig seals in order to drive it in reverse. A bidi type drive cup is also considered. An axi-symmetric analysis is given and a linear material is used to model the cup. Consideration is given to pigging around bends and connections, and insuring that the cups can deform adequately in all parts of the pipeline without the central metal shaft contacting the pipewall. Contributions to the deformation from the differential across the cup and the wall force are considered.

The authors claim agreement for start-up differential pressures with the manufacturers' data with an accuracy of $\pm 2.5\%$. The type of pipe used in the tests is not mentioned in the paper, but for this degree of accuracy the analysis must have been compared with smooth walled stainless steel or plastic pipe pigging tests. This is since rough wall carbon steel pipes will wear the pig cups and third body rolling may result from rust and wear particles. This would give rise to a large spread of results. However, friction coefficients of the order of 0.25 are quoted. This appears low, especially compared with measured friction coefficients (see chapter 6) if smooth wall plastic or stainless tube is used with polyurethane.

In an earlier paper, Saevick and Soreide (1988), adopted a similar approach. Comparison is made with test results and good agreement is reached in the case of restart pressure and again overflow. Again the material is assumed linear and the pig body is rigid. The only inaccuracy seen with axi-symmetric analysis is the problem at the bends and no attention is paid to the effect of the sit down or centreline offset due to lack of support. The frictional force is again calculated by using the coefficient of friction which will undoubtedly need to be measured (static friction) for polyurethane against the pipe surface. The parameters of interest in considering the overflow question are the oversize, the friction coefficient and the angle between

the pig cup and pipewall. Neither of these two papers pay any attention to the contact stress distribution between the pipewall and the pig cup, although this is unnecessary for rough restart differential pressure calculations.

Models

O'Donoghue (1993) describes the characteristics of the pipeline pig in general terms. In addition to the characteristics outlined in this work, the fact that pigs do not run axi-symmetrically is mentioned. However, the difficulty of calculating the overturn moment is not underestimated. This would introduce an extra level of complexity for a very small result - the uneven wear on the seals and guide discs.

Very little work has been done to model the motion of the pipeline pig. Any such model must incorporate the parameters as outlined in the sections above, and must attempt to predict the characteristics of the pig in motion. For example, all aspects of the seal with the pipe wall must be considered such as the drive pressure, frictional characteristics and leakage. The models found in the literature concentrate on pigging with a compressible medium and steady state, incompressible pigging is considered trivial. However the models presented generally fall short due to their disregard for this interaction between the seal and pipewall and failure to predict any of the characteristics particular to that pig. In addition the ability to model different types of pigs and predict the differences between these has been omitted - the pig is treated as a plug of mass M usually.

Weingarten, Chapman and Walker (1984) describe the dynamics of the pig, with compressible drive, and a bypass port through the pig. However, constant friction is assumed, as is isothermal gas flow with a quasi-static pig, and a certain amount of confusion exists as to the nature of the non-dimensional equations employed. Again Webb (1987) uses constant friction in his attempt to model the removal of

liquid with a gas driven pig. In addition, his pig has no leakage and pig velocity is the same as fluid velocity.

In general, all the models for pig motion in gas pipelines - even in the presence of a liquid - use a constant frictional term. Out (1993) assumes a two stage friction against velocity relationship. He reports that this is necessary due to hydrodynamic effects in the seal area. In terms of differential pressure, the two stages are:-

- (i) An initial rapidly decreasing logarithmic ΔP against velocity
- (ii) A subsequent gradual decrease in differential pressure using a quadratic relationship

The logarithmic model is used for low velocities and the quadratic model for higher velocities, resulting in a piece-wise continuous differential pressure curve against velocity.

Little is reported on the topic of leakage. Azevedo and Gomes (1994) use an effective gap model. This results an expression for the net leakage through this gap. The expression is similar to that derived in lubrication theory. However, a constant gap is considered against velocity. Forward leakage is then estimated from the velocity profile - that fraction of the flow travelling faster than the pig. Reverse leakage is the remainder, travelling slower than the pig. The graph presented for forward and reverse leakage against velocity shows a high initial forward leakage, reducing rapidly. Reverse leakage appears to increase linearly with velocity. This matches the predictions of Hara, Hayashi and Tsuchiya (1979) for sphere leakage. The shapes of the curves differ however, in this analysis linearly reducing forward leakage and exponentially rising forward leakage. This could possibly be since the sphere is not a self-acting seal.

2.2. Review of tribological considerations

A pig disc can be regarded as a seal moving in the pipeline and as such it can perform or fail just like any other seal. Seal parameters of interest such as leakage, friction and film profile are also relevant in the case of pig disc/pipe wall sliding contacts. This section reviews the methods available for modelling the pig disc seal and ultimately the steady state motion of the pig in a pipeline.

When the seal is sliding on the pipewall, the wall force is distributed over the contact area. This load is supported by both the fluid trapped between the pipewall and the roughness asperities of the pipe. A review of lubrication and sealing methods available is now presented which focuses on the following aspects:-

- (i) Calculation of total pressure and contact parameters (Contact analysis)
- (ii) Calculation of fluid pressure in the seal and film thickness (Lubrication theory)
- (ii) Estimation of load support by the rough surface (Rough surface effects)
- (iv) Calculation of leakage and friction in the seals (Leakage and friction)

The emphasis of this review is to outline methods available to model the seal. Since there are many interacting variables and iterative loops to be considered in the analysis of pig motion, simple and approximate techniques will be more useful and reduce calculation time. However, an appreciation of the limitations of these techniques is vital.

Contact Mechanics

In the static position, the seal will deform slightly at the contact with the pipe wall. The contact is represented by a characteristic footprint or contact length, a contact pressure distribution and a local deformation. This is dependent on the wall force

per unit length, w , since $w = \int P_t dx$ (P_t is the contact pressure distribution), the properties of the seal material and the geometry of the seal.

If the wall force can be calculated, then a line contact problem can be set up in the case of the pig disc seal. Line contact implies that the maximum deformation lies along a line, in this case in the circumferential direction. Gohar (1988) shows how the resulting local deflection is related to the contact pressure (which when integrated gives the load), the shape as typified by the radius of curvature, and the material properties. The resulting deflection formula is given by:-

$$\delta_1(x,y) = \frac{(1-\nu^2)}{\pi E_c} \iint \frac{p \, dx_1 \, dy_1}{\sqrt{(x - x_1)^2 + (y - y_1)^2}} \quad \dots 2.1$$

Where (x_1, y_1) is the location of the pressure over a small element, and (x, y) is the point at which there is a resulting deflection. This is expanded to the full surface and lends itself to numerical analysis. If a point load is applied at (x, y) then the deflection $\delta(x, y)$ tends to infinity. However if the load is distributed this is not the case.

A uniform normal pressure distribution P , distributed over $-a \leq x \leq a$, yields (Johnson K., (1987)):-

$$\delta_1(x) = -\frac{(1 - \nu^2) P}{\pi E_c} \left((x + a) \ln \left(\frac{x + a}{a} \right)^2 - (x - a) \right) \quad \dots 2.2$$

This could be extended to a numerical analysis by estimating δ_1 at all x in the contact region, and working back to $P(x)$. This method also allows calculation of deformation outside the contact area. However, the analysis can be time consuming

since several attempts may be needed to get the correct deformation such that the contact pressure exactly balances the wall force.

Hertzian theory can be employed to estimate the contact parameters for two solids brought into contact along a line. This method concentrates on smooth profiles which can be described by $z = Ax^2 + By^2$, a paraboloid nominal point contact. For the two dimensional or line contact problem, where B equals 0 (or the radius of curvature is infinite in the y -direction), Hertz estimated (Gohar R., (1988)):-

$$a = \sqrt{\frac{4wR(1 - \nu^2)}{\pi E_c}} \quad \dots 2.3$$

for the half contact footprint length, and maximum contact pressure of:-

$$P_{t_o} = \sqrt{\frac{wE_c}{\pi(1 - \nu^2)R}} \quad \dots 2.4$$

This assumes a parabolic contact pressure distribution.

The Hertz theory of contact is restricted to surfaces of smooth and continuous profile. This assumes that stresses are finite at all points. The treatment of a sharp point or discontinuity in slope is presented by Johnson (1987). The pressure calculation leads to a logarithmic singularity at this discontinuity. Therefore, the full pressure distribution will remain unknown.

Numerical methods can be employed to model non-Hertzian contact problems, where the shape cannot be described by a simple quadratic equation. Numerical methods employ discretisation of the problem using a series of uniform, point or

triangular pressure distributions acting over the small increments, dx . Johnson (1987) describes two methods - Matrix inversion and the variational method. A matrix of influence coefficients is built up relating deformation at each point to pressure at each point. A matrix analysis is then used to estimate P_i along the contact. The contact footprint must be guessed at first. Any negative pressures calculated imply that they lie outside the contact area, and the footprint altered accordingly. Hence, an iterative approach is used to estimate P_i .

The main difficulties in contact analysis of the pig seal arise due to:-

- (i) The discontinuity in seal slope
- (ii) The seal shape is sharp initially, prior to wearing in
- (iii) Integral equations are required to solve for $P_i(x)$

Winkler, or elastic foundations provide one easy way of approximating the contact problem. Here there is no interaction between elements in the discretised problem. Pressure at a point is assumed to be merely proportional to deformation at this point:-

$$P_i(x, y) = \frac{K_w}{h_w} \delta(x, y) \quad \dots 2.5$$

Johnson (1987) compares this method with Hertzian contact to estimate a relationship between K_w/h_w and the material properties. This model is only an approximation and does not calculate deformation outside the contact area.

Lubrication theory

Osbourne Reynold's theory of lubrication describes how fluid gets dragged into a sliding converging wedge and sets up a pressure in this fluid, which limits new

lubricant coming in and also to boost out lubricant already in the bearing, thus conserving continuity. The term bearing is used here since Reynold's analysis is often concerned with their analysis (Cameron A., (1987), and also Szeri A., (1987)).

Fig 2.5 shows the pressure generated beneath the converging wedge and the subsequent velocity distributions along the length of the bearing. The area under each of these velocity distribution curves is equal, demonstrating that continuity of flow is conserved throughout. It is this pressure, P_f which helps support the slider and lubricate the seal.

Reynold's equation itself is highly non-linear and in order to solve it analytically in most cases it is necessary to make some simplifications. One such simplification is known as the long bearing approximation and was first solved by Sommerfeld (Cameron A., (1987)). The pressure gradient is ignored in the y -direction, or into the page, as this is considered to be very long. This is the case with pigs since the circumferential pressure gradient will be negligible compared to the component in the direction of motion. Indeed for the axi-symmetric case, the circumferential pressure gradient will actually be zero, and so the long bearing case is very useful.

The resulting expression is simply (Perkins A., (1993) and Cameron A., (1987)):-

$$\frac{dP_f}{dx} = -6V_p\eta\left(\frac{h - h^*}{h^3}\right) \quad \dots 2.6$$

relative to the pig. The fluid pressure in the seal is found by integrating this expression, and using known boundary conditions to evaluate the constant of integration and h^* , the height at which $dP/dx = 0$.

However, the generated pressure can in itself cause the seal to deform if the material

is soft or if the fluid pressure magnitudes are high enough. Elastohydrodynamics or EHL, considers this deformation in the material at a local level due to the pressure generated by a fluid film separating surfaces with relative sliding motion.

Dowson and Higginson (1986) shows how, in highly loaded metal contacts, the pressure can deform the surface of the material. The local displacements are calculated for a semi-infinite slice in a condition of plane strain. The boundary conditions are set such that $p = 0$ at the inlet and at the outlet $p = dp/dx = 0$. The viscosity is made pressure dependent due to the high pressures involved. Unfortunately, the iteration scheme Pressure - Deformation - Film shape - Pressure doesn't always converge. Simplification results from considering that the film thickness is small with respect to the elastic displacements and therefore the pressure profile is not too dissimilar to the original static contact pressure distribution. This must be true since the fluid is required to support the contact load at all points in the seal.

Use of numerical analysis to solve the EHL problem is very unstable. Here the initial seal shape is assumed and fluid pressure calculated. This causes a deformation in the seal and a new film shape results. A finite difference scheme can be set up to solve Reynold's equation. Deformation as a result of differences between fluid and total pressure can be calculated using methods outlined in the contact mechanics discussion earlier. However, a large relaxation factor is required as the solution can diverge easily.

A simple method of determining the film profile or film thickness is the inverse Hydrodynamic theory or IHL (Kanters A., (1990)). Here the fluid pressure distribution is assumed and based on this a single value for film thickness, called the flow criterion, is calculated:-

$$h^*_{IHL} = \sqrt{\frac{8}{9} \left[\frac{1}{\eta V_p} \frac{dP_f}{dx_{\max}} \right]^{-1}} \quad \dots 2.7$$

This occurs at the point of maximum fluid pressure. This method is valid provided:-

- (i) The pressure gradient reaches a maximum at some point in the film.
- (ii) The film must be larger than $1.5h^*_{IHL}$ some where in the film. This is usually satisfied at the inlet to the seal.

Therefore, if a fluid pressure profile is assumed, the film thickness due to fluid pressure support can be estimated from 2.7 above. The difficulty arises in the analysis of the seal film since fluid pressure is not equal to total pressure due to the existence of a rough surface, where asperities support some of the normal load.

Rough Surfaces

The presence of a rough pipe surface affects the friction, leakage and lubrication of the pig cup seal. Rhode (1980) showed that it was possible to use an expected or stochastic version of the Reynolds equation using flow and shear factors derived from randomised surfaces, to model the mixed friction lubrication regime. This was applied to energy losses in piston rings and a Streibeck type curve results (see figure 2.6 for example of Streibeck curve). A force balance between the actual load due to the ring, and the proportion of this load supported by the asperities and the lubricating film was investigated. One criticism of this paper is the lack of consideration for thermal effects, considering that it was a motor engine under analysis.

Patir and Cheng's average flow model (1978, 1979) is used by Rhode in this analysis. Using flow and shear factors, the effects of roughness on load carrying capacity,

leakage and friction can be considered for different types of roughness including isotropic and longitudinal roughness. The advantage of this model is that the differences between a smooth slider on a rough wall and a rough slider on a smooth wall can be investigated. They also report that for film heights above three times the standard deviation of the roughness, then roughness effects can be ignored. However, this assumes a normal distribution of surface roughness heights.

The methods outlined for treating rough surface in the lubrication problem are detailed and involved, thus adding another layer of complication to the problem. The aim of this thesis is to set up and validate an initial model for use by pigging operators. Inclusion of this level of detail can be added later. Therefore the effects of roughness on leakage, fluid pressure generation and viscous friction are not considered.

The main interest in rough surfaces therefore is in the load support and mechanical contribution to friction due the roughness. Although a small fraction of the load shall be supported by the fluid, the majority will be supported by the rough pipewall. This is because of the relatively low sliding speeds, usually less than 10m/s.

Greenwood and Williamson employed a statistical method to calculate the variation in roughness asperity load support with clearance. Using a Gaussian or exponential distribution of asperity summit heights, the following expressions can be evaluated:-

$$N = \eta_s A_N \quad \dots 2.8$$

$$n_s = N \int_h^{\infty} \phi(z_s) dz_s \quad \dots 2.9$$

$$A_R = \pi N R_s \int_h^{\infty} (z_s - h) \phi(z_s) dz_s \quad \dots 2.10$$

$$W = \frac{4}{3} N \frac{E_c}{(1 - \nu^2)} R_s^{1/2} \int_h^{\infty} (z_s - h)^{3/2} \phi(z_s) dz_s \quad \dots 2.11$$

$$P_a(x) = \frac{4}{3} \eta_s \frac{E_c}{(1 - \nu^2)} R_s^{1/2} \int_h^{\infty} (z_s - h)^{3/2} \phi(z_s) dz_s \quad \dots 2.12$$

At high loads or low sliding speeds, the separation will be low and therefore the load support from the asperities will be high. As the loading reduces due to wear, the pressure generated in the fluid will increase and the asperity contribution will reduce.

Wear

Moore (1972) identifies three direct mechanisms of wear when an elastomer slides on a rigid base surface:-

- (i) Abrasive wear as a result of sharp texture in the base surface causing abrasion and tearing of the sliding elastomer.
- (ii) Fatigue wear due to blunt base surface projections
- (iii) Roll formation in highly elastic materials sliding on smooth surfaces

Abrasive wear and fatigue wear result from sliding on rough surfaces. Roll formation is characterised by high friction sliding on smooth surfaces. Also, fatigue wear is usually very mild. For this reason, only abrasive wear will be considered in the pig seal wear problem (Although very high differential pressure pigs could suffer from adhesive wear).

Halling (1978) describes a relationship between distance travelled, load and volume of material lost due to wear:-

$$V_{wear} = k_{wear} W X \quad \dots 2.13$$

This literature review demonstrates that very little design information is available to the pig designer. However, techniques from lubrication analysis and tribology can be adapted to analyse the motion of the pig. The remainder of this thesis is concerned with deriving and verifying such a model to describe the motion characteristics of the sliding pig and the effect of distance and velocity on these characteristics.

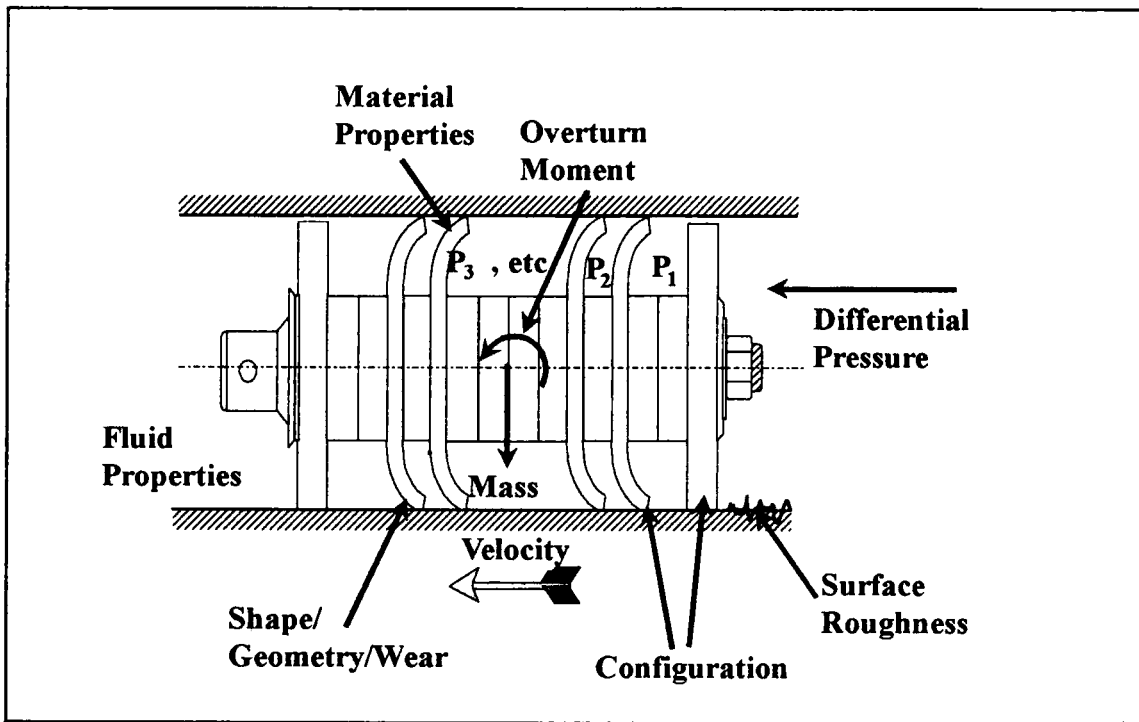


Figure 2.1 Variables involved in the analysis of motion of the conventional pipeline pig.

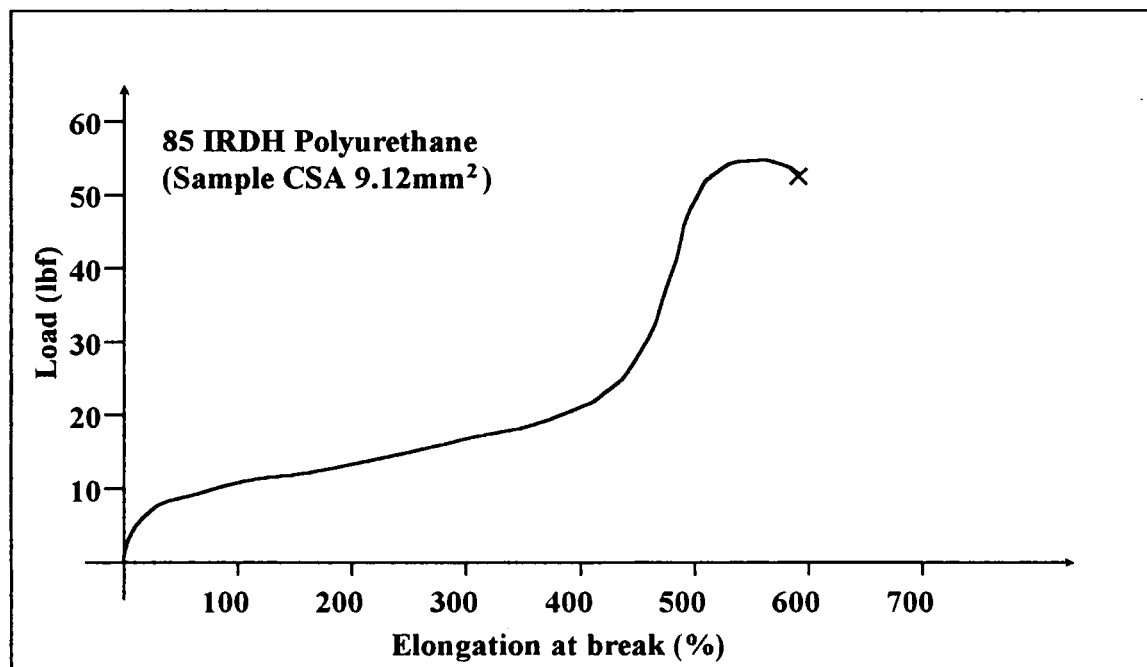


Figure 2.2 Typical load extension curve for 85 IRHD hardness urethane

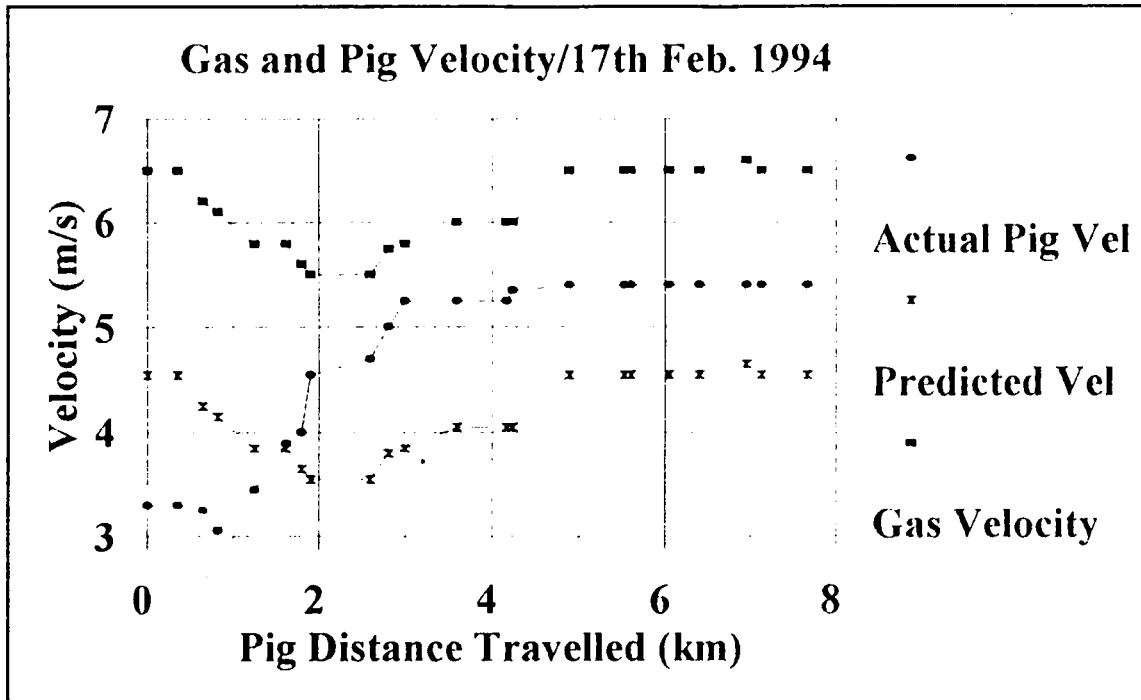


Figure 2.3 Increase in bypass pig velocity for 20", two-phase pipeline as reported by Wu et al

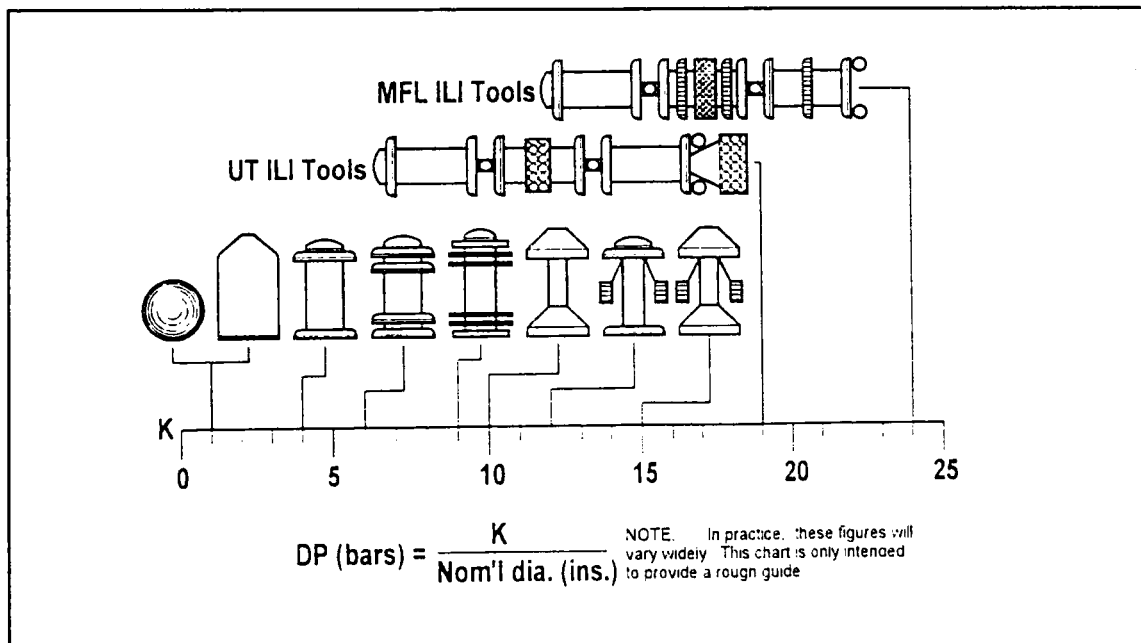


Figure 2.4 Guide to differential pressures for different pigs

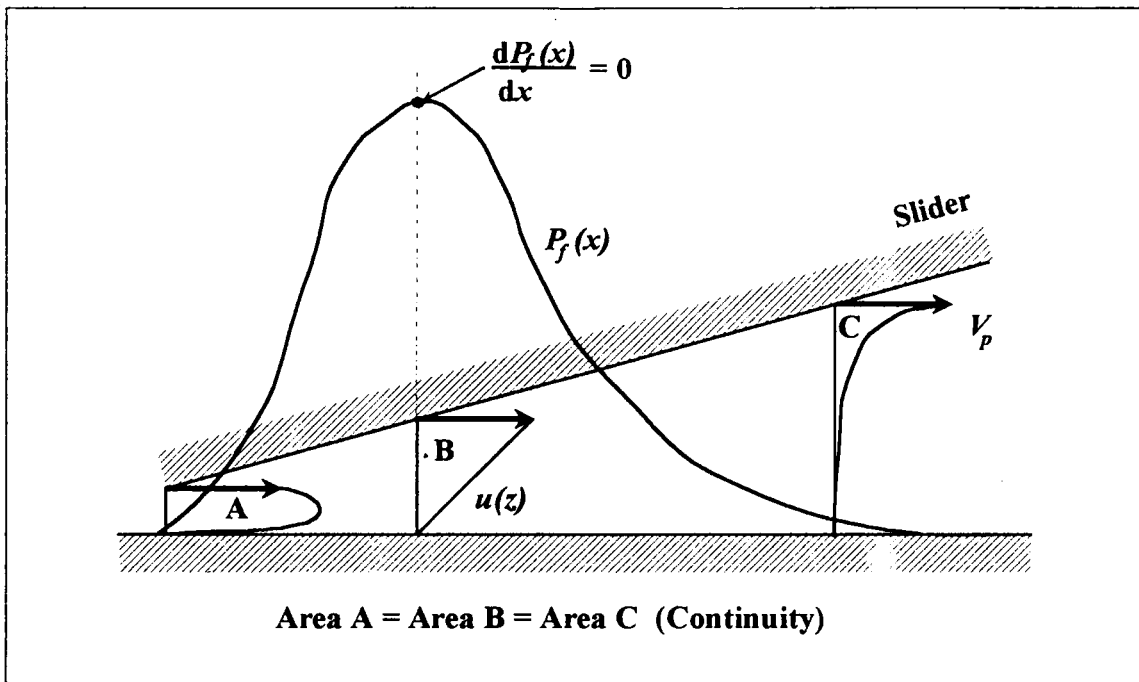


Figure 2.5 Pressure generation in a sliding seal showing continuity of flow

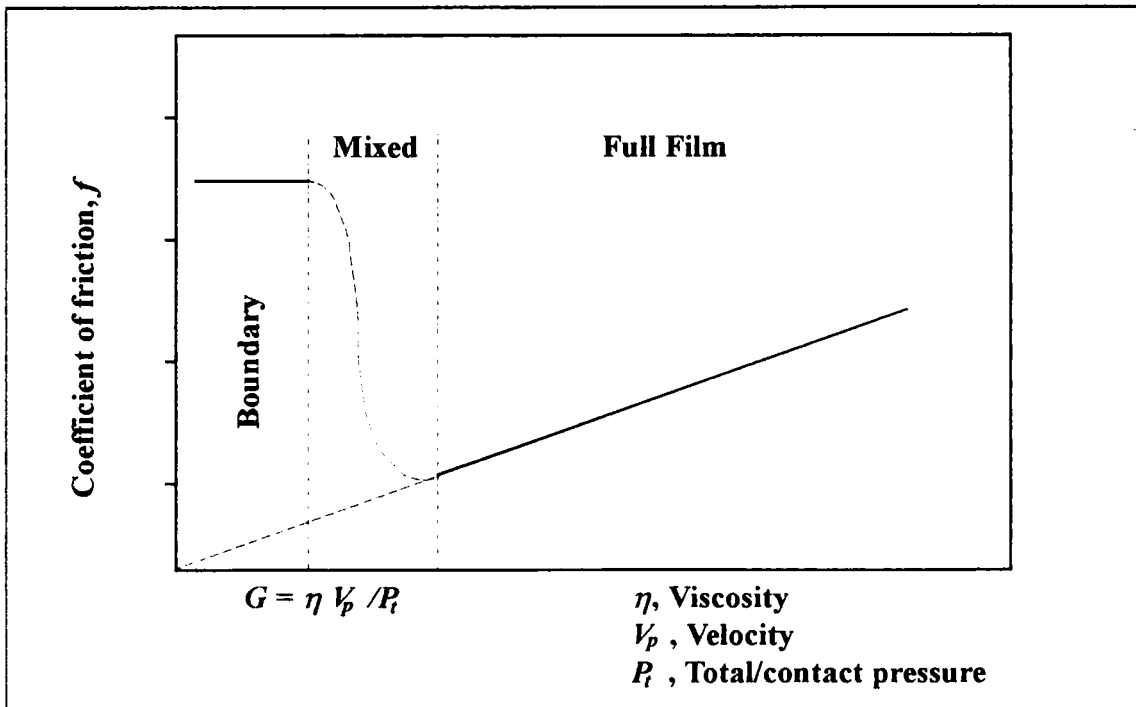


Figure 2.6 The Stribeck curve

CHAPTER 3

SELECTION OF LUBRICATION ANALYSIS TECHNIQUES

3. SELECTION OF LUBRICATION ANALYSIS TECHNIQUES

The previous chapter introduced a variety of techniques applicable to analysis of the sliding pig seal/pipe wall contact problem. In order to analyse the motion and wear of the conventional pipeline pig efficiently and fully, it is necessary to select appropriate techniques that can be handled easily and allow a solution to be obtained quickly. However, if this selection process involves choosing a less recognised method, then some justification for this is demanded.

A QUICKBasic program has been written to calculate the characteristics of the pig against velocity and distance (wear effects). This program is known as *PIGPlus*. The overall solution scheme used in the *PIGPlus* program, as developed in this project, is:-

- (i) Estimate wall force acting on the pipewall due to the oversized pig discs.
- (ii) Using this wall force, and a simplified geometry of the contact, calculate the contact parameters - footprint or contact length, local deformation and contact pressure distribution.
- (iii) Using a lubrication technique, the film profile during motion is calculated.
- (iv) Once this is established, the friction due to shear with the fluid and rough pipe wall is estimated. Differential pressure can be found from a force balance across the pig.
- (v) Calculation of reverse leakage, forward leakage and net leakage is then possible.

Wear of the seal can be considered using the abrasion relationship detailed in the previous chapter.

Due to the iterative solutions required in this program, a number of simplified

techniques have been adapted to aid the analysis process. These are:-

- (1) A simplified wall force model is introduced in order to calculate the force exerted by the oversized pig disc on the pipe wall. This is based on the equilibrium of the forces involved - wall force w , friction f , differential pressure ΔP , and hoop and radial stresses in the deformed material. Justification of this approach is offered in section 3.3 below, in which results of this calculation are compared with those of a finite element analysis.
- (2) In the analysis of the contact between the pig disc and the pipe wall, the local deformation is analysed using *Winkler foundations*. This assumes that a force at a point only causes a deflection at this point alone. Since this is highly simplified, a comparison with other more rigorous techniques is discussed in section 3.4.
- (3) The roughness of the pipewall is modelled using a statistical technique. A sensitivity analysis is offered in section 3.5, in order to examine the relative effects of the three main roughness parameters - σ_s , the standard deviation of summit heights, η_s , the number of summits per unit area and R_s , the mean radius of curvature of the asperity summits. Little information is normally available in the Oil & Gas industry on some of these parameters and therefore it is important to understand the relative effect of each so that some guidance can be given.
- (4) Use is made of the Inverse Hydrodynamic Theory (IHL) of lubrication, which allows calculation of the lubrication film thickness in elastomers relatively easily when compared with the highly unstable iterative solutions. A simplified fluid pressure distribution is assumed in the seal area. However, it is necessary to compare both methods to ascertain the IHL method's accuracy. This is discussed in section 3.6.

The methods selected will be applied in the following chapter which presents details of the pig motion model. The main area of interest in this analysis is the disc seal/pipe wall contact area. A model of the pig disc seal is now presented.

3.1 Model of the pig sealing disc

The pig seal model is based on the discs found on most bidirectional pigs, which are commonly used in the industry. Figure 3.1 shows the sealing disc in contact with the pipe wall. The disc is rigidly clamped at A , where the disc is held by the pig body. The undeformed disc is stressed by a wall force, w , such that the tip of the centreline moves inwards radially by Δ , the real seal oversize¹. The disc geometry is characterised by a thickness t , and this oversize Δ . The material, usually polyurethane is described solely in terms of linear material properties, Compressive Youngs Modulus, E_c , the tensile Modulus, E_t and the Poissons ratio, ν .

A close-up of the contact between the pipewall and the disc is shown in figure 3.2. The disc is deformed locally due to the contact pressures. This results in a footprint length $2a$, along which these pressures act. When the pig is static, the roughness of the pipewall alone supports the disc. This results in a small gap, $h_s(x)$. When the pig moves, hydrodynamic pressure is generated and the fluid helps to support the disc too. The film thickness increases to $h(x)$, the final film profile, due to this pressure generation in the fluid.

The remainder of this chapter discusses methods employed to model various parts of this seal. The first investigation involves calculation of w , the wall force, using

¹ The real oversize as shown in figure 3.1 is based on the distance the tip of the centre line moves radially, rather than the usual oversize quoted in pigging brochures which is merely the percentage difference between the disc and pipe diameters. This may not change even when a chamfer is worn or machined onto the disc.

the Equilibrium Wall Force Model. This is compared with a finite element analysis for validation.

3.2 Calculation of wall force

Figure 3.3 shows the basis for the wall force calculation. The forces and stresses acting on the pig disc segment are:-

- (i) The wall force, w
- (ii) The frictional force, f
- (iii) Differential pressure, ΔP
- (iv) Hoop stress, σ_θ
- (v) Radial stress, σ_r

The basic premise is that all five of these forces and stresses on the disc are in equilibrium, and therefore the sum of the moments around A , is zero. The differential pressure and the frictional forces can be calculated later as a result of the lubrication analysis and therefore only the wall force w is unknown. Firstly, the geometry of the deflected disc must be described. Figure 3.4 shows this geometry. It is assumed that the disc centreline forms the arc of a circle. This is based on observations made by O'Donoghue and Russell (1992) from pig discs in visual sections in an 8" pipeline. This is valid for a mid range of seal oversize, in the region of 3 to 6% of line internal diameter. However, small oversizes or indeed very large oversize the assumption must be questioned. The original length, l is therefore given by:-

$$l = R\beta \quad \dots 3.1$$

Also the deflected length, l' can be written as:-

$$\frac{l'}{R} = \text{Sin}\beta \quad \dots 3.2$$

Equating 3.1 and 3.2, an expression in β alone can be derived:-

$$\frac{l}{\beta} = \frac{l'}{\text{Sin}\beta} \quad \dots 3.3$$

Therefore, β can be evaluated, where:-

$$l = \frac{D-\phi}{2} \quad \dots 3.4$$

and

$$l' = \frac{d-\phi}{2} - \frac{t\text{Sin}\beta}{2} + \delta_o + x'\text{Sin}\beta\text{Cos}\beta \quad \dots 3.5$$

where δ_o is the small deflection in the seal at the point of contact. The chamfer length is x' , which is either machined onto the disc or worn as the pig slides along. Note that the real oversize, Δ , which is given by $l - l'$, is affected by this chamfer length. This then in turn affects the wall force. If the difference in diameters was used as oversize, then this effect would not be observed.

Now, the moment contribution of each of the forces in turn is discussed. A complete derivation of this wall force model is given in Appendix A.

Wall force and frictional moments

Figure 3.5 shows the positive moment contributions due to the wall force, w , and the frictional force f . The resulting expressions for moments about A are:-

$$M_w^+ = wr_o R(1 - \text{Cos}\beta)d\theta \quad \dots 3.6$$

and

$$M_f^+ = fr_o (r_o - r_i) d\theta \quad \dots 3.7$$

where $r_i = \phi/2$ and $r_o = d/2$.

Differential pressure

Figure 3.6 shows the method of calculating the total negative moment contribution due to the differential pressure. A small section, denoted by $d\alpha$ is considered first. The force on this section due to the differential pressure is resolved into two components - one axial and one radial. The moments due to these two components about the point A are calculated resulting in the final moment:-

$$M_{\Delta P}^- = \Delta P R^2 \left(\frac{R\beta}{2} - \frac{R\sin 2\beta}{4} + r_i - r_i \cos \beta \right) d\theta \quad \dots 3.8$$

Radial and hoop stresses

The properties of the material are important in this instance. Due to the mainly compressive nature of both these stresses, the compressive Youngs Modulus is used primarily. Figure 3.7 shows how the radial stress is calculated. A thin membrane of the urethane is considered first. The strain is estimated by considering the change in length, assuming that the neutral axis remains in the middle of the disc. In reality, equilibrium conditions would possibly shift the neutral axis. This would ultimately have the effect of reducing the calculated wall force slightly. From this the radial stress is calculated, which results in a force over this thin element. Taking the distance away from the neutral axis, the moment contribution is estimated. However, for forces on the compressive side, E_c is used and for the tensile side E_t is used. This results in two different moment expressions for the radial stress:-

$$M_{\sigma_{rc}}^- = E_c r_i \frac{t^3}{24R} d\theta \quad \dots 3.9$$

$$M_{\sigma_{rr}}^- = E_t r_i \frac{t^3}{24R} d\theta \quad \dots 3.10$$

The hoop stress moment is entirely compressive and also negative. Figure 3.8 shows the hoop stress calculation diagrammatically. A small section is considered first. Due to a change of radius, a compressive stress is induced. This leads to a stress at this point. Considering the stress acting over this small element, and its moment contribution, the following integral expression can be calculated:-

$$M_{\sigma_{\theta}}^- = \frac{E_c R^2 t d\theta}{(1 - \nu^2)} \int_0^\beta \frac{(\alpha - \text{Sin}\alpha)(1 - \text{Cos}\alpha)}{(\alpha + \frac{r_i}{R})} d\alpha \quad \dots 3.11$$

The integral expression can be evaluated numerically using Simpson's rule as all of the integrand is known. Using all these expressions, equations 3.6 to 3.11, a final moment equation can be written, since ΣM_A is equal to zero:-

$$M_w^+ + M_f^+ - M_{\Delta P}^- - M_{\sigma_{rr}}^- - M_{\sigma_{rt}}^- - M_{\sigma_{\theta}}^- = 0 \quad \dots 3.12$$

The only unknown, as stated above is w , the wall force per unit length, and therefore, this can be evaluated. It should be noted that $d\theta$ cancels out in this expression as one might expect due to the axi-symmetrical nature of the calculation. In order to have confidence in this, the method has been compared with a finite element analysis. This is now described and the comparison given.

3.3 Comparison with Finite Element Analysis, FEA

Desktop Engineering Limited were commissioned to carry out a finite element analysis of the pig sealing disc. The following data was supplied:-

-
- Elastic Modulus range, E 3.5, 4.8, 6.2MPa
 - Disc diameter, D 269mm
 - Clamp diameter, ϕ 172mm
 - Disc thickness, t 15mm

Two cases were studied:-

- (i) Given a friction to wall force relationship of $f = 0.8w$, and a 0.5bar differential pressure, calculate the wall force required for a mid-plane disc displacement of 15mm for each of the elastic moduli above. The results from this analysis are summarised in table 3.1 at the end of the chapter.
- (ii) For the same wall force/friction relationship and a differential pressure of 0.1bar, calculate the mid-plane disc deflection for each of the elastic moduli values. Values of wall force were taken from case (i) above. This is summarised in table 3.2 at the end of this chapter.

In addition, the values as calculated from the equilibrium wall force model, or analytical method as summarised above are given. The complete report from Desktop Engineering Limited is presented in Appendix B. Figure 3.9 shows the grid used in the analysis, while figure 3.10 shows a typical deflection plot.

Figure 3.11 shows wall force against elastic modulus for a constant oversize of 15mm. Good agreement is obtained, but the finite element output is higher with increasing modulus value. Figure 3.12 shows a plot of wall force against deflection for the three different moduli. This is for very small deflections, in the order of 2-3mm. The analytical model gives smaller wall force values than the FEA, or finite element output, by about 50%. However, the trend is correct.

Figure 3.13 shows similar output for large deflections in the order of 18-22mm. Again the analytical model gives wall force values approximately 30% less than the FEA results.

For typical pig seal deflections, the two methods compare well. However, increasing elastic modulus appears to increase the error. For large and very small deflections, the results are less promising, but the trends are similar. Again the error is greater for greater elastic moduli inputs. Possible explanations for the deviation between the two methods are:-

- (i) For very small and very large deflections, the seal cross section may not take the shape of the arc of a circle.
- (ii) The analytical model does not take end effects into account, especially at the free end of the disc.

However, given that the analytical approach provides a very stable solution, and the correct trends in comparison with the finite element approach, it is acceptable for this study. However, the apparent error in results will probably yield reduced differential pressure output at the beginning of the pig travel, in the run-in phase.

3.4 Contact analysis - calculation of $P_t(x)$

The main technique to be employed in the seal contact analysis is the Winkler foundation method. The net wall force, w , as a result of the bulk deflection of the disc is distributed over a finite contact area over which the local contact pressure varies. Winklers method shall be used to predict the extent of the contact length, or footprint, and the distribution of contact pressure for a given net wall force. The method is described below, and there follows a critical comparison between this method and another well documented method - Hertzian Contact. These analyses

are compared for a long parabolic shape contacting on a flat surface.

Winklers foundations

The main difficulty in elastic contact analysis arises from the fact that displacement at a point is dependent on the whole pressure distribution. This leads to integral equations which are difficult to handle. In the Winkler foundation method, the solid is modelled by a simple "mattress" rather than an elastic half space. An arbitrarily shaped punch demonstrates this in figure 3.14. Since no interaction between the springs is assumed, or shear between elements is ignored, the displacement at a point is dependant only on the pressure at that point. No deformation outside the footprint occurs as would happen in reality, because of this (Johnson K., (1987)). This assumption affects the shape of the seal and in particular the inlet region. This will in turn influence the lubrication analysis. Therefore if the displacement at a point is $\delta(x)$, then the total pressure at this point is

$$P_t(x) = \frac{K}{h_w} \delta(x) \quad \dots 3.13$$

Here K is the elastic modulus of the foundation and this can be related to the Youngs modulus E_c . The exact relationship between K and E_c , shall be determined below when the different methods are compared, but it will take the form

$$\frac{K}{h_w} = \frac{C E_c}{a (1 - \nu^2)} \quad \dots 3.14$$

The value of C can be estimated when the Winkler method is compared with Hertzian contact.

The main parameters of comparison between the Winkler method and the Hertzian method are a , the half footprint length and P_{to} , the maximum total pressure. C is

selected to give the best match between the Winkler method and Hertzian method.

Comparison based on parabolic shape

Figure 3.15 shows the parabolic punch used in this comparison. A parabola with tip radius of curvature of R , and of length l is acted upon by a force W . In the Winkler foundation approach, the half footprint can be evaluated directly from geometry once the maximum deformation is known. Full derivation is given in appendix C.

Hence:-

$$a = \sqrt{\frac{3}{2C}} \cdot \sqrt{\frac{(1 - \nu^2)Rw}{E_c}} \quad \dots 3.15$$

The maximum pressure can be determined directly from equation 3.13, given that the pressure is directly proportional to deformation:-

$$P_{t_o} = \sqrt{\frac{3C}{8}} \cdot \sqrt{\frac{E_c w}{(1 - \nu^2)R}} \quad \dots 3.16$$

Expressions for the same parameters have been obtained for a Hertzian analysis, from the literature (Johnson K., (1987)). These are:-

$$a = \sqrt{\frac{4}{\pi}} \cdot \sqrt{\frac{(1 - \nu^2)Rw}{E_c}} \quad \dots 3.17$$

$$P_{t_o} = \sqrt{\frac{1}{\pi}} \cdot \sqrt{\frac{E_c w}{(1 - \nu^2)R}} \quad \dots 3.18$$

There is a fundamental dilemma in selecting C , the foundation constant. Comparison of equations 3.15 and 3.17 yield $C = 1.178$. This is based on correctly modelling the footprint. However, the peak pressure P_{t_o} will be wrongly predicted,

by comparison with equation 3.18. Alternatively, equating 3.16 and 3.18 yields $C = 0.849$. Here the peak pressure is correct but the footprint is wrongly predicted.

The compromise is to choose C as the mean of the values suggested by either comparison so that neither is too far in error. This approach gives $C = 1.013$. This results in an error of $\pm 7.8\%$ on contact footprint length and an error of $\pm 9.2\%$ on peak pressure at the centre of the contact zone.

General agreement is therefore obtained for the pressures and footprint length for smooth parabolic shapes in contact. Winkler foundations are not generally considered good practice when sharp contacts are considered. However, even if the pig disc shape is initially very sharp, as indeed shown in figure 3.1, this will not last long in general due to rapid initial wear. For example, Kennard (1993) has shown that after only $\frac{1}{4}$ of a kilometre a 5mm chamfer can be worn onto the pig disc due to high initial wear. This will result in a relatively long chamfer length covering most of the contact, and the Winklers method will be valid. In addition, many pig manufacturers machine or mould a chamfer onto the pig disc when it is new.

This method will be used for the local deformation of the pig disc. The above analysis is performed on a flat surface to establish the contact stress levels (known as total pressure). From 3.13 and 3.14, this total pressure at a point in the seal/pipewall contact is given by:-

$$P_t(x) = \frac{1.013 E_c}{(1 - \nu^2) a} (\delta_o + h(x) - h_{orig}(x)) \quad \dots 3.19$$

Where $\delta_o + h(x) - h_{orig}(x)$ is written to indicate the total deflection at a point. Here, $\delta_o - h_{orig}(x)$ is the deformation when the pig is stationary whilst $h(x)$ is the additional deformation of the seal due to hydrodynamic pressure generation.

It should be noted that the seal tip, over which the wall force is distributed is much stiffer than the main seal from which this wall force results. This can be viewed as two springs in series with stiffnesses K_{bulk} and K_{local} . The local "spring constant", K_{local} is much greater than the bulk constant K_{bulk} . For example, a typical seal of modulus 6MPa and a contact footprint of about 10mm yields a local stiffness of about 5.7MPa, while the bulk stiffness is only in the region of 0.09MPa². This means that most of the deflection will be taken by the bulk of the seal rather than the sliding contact. This is taken into account in the *PIGPlus* program as an iterative solution for wall force and local contact pressure is sought.

3.5 Statistical method for surface roughness - calculation of P_a

In the literature review a statistical method for treating surface roughness was presented, based on the work of Greenwood and Williamson (1966). Using this the seal support pressure due to contact with the pipewall surface roughness is given by:-

$$P_a(x) = \frac{4}{3} \eta_s \frac{E_c}{(1 - \nu^2)} R_s^{\frac{1}{2}} \int_h^{\infty} (z_s - h(x))^{\frac{3}{2}} \phi(z_s) dz_s \quad \dots 3.20$$

For the model shown in figure 3.16, this is evaluated using a negative exponential asperity height distribution function as, see appendix D:-

$$P_a(x) = 0.707 \frac{E_c}{(1 - \nu^2)} K_s e^{\frac{-h}{\sigma_s}} \quad \dots 3.21$$

where K_s is $R^{\frac{1}{2}} \eta \rho^{3/2}$, a dimensionless number. Johnson (1987) quotes a relationship between σ_s , the standard deviation of asperity heights, R_a , the average

² Neither of these "spring constants" are linear. Both vary with displacement, and hence the values quoted are average values.

roughness as measured by a profilometer as $\sigma_s = 1.253R_a$, for Gaussian distributions of roughness. However, whereas σ_s is generally known for this reason, the other elements or terms in this expression are less widely available. It will be seen later that a value of 0.012 approximately has been taken for K_s when applying the model to the 10" test loop. An errors analysis reveals the extent to which under or over estimation of this parameter can affect the results. In the static case, with no fluid pressure, the asperity load support equals the total pressure:-

$$.707 \frac{E_c}{(1 - \nu^2)} K_s e^{-\frac{h_s}{\sigma_s}} = \frac{1.46E_c}{(1 - \nu^2)\alpha} \delta(x) \quad \dots 3.22$$

For the parabolic shape taken earlier, at the centre the maximum deformation is $\delta_0 = \alpha^2/2R$. Differentiating and dividing by h_s , the following expression results:-

$$\frac{dh_s}{h_s} = \frac{\sigma_s}{h_s} \frac{dK_s}{K_s} \quad \dots 3.23$$

Figure 3.17 shows the percentage change in h_s calculation against change in K_s , for different values of h_s/σ_s . For high values of h_s/σ_s , i.e. low load, the change is small but still appreciable. At low film thickness levels, the errors band rises and is very substantial. For significant contact, we might expect h_s/σ_s to be about 1.5, so that a 10% error in estimated K_s would translate to a 6.6% error in h_s .

Therefore, when the pig seal is new or a high load is present, the potential error in film thickness will be large. This effect shall reduce, but not disappear as the seal wears and the load reduces. Of potentially more serious concern is the implication for leakage since leakage is proportional to the cube of the film thickness. Thus:-

$$\frac{dQ}{Q} = \frac{3 \sigma_s}{h_s} \frac{dK_s}{K_s} \quad \dots 3.24$$

However, for significant leakage, h_s/σ_s must be large as so the error will be smaller. For high loads it is expected that the cubic relationship will breakdown due to the existence of very small films and the difficulty the fluid would experience in flowing around the asperities.

In summary, since the majority of the load will be taken by the surface roughness asperities:-

- (i) K_s will not affect friction and wear calculations greatly, since most of the load is supported by the asperities. Friction is therefore directly proportional to the total load, approximately.
- (ii) K_s will affect leakage rates to a larger extent since it will alter the film thickness prediction as seen in figure 3.17. A simple Poiseuille flow calculation to establish leakage rates is very sensitive to gap height changes. However, the error is lower for larger gap sizes and little or no leakage would be expected for very small film thicknesses.

Leakage will also be affected by roughness on the sliding seal. This is not considered in this work. It is assumed throughout that the slider remains flat and smooth. This is clearly in error since as the pig moves, a directional roughness is worn onto the lip of the seal. Cheng and Dyson (1976) have modelled two rough sliders by an addition process resulting in a smooth slider on a combined roughness surface. It is evident from this analysis that the contact analysis will not be affected significantly by the roughness on the pig seal since it is much softer than the hard steel pipe. However, it is the effect of such directional roughness on leakage that is of greater concern. Patir and Cheng (1978, 1979) proposed an average flow model based on Reynolds' equation capable of taking the effect of roughness and direction of roughness into account. This is not included in the current analysis.

Therefore it is expected that leakage will be underpredicted, since axi-directional roughness will increase leakage rates.

3.6 Comparison between IHL and iterative EHL scheme - calculation of P_f

When the seal is moving at a steady state velocity, the film thickness increases due to pressure support from hydrodynamic pressure generation. To evaluate this new film thickness, the Inverse Hydrodynamic Lubrication (IHL) theory is invoked. This gives an approximation of the film thickness in the seal, as opposed to the more rigorous EHL, or Elastohydrodynamic method where an iterative scheme is used. In addition, the shape of the fluid pressure distribution is important. This determines forward and reverse leakage through the seal. Firstly, the background behind both of these methods is discussed.

Iterative Elastohydrodynamic (EHL) Method

Reynolds' equation for an infinitely wide bearing is given by (Cameron (1987)):-

$$\frac{d}{dx} \left(h^3 \frac{dP_f}{dx} \right) = -6 V_p \eta \frac{dh}{dx} \quad \dots 3.25$$

A finite difference scheme is used to solve for the fluid pressure, P_f , for a given film shape. This yields, for pressure at a point i with a grid mesh spacing of Δx :-

$$P_i = \frac{A + B + C}{D} \quad \dots 3.26$$

where

$$A = h_i^3 (P_{i+1} + P_{i-1}) \quad \dots 3.27$$

$$B = 3 h_i^2 (h_{i+1} - h_i) P_{i+1} \quad \dots 3.28$$

$$C = 6 V_p \eta (h_{i+1} - h_i) \Delta x \quad \dots 3.29$$

and

$$D = h_i^2 (3 h_{i+1} - h_i) \quad \dots 3.30$$

Initially all pressures are set to zero and the program calculates each P_i until an equilibrium fluid pressure distribution is calculated. Once this is achieved, a deformation occurs at each point if the sum of the fluid and asperity pressures are not equal to the total pressure, P_t . The incremental deformation at a point is given by:-

$$\delta_i = \frac{(P_{f_i} + P_{a_i} - P_{t_i}) (1 - \nu^2) a}{1.013 E_c RELAX} \quad \dots 3.31$$

where *RELAX* is a relaxation factor designed to reduce the effect of the deformation. This results in a new film shape and the fluid pressure must be calculated again. This process continues until a steady film shape and fluid pressure is obtained. A QUICKBasic program, EHLPROG.BAS has been written to do this. Figure 3.18 shows the flow chart for this program. A listing of the program can be found in Appendix E. If *RELAX* is too small then convergence may not be achieved as the seal shape will distort grossly and cause the program to crash. The EHL analysis takes some time to run on a standard Pentium PC for just one analysis. Since there are other iterations to be dealt with in the pig model this would be an unfeasible way of calculating the necessary parameters.

The Inverse Hydrodynamic Lubrication method (IHL)

Figure 3.19 shows the assumed fluid pressure distribution in the seal. This is assumed to be flat in the mid seal area. This is a simplification to allow ease of

analysis. As a result, the film thickness will be constant in the seal area. At the entry zone, the fluid pressure is assumed to be zero. At the exit side of the seal, the pressure is higher, due to the fact that there is a pressure drop across the pig. The pressure drop across one seal is simply taken as the total pig pressure drop divided by the number of seals. When the pig is stopped, the film thickness, h_s , is determined by equation 3.22, setting $P_t = P_a$. When the seal is moving, pressure is generated in the fluid, causing an increase in film height from h_s to h , where $h = h_s + 1.5h^*$. The IHL theory assumes that the entry height into the seal is $1.5h^*$, where h^* is the flow criterion (Kanters A., (1990)). An approximation of the IHL approach as outlined by Kanters (1990) is put forward. Here, a force balance at the point x' means that the sum of the fluid pressure and the asperity pressure must equal the total pressure:-

$$P_t = P_a + P_f \quad \dots 3.32$$

Letting the fluid pressure be equal to a constant times the total pressure at this point x' , yields the following important relationships:-

$$P_f = s P_t \quad \dots 3.33$$

and

$$P_a = (1 - s) P_t \quad \dots 3.34$$

Where s is known as the pressure factor. This allows easier treatment of both fluid pressure and surface roughness effects in the seal area. At x' , when the pig is moving, P_t is given by:-

$$P_t = \frac{1.013 E_c}{(1 - \nu^2) a} (\delta_o + 1.5 h^*) \quad \dots 3.35$$

Now, by the Inverse Hydrodynamic Lubrication (IHL) theory, the additional lift by the fluid is given by:-

$$h^* = \sqrt{\frac{8}{9} \eta V_p \left(\frac{dP_f}{dx} \right)_{\max}^{-1}} \quad \dots 3.36$$

The maximum pressure gradient at the entry zone to the seal is the pressure at x' over the length $a^+ - x'$. Therefore it can be expressed as:-

$$\frac{dP_f}{dx}_{\max} = - \frac{1.013 E_c (\delta_o + 1.5 h^*)}{(1 - \nu^2) a (a^+ - x')} \quad \dots 3.37$$

Equation 3.34 is now used in conjunction with 3.36 and 3.37 to solve for the pressure factor, s . The resulting expression is:-

$$0.707 \frac{E_c}{(1 - \nu^2)} K_s e^{-\frac{h_s + 1.5 h^*}{\sigma_s}} = \frac{1.013 E_c (1 - s)}{(1 - \nu^2) a} (\delta_o + \dots 3.38$$

Once s has been established, the h^* can be calculated from equation 3.36. The following points must be made about this simplified approach at this stage:-

- The film thickness is taken to be $h_s + 1.5h^*$ through out the entire seal. This is not strictly true since the pressure drop across the seal will govern the film thickness on the high pressure seal side.
- The lift due to fluid pressure generation is taken to be additive. This simplifies the rough surface calculation greatly, by use of the pressure factor, s .
- In reality most of the load is taken by the rough surface. However, as will be seen below, when the film thickness is low, the EHL approach generates

much pressure in the fluid. This is overcome in the additive approach suggested here where *negative film heights* are allowed. This is not a contradiction since the datum level is an arbitrary choice. The EHL approach cannot allow any negative film heights however, and the fluid appears to support much of the load even when it is known that this is not possible.

Comparison between IHL and iterative EHL

Both methods have been compared using a base case seal design and varying one of the main parameters in turn. The base case is:-

w	= 1000 N/m	(Wall force)
m	= 1	(Entry slope)
x'	= 8 mm	(Chamfer length)
V_p	= 1 m/s	(Pig velocity)
P^+	= 10000 Pa	(Seal exit pressure)
E_c	= 6 Mpa	(Compressive modulus)
σ_s	= 6 μm	(Standard deviation of asperity peak heights)
K_s	= 0.07	(Surface parameter)
η	= 0.001 Pa.s	(Viscosity)

The wall force, entry slope, chamfer length, velocity and pressure drop or exit pressure have been varied and the results of the IHL and EHL analyses compared. Figures 3.20 to 3.24 show the results of this comparison. The value of film thickness taken from the EHL analysis is the average reading from the seal central section, unless otherwise stated.

In general the two methods agree well with the IHL method predicting a film thickness about $3\mu\text{m}$ (approximately $0.5H$ difference, where H is h/σ_s) greater than

the EHL method on average. The chamfer length, entry slope and wall force graphs show strong agreement in trend. However, the velocity effects and the seal pressure drop graphs show less promise.

With increasing velocity, the IHL method predicts an initial rapid rise in film thickness and then a more gradual rise. However, in the EHL method this is less marked. Although it is difficult to see, the EHL curve drops slowly at first and then rises again at a very slow rate. This is probably due to the slow sliding speeds, which for an EHL analysis will not cause much increase in film thickness. However, for the IHL analysis, h^* increases with the square root of the velocity and this is evident in the curve.

The initial decrease in film thickness in the EHL approach is symptomatic of the datum level selection problem in this iterative approach. A paradox of sorts results - due to the lack of lift at these very low velocities, the film thickness drops, thus generating more pressure! Convergence is very difficult to obtain at these conditions also.

Despite the initial rapid rise the subsequent rise is less marked and therefore it is felt that the IHL method is still valid. However, care must be taken to interpret the model outcome correctly in the light of this information.

This effect is also seen, but to a greater extent in the chamfer graph. Here, it is quite clear that the EHL method cannot go below the zero datum level. However, the IHL method allows negative levels.

The pressure drop graphs shows no change for the IHL method, as this does not affect it. However, for the EHL approach the maximum film thickness at the rear

of the seal or exit zone rises rapidly as a result of the pressure drop. However, the minimum seal film thickness is largely unaffected.

Despite the differences, the IHL method appears to be close to that of the EHL and therefore can be considered adequate for the model of pig motion. However, care must be taken when considering negative film levels as leakage is unlikely under such loads, and the negative exponential asperity distribution was only chosen as an approximation to the Gaussian for the upper level of asperity heights.

3.7 Summary

This chapter has introduced some simplified methods of calculation to allow easier analysis of the pig disc seal. However, the methods selected have been compared with more widely investigated methods and as such the reliability and limitations of such analysis has been shown. Therefore in summary it has been decided to use:-

- (i) *Winkler foundations*, for the analysis of the local deformation of the pig seal/pipewall contact.
- (ii) *Statistical roughness model*, has been found to be useful even though one of the parameters K_s is difficult to measure. It must be remembered that this parameter will affect leakage predictions to a large extent.
- (iii) *IHL method*, is regarded most efficient method of calculating the average film thickness but care must be taken with initial high loads before run-in occurs.
- (iv) *Equilibrium wall force calculation*, is used to calculate the force exerted by the pig disc on the pipewall. This eliminates the need for finite element analysis with which it has been compared.

The methods outlined in this chapter shall now be used to model the motion of the

pig under steady state conditions, in the following chapter, chapter 4.

Modulus E (MPa)	Wall force, w (FEA)	Wall force, w (Analyt.)
3.5	1292	1297
4.8	1682	1557
6.2	2104	1749

Table 3.1 Comparison between Finite Element Analysis and Analytical approach for 15mm oversize deflection (Seal pressure drop of 0.5 bar)

Wall force, w (FEA)	Resulting Deflect., Δ (mm)	Modulus, E (MPa)	Wall force, w (Analytical)
646	2.39	3.5	342
841	2.52	4.8	408
1052	2.59	6.2	471
1292	21.2	3.5	1062
1682	19.33	4.8	1250
2104	18.3	6.2	1494

Table 3.2 Comparison based on different oversize deflections and moduli (Seal pressure drop of 0.1 bar)

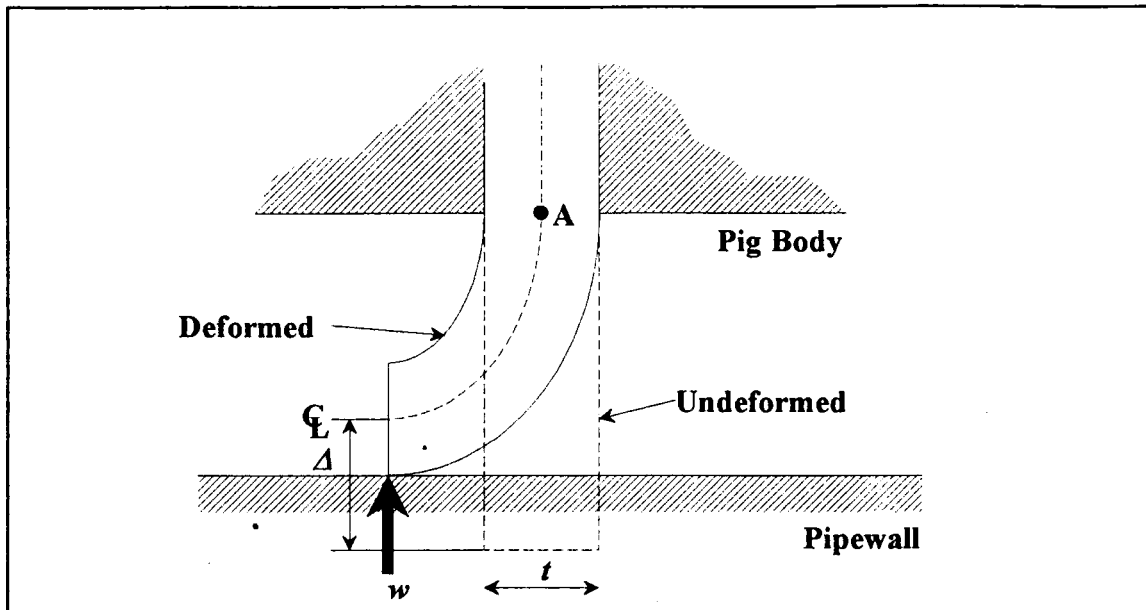


Figure 3.1 Pig sealing disc in contact with the pipewall

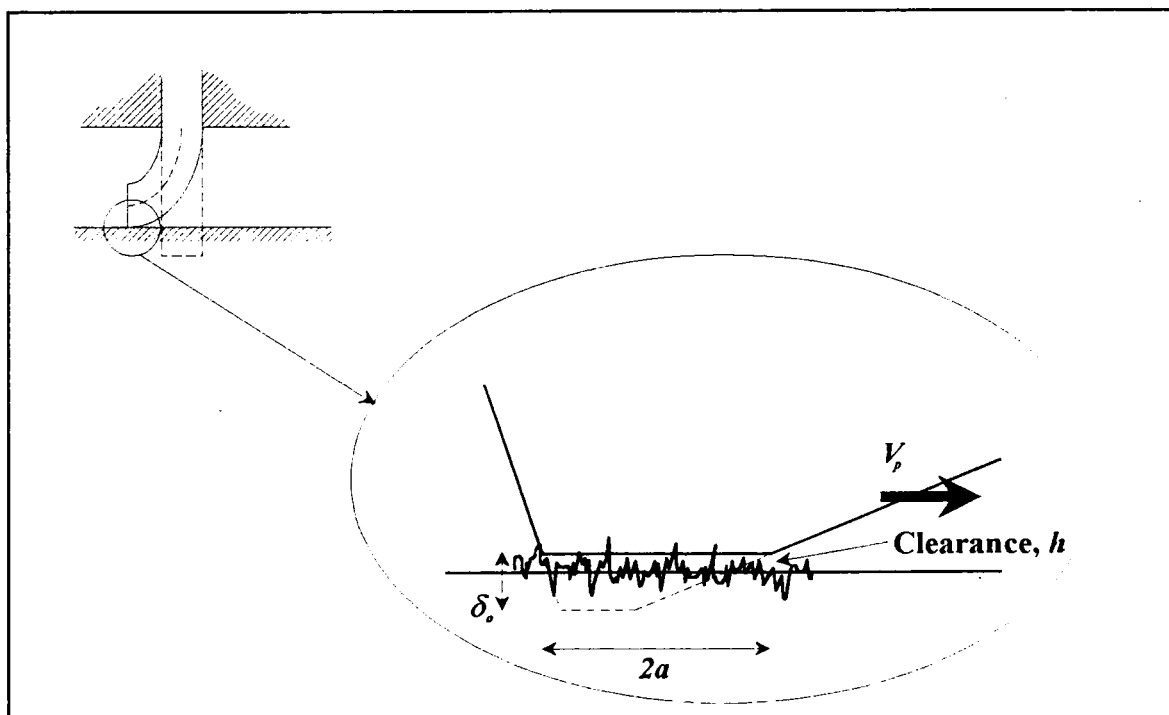


Figure 3.2 Contact between seal and pipewall

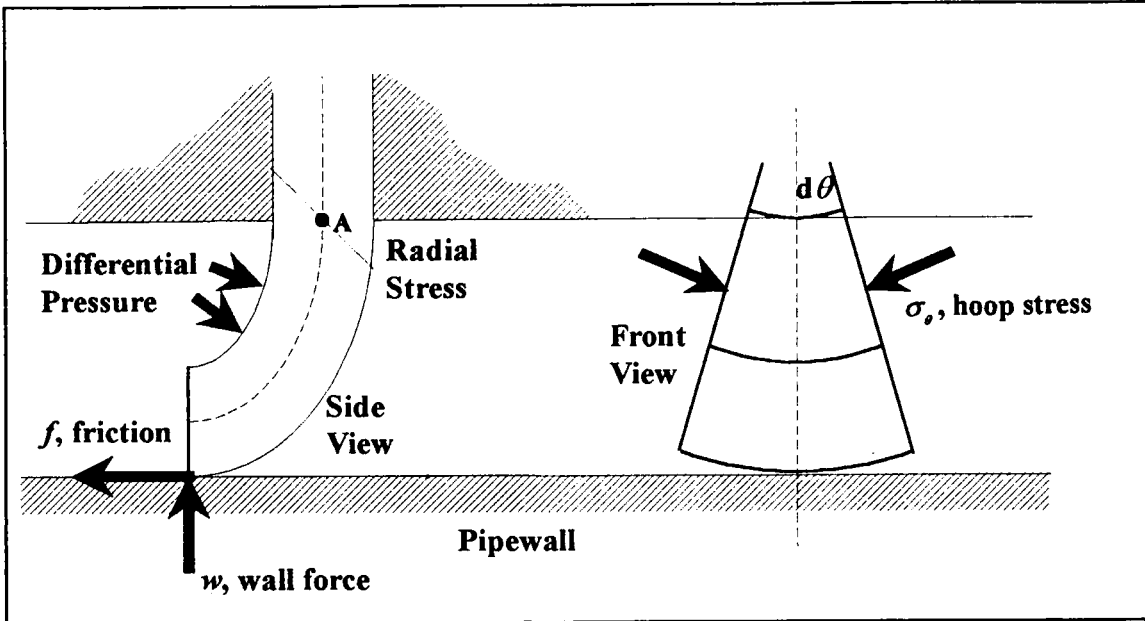


Figure 3.3 Basis of the wall force calculation

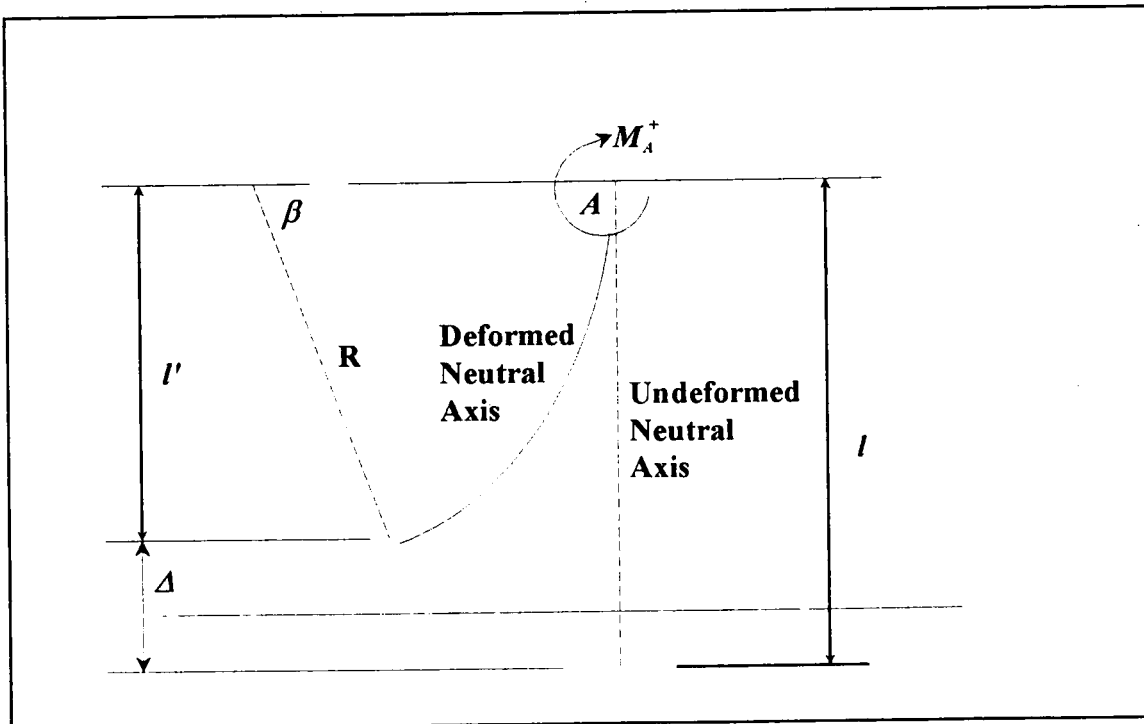


Figure 3.4 Geometry of the stressed pig sealing disc

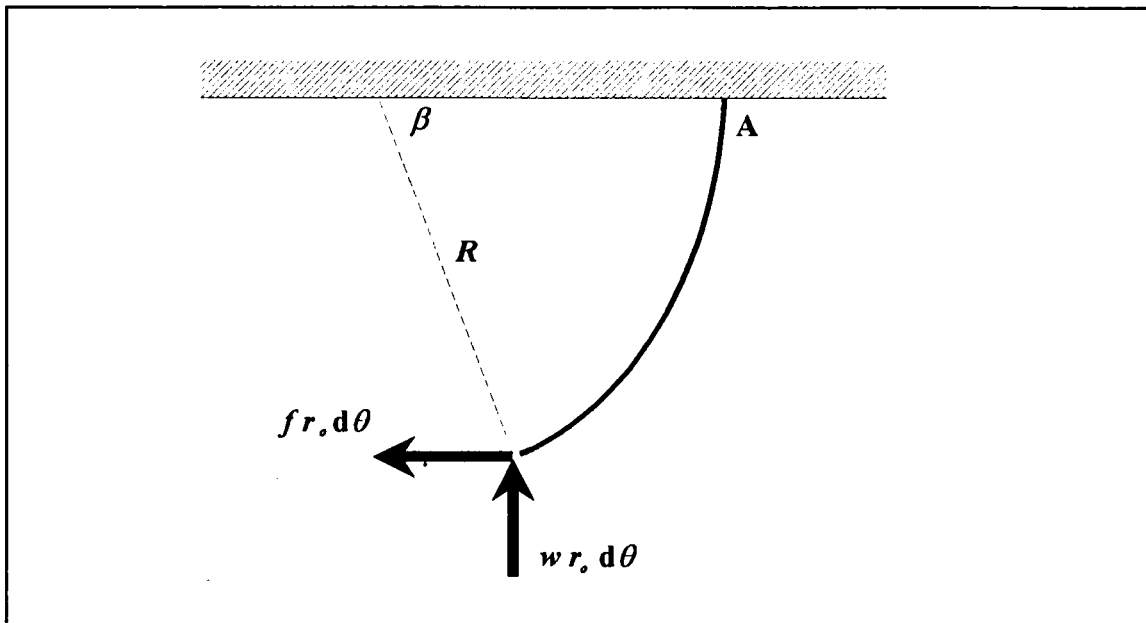


Figure 3.5 Positive moments due to wall force and friction

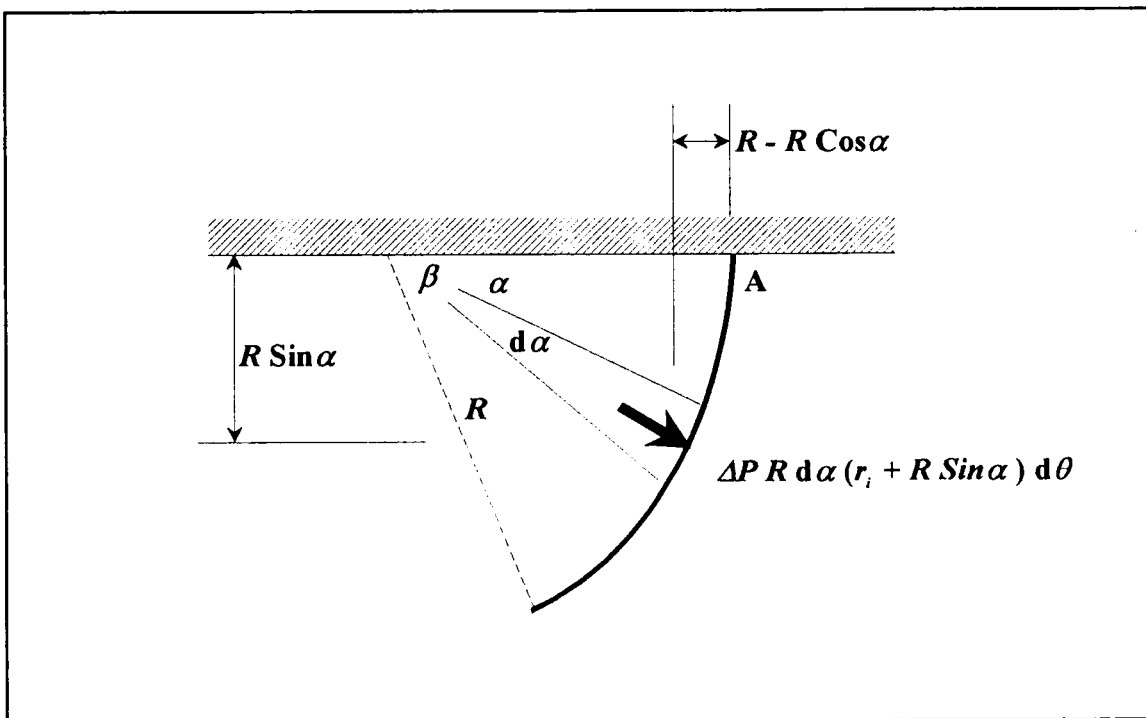


Figure 3.6 Negative moment due to differential pressure

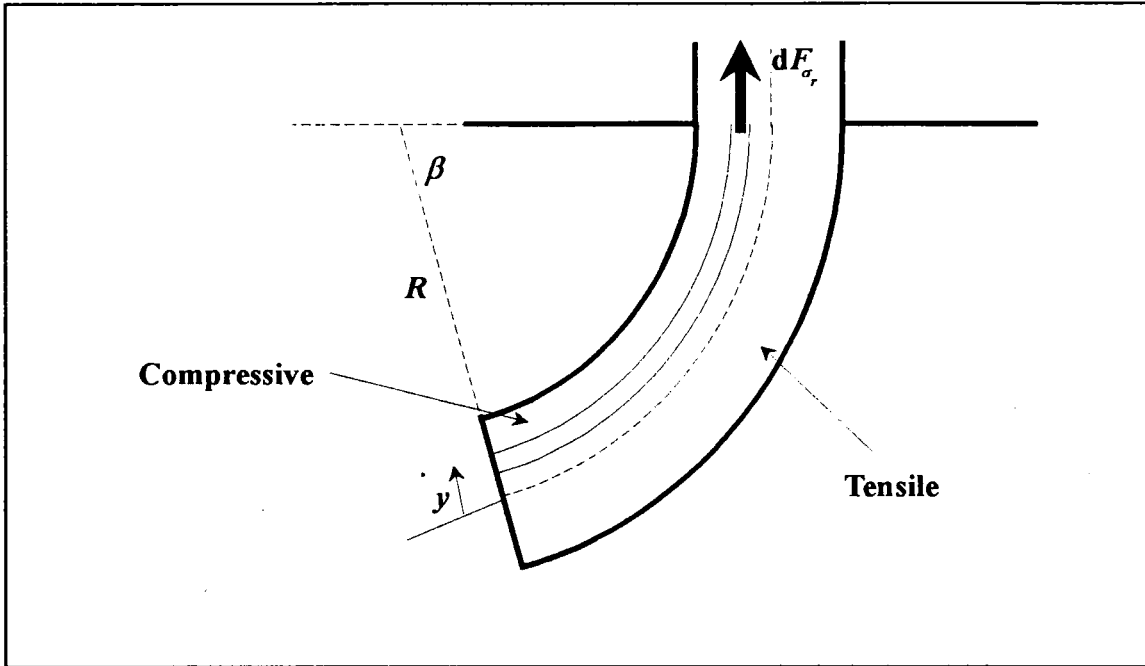


Figure 3.7 Negative moment due to radial stress in the disc

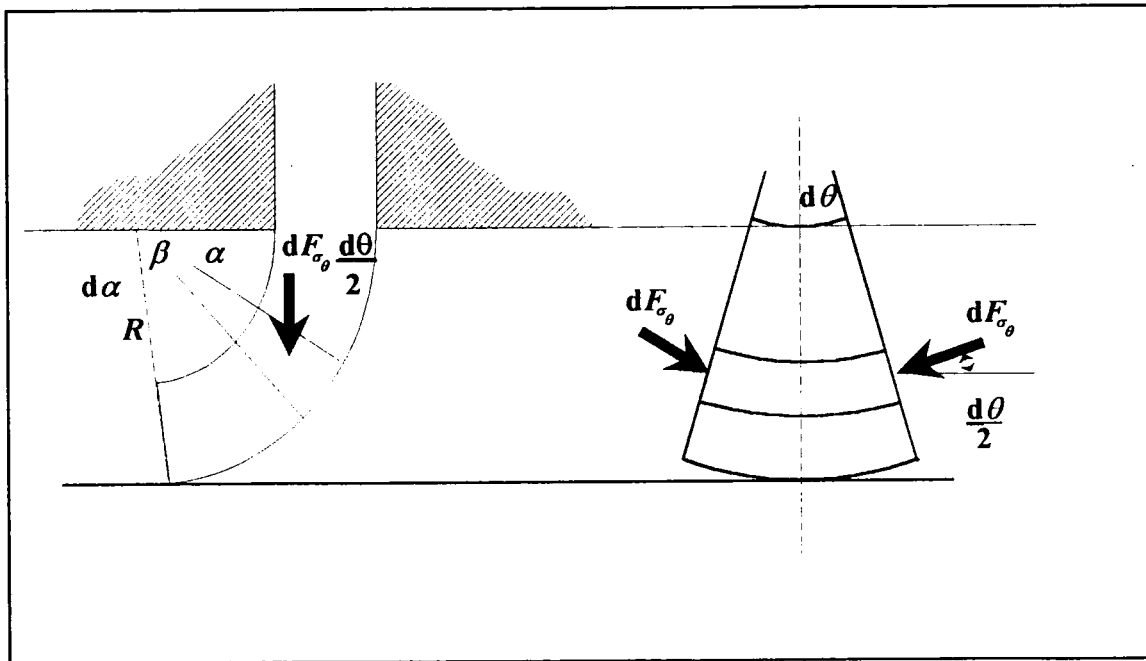


Figure 3.8 Negative moment due to hoop stress components

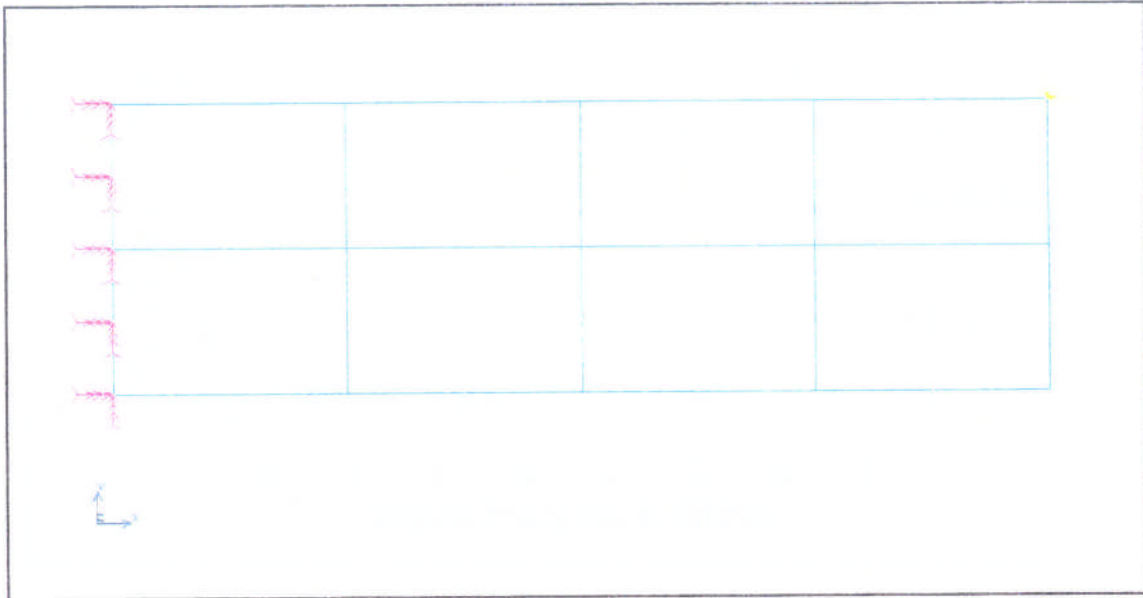


Figure 3.9 Grid used in Finite Element Analysis

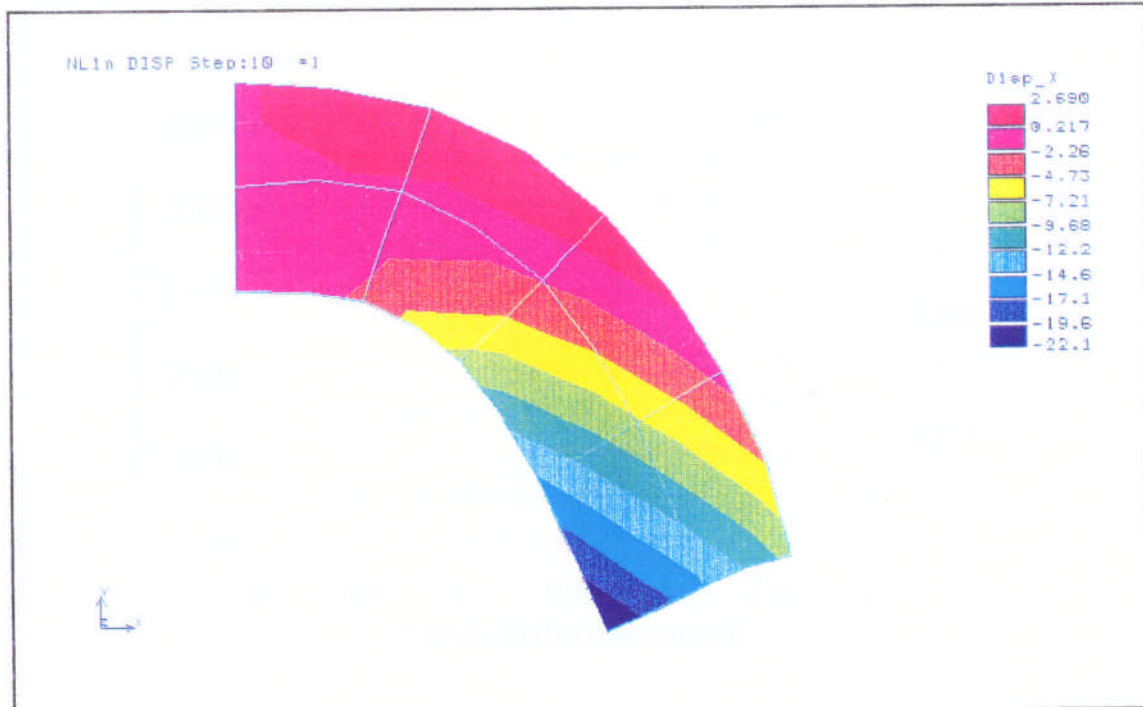


Figure 3.10 Typical 15mm oversize deflection plot from Finite Element Analysis

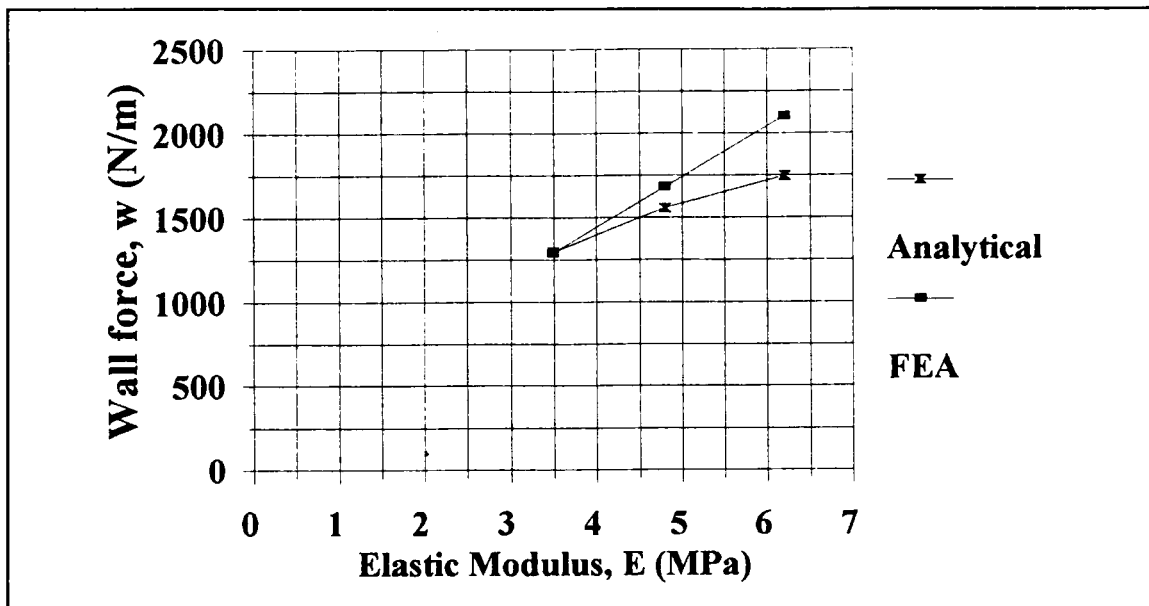


Figure 3.11 15mm oversize deflection output comparison

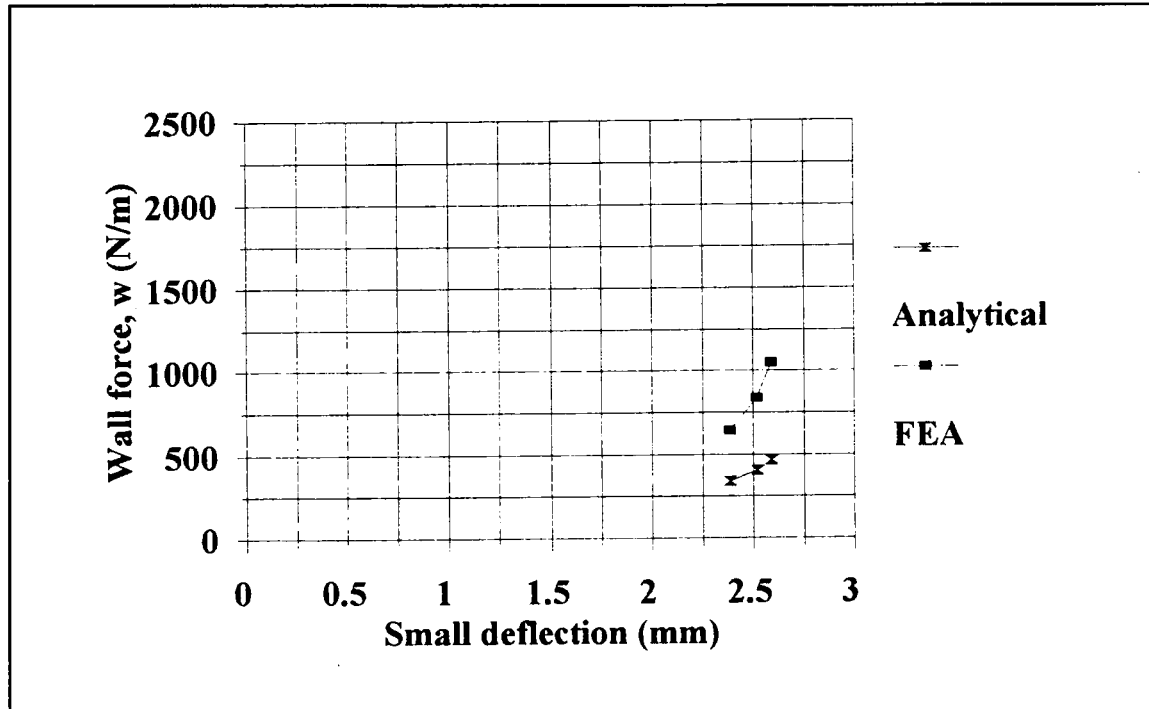


Figure 3.12 Wall force against deflection comparison (Small deflections)

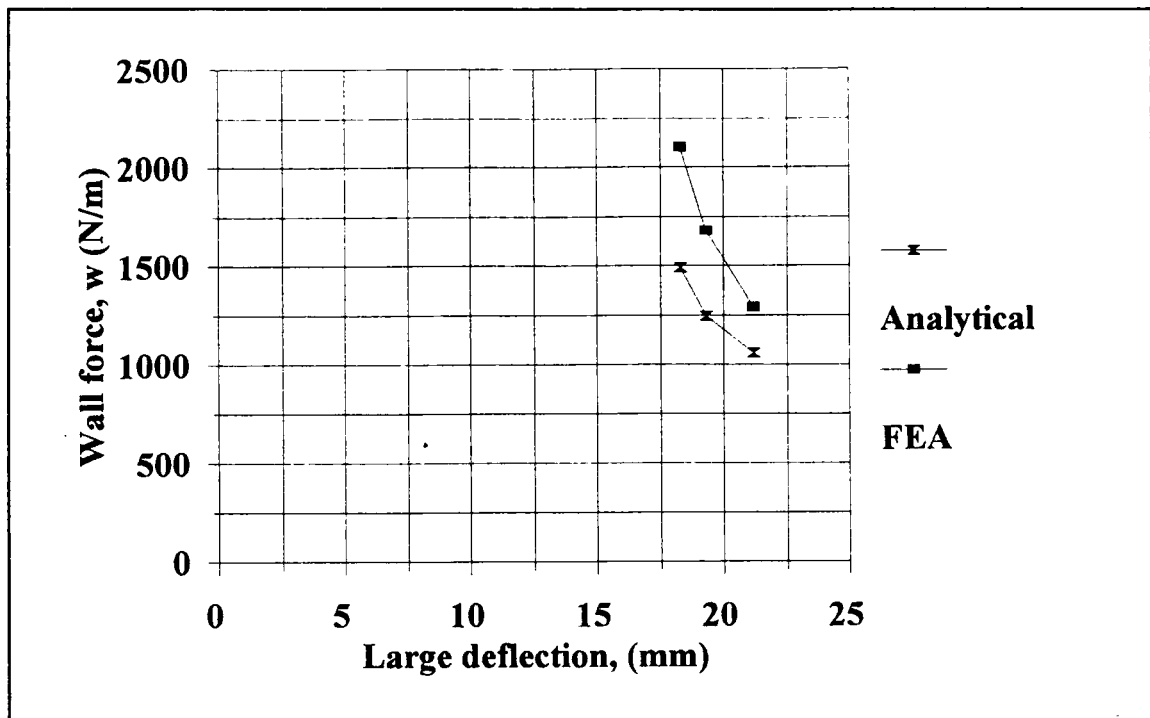


Figure 3.13 Wall force against deflection comparison (Large deflections)

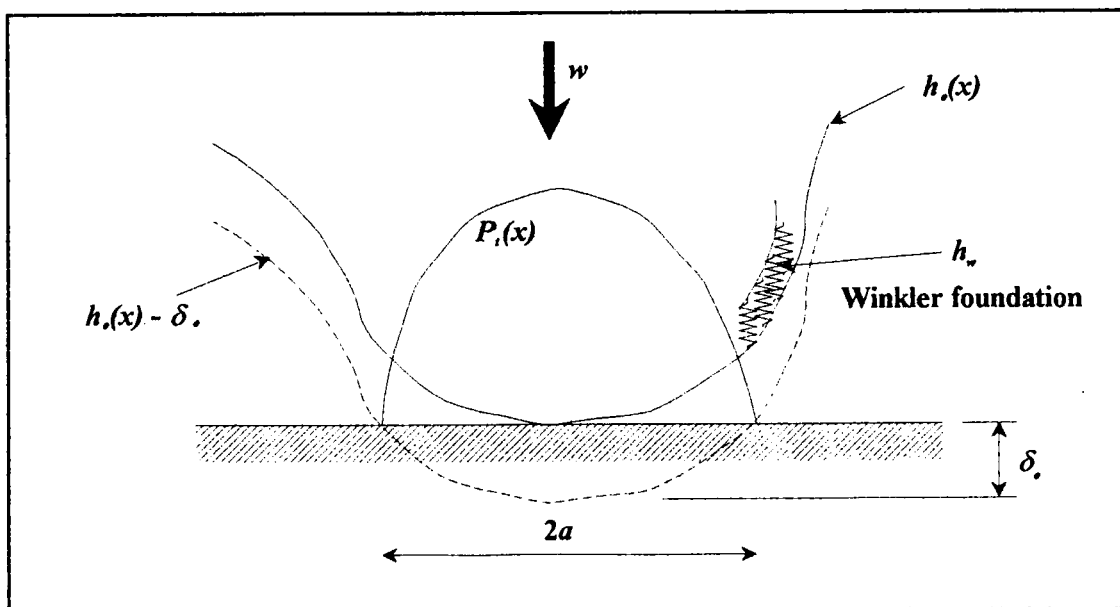


Figure 3.14 Winkler foundation method applied to an arbitrary shaped punch

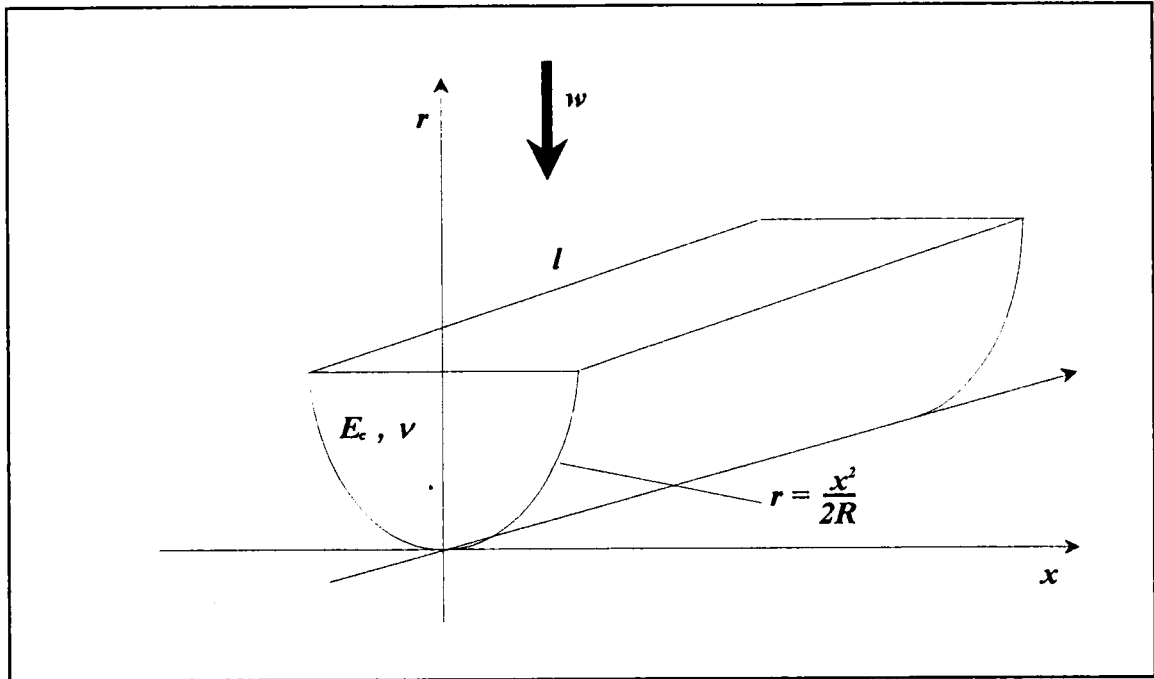


Figure 3.15 Parabolic line contact shape for comparison purposes

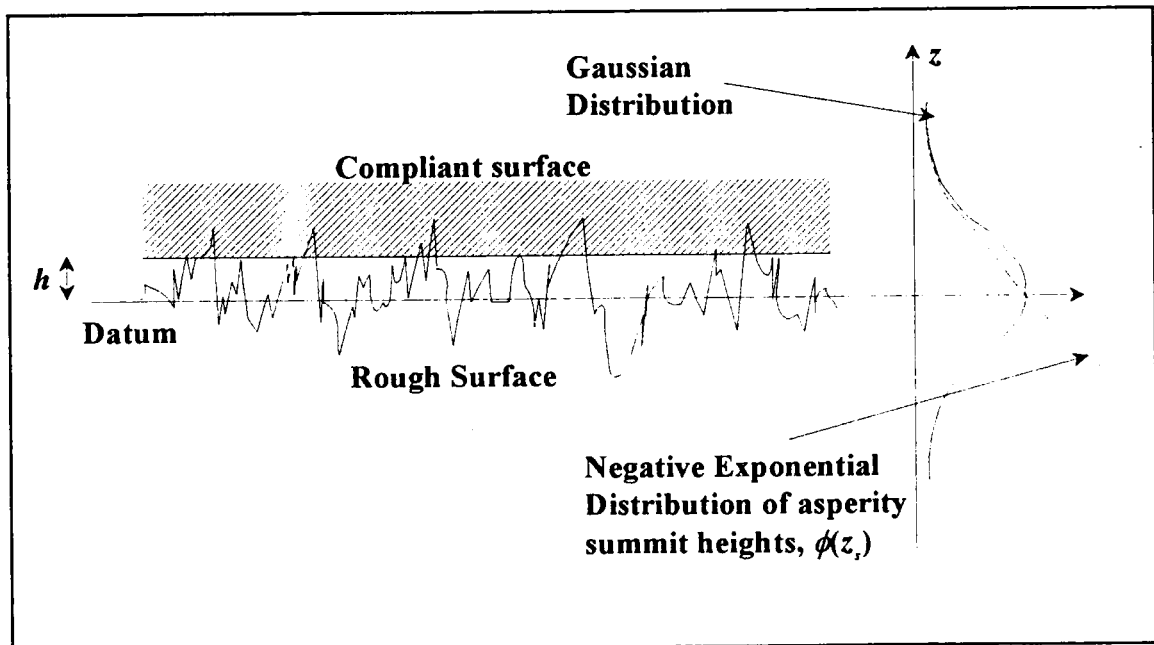


Figure 3.16 Rough surface model

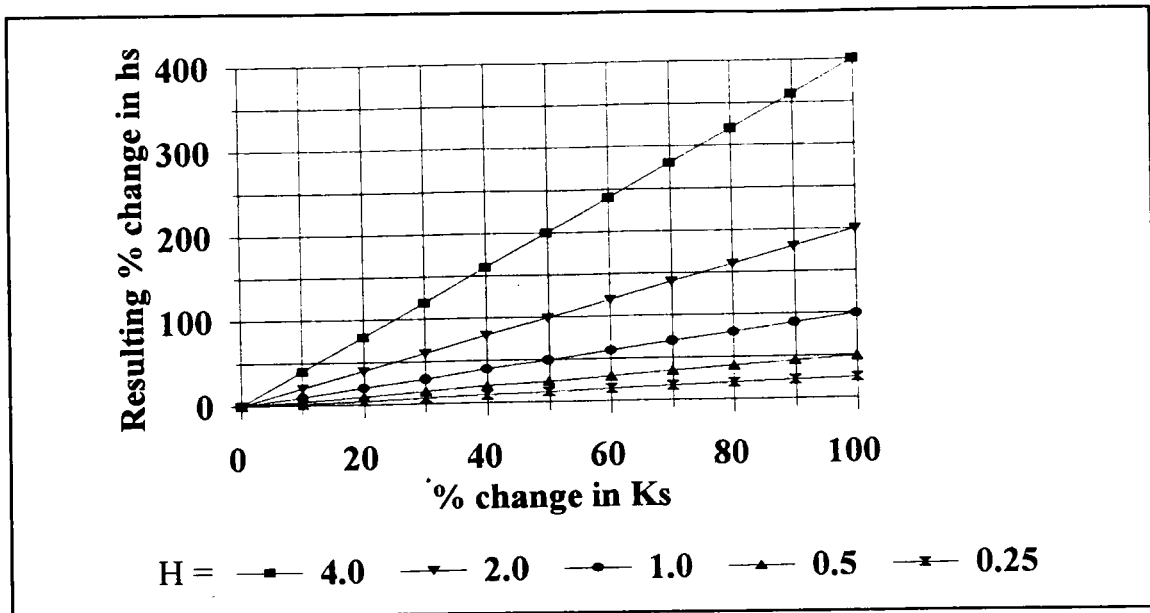


Figure 3.17 Error analysis on K_s , the roughness parameter

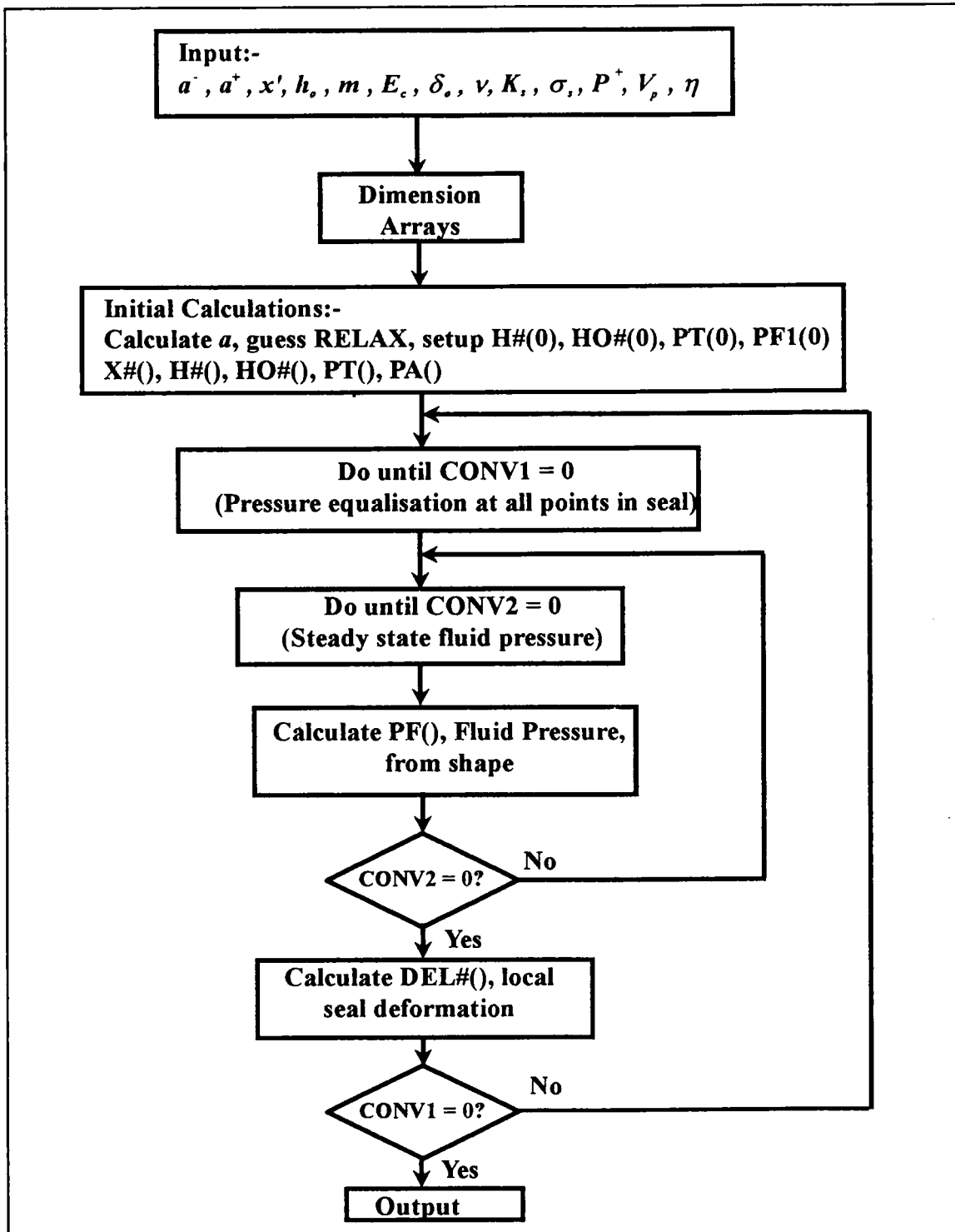


Figure 3.18 Flowchart for iterative EHL program, EHLPROG.BAS

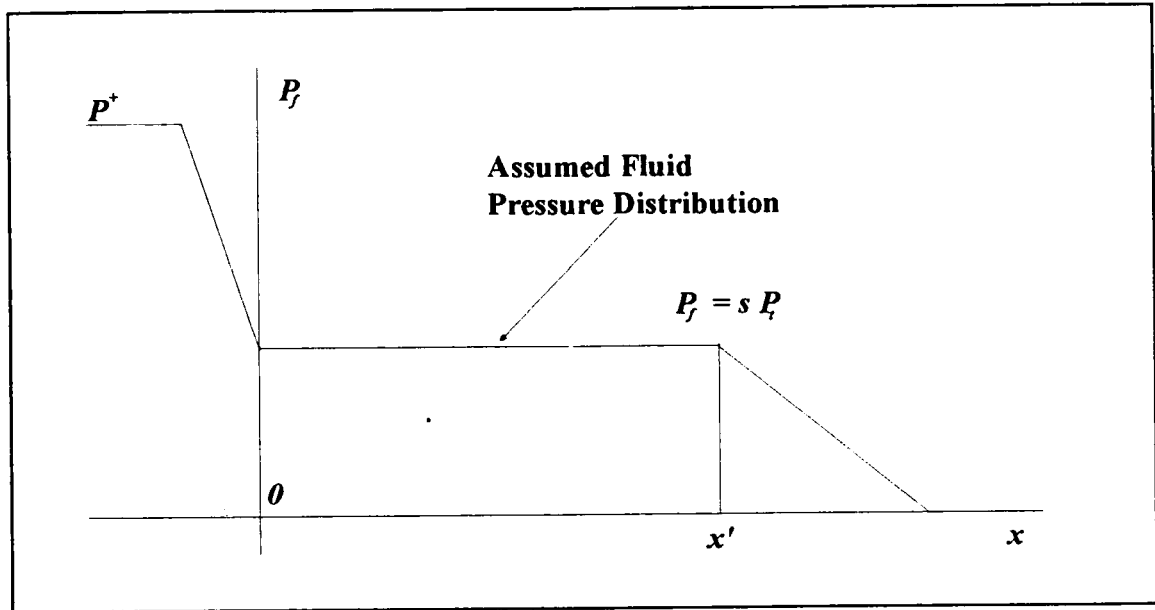


Figure 3.19 Assumed pressure distribution in seal area

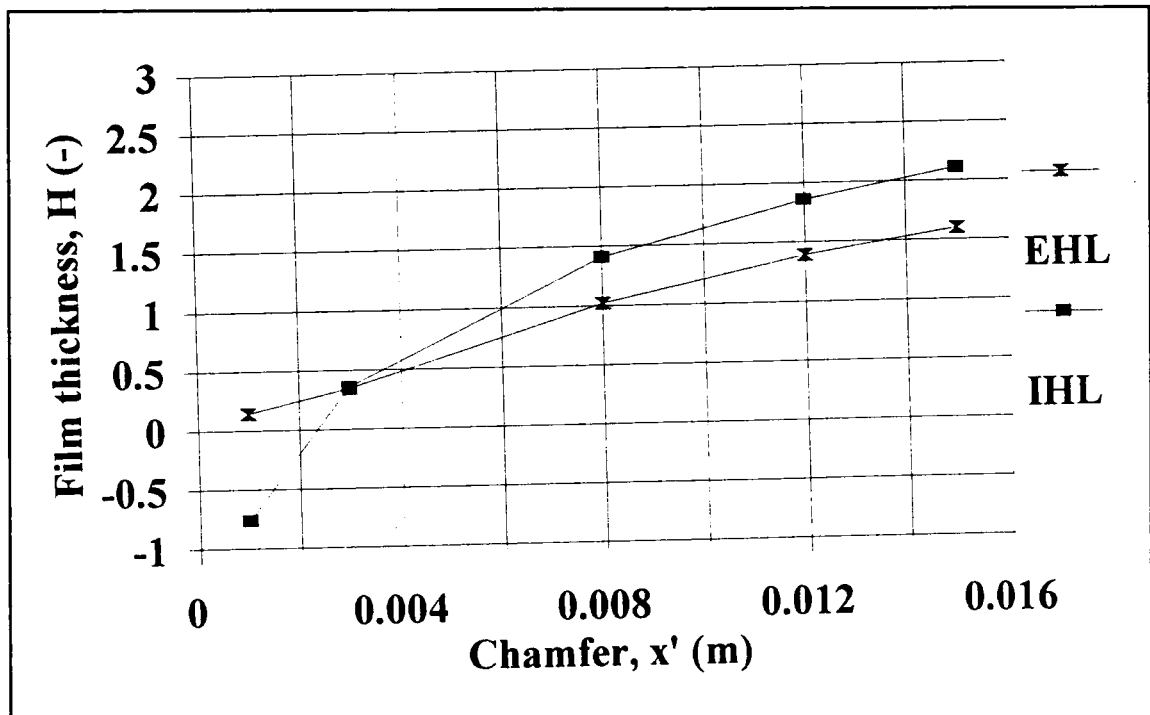


Figure 3.20 IHL against EHL - Chamfer length

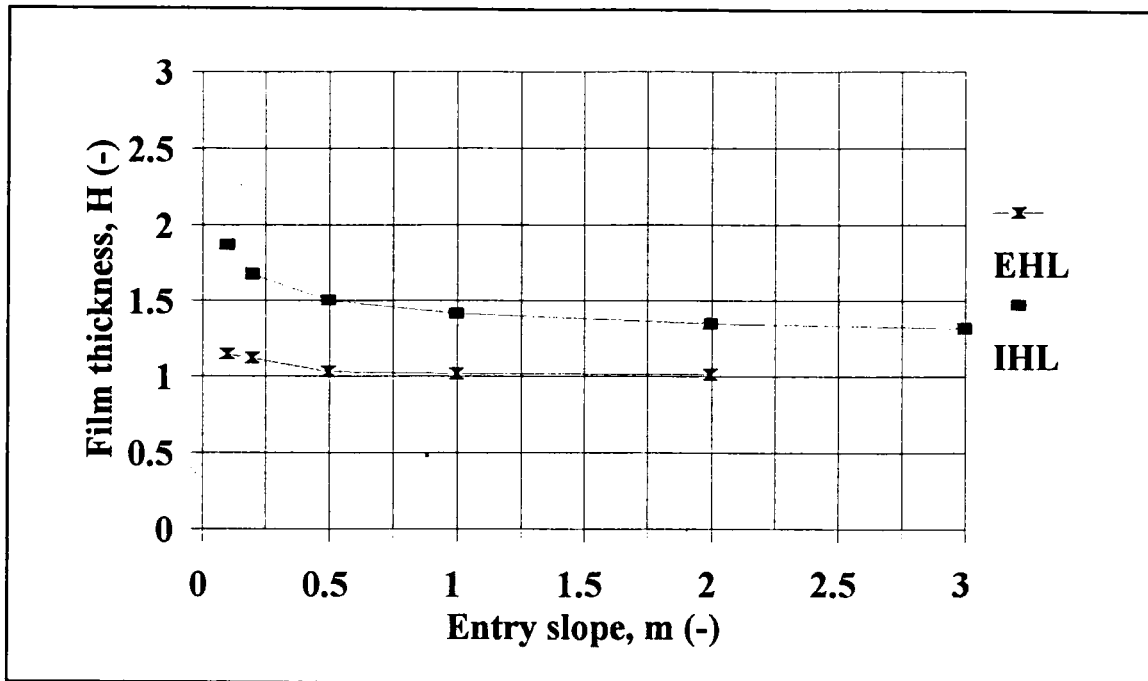


Figure 3.21 IHL against EHL - Entry slope

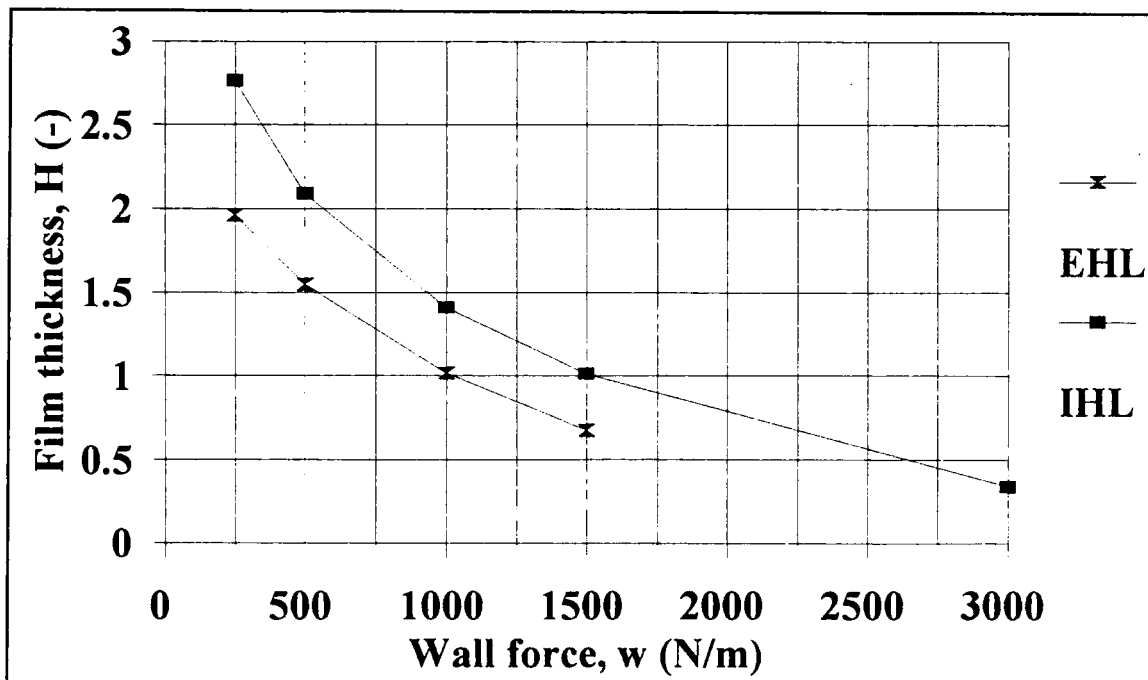


Figure 3.22 IHL against EHL - Wall force

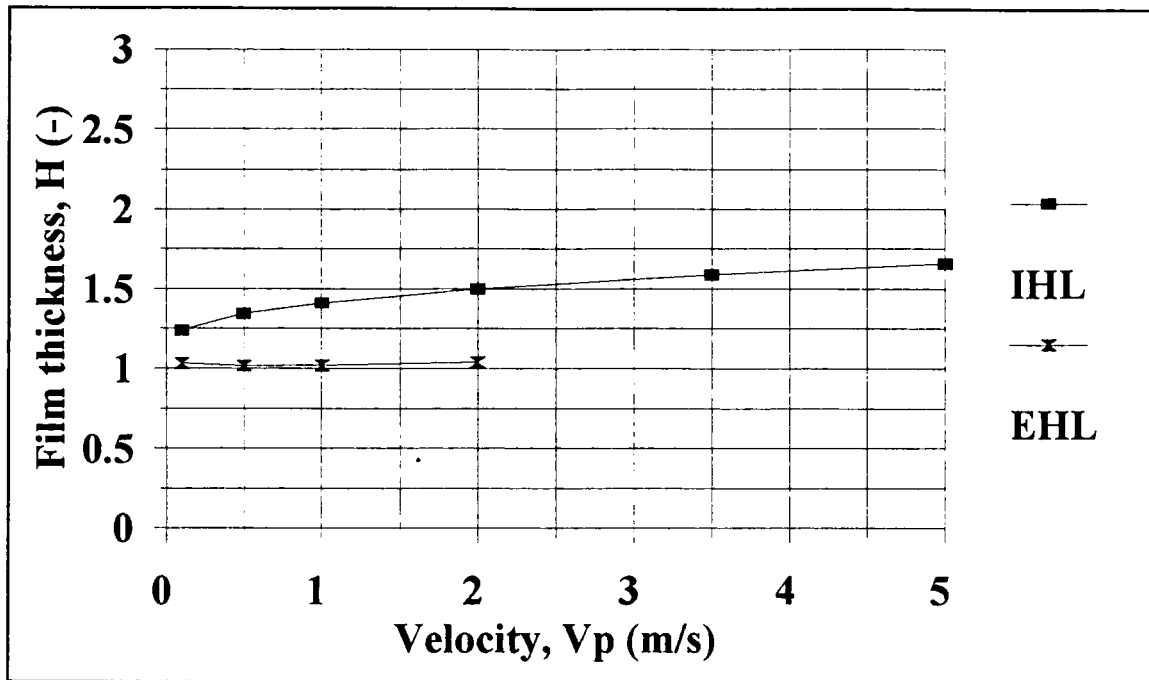


Figure 3.23 IHL against EHL - Velocity

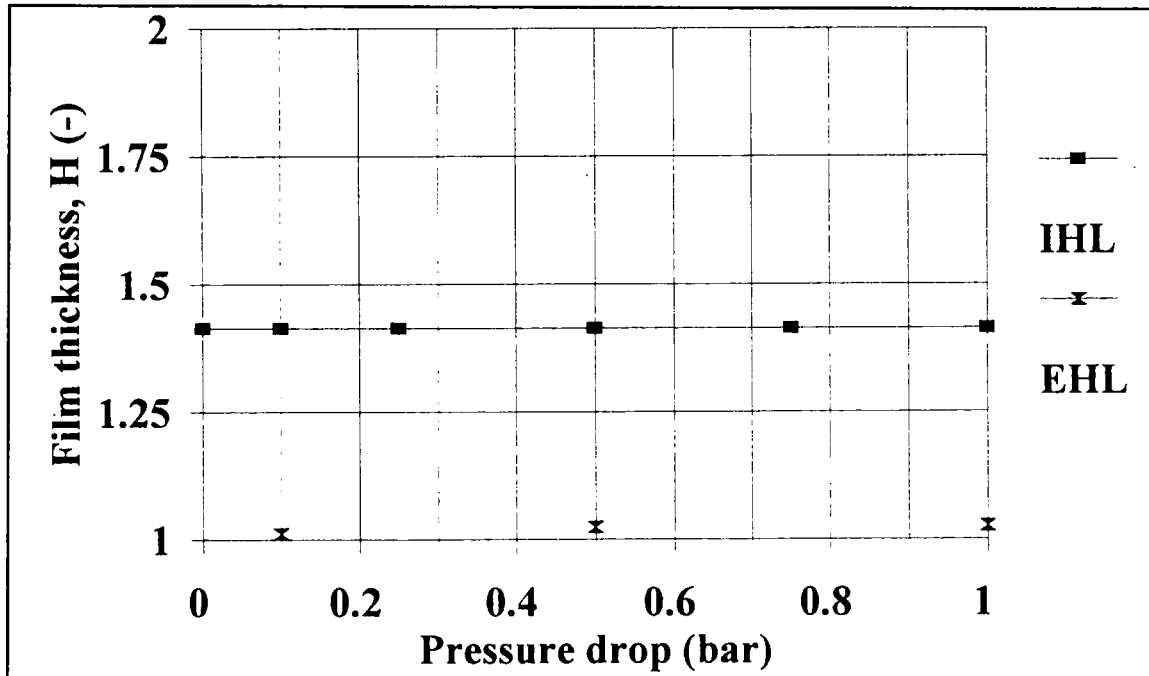


Figure 3.24 IHL against EHL - Pressure drop

CHAPTER 4

STEADY STATE MOTION MODEL

4. STEADY STATE MOTION MODEL

An engineering model of conventional pipeline pig steady state motion is described in this chapter. This model is based on the methods selected in the previous chapter. Where overlaps occur between this chapter and the last, a summary is given. The model is intended for use in the Oil and Gas environment in particular, but can also be applied to pigging applications in other industries. The working assumptions are outlined. The analysis is followed through, showing how all the characteristics required such as differential pressure and leakage, can be calculated. Investigations into the effects of wear on these characteristics is also possible using this method. Efficient calculation of these parameters requires the power of a computer due to the number of iterations in one run, and a program with this ability will be detailed in Chapter 5.

4.1 Overall model of the pig

Figure 4.1 shows the overall model of the bidirectional pipeline pig. The type shown is typical of that found in the field, with four sealing discs and two guide-discs to take the weight of the body. The model is by no means limited to this disc configuration however.

Frictional resistance to motion results in a pressure drop across the vehicle in order for motion to occur. Friction is primarily due to seal contact with the pipewall, but also from the guide-discs. The resulting pressure drop is used to calculate leakage. A number of assumptions are made in this analysis of the motion, and these are now outlined.

Assumptions

The main assumptions made in the ensuing analysis are:-

- (1) The force exerted on the wall due to the seals is far in excess of the weight of the pig. Therefore, most of the friction is due to the sliding contact between the seals and the pipewall. This is almost always true when the pig

is new, i.e. the oversize of the seals is large. However, as the seals wear, the wall force reduces along with the oversize and this assumption becomes less and less valid. Therefore, output for long distances may not be as accurate as for shorter distances.

- (2) The pig analysis is treated as an axi-symmetrical problem. That is the centreline of the pig matches the centreline of the pipeline. This means that wear, leakage and friction are uniform all round the circumference of each seal. In reality, a moment is induced due to the weight of the pig causing the friction to be greater on the bottom of the pig, making the pig travel in a “nose-down” fashion. This leads to uneven wear and leakage around the seal. Because of this the film thickness is not constant around the seals, and this leads to greater leakage than calculated.
- (3) The pressure drop across the pig is assumed to be stepped equally over the sealing discs. That is, the pressure drop across each of the seals are equal, and obviously the sum of these make up the total pig pressure drop. There is no pressure drop across the undersized guide-discs, since they offer relatively little resistance to flow due to their undersize. It will be seen later that this assumption is incorrect. However, attempts to calculate the different internal pressures adds another layer of complication for very little return. Therefore this is not considered.
- (4) The wall force is assumed to be related to:-
 - The differential pressure across the disc
 - The real oversize of the disc, Δ
 - The axial frictional force acting on the disc

All of these can vary in the analysis due to wear and velocity changes. The constant material and geometric properties of the disc are also included in

the wall force model. The non-linear properties of typical seal material, for example Urethane, is ignored. In addition, no account of hysteresis effects due to time or temperature is made. It has been observed by the author during validation trials, that the pig seals tend to retain some of their curvature if left in the pipeline for a long time. This is due to the time-dependant nature of the material. The result is to reduce differential pressure.

- (5) The contacting seal surface is modelled using a *Winkler foundation*, or "spring mattress", as discussed in chapter 3. The simplifying assumption made here is that a force acting at a point on this foundation will cause a displacement only at this point. The effect of this assumption has been discussed in chapter 3.
- (6) A chamfer is worn onto the disc as it travels along the pipeline. The seal is assumed to contact the pipewall along all of this chamfer. Neither of these are strictly true, since as the seal wears, the oversize reduces, allowing the seal to relax. This causes a slightly rounded chamfer.
- (7) The height of the surface asperities are distributed statistically according to the Gaussian distribution. The upper end of this distribution can be approximated by the simpler exponential distribution. Many pipeline surfaces have been shown to be distributed in this way, and so this assumption is valid. However, no directional effects of roughness are accounted for in the model (Greenwood J., Williamson J., (1966)). Directional roughness will affect leakage. In addition, the seal is roughened during the wear process, resulting in grooves in the axial direction on the seal contact face. Such grooving will lead to an increase in leakage.
- (8) The effects of roughness are ignored when calculating leakage and fluid viscous friction, but the contribution of friction at the asperity contacts is included. Although roughness will undoubtedly affect the fluid flow parameters, the information required is not readily available in the Oil & Gas

industry, and so it has been decided to attempt to validate these aspects of the model based on a smooth walled analysis.

- (9) Leakage past the seal is calculated using Poiseuille's formula based on the pressure drop across one seal, the film thickness and the chamfer length.
- (10) Removal of material due to wear is due to abrasion only, and is therefore related to the material abrasion resistance, the load borne by the pipe surface and the distance travelled.

The effects of these assumptions and further justification is offered in the ensuing analysis, the verification chapter and the discussion at the end of this work, where appropriate.

The bidirectional pig model

As stated, figure 4.1 shows the simplified model of the pipeline pig. The analysis proceeds as follows:-

- Estimate wall force acting on the pipewall due to the oversized pig sealing discs.
- Using this wall force, and a simplified geometry of the contact, calculate the contact parameters - footprint or contact length, local deformation and contact pressure distribution.
- The statistical nature of the pipe surface is used to estimate the initial film when the pig is stopped. This height is then taken as a datum.
- The Inverse Hydrodynamic Theory of Lubrication (IHL) is used to establish a representative film height once the pig is in motion at a given velocity.
- Once this is established, the asperity contact friction is estimated along with the frictional component due to the fluid. The total friction acting on the pig leads to the differential pressure acting across the pig using a simple force balance.

- Leakage rates are then estimated.

One consideration in particular acts to complicate the analysis. The wall force is dependent on the differential pressure to begin with. Therefore, an iterative approach is adopted, where the differential pressure across each of the seals is initially taken to be zero. Friction is then calculated for this case and hence the differential pressure. This is distributed across each of the seals, and the wall force is re-calculated. This is performed a number of times until a steady wall force and differential pressure is reached.

This model has been coded in QuickBASIC. This is discussed in chapter 5. This chapter is concerned with a more detailed explanation of the theory as outlined above. The starting place is calculation of the load on the pipewall due to the oversized seals, or the wall force. A summary of the equilibrium wall force method employed in the last chapter is given.

4.2 Estimation of the wall force, w

The equilibrium wall force model allows calculation of the wall force assuming that the sum of the moments due to the friction, differential pressure, hoop stress, radial stress and of course the wall force is zero. Friction and differential pressure are calculated from the lubrication analysis. These can be initially set to zero each, and an iterative type solution employed.

The equilibrium wall force formula is as follows:-

$$M_w^+ + M_f^+ - M_{\Delta P}^- - M_{\sigma_{rc}}^- - M_{\sigma_{rt}}^- - M_{\theta}^- = 0 \quad \dots 4.1$$

where:-

$$M_w^+ = wr_o R(1 - \text{Cos}\beta)d\theta \quad \dots 4.2$$

$$M_f^+ = fr_o(r_o - r_i)d\theta \quad \dots 4.3$$

$$M_{\Delta P}^- = \Delta PR^2 \left(\frac{R\beta}{2} - \frac{R\text{Sin}2\beta}{4} + r_i - r_i \text{Cos}\beta \right) d\theta \quad \dots 4.4$$

$$M_{\sigma_{rc}}^- = E_c r_i \frac{t^3}{24R} d\theta \quad \dots 4.5$$

$$M_{\sigma_{rr}}^- = E_c r_i \frac{t^3}{24R} d\theta \quad \dots 4.6$$

$$M_{\sigma_\theta}^- = \frac{E_c R^2 t d\theta}{(1 - \nu^2)} \int_0^\beta \frac{(\alpha - \text{Sin}\alpha)(1 - \text{Cos}\alpha)}{(\alpha + \frac{r_i}{R})} d\alpha \quad \dots 4.7$$

A full derivation of this can be found in appendix A. The segment angle, $d\theta$, can be ignored in the above since it cancels out in equation 4.1 due to the axi-symmetrical nature of the analysis. Given a value of friction and differential pressure, wall force w , can be calculated from this.

Finally the entry slope, m , (see figure 4.2) into the seal is given by:-

$$m = \text{Tan}\left(\frac{\pi}{2} - \beta\right) \quad \dots 4.8$$

4.3 Contact Analysis

The next step is to consider what is happening at the contact between the pipewall

and the pig sealing disc. The wall force w , will act at this location and cause a local deformation of the disc. Figure 4.2 shows a close-up of the contact between the disc and wall. Figure 4.3 then shows this generalised contact model. The undeformed shape is "squashed" against the pipewall resulting in a local deformation δ_o , and a footprint of length $2a$. Initially when the pig disc is new the chamfer length x' is zero, unless a chamfer has been machined onto the disc. To analyse this contact problem, the Winklers foundation approach is adopted as discussed in chapter 3.

Footprint length

From simple geometry consideration, the following footprint characteristics can be calculated, referring to figure 4.3. The negative extreme of the contact is:-

$$a^- = -\delta_o m \quad \dots 4.9$$

The positive extreme is:-

$$a^+ = x' + \frac{\delta_o}{m} \quad \dots 4.10$$

and finally the footprint length is given by:-

$$2a = \frac{m^2\delta_o + x'm + \delta_o}{m} \quad \dots 4.11$$

If the initial chamfer length x' , is small, then the wall force will be distributed over a very small length and so contact pressures will be high. Thus we would expect high wear rates to begin with, leading to an increase in x' , and thus a reduction in contact pressure magnitudes. Hence, wear rate is reduced as the pig travels further and further. For this reason, an initial severe run-in period is expected followed by a more gradual wearing of the discs.

Contact Pressures

The contact pressures are different in each of the three regions, 1, 2 and 3. These contact pressures relate directly to the deformations at each point according to equation 3.13. These deformations are:-

$$\text{Zone 1,} \quad \delta(x) = \delta_o + \frac{x}{m} \quad \dots 4.12$$

$$\text{Zone 2,} \quad \delta(x) = \delta_o \quad \dots 4.13$$

$$\text{Zone 3,} \quad \delta(x) = \delta_o - m(x - x')$$

Therefore, equation 3.13 can be used to calculate the total pressure $P_t(x)$, at each point in the contact footprint length:-

$$P_t(x) = \frac{1.013 E_c}{(1 - \nu^2) a} (\delta_o - h_o(x)) \quad \dots 4.15$$

When the pig is moving, this deformation increases to $\delta_o + h - h_o(x)$.

Local deformation

However, none of the above can be calculated until δ_o , the local deformation is known. This is done by equating the wall force with the integrated contact pressure along the footprint length. This is due to the fact that for equilibrium, the wall force must be exactly balanced by the contact pressure:-

$$w = \int_{a^-}^{a^+} P_t(x) dx \quad \dots 4.16$$

This simply yields:-

$$w = \frac{1.013 E_c}{(1 - v^2)a} \left(\frac{m\delta_o^2}{2} + \delta_o x' + \frac{\delta_o^2}{2m} \right) \quad \dots 4.17$$

Since a is a function of δ_o , the only unknown is δ_o . Solving for this using an iterative routine such as Newton-Raphson allows calculation of all the other contact parameters.

4.4 Rough surface model

A statistical method has been used to model the rough surface. This is based on the work done by Greenwood and Williamson (1966). When the pig is stationary all the load or wall force is supported by the asperities or roughness peaks. When the pig is moving, a thin film of liquid is built up and part of the load is then borne by the fluid. The film of liquid is characterised by a clearance between the disc and the mean roughness height. A relationship between asperity pressure and clearance, h , is derived in Appendix D as:-

$$P_a(x) = 0.707 \frac{E_c}{(1 - v^2)} K_s e^{-\frac{h}{\sigma_s}} \quad \dots 4.18$$

Initial, stationary rough surface contact

Equation 4.18 can be used to evaluate the asperity pressure at a point in the seal. When the pig is stationary, the contact pressure is matched exactly by the asperity pressure, i.e. all the load is taken by the rough surface, so asperity pressure is equal to total pressure at each point. Therefore, an expression for film thickness at each point can, in general, be written:-

$$0.707 \frac{E_c}{(1 - v^2)} K_s e^{-\frac{h_s(x)}{\sigma_s}} = \frac{1.013 E_c}{(1 - v^2) a} \delta(x) \quad \dots 4.19$$

4.5 Calculation of the film thickness

The film thickness is calculated using the Inverse Hydrodynamic Theory (IHL), as outlined in chapter 3. This method is now applied to the disc seal in order to establish the film thickness as the pig is in motion at a velocity of V_p .

Balancing the load to calculate film thickness

The final film thickness, when the pig is in motion, is made up from two components, the static component as detailed in 4.4, and the steady state component, h^* . Therefore:-

$$h = h_s + h^* \quad \dots 4.20$$

Press

ure is generated by the fluid in the seal, P_f , due to the sliding motion. This causes the seal to lift off the surface. However, a force balance must still be maintained as demonstrated in figure 4.4 at the point x' . Note that the fluid pressure distribution is assumed in this case. The sum of the fluid and asperity pressures at this point in the contact zone must equal the total or contact pressure.:-

$$P_t(x') = P_a(x') + P_f(x') \quad \dots 4.21$$

A

pressure factor, s , is now introduced in zone 2 of the seal. This is defined as follows:-

$$P_f = s P_t \quad \dots 4.22$$

The pressure factor is assumed to be an average relationship between fluid pressure and total pressure at x' . This is a simplification to allow both the fluid and asperity support loads to be calculated easily. Combining equations 4.21 and 4.22 the following expression is obtained:-

$$P_a = (1 - s) P_t \quad \dots 4.23$$

Now

, at the point x' in the seal, equation 4.23 can be expanded to:-

$$0.707 K_s e^{-\frac{h_s + 1.5 h^*}{\sigma_s}} = \frac{1.013 (1 - s)}{a} (\delta_o + 1.5 h^*) \quad \dots 4.24$$

The pressure factor s can be evaluated from this using an iterative solving technique, given that:-

$$h^* = \sqrt{\frac{8}{9} \eta V_P \left(\frac{dP_f}{dx} \right)^{-1}} \quad \dots 4.25$$

The fluid pressure distribution is taken to be at the inlet. This is:-

$$\frac{dP_f}{dx} = \frac{1.013 E_c (\delta_o + 1.5 h^*)}{(1 - v^2) a (a^+ - x')} \quad \dots 4.26$$

This allows calculation of a representative final film shape in the seal.

Final film shape

The film shape can now be determined at each point in the seal. In zone 1, equation 4.21, the force balance equation, is used to determine the film profile. The resulting expression is:-

$$\begin{aligned} (P^+ - P_o) \frac{x}{a} + P_o + 0.707 \frac{E_c}{(1 - v^2)} \\ = \frac{1.013 E_c}{(1 - v^2) a} (\delta_o + \frac{x}{m} + h(x)) \end{aligned} \quad \dots 4.28$$

where P_o is the fluid pressure at $x = 0$, or

$$P_o = \frac{1.013 s E_c}{(1 - v^2) a} (\delta_o + h(0)) \quad \dots 4.29$$

In the central zone, zone 2, the film thickness is taken to be constant and can be evaluated by applying equation 4.23:-

$$0.707 K_s e^{-\frac{h(x)}{\sigma_s}} = \frac{1.103 (1 - s)}{a} (\delta_o + h(x)) \quad \dots 4.30$$

The

value of $h(x)$ from this expression can be used in 4.29 as $h(0)$. Finally, the same approach is used for zone 3, the entry into the seal:-

$$0.707 K_s e^{-\frac{h(x)}{\sigma_s}} = \frac{1.013 (1 - s)}{a} (\delta_o - m (x - x') + \dots 4.31$$

Each

of these expressions for the film thickness profile require an iterative solution such as Newton-Raphson for estimation of h at each x . A detailed description of the film can now be used to estimation friction and then differential pressure.

4.6 Friction and differential pressure

Friction in the seal is due primarily to the contact between the pipewall and the pig seal, i.e. rough surface contact. In addition a small component of friction is due to

fluid shear. Asperity friction reduces with increasing film thickness. This is due to the reduction in real area of contact as the seal moves further and further away from the datum line. This shall now be demonstrated.

Asperity friction

Asperity friction is simply given by the load and the dynamic friction coefficient according to the relationship, $F_a = f_o \cdot W_a$. Applying this to a point in the seal with a film thickness of h , the friction acting on a small length of the seal, dx , is given by:-

$$dF_a = 0.707 f_o \pi d \frac{E_c}{(1 - \nu^2)} K_s e^{-\frac{h(x)}{\sigma_s}} dx \quad \dots 4.32$$

This equates to asperity pressure at a height h , times the small circumferential nominal contact area this pressure is acting over with a nominal dynamic friction coefficient included. This must be calculated along the length of the seal and summed to evaluate the final friction due to the seal/asperity contact for a single seal.

Fluid friction

The fluid friction due to seal/fluid shear is obtained from Reynolds' lubrication equation. The general expression is (Cameron A., (1987)):-

$$dF_f = \pi d \left(\frac{dP_f(x)}{dx} \frac{h}{2} - \frac{\eta V_p}{h} \right) dx \quad \dots 4.33$$

The pressure gradient in each area is:-

$$\text{Zone 1,} \quad \frac{dP_f}{dx} = \frac{P^+ - P_o}{a^-} \quad \dots 4.34$$

$$\text{Zone 2,} \quad \frac{dP_f}{dx} = 0 \quad \dots 4.35$$

$$\text{Zone 3,} \quad \frac{dP_f}{dx} = -\frac{P_o}{a^+ - x'} \quad \dots 4.36$$

Here the sign convention is different. A positive asperity friction acts to oppose pig motion and induce a differential pressure. A negative fluid friction acts to oppose the motion of the pig. This is due to the fact that pig velocity is taken as negative in the Reynolds' equation to comply with convention.

The frictional component is ignored in zone 1, since much turbulence will be generated in this outlet region and the overall effect is also judged to be negligible.

Total friction and differential pressure

These small components of fluid friction are summed up over the length of the seal.

The final total friction is then given by:-

$$F_{tot} = n \Sigma (dF_a - dF_f) + f_o M g \quad \dots 4.37$$

Note that the last term in this expression gives the frictional contribution due to the guide-discs. This is expected to be relatively small initially, since the highest wall force is due to the seals. However, if it becomes significant then the model will not be as accurate since no lubrication effects are included here.

The differential pressure is found by a simple force balance across the pig

$$\Delta P = \frac{4 F_{tot}}{\pi d^2} \quad \dots 4.38$$

4.7 Leakage past the seal

Figure 4.5 shows a typical fluid velocity distribution in the seal area. Forward leakage is that proportion of this flow which is moving faster than the pig, V_p . Reverse leakage is that proportion moving slower than this. It must be noted that forward leakage will be "recycled" as reverse leakage in reality. This must be taken into account in any attempt to measure forward leakage rates.

Massey (1979) derives an expression for $u(z)$, the velocity distribution arising from a pressure driven flow through two parallel flat surfaces:-

$$u(z) = \frac{1}{2} \frac{dP_f}{\eta dx} (z^2 - h z) + \frac{V_p z}{h} \quad \dots 4.39$$

The leakage rates can then be calculated from this expression, by discretisation in the z -direction, or axial direction. The pressure gradient is taken as the pressure behind the seal, P^+ , dropped linearly across the length of the seal, $2a$, for simplicity.

4.8 Pig disc wear

After the pig travels a distance ΔX , material is removed from the pig discs due to wear. The volume of material removed depends on the load supported by the asperities, the distance travelled and the abrasion resistance of the material. The classical relationship used is:-

$$V_{wear} = K_{wear} w_a \pi d \Delta X \quad \dots 4.40$$

Figure 4.6 shows the "area" of material removed, in two dimensions. As a result of this the chamfer length x' , increases to x'_{new} . From equation 4.40, the area of wear

is:-

$$A_{wear} = K_{wear} w_a X \quad \dots 4.41$$

where w_a is the load supported by the asperities.

From geometric considerations, this area of material removed is:-

$$A_{wear} = 2 a \delta_{wear} + \frac{\delta_{wear}}{2} \left(m + \frac{1}{m} \right) \quad \dots 4.42$$

where δ_{wear} is the depth of wear as shown in figure 4.6, and $2a$ is the seal length. Equating 4.41 and 4.42, then δ_{wear} can be estimated. Once δ_{wear} is established then the new chamfer length, x'_{new} is:-

$$x'_{new} = 2 a + \delta_{wear} \left(m + \frac{1}{m} \right) \quad \dots 4.43$$

The real oversize, Δ , is also assumed to reduce by δ_{wear} .

Removal of material from the pig disc results in a reduction in wall force, due to the reduction in oversize. In addition, the load is spread over a longer footprint, and so the contact pressure magnitude will reduce. The consequence of this is that the wear rate is initially high, during the run-in period, due to high wall forces and contact pressures. For this reason, the distance increment ΔX , is short initially, but can grow progressively longer as the wear calculation proceeds. After a few kilometres of travel, the wear rate drops considerably and less material is removed.

The model as described above, has been coded in QuickBASIC, and is described in the next chapter. The program is called *PIGPlus*. The chapter describes how the above formulae are used to describe the motion of the pig at a steady velocity along the pipeline, and how wear affects characteristics such as differential pressure, and

leakage.

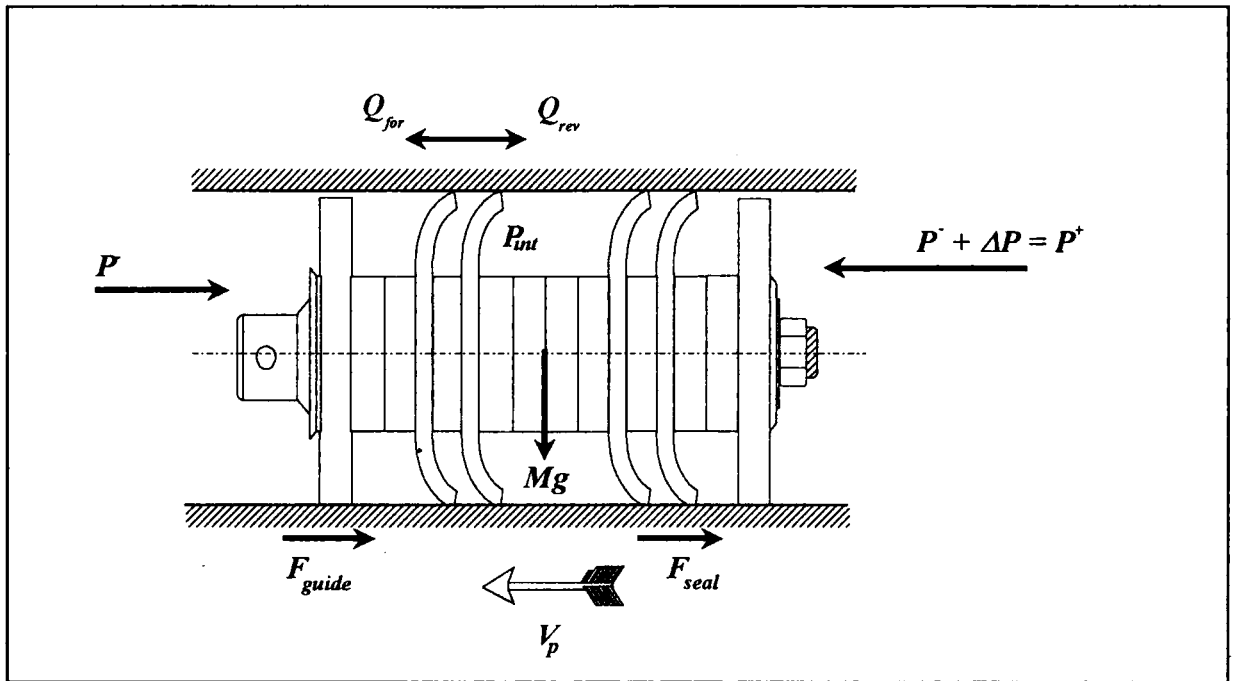


Figure 4.1 Overall bidirectional pig model

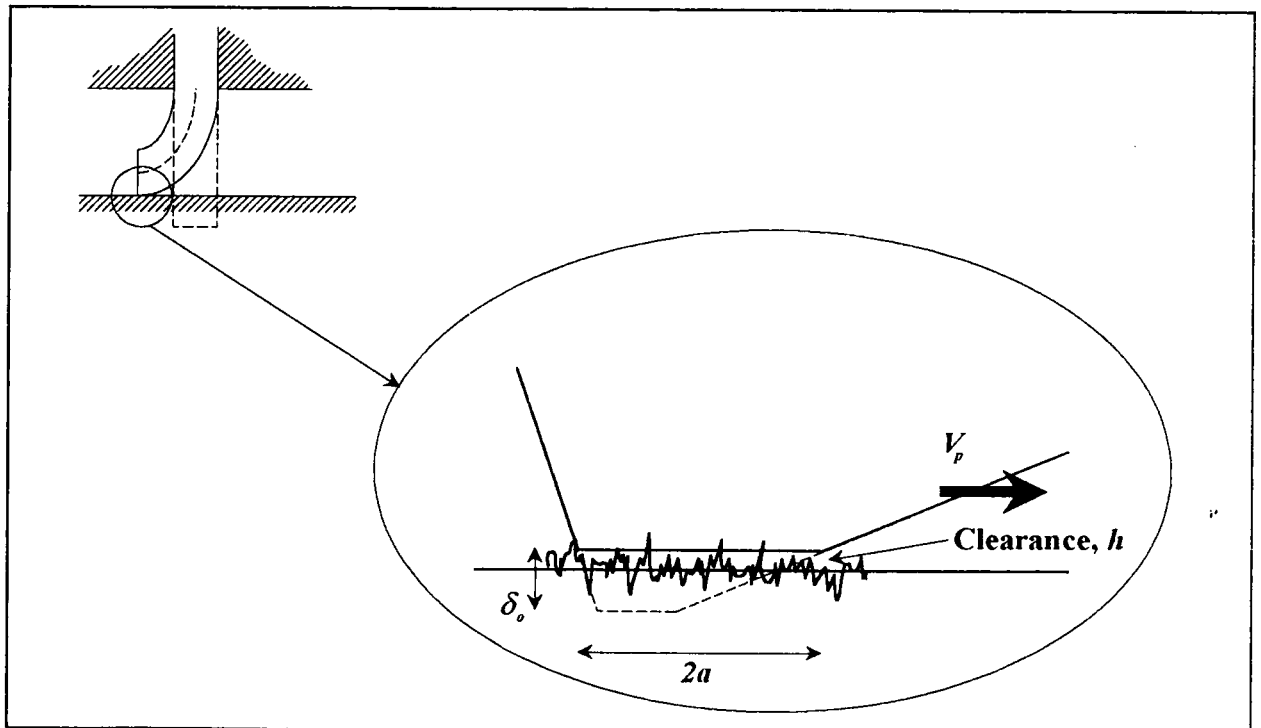


Figure 4.2 Close-up of pig disc/pipewall contact

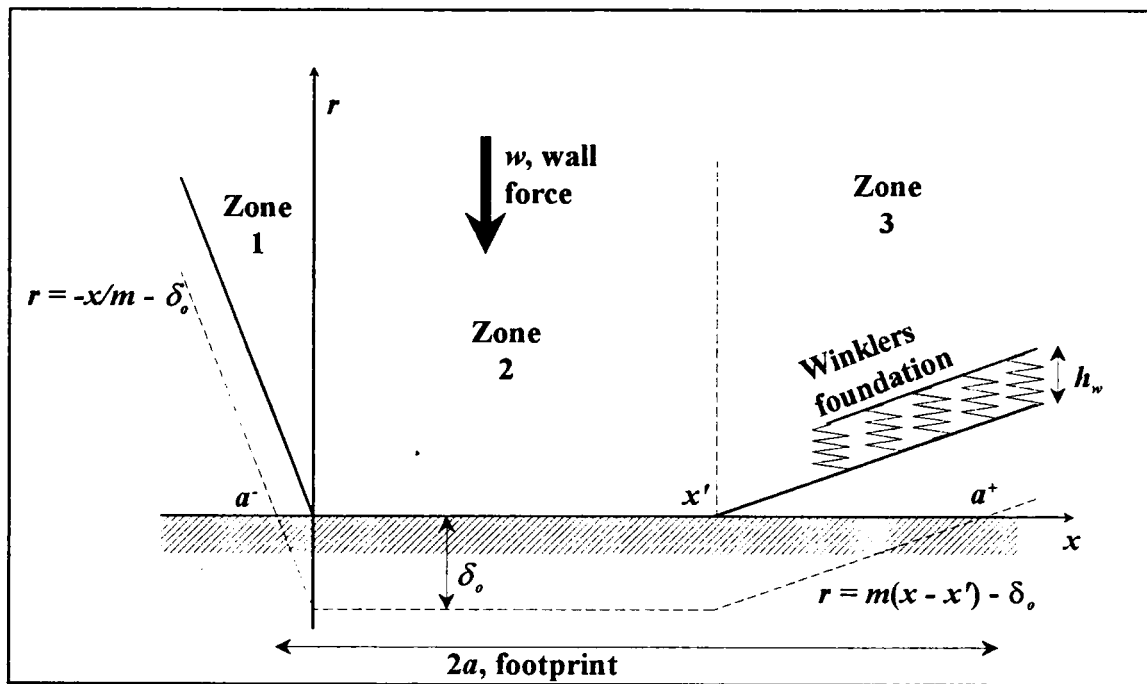


Figure 4.3 Generalised pig seal/pipewall contact model

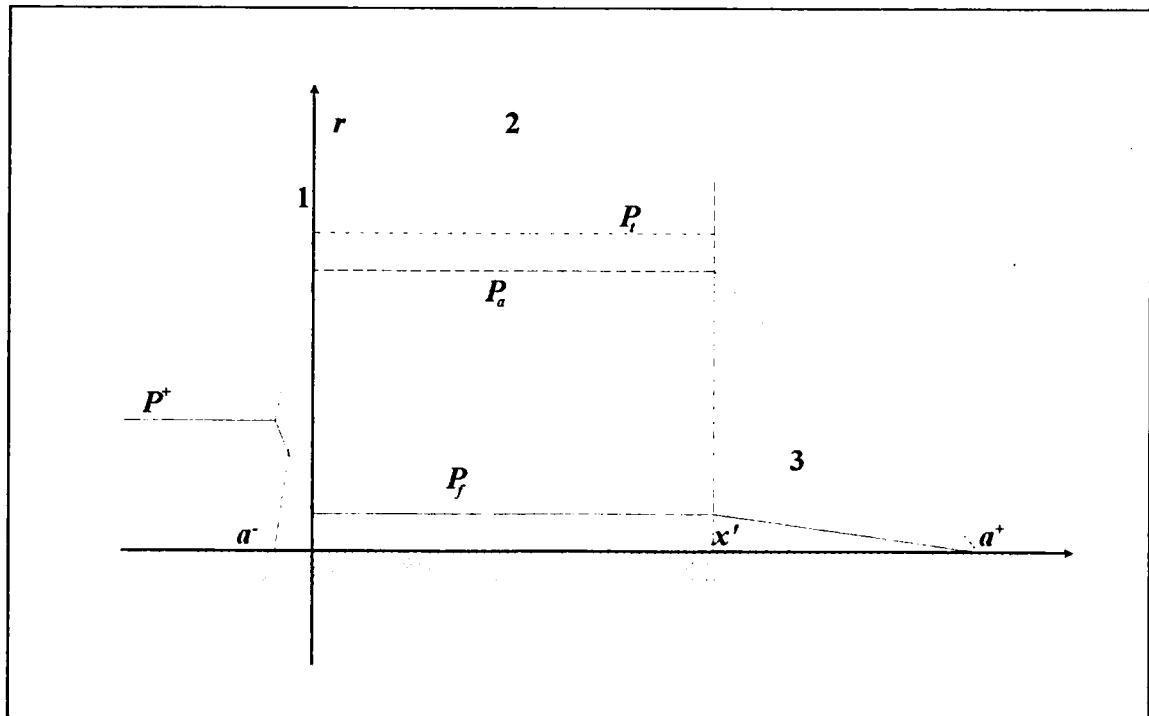


Figure 4.4 Pressure distribution in seal showing $P_f + P_a = P_t$

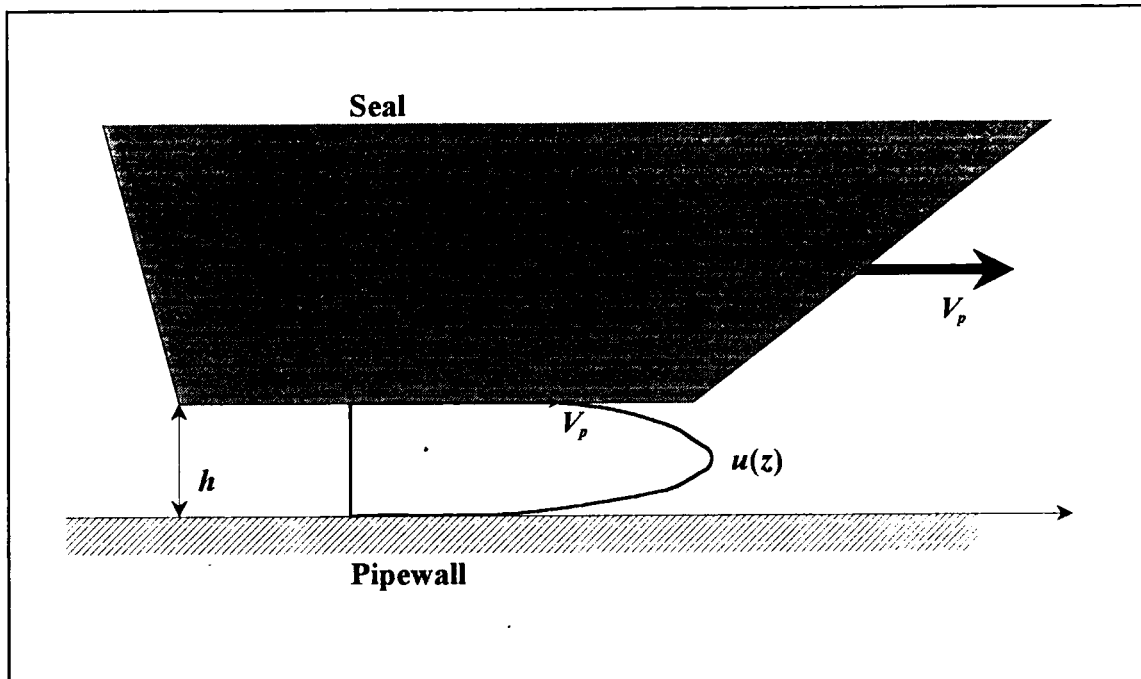


Figure 4.5 Velocity profile in the seal area

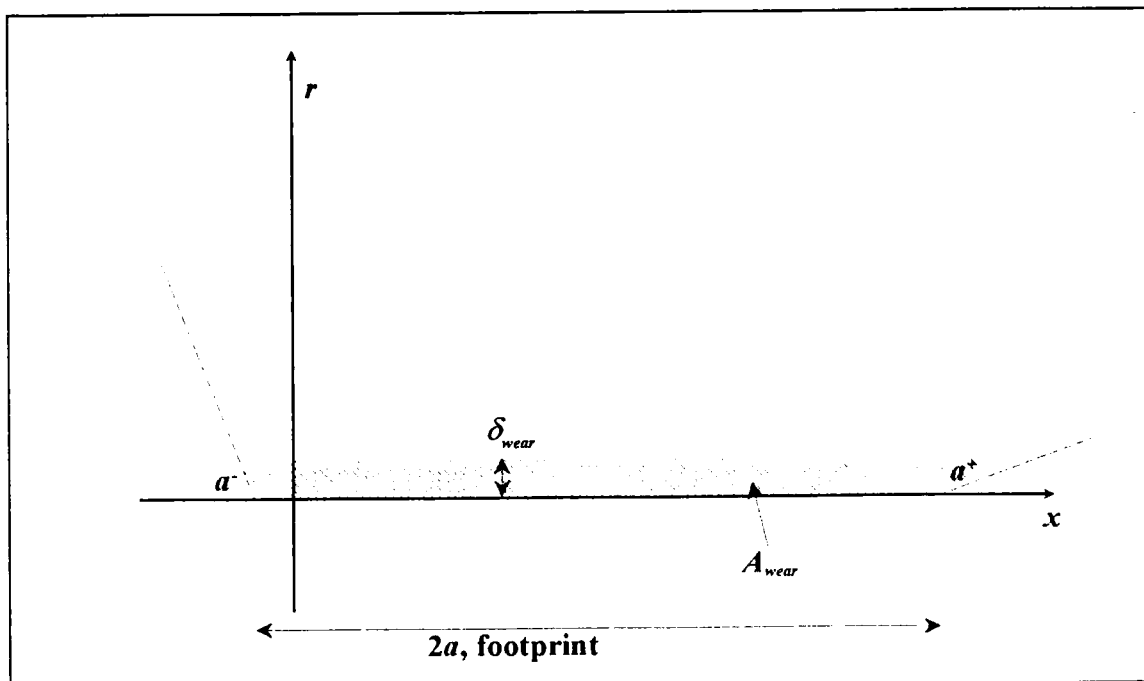


Figure 4.6 Area of wear on seal due to abrasion

CHAPTER 5

***PigPlus*, COMPUTER PROGRAM**

5. *PigPlus*, COMPUTER PROGRAM

The model described in chapter 4 has been coded in QuickBASIC, to allow ease of calculation of pig characteristics. The program allows the user to define the following details:-

- Pig configuration, geometry and physical properties
- Pipeline details
- Operational details
- Program details

The pig is modelled over the length of the pipeline, showing the variation in characteristics such as differential pressure, leakage and film thickness as the pig seals wear. This is performed at a constant velocity. However, it is possible to stop the pig at any node, or distance step and explore the variations of the pig characteristics with velocity at this stage.

Variables and arrays in this chapter in **BOLD** correspond to the variable name in the programme. Variables in *ITALICS* are as per the theory section in chapter 4. Subroutine names are in normal print.

The program is accessed as follows¹ :-

- (1) Enter QuickBASIC
- (2) Type ALT-File, Open
- (3) Double click the mouse cursor on PIGPLUS.BAS, or type this name in and press RETURN
- (4) When the program is shown on the screen, type ALT-Run, Start

1

The program must be on disc in the A drive.

This starts the *PigPlus* program running. Initially input is asked for. Then the user is asked to highlight the nodes to stop the pig running and look at the variations in pig characteristics with velocity.

The program has not been compiled since due to the research nature of the work behind it and in verification, it was felt that many changes would have to be made as it evolved.

5.1 *PIGPlus*, the core programme

Figure 5.1 shows the overall flow chart for *PIGPlus*. A print out of this programme is shown in Appendix F. The programme is set up to run as follows:-

- (1) Firstly, the subroutines used in the programme are declared. These subroutines are used to allow the programme structure to be understood more fully. The subroutines used are:-
 - **TITLE()**, sets up a title on the screen when the programme is first invoked
 - **WIND()**, sets up a graphics view port within which the progress of the programme can be viewed as it proceeds
 - **PUTIN()**, accepts input into the programme. These inputs are discussed below.
 - **SAMPLE()**, sets up the sampling node points at distances along the pipeline.
 - **FILER()**, sets up output files for use by the **MAINS** routine. This is the routine which calculates the variation in pig characteristics with velocity.
 - **RESETTER()**, this subroutine empties the output files, i.e. clears away data from previous programme runs.
 - **MAINS()**, calculates the variation in pig characteristics with velocity at any node along the pipeline
 - **WEARS()**, deals with the pig characteristic variation with distance along the

pipeline due to wear

- **INIT()**, sets up initial conditions for use by both the MAINS and WEARS routines.
- **FORCE()**, calculates wall force given material properties, geometry and friction and differential pressure across the seal.
- **CONTACT()**, determines the contact parameters in the seal
- **SCALC()**, calculates s , (S), the pressure fraction or the fraction of load supported by the fluid when the pig is in motion.
- **PROFILE()**, estimates the profile of the pig seal film due to the lubrication analysis.
- **PRESSURE()**, calculates seal friction and the differential pressure based on a force balance across the pig.
- **CONVGT()**, checks for convergence in the estimation of differential pressure and friction. This is necessary since wall force changes as both of these change, and so an iterative process is required.
- **LEAKAGE()**, for calculating forward and reverse leakage past the seal
- **STORE1()**, **STORE2()**, the first of these saves output data for the WEARS routine. The second saves output characteristics for the MAINS routine.
- **REMOVE()**, deals with the removal of material from the pig seal and calculates the subsequent increase in chamfer length

Once the subroutines have been declared, the programme displays the title and subsequently sets up a graphics view port using **TITLE()** and **WIND()**. These are not expanded upon here, only to say that the graphics view port allows the user to view how the programme is proceeding and to stop if there is any problems.

The next step is to define the arrays used in the programme, and to give them dimensions. The arrays used are:-

- **WEAR(20)**, distance steps along the pipeline in meters
- **NODE(20)**, this array stores the distance increment between one node and the next
- **VPIG(20)**, velocity steps for characteristics against velocity
- **MAIN(20)**, if $\text{MAIN}(I) = 1$ at a node, then the programme branches to the **MAINS()** subroutine and the pig characteristics against velocity are calculated at this node
- **FILES(20)**, stores files "A:\MAINXX.DAT", for storage of pig characteristics against velocity from the **MAINS** routine
- **QFOR(20)**, **QREV(20)**, **QTOT(20)**, temporary leakage information storage before it is stored into output files
- **XDASH#(20)**, temporary seal chamfer length storage prior to storage in output files
- **H#(60)**, film heights in seal
- **X#(60)**, local distance along the seal

Once the arrays are dimensioned, the program accepts user input using **PUTIN()**. Previous inputs are already stored so the user does not have to input all the data again. The data inputted by the user is:-

(1) **Pipeline:**

L, length of the pipeline, l_p

D, internal diameter of the pipeline, d

KS, roughness parameter, K_s

SIGS, standard deviation of pipeline roughness asperity heights, σ_s

(2) **Pig:**

EC, Compressive Youngs Modulus, E_c

ET, Tensile Youngs Modulus, E_t

FO, dynamic coefficient of friction, f_o

KWEAR, material wear coefficient, k_{wear}

MASS, mass of pig, M

N, number of seals, n

XDASHO#, initial chamfer length on the seal, x'_o

NU, Poissons ration, ν

PHI, pig spacer or hub diameter, ϕ

DD, pig seal diameter, D

T, pig seal thickness, t

CD, discharge coefficient for leakage, C_d

(3) **Operation:**

VP, pig velocity along the pipeline, V_p

ETA, fluid viscosity, η

(4) **Control:**

VPMAX, maximum velocity for characteristics against velocity

Each data set - pipeline, pig, operation and control - is treated in turn. For example, in the case of the pipeline data input:-

- The storage file is opened and the existing data retrieved
- This data is then presented in the graphics view port to the user
- The user selects which parameter to change and the new data is displayed
- To move along to the next data set, the user types 0
- The program then saves the new data and the same operation is performed for pig data input

The MAINS routine, for the calculation of pig characteristics against velocity at particular points in the pig travel, is called if the programme encounters that the array value for **MAIN(I)** is 1. The user can decide when to branch to the MAINS routine. This is done in the SAMPLE routine. This routine sets up distance steps

for the WEARS routine and velocity steps for the MAINS routine. In each, there are 20 steps.

Since there are 20 potential MAINS routine output sets, 20 files are required. The FILER subroutine sets up 20 different files for this data to be stored in. These files are called A:\MAINXX.DAT, where XX is between 01 and 20 depending on the node at which the MAINS routine is called. However, since the programme appends these files, i.e. it adds data to the end of the file rather than over-writes, it is necessary to clear the old data from any previous run. For this purpose the subroutine RESETTER is used.

Once this is complete the core of the programme is reached. The chamfer length of the seals are set to the initial value entered by the user, and the pig "starts moving" along the pipeline. As it travels, data recording the change in pig characteristics due to wear is stored in the file A:\WEARS.DAT. If the programme sees that $MAIN(I) = 1$ then it branches to the MAINS routine and calculates change in pig characteristics against velocity. When the end is reached, $I = 20$, then the PIGPlus programme terminates after all data is stored.

5.2 The MAINS and WEARS routines

Figure 5.2 shows the flow chart for the WEARS subroutine. A listing of this is given in Appendix F. This routine proceeds as follows:-

- The process is firstly initialised using INIT. This sets the initial differential pressure across the pig **DP1** to 1000 Pa. The initial pig seal friction is set to zero (N/m).
- An iterative loop is then setup where a steady pig differential pressure is the convergence criteria. When this is achieved the convergence factor **CONV1** will be greater than .99. **CONV1** is defined as the ratio of the new pig

differential pressure to old from the last iteration step. This will change due to the fact that wall force is dependent on differential pressure and friction. It is this interconnection that makes the need for a computer programme so necessary. The initial differential pressure across the seal **PPLUS** (P^+), is calculated by dropping the pig differential across the number of seals on the pig, **N** (n)

- The iteration proceeds by calculating the wall force **W** in **FORCE**.
- From this the contact parameters are estimated by **CONTACT**. These are:-

Negative contact extreme, **AN#** (a^-)

Positive contact extreme, **AP#** (a^+)

Seal footprint half length, **A#** (a)

Local deformation at the seal lip, **DELO#** (δ_o)

The hash sign, #, in QuickBASIC is used to define variables which are double precision. The very small parameters involved in the analysis of the seal contact and in the lubrication analysis are all treated as double precision.

- The pressure factor, **S**, or s in the theory is then calculated. This determines the fraction of the load carried by the fluid in the seal.
- Using the pressure factor and the seal contact parameters the film profile along the seal is estimated. This is stored in the array **H#()** along with the x-coordinate **X#()**.
- Knowledge of the film profile is then used to determine a new value of friction, **FRICT**. This is then used to calculate the new estimate of pig differential pressure, **DP**. Using this **CONV1** is calculated by either **DP/DP1** or **DP1/DP**, which ever is less than one. If this is greater than .99 as stated before then convergence has been reached. Otherwise the process is repeated using the new values of friction and differential pressure.
- Once convergence has been attained, leakage can be assessed using

LEAKAGE. This calculates total, forward and reverse leakage.

- At this stage all the pig characteristics at this point in the pipeline are known. Therefore A:\WEARS.DAT is opened to add in the data. The data stored is distance travelled, differential pressure, leakage rates, chamfer length and seal entry slope.
- Finally, in preparation for the next loop, the abrasion process takes place and material is removed from the pig seal. This causes the chamfer length to get longer.

The MAINS routine is similar to the WEARS routine except that instead of distance increments there are velocity increments. The same convergence criteria is used, except with CONV2. Storage of the files is also slightly different with only differential pressure and leakage rates saved to the appropriate file for this node. Obviously material is not removed from the seal as the pig motion is considered against velocity and not distance.

Due to the similarity between the MAINS and WEARS routines, a flow chart is not given but a full listing is found in appendix F.

5.3 Examples of input and output

The following data was entered into the programme by way for demonstration:-

1. Pipeline data:

L, Pipeline length = 20,000 (m)

D, Pipeline diameter = .254 (m)

KS, Roughness parameter = .07 (-)

SIGS#, Standard deviation of asperity heights = 6e-6 (m)

2. Pig data:

EC, Compressive Youngs Modulus = $8e6$ (Pa)

ET, Tensile Youngs Modulus = $5e6$ (Pa)

FO, Dynamic coefficient of friction = 1.1 (-)

KWEAR, Wear coefficient = $1e-13$ (msKg⁻¹)

MASS, Mass of pig = 15 (Kg)

N, Number of seals = 4 (-)

XDASHO#, Initial chamfer length = .001 (m)

NU, Poissons ratio = .45 (-)

PHI, Pig hub diameters = .17 (m)

DD, Sealing disc diameter = .269 (m)

T, Sealing disc thickness = .015 (m)

CD, Coefficient of discharge = 1 (-)

3. Operational data:

VP, Pig velocity = 1 (m/s)

ETA, Fluid viscosity = .001 (Pa.s)

4. Control data:

VPMAX, Maximum pig velocity = 10 (m/s)

The data shown represents a pig run through a 10" nominal bore pipeline for 20km. The velocity of this pig is a constant 1 m/s. The pig geometry and material properties are described as in chapter 4.

At nodes 0, 14, 18 and 20 the pig was "stopped" and the variation in pig characteristics against velocity was investigated. This corresponds to distances of approximately 0km or new pig, 2km, 10km and finally 20km. Figures 5.3 to 5.5 show output data from this analysis.

Figure 5.3 shows pig differential pressure against velocity at the four nodes selected. The characteristic drop in differential pressure against velocity is noted. As the pig wears the pressure required to drive the pig reduces. This is also shown in figure 5.4, differential pressure against distance. This is in agreement with expectation.

Figure 5.5 shows the increase in seal chamfer length as the pig wears in. The initial rapid run-in period is shown with the subsequent less rapid increase. The programme will now be checked against experimental data taken from CALtecs (Oil and Gas division of BHR Group Limited) 10" pipelooop. The various outputs from both the MAINS and WEARS routines shall be verified against this experimental data.

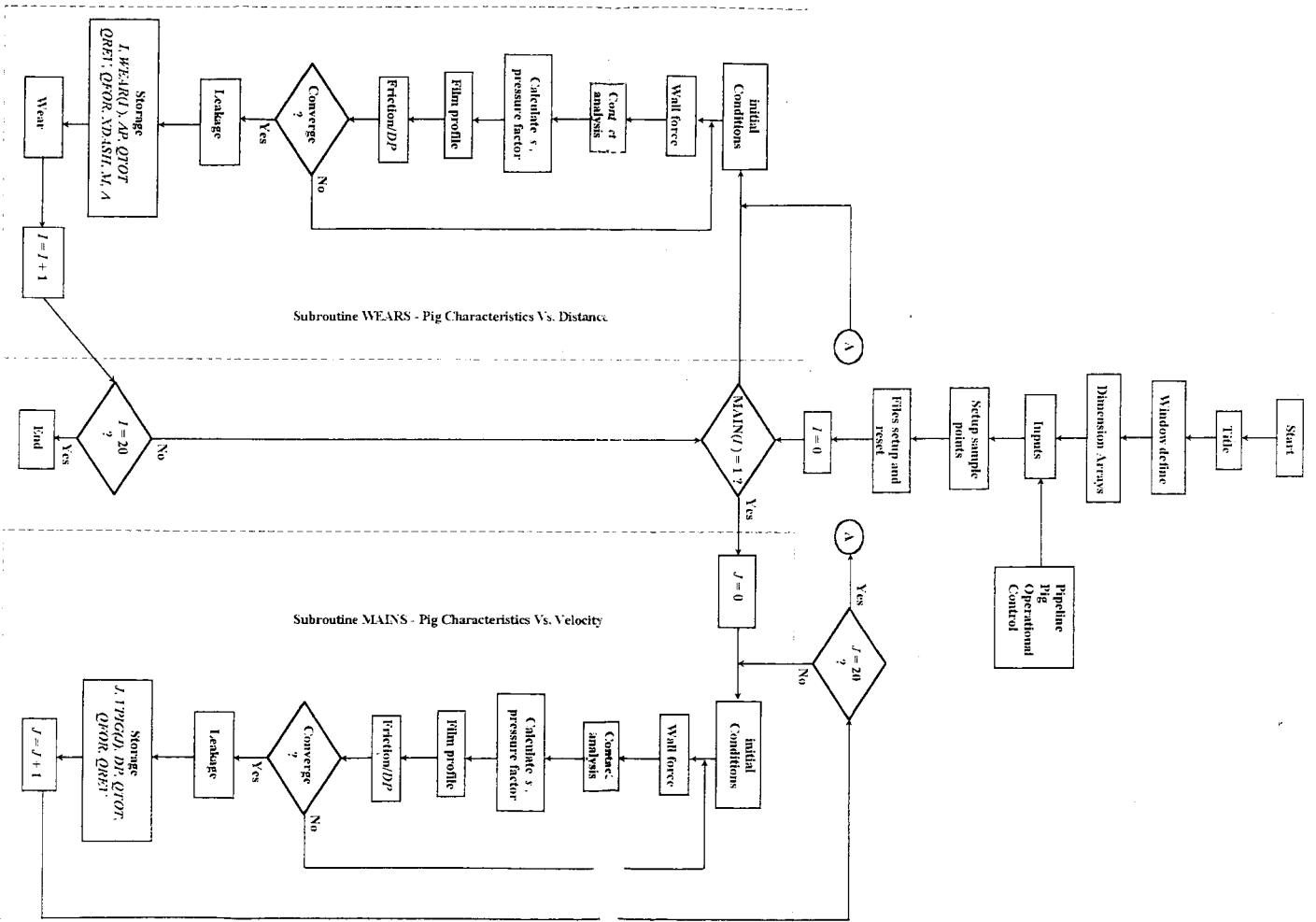


Figure 5.1 Flowchart for PIQPPlus

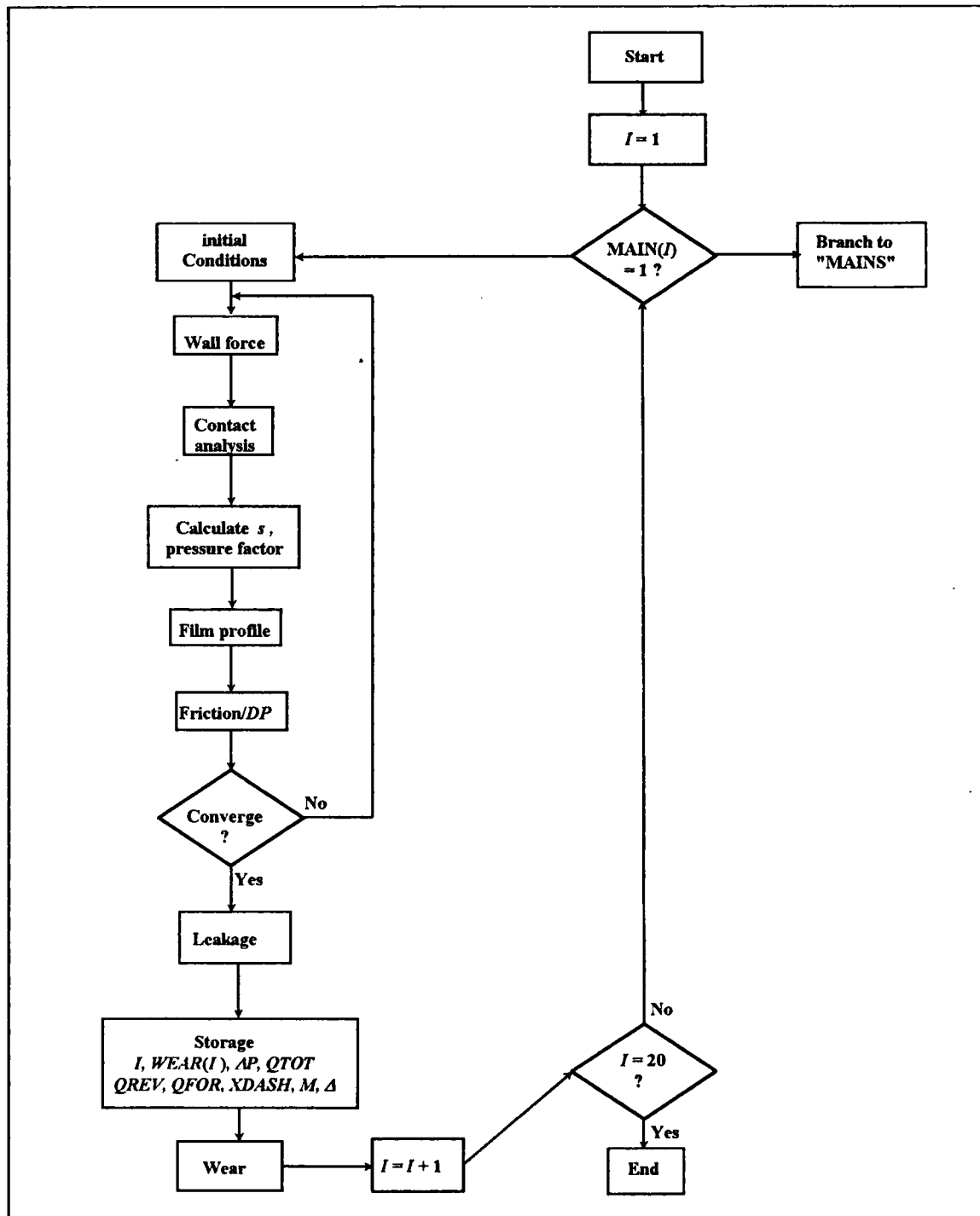


Figure 5.2 Flowchart for WEARS routine

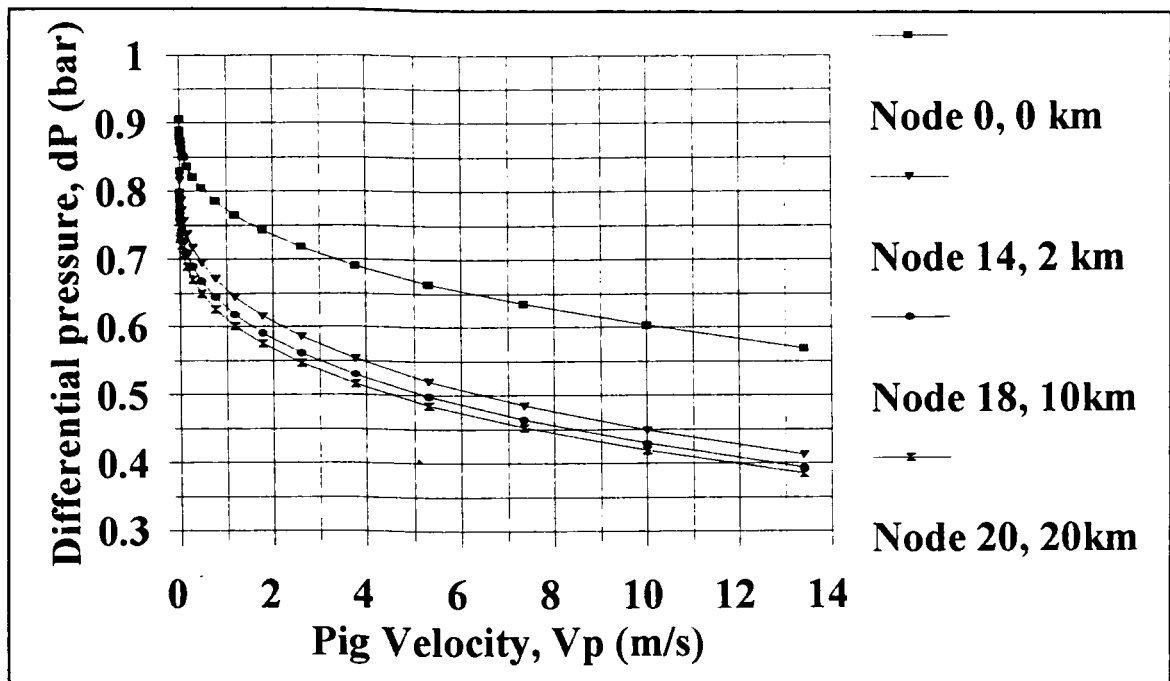


Figure 5.3 Sample output from the MAINS routine

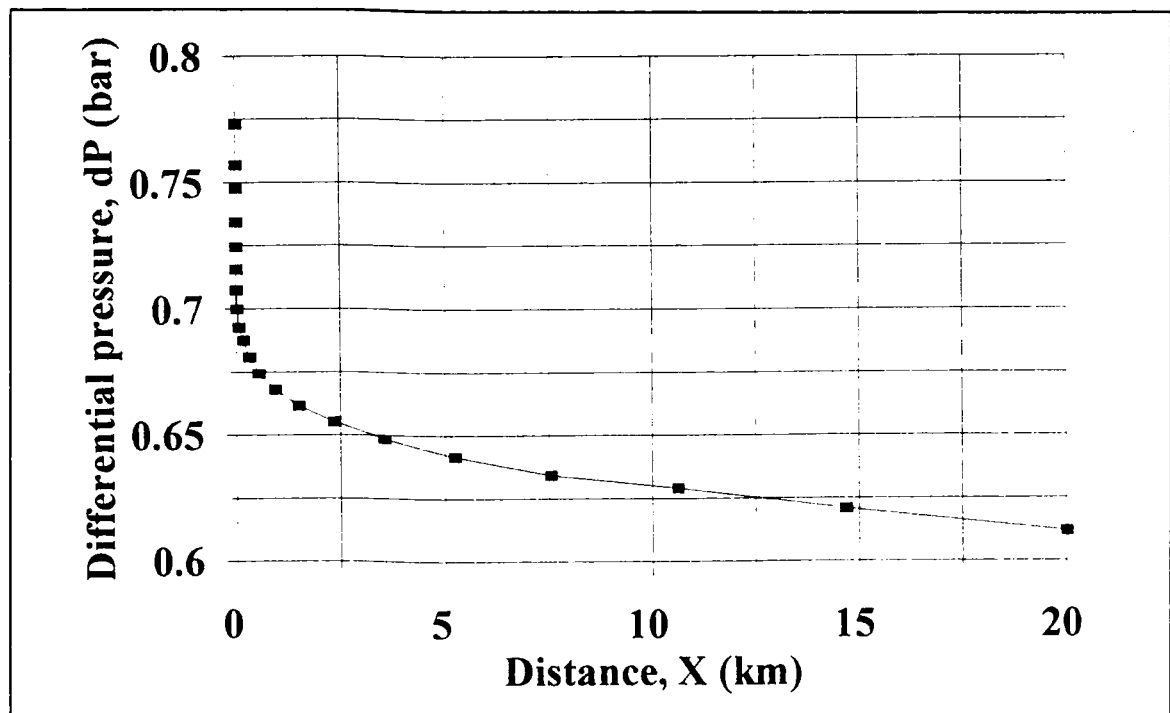


Figure 5.4 Sample output from the WEARS routine, ΔP Vs. X

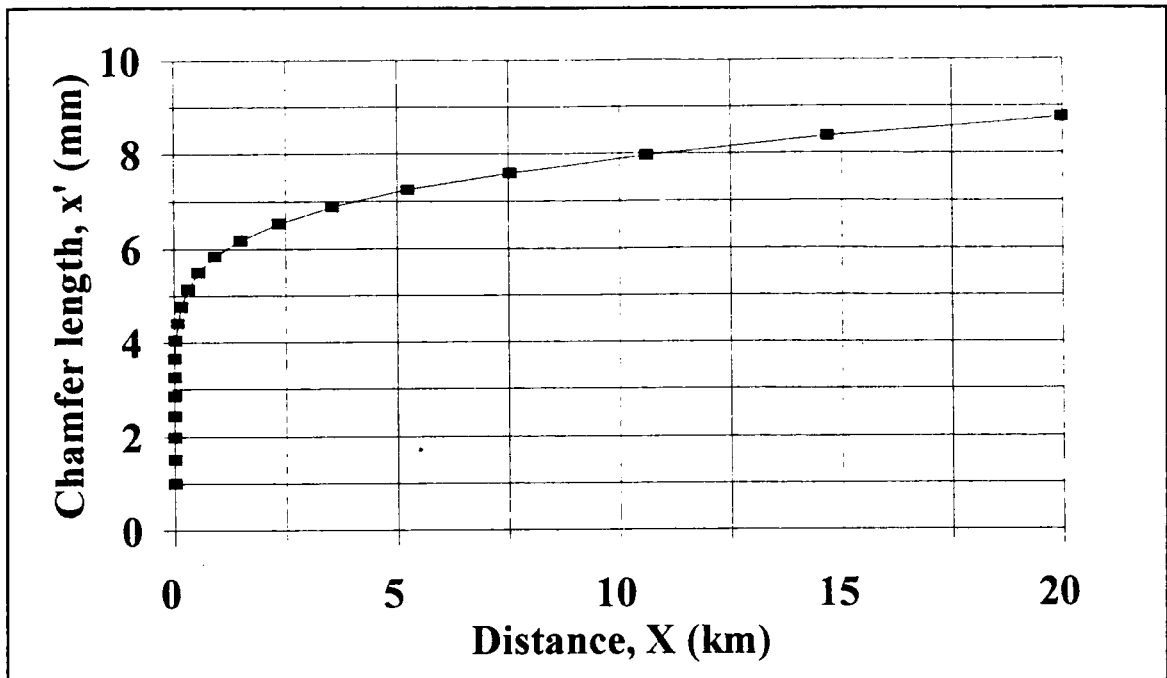


Figure 5.5 Sample output from the WEARS routine, x' Vs. X

CHAPTER 6

VERIFICATION OF THE MODEL

6. VERIFICATION OF THE MODEL

The aim of this chapter is to demonstrate that the model can be used to calculate the main pig characteristics against both velocity and distance travelled. The test facility is introduced and its operation is explained. In addition the main measurement techniques are explained. The data used has been taken from CALTEC's Pigging Technology Project. This project consisted of three main investigations:-

- Wear trials, from which the variations in differential pressure, chamfer length and seal entry slope with distance travelled can be compared with the model predictions
- Cleaning trials, from which the variation in differential pressure against velocity can be compared
- Swabbing trails¹, from which reverse leakage readings have been taken against distance and velocity

The inputs into the programme have been taken from available polyurethane in the public domain as far as possible. It is felt that this approach is more useful as it allows the user to find data on his/her own particular urethane sample.

Unfortunately, there is no data available for forward leakage due to the expense of setting the facility up to allow this measurement to be taken. Differences between pig velocity from pig signallers and flow measurement were too unreliable to be of use.

The bypass pig used by Wu et al (1995), as described in the literature review, has also been investigated and the increase in velocity due to wear of the seals has been

1

Removal of liquids from gas pipelines using conventional pipeline pigs. This is a compressible drive project, but the volume of liquid remaining is as a result of reverse leakage.

modelled. A simplified spreadsheet program of *PIGPlus* was used for this study in order to include the gas dynamics through the pig. Although gas is the driving medium for this pig, it is assumed that the pig is travelling at a quasi-steady speed, i.e. there is no sudden accelerations or decelerations. The resulting increase in velocity, over about 15km, is demonstrated for a constant gas flow.

6.1 The Test Facility

A general schematic of the test facility is shown in figure 6.1. This shows two possible configurations:-

- A once through facility where the pig is basically launched and then received after the test section (approximately 130m long). This was used for the cleaning and swabbing trials.
- The continuous loop, which allows the pig to be pushed around a never ending loop for as long as the user requires. One loop is approximately 260m long. This was used for the wear trials.

The photographs in figures 6.2 to 6.4 show photographs of the facility. The overall specification is as follows:-

- Nominal bore of pipeline, 10" (Schedule 40 Carbon steel)
- Actual bore, 254mm (Seamless tubing)
- Raised face, weld neck flanges (Internal welds are ground down to flat)
- Maximum water flowrate, 3m/s in 10" pipe
- Maximum air flowrate, 10m/s in 10" pipe (using sonic nozzle blowdown technique, see operation of once-through facility with air drive)
- Instrumentation:-
 - Magnetic water flow meter
 - Turbine air flow meter

-
- Optical pig signallers (for pig velocity measurement, spaced every 3m approximately)
 - Mechanical pig signallers (for pig velocity measurement, spaced every 6m approximately)
 - Pressure transducers for absolute pressure measurement and for measurement of pig differential pressure². Six such transducers are spaced along the loop with a range of 0 to 12barg.
 - Temperature transducers for measurement of both ambient and fluid temperature.

The operation of the facility can be broken down into three sections:-

- Once-through, water drive
- Once-through, air drive
- Continuous loop, water drive only

Once-through facility, water drive

Figure 6.5 shows a schematic of the facility for once-through use with water drive.

The facility is operated as follows:-

- The pig is inserted in the launcher and pushed into the reducer
- All air is vented from the line by slowly running water into the facility with vent valves open. Occasionally, it was required to run the pig with air in front of the pig and therefore the launcher bypass line was closed, thus venting the launcher only.
- The data acquisition system is set to trigger on the first pig signaller. All

2

A single pressure transducer can be used for differential pressure measurement since the pig passed the transducer, thus yielding a reading both upstream and downstream of the pig.

pressure transducers are zeroed to avoid errors due to drift.

- A flowrate is setup through the launcher kicker valve and bypass line.
- By quickly shutting the bypass valve, the pig is launched into the pipe and the test performed.

Restart tests in the 10" line were performed by running the pig only as far as the stopping section. This enabled the pig restart differential pressure to be measured.

This configuration was used for the cleaning trials where the following data was obtained:-

- Differential pressure against velocity
- Pig internal pressure levels, i.e. the pressure between the sealing discs

Once-through, air drive

Air drive tests usually involved filling the dip section with water in order to assess the liquid sweep-out or swabbing efficiency. Figure 6.6 shows a schematic of this configuration. The facility was operated as follows:-

- The pig is inserted into the launcher as before.
- Under low system pressure and input flowrate the pig is pushed to just before the beginning of the dip.
- The dip is filled using the service water line.
- With the isolation valve open and the sonic nozzle valve shut the entire pipe system is charged to 12 barg pressure.
- To launch the pig the isolation valve is shut and the sonic nozzle valve is opened. The average pig velocity is dependant on the size of this nozzle.

The nozzles were sized using critical flow equations. The principle behind this is

that the volumetric flowrate in the pipeline is independent of the system pressure so long as a pressure ratio in excess of 2:1 is maintained across the nozzles (Massey, B (1979)). The accumulator has been sized to ensure that this is always the case.

- Several methods of determining the volume of liquid remaining in the pipeline were investigated. The most effective methods was using two soft foam pigs or swabs to both push the remaining liquid from the system and soak it up. The majority of the liquid was removed in this way with only a very small proportion remaining on the pipewall. A crawler, complete with video and umbilical was used to relay back pictures of the "almost dry" pipeline after the foam swabs were run.

The velocity of the pig was not entirely steady due to compressible effects, change in upstream and downstream accumulator volumes, and the natural stick-slip tendency of pig motion in compressible drive systems. However, large velocity excursions were avoided³.

This configuration was used for the swabbing project, from which the following data is available:-

- Reverse leakage rate estimate against velocity and distance
- Differential pressure against velocity

3

A velocity excursion can be defined as a large initial acceleration and subsequent deceleration of the pig in a compressible medium. In low pressure media, these can be very large and highly dangerous. By increasing the system pressure to 12 barg and introducing a sonic nozzle, the effective excursion length was limited and a quasi-steady state motion was achieved.

Continuous loop with water drive

Figure 6.7 shows the continuous loop for use with water drive. This configuration is operated as follows:-

- The pig is inserted in the hatch-box. A special bolting technique is employed to ensure that the discs of a bidirectional pig are pushed backwards so that it is ready to launch without flip over.
- Air is vented from the loop by opening all vent valves and both inlets. The outlets to the break tank are closed.
- The pig is launched by opening valves CV4, 6 and 2. The others remain closed.
- On passing CMPS1 (Control Mechanical Pig Signaller, No. 1), the system changes over such that valves CV1, 3 and 5 are open and the rest closed. This pushes the pig down the main loop section.
- CMPS2 changes the valving system back again, thus allowing the pig to travel around the loop continuously.

This configuration was used for the wear project, from which the following data is gathered:-

- Differential pressure against distance
- Change in chamfer length and entry slope with distance (from the geometry of the worn disc)

6.2 Description of the test pig

The test pig was supplied by International Pipeline Products. It is known as a high seal pig. This pig is shown in figure 6.8. The sealing discs are 269mm in diameter, with a thickness of 15mm. This constitutes a nominal oversize of about 6% on diameter. The pig is approximately 21kg in mass. Three disc hardnesses are

available - Shore A 60, 65 and 70. The guide discs are 253mm in diameter when new, 25mm thick and available only in Shore A 85 hardness.

A small chamfer of about 1.14mm has been pre-moulded onto the edge of the disc. It is assumed that this chamfer lies flat on the pipe wall. This is not unreasonable since it is such a small chamfer length.

6.3 Inputs into the *PIGPlus* model for verification against experiment

It is appreciated that detailed information on some of the parameters required in the *PIGPlus* model are not readily available to the Oil & Gas industry. For this reason, rather than measure all the required inputs, available data from handbooks has been used where possible. If this is not possible, then guidance is given using the finding from the previous chapters, especially chapter 3, comparison and selection of models. However, a word of warning is required since as improved polyurethanes are made available, the properties found in industry will not be applicable. However, a similar test should be performed on the material, or the pipeline or whatever aspect of the problem has been improved.

A summary of the data input is now given. Where applicable, a more detailed explanation of the source of the input or how it was measured is given later.

l	distance travelled, 15,000m for most Wear trial tests. However a number were run to 100,000m or 100km.
d	pipeline diameter, 0.254m internal diameter based on 10" nominal bore schedule 40 carbon steel pipe
K_s	roughness parameter, 0.0115 (see below)
σ_s	standard deviation of surface roughness, 6.7 μ m (see below)
E_c	Shore A 60 5.9 MPa Shore A 65 6.9 MPa

	Shore A 70	7.7 MPa	(see below)
E_t	Shore A 60	3.1 MPa	
	Shore A 65	3.6 MPa	
	Shore A 70	4.1 MPa	(see below)
f_o	Dynamic coefficient of friction,	Shore A 60, 0.90	
		Shore A 65, 0.86	
		Shore A 70, 0.91 (see below)	
M	Mass of pig, 21.1kg		
K_{wear}	Wear coefficient, 3.9×10^{-12}		
N	Number of seals, 4		
x'_o	Initial seal chamfer, 1.414mm		
ϕ	Pig body diameter, 172mm		
D	Seal diameter, 269mm		
t	Seal thickness, 15mm		

A note of explanation is required for some of these parameters to explain where the information came from.

Roughness parameters, K_s and σ_s

Figure 6.9 shows a typical output from surface topography measurements taken on the test facility. The magnification is times 400 in the z-direction and times 40 in the x-direction. The average peak-to-peak reading from this output and from another 3 measurements is approximately $33.5\mu\text{m}$. The standard deviation is taken to be roughly one fifth of this peak-to-peak value, i.e $6.7\mu\text{m}$. This corresponds well with the surface R_a value of $6\mu\text{m}$.

As stated before, the surface parameter K_s , is defines as

$$K_s = R_s^{1/2} \eta_s \sigma_s^{3/2} \quad \dots 6.1$$

The number of asperity summit heights per unit area was estimated by counting the number of summits in the surface profile outputs (a two dimensional output), squaring this and normalising to be per m². This value is then multiplied by 1.8, a correction suggested by Johnson (1987). The average radius of curvature was estimated by considering a sample of summits to be roughly a parabola and working back to the radius. This was done for a large sample and an average taken. The final value of K_s was estimated as 0.0115. This is very small and the risk of sub-zero static film heights is quite significant. This is since the loads can be initially so high that the roughness alone cannot support it. The arbitrary selection of the surface roughness datum level is important here as discussed in chapter 3. In addition the negative exponential distribution will not be accurate if negative film heights are encountered. Fortunately, due to wear, this scenario does not last for very long, eg about a quarter of a kilometre.

Youngs Modulus, compressive and tensile

The compressive and tensile elastic moduli are estimated by using a Neo-Hookean model. 100% extension data is used in this model to estimate the stress levels at +30% extension (tensile) and -30% (compressive). The Neo-Hookean model is:-

$$\sigma = 2 C_o \left((1 + \epsilon) - \frac{1}{(1 + \epsilon)^2} \right) \quad \dots 6.1$$

The coefficient C_o is calculated from stress data corresponding to +1.0 strain levels.

This has been found from uniaxial stress-strain handbook data (Inpipe, (1995)):-

Stain level	+1.0	
Stress levels:-	Shore 60	2.3MPa
	Shore 65	2.7MPa
	Shore 70	3.0MPa

The following coefficients were estimated from this data:-

Coefficients C_o	Shore 60	0.66
	Shore 65	0.77
	Shore 70	0.86

Now, these coefficients can be used to calculate the stress levels for strain levels of +30% and -30%. Once these are known, the elastic modulus is calculated using the simple formula:-

$$E = \frac{\sigma}{\epsilon} \quad \dots 6.2$$

The compressive nature of polyurethane is misleading in one way. It could be argued that a sample of polyurethane gets a degree of its compressive strength from its tensile properties. This can be seen in figure 6.10. Therefore, a compressive test on a sample may over-estimate the compressive modulus.

The large difference between the compressive and tensile moduli is evident from figure 6.11. This shows a stress/strain curve for Shore A 85 urethane. The slope of the compressive side is much greater and will become non-linear quicker.

The dynamic coefficient of friction, f_o

The dynamic coefficient of friction was measured using a simple setup as shown in figure 6.12. This shows a urethane block on an inclined pipe. The time taken to travel the distance s , can be used to calculate f_o , the dynamic coefficient of friction according to:-

$$f_o = \text{Tan}\theta - \frac{2 s}{g t^2 \text{Cos}\theta} \quad \dots 6.3$$

After a number of trials, a value of f_o for each Shore hardness was estimated. It is interesting to note that these figures are for a worn sample. The values for new samples is approximately 10% higher in each case.

6.4 Validation of PIGPlus using the Wear trials

The following matrix of tests was conducted during the wear trials:-

Test No.	Pig Type	Distance (km)	Fluid Vel (m/s)	Shore A
1	Bidirectional	15	0.7	60
2	Bidirectional	15	0.7	70
3	Bidirectional	15	1.4	60
4	Bidirectional	15	1.4	65
5	Bidirectional	15	1.4	70
6	Bidirectional	15	2.1	60
7	Bidirectional	15	2.1	70
8	Bidirectional	100	1.4	65

Table 6.1 Wear trials

The data available from these tests is mainly:-

- Differential Pressure
- Chamfer length on seal
- Seal entry slope (from the geometry of the worn seal)

All of these are graphed against distance. Figures 6.13 to 6.20 show the results of these tests compared with PIGPlus using appropriate input data. Figure 6.21 shows the bidirectional pig tested in the loop trials.

6.5 Verification using the Swabbing trials

The following series of trials have been compared with *PIGPlus* from the swabbing trials:-

Test No.	Pig Type	Distance	Vel. Range	Shore A
9	Bidirectional	0	0 to 10m/s	65
10	Bidirectional	15	0 to 10m/s	65

Table 6.2 Swabbing trials

The data available from these tests are:-

- (i) Differential pressure
- (ii) Reverse leakage

Both of these parameters are graphed against increasing velocity. However, since a new bidi and a worn-in bidi are used, then a comparison against distance is also available.

Due to the rapid increase in chamfer length when the pig is new, measured leakage rates for the new bidi are measured using the WEARS module over 80m distance in each case. The chamfer length at the end is used as the initial chamfer for the next run. However, for the 15km case, it is assumed that the chamfer length has reached a steady state, and therefore the MAINS module is used for comparison.

Figures 6.22 to 6.23 show the comparison of this data using output from the programme, *PIGPlus*.

6.6 Verification using the cleaning trials

The following trials have been compared with *PIGPlus* using data from the cleaning trials:-

Test No.	Pig Types	Distance (km)	Vel. Range	Shore A
11	Bidi	15	0-2m/s	65

Table 6.3 Cleaning trials

The following data is available:-

- Differential pressure against velocity
- Internal pressure levels

Figure 6.24 shows differential pressure against velocity from both the trials and *PIGPlus*. Figure 6.25 shows internal pressure levels taken using a high data acquisition rate as the pig passes a pressure transducer. Unfortunately, since the pig sealing discs are so close together, it is impossible to determine pressure levels between two adjacent seal pairs. Figure 6.26 shows the measurable internal pressure levels against increasing velocity. It is clear that uniform pressure drop across each seal is not strictly a valid assumption. In addition, there is clearly a pressure drop across the guidediscs.

6.7 Further validation

Another source of verification is the application of *PIGPlus* to a particular problem described by Wu et al (1995). This concerns the passage of a high bypass pig along a 20" pipeline multiphase pipeline. If a typical pig is used, all the liquid is pushed from the pipeline at once. This could potentially flood the slug-catcher at the processing facilities. To avoid overloading the slug-catcher separator, a bypass pig

was used. This is a pig which allows a certain amount of the flow to pass through the pig via holes in the body. This has the effect of aerating the slug of liquid in front and slowing down the pig. Hence, liquid arrives at the slug-catcher at a much reduced rate and the separator can handle the smaller liquid flow.

Bypass flow through the body is driven by the differential pressure across the pig. Due to wear on the seals, the differential pressure reduces because interference reduces as material is removed from the seals. Hence, the bypass flow reduces and the pig velocity increases, tending towards that of the gas velocity. Figure 6.27 shows the measured velocity increase against the authors' predicted velocity and the gas velocity. As explained before, the pig is assumed to travel in a steady state manner and since there was a liquid slug in front of the pig, it is assumed that it is lubricated fully. Using a simplified version of *PIGPlus*, coded into a spreadsheet, this increase in velocity due to wear and lubrication effects has been modelled. The result of using this, as seen in figure 6.28, compares well with the actual measured values. Note that a constant gas velocity has been used in this analysis. It would be possible to vary the gas velocity, but for clarity it was kept constant.

The main simplifications used in this spreadsheet analysis are:-

- (i) Wall force is considered to be affected by oversize, Δ only according to the relationship $w = K\Delta^3$, where K is a "spring constant". K is determined by relating this expression to the assumed restart differential pressure, ΔP_o and the static coefficient of friction.
- (ii) Pig seal entry slope is constant throughout the analysis
- (iii) There is no differential pressure across the seal. This is a gross assumption, but simplicity was required in order to perform the analysis on a spreadsheet.

The gas flow dynamics was determined using a discharge coefficient for the bypass

flow system. The start-up differential pressure was calculated by the intersection of two curves:-

- (i) Differential pressure against gas flowrate (Pig stopped)
- (ii) Pig differential pressure against velocity (No bypass)

The intersection of these two curves resulted in the start-up velocity. Calculation of a negative start-up velocity indicated that the bypass ports were open too far, and motion could not be initiated. The study concluded that maximising the bypass is the only way to avoid pig velocity increasing excessively. However, this is risky, as the pig can get stuck easily, in reality at bends and weld-beads for example.

It is clear that the model works satisfactorily in most areas with the possible exception of leakage which has been difficult to verify. The following chapter discusses both the experimental and theoretical results and the apparent limitations of the model. The final chapter recommends possible future work required to improve upon this model.

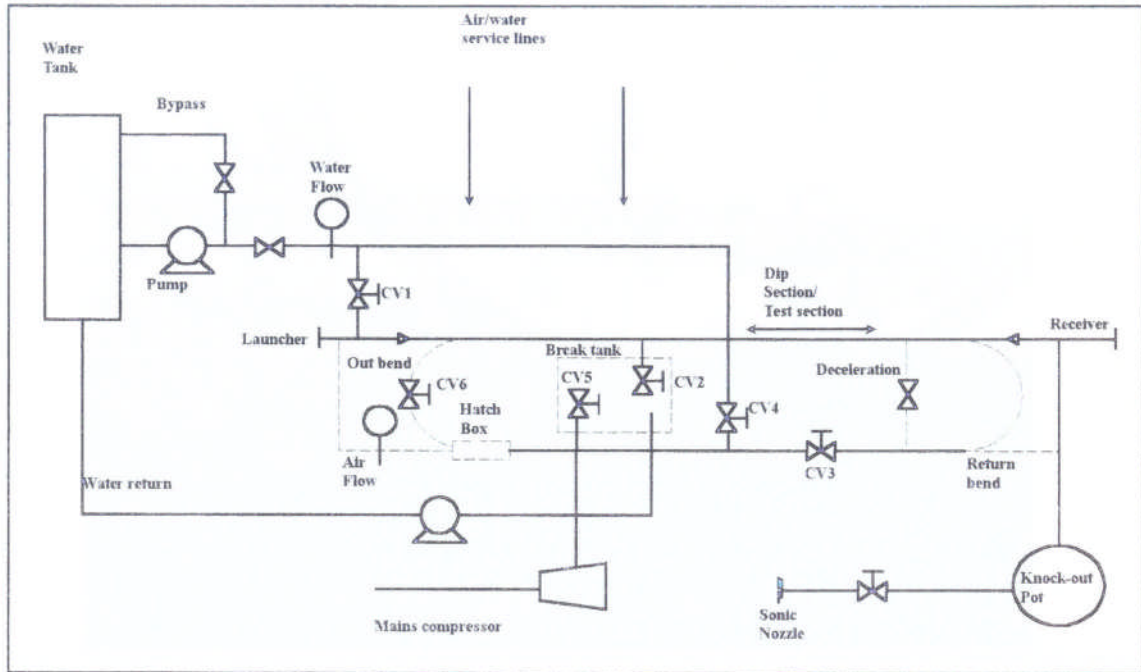


Figure 6.1 General schematic of the facility

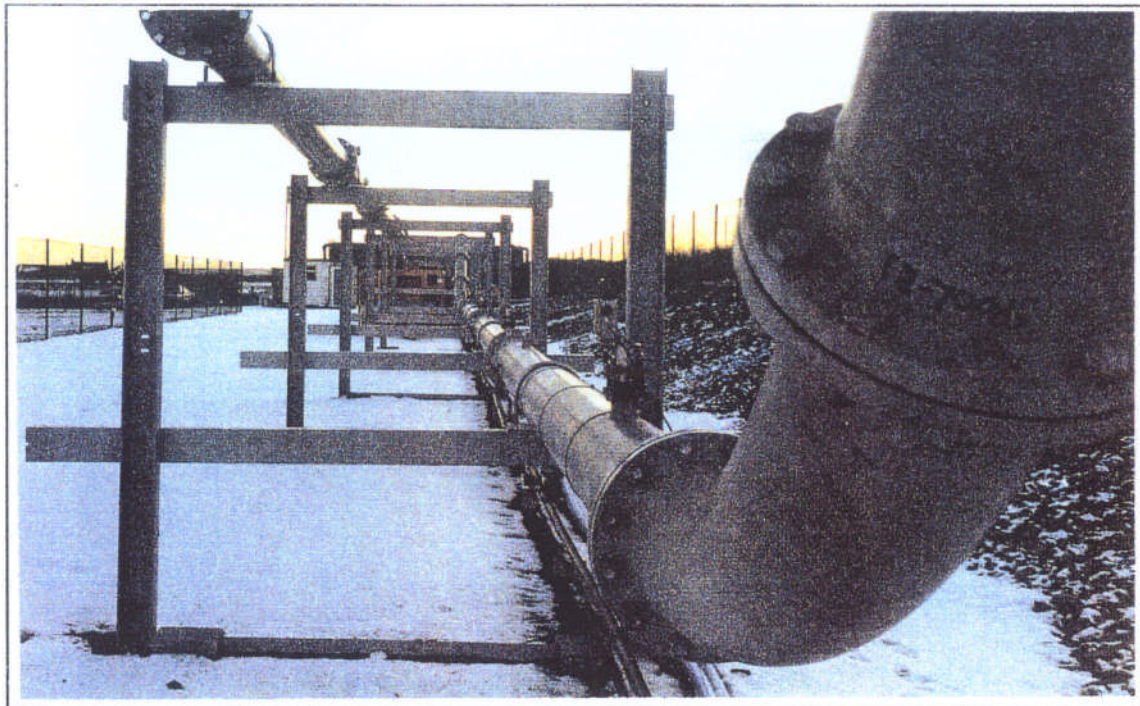


Figure 6.2 The dip section



Figure 6.3 The launcher



Figure 6.4 Overview of the entire facility

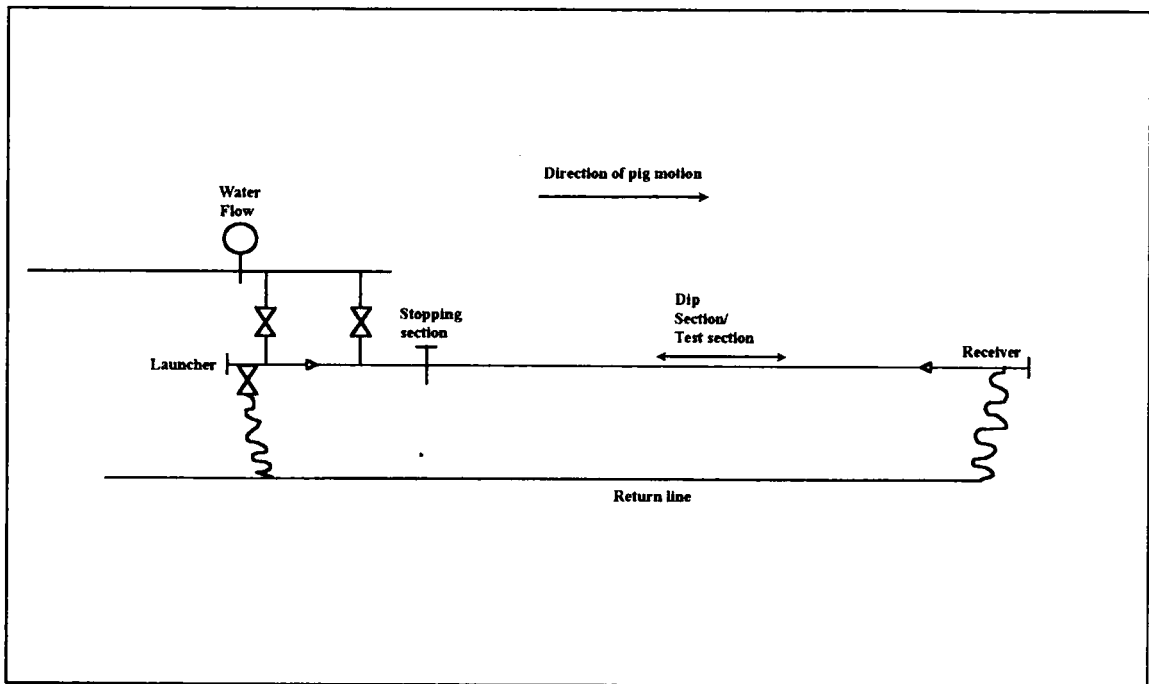


Figure 6.5 Schematic of once through facility - water drive

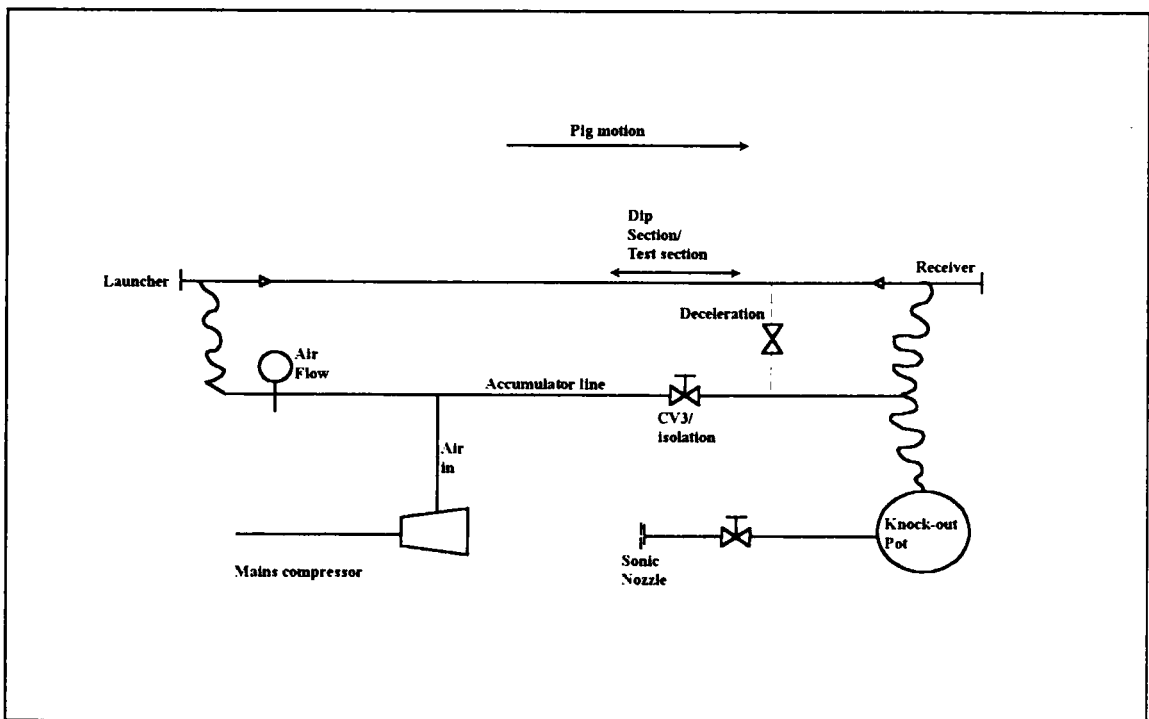


Figure 6.6 Schematic of once through facility - air drive

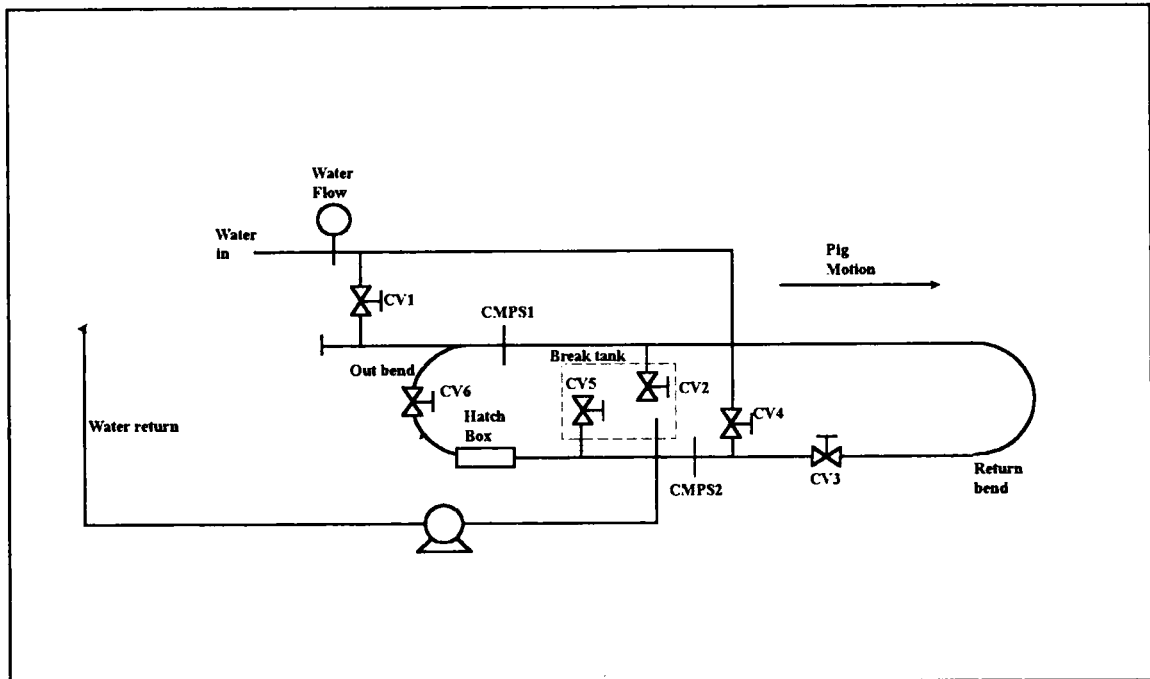


Figure 6.7 Schematic of continuous loop facility

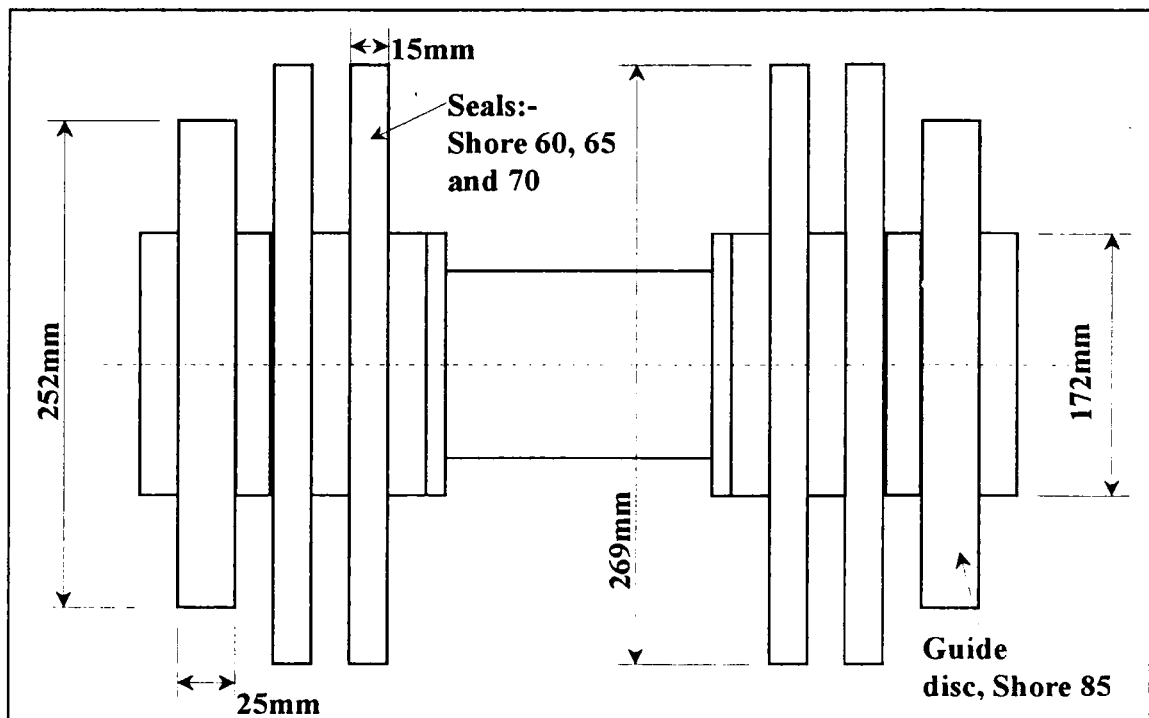


Figure 6.8 Description of bidirectional pig

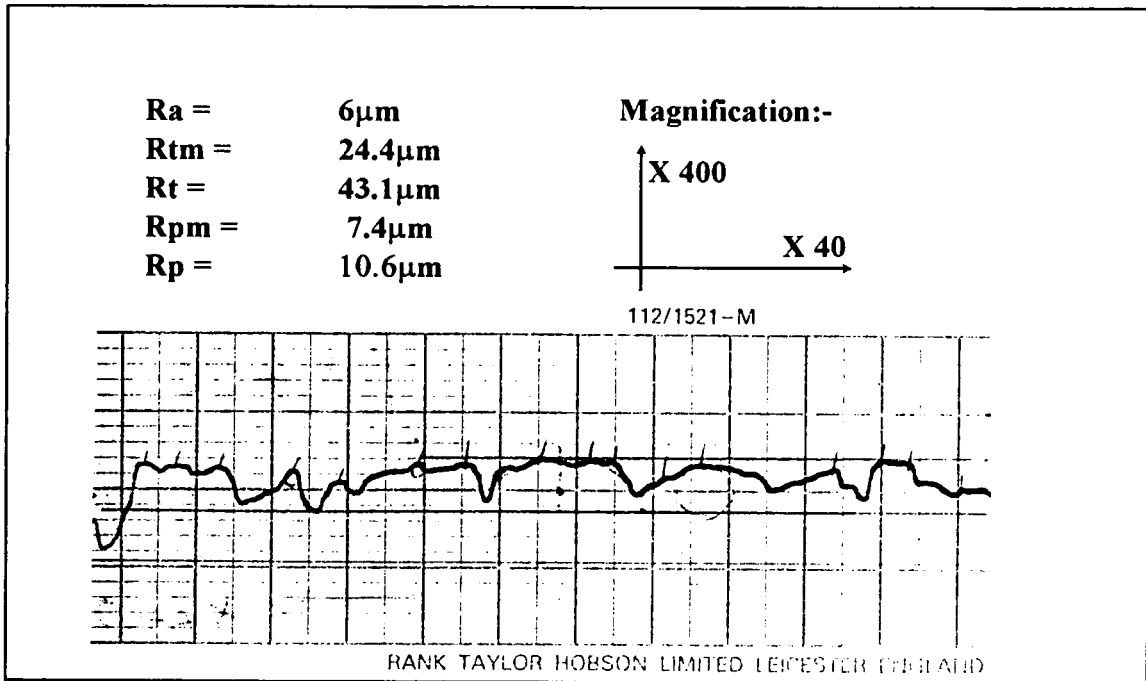


Figure 6.9 Surface topography measurements

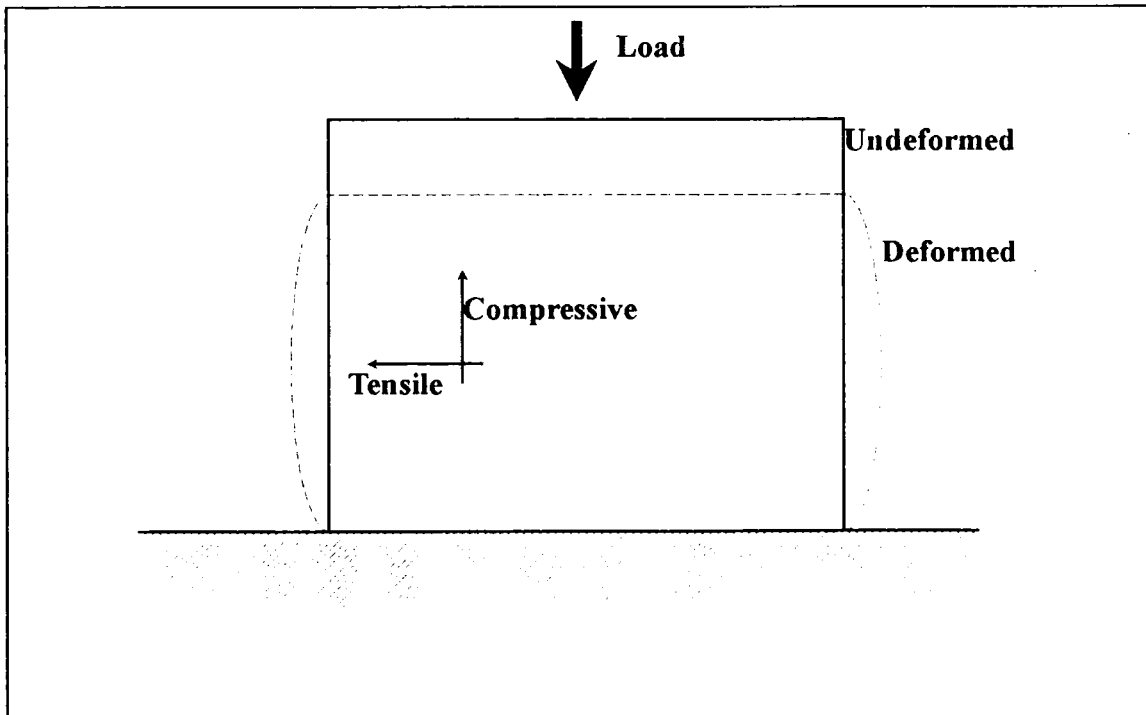


Figure 6.10 Compression with tensile component

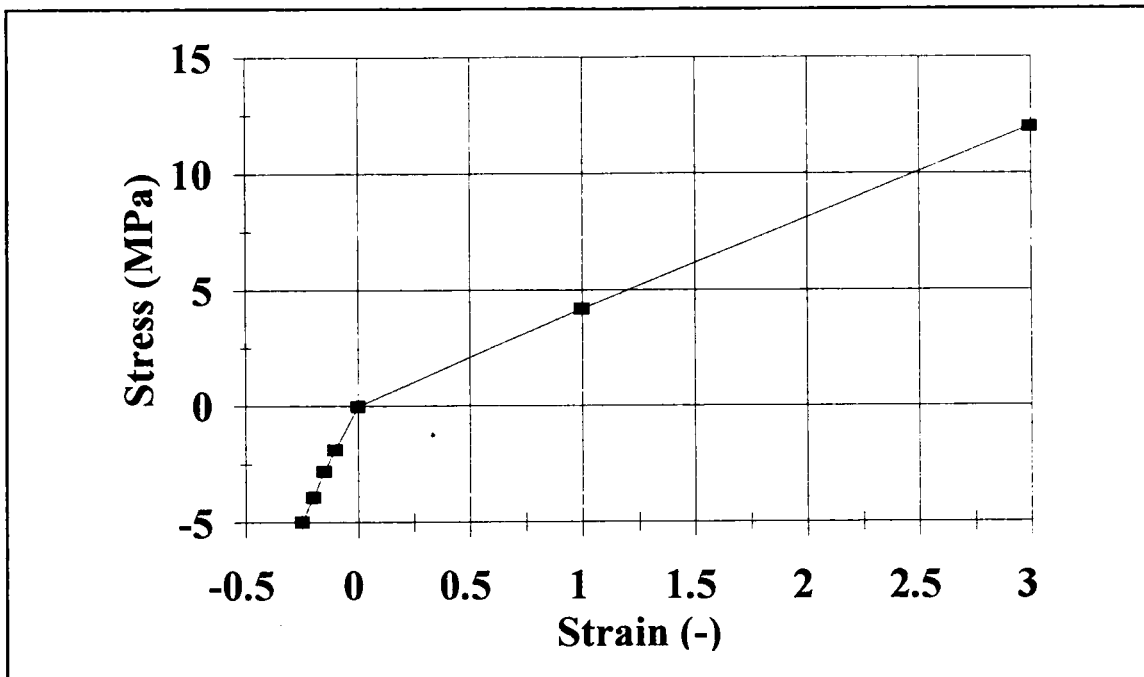


Figure 6.11 Shore 85, extension and compression results

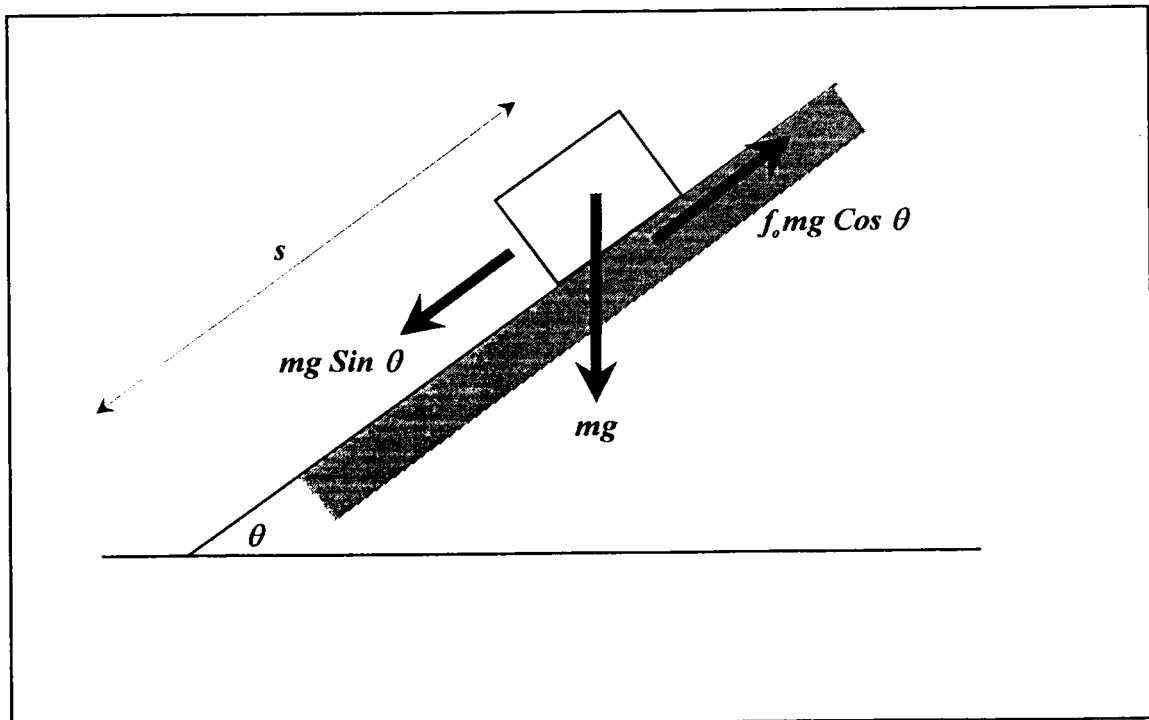


Figure 6.12 Measurement of f_o , coefficient of friction

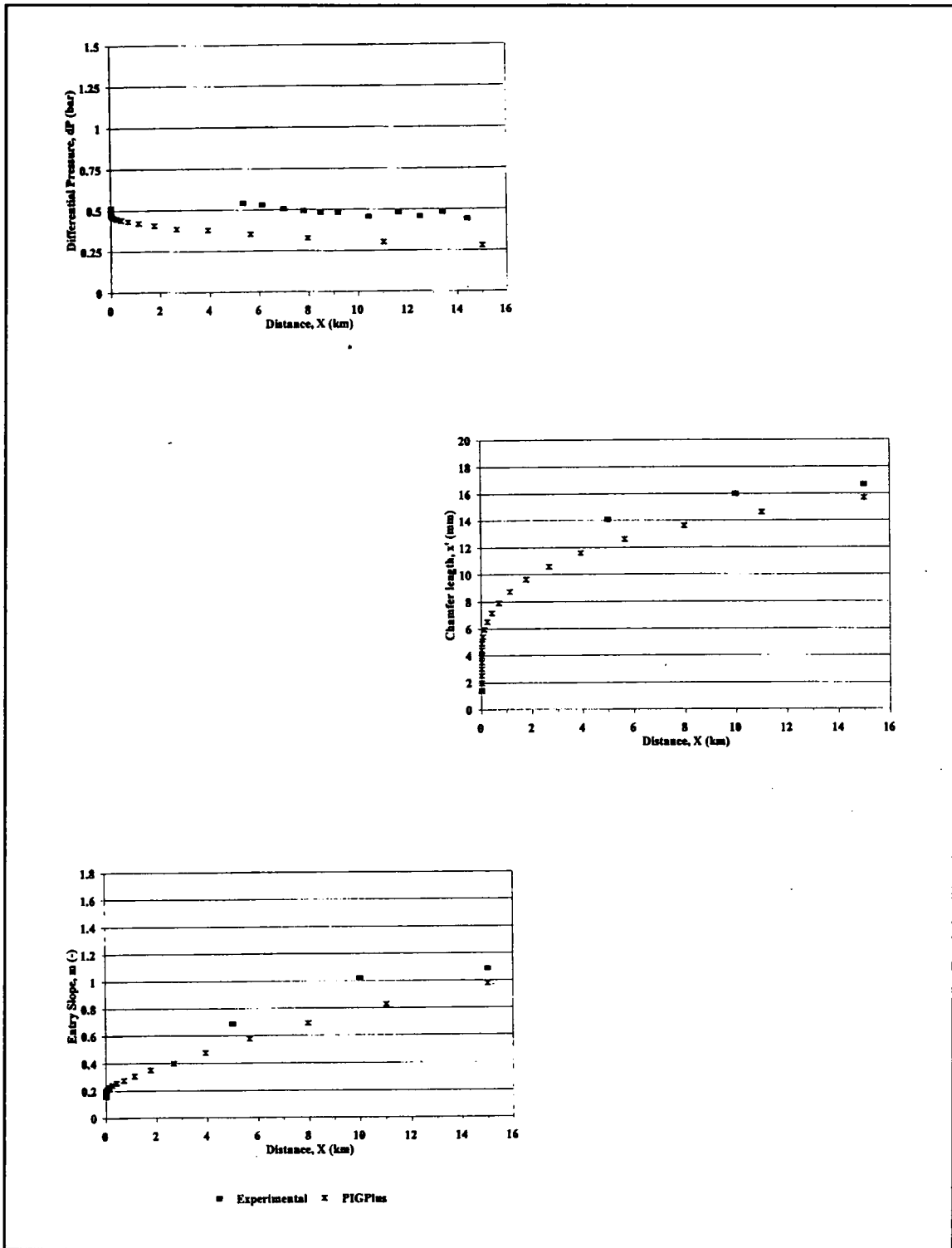


Figure 6.13 Wear test 1, 15km, Shore 60, 0.7m/s

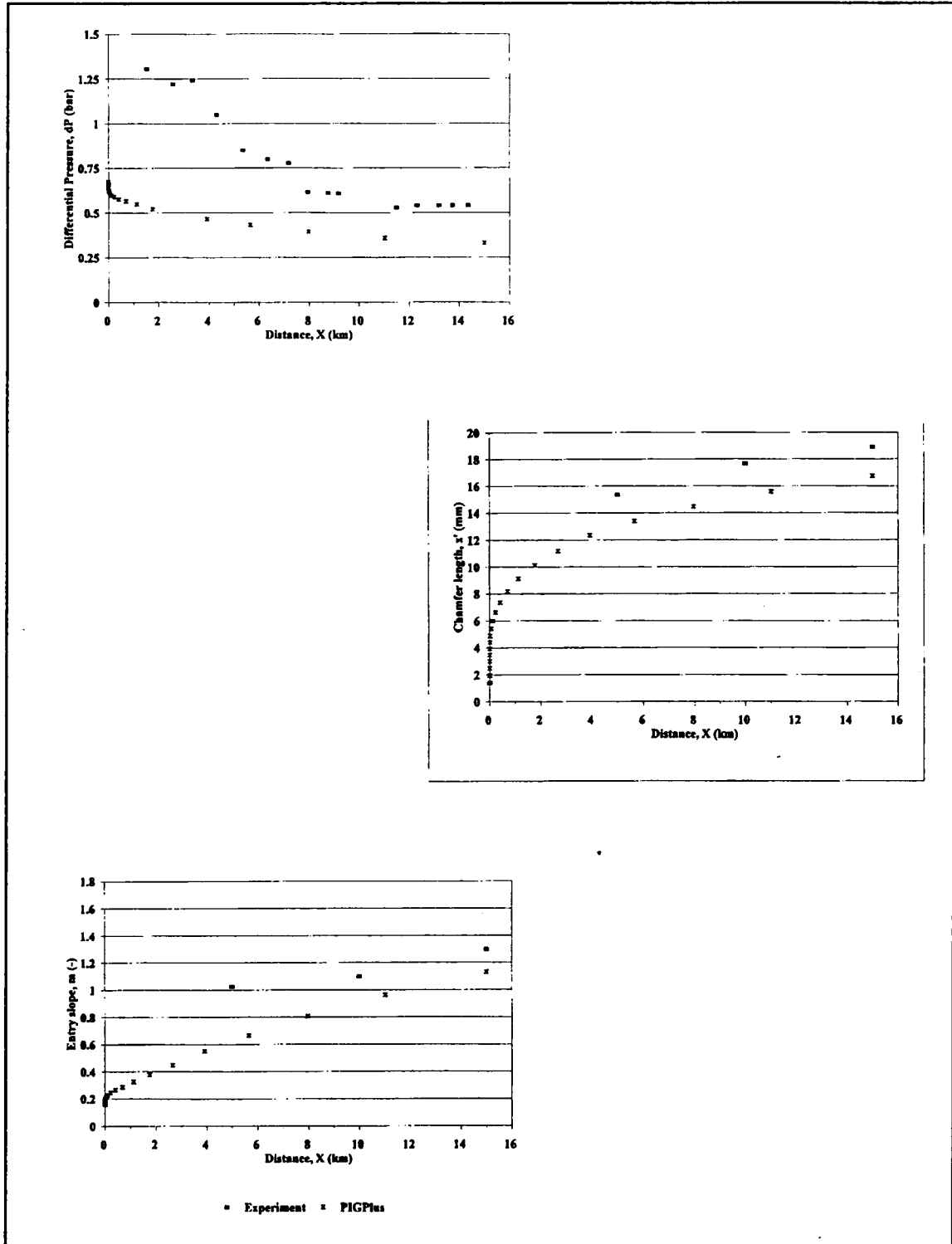


Figure 6.14 Wear test 2, 15km, Shore 70, 0.7m/s

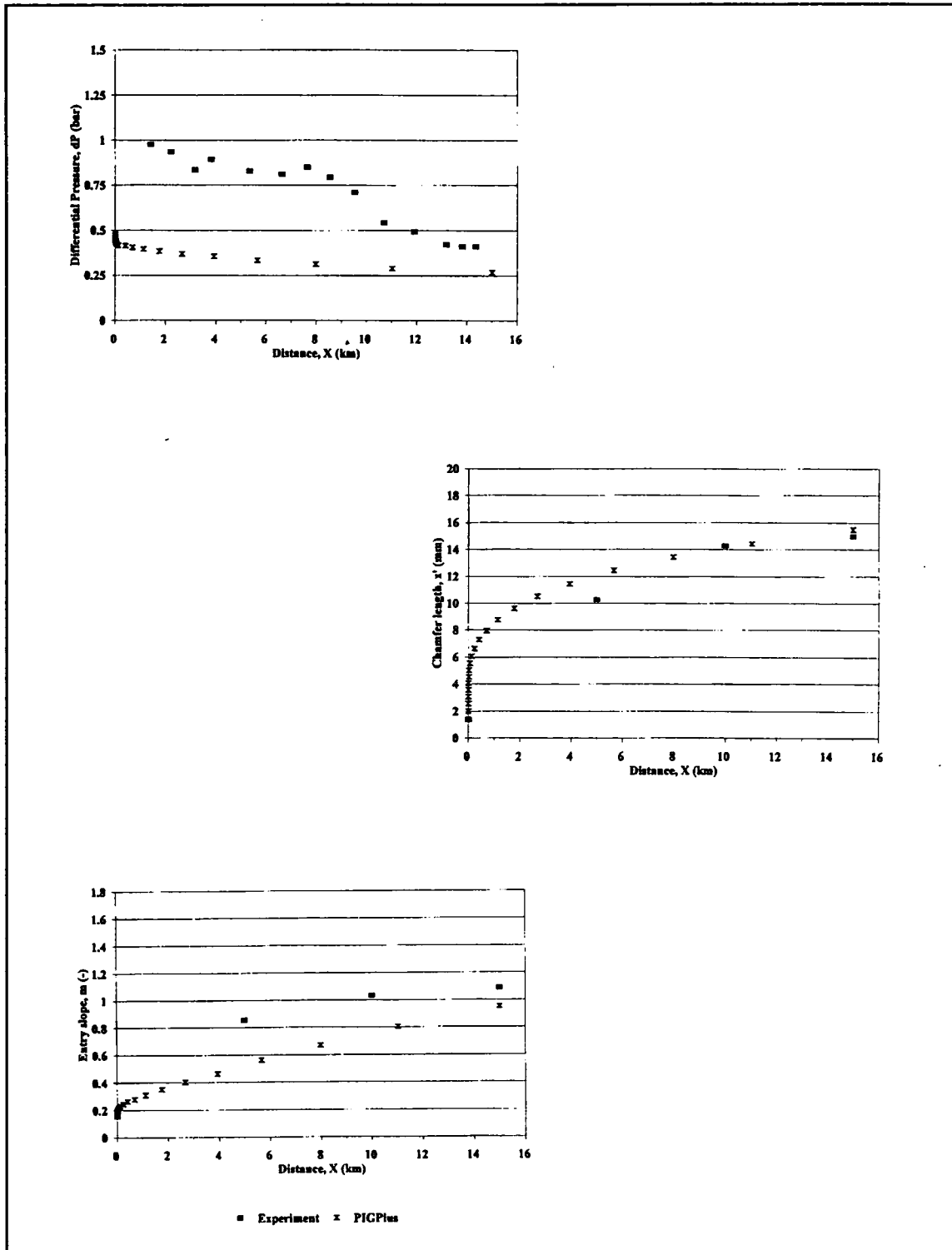


Figure 6.15 Wear test 3, 15km, Shore 60, 1.4m/s

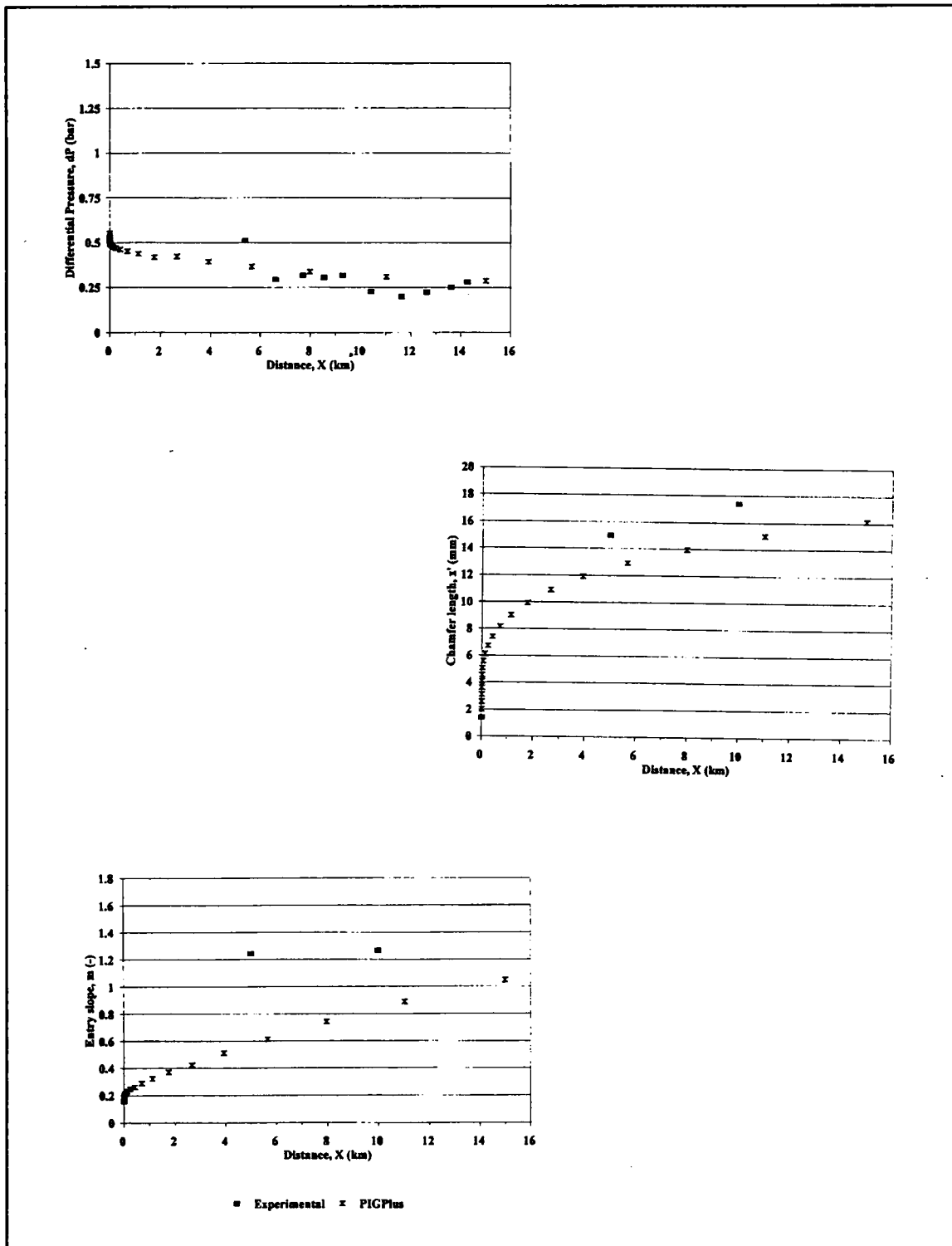


Figure 6.16 Wear test 4, 15km, Shore 65, 1.4m/s

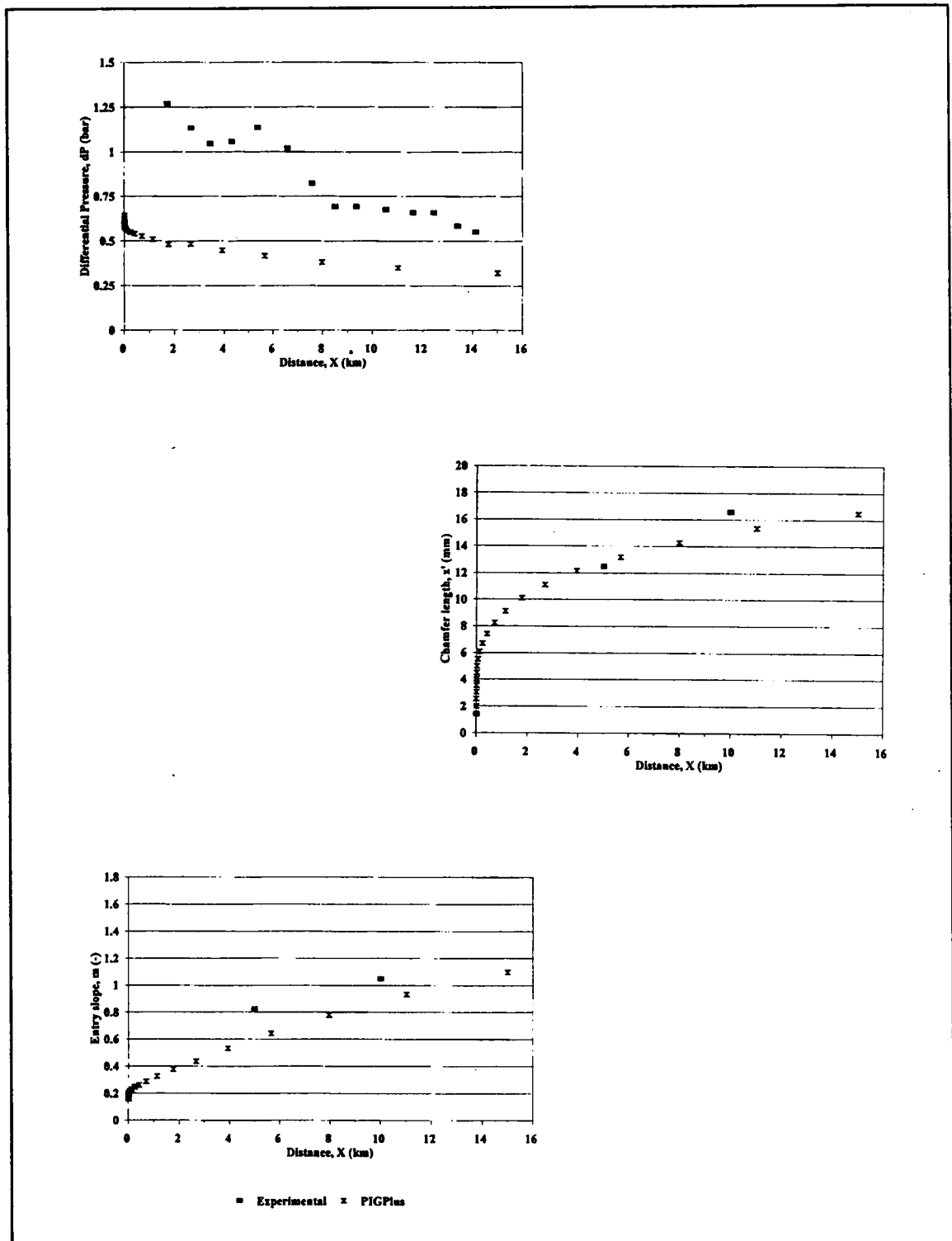


Figure 6.17 Wear test 5, 15km, Shore 70, 1.4m/s

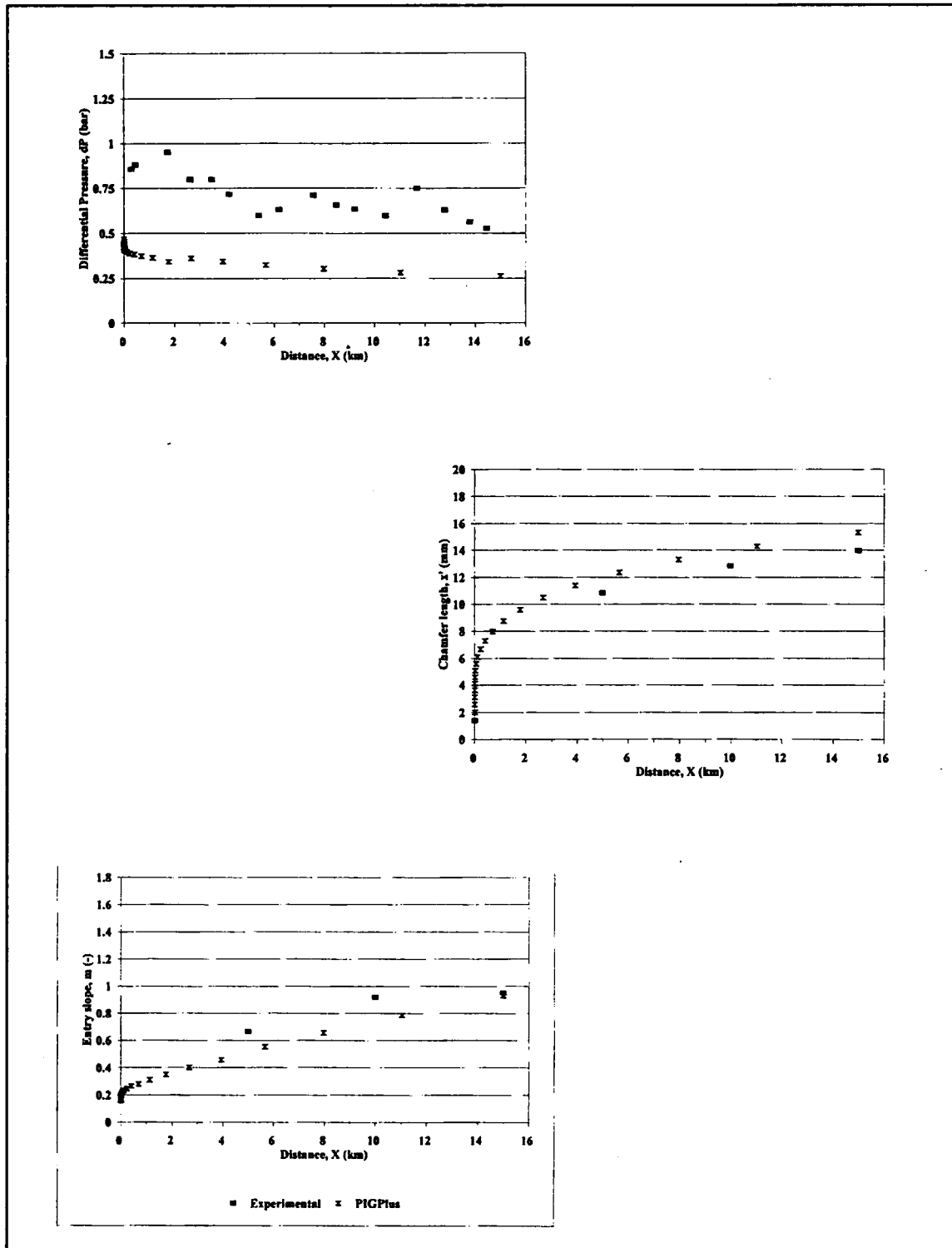


Figure 6.18 Wear test 6, 15km, Shore 60, 2.1m/s

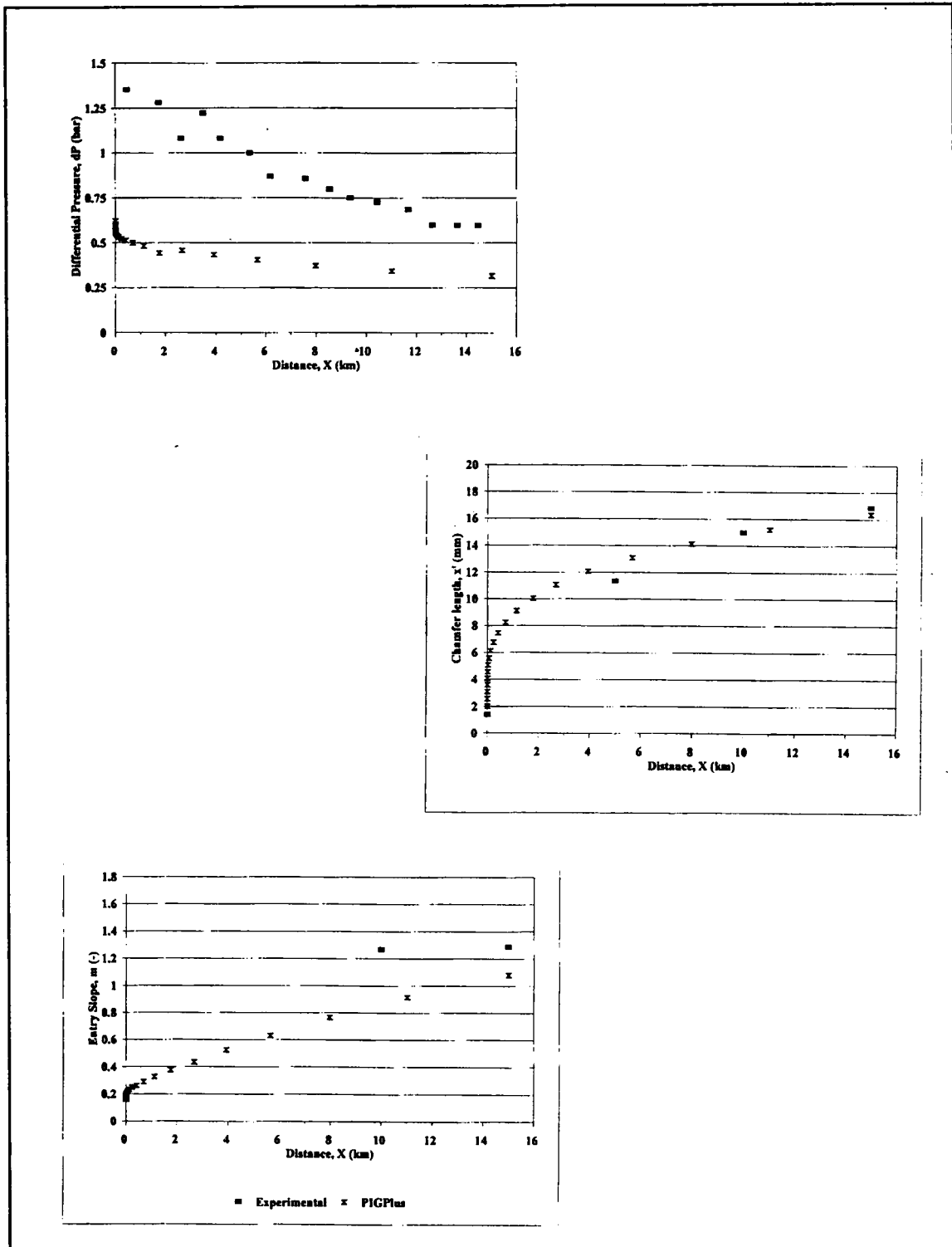


Figure 6.19 Wear test 7, 15km, Shore 70, 2.1m/s

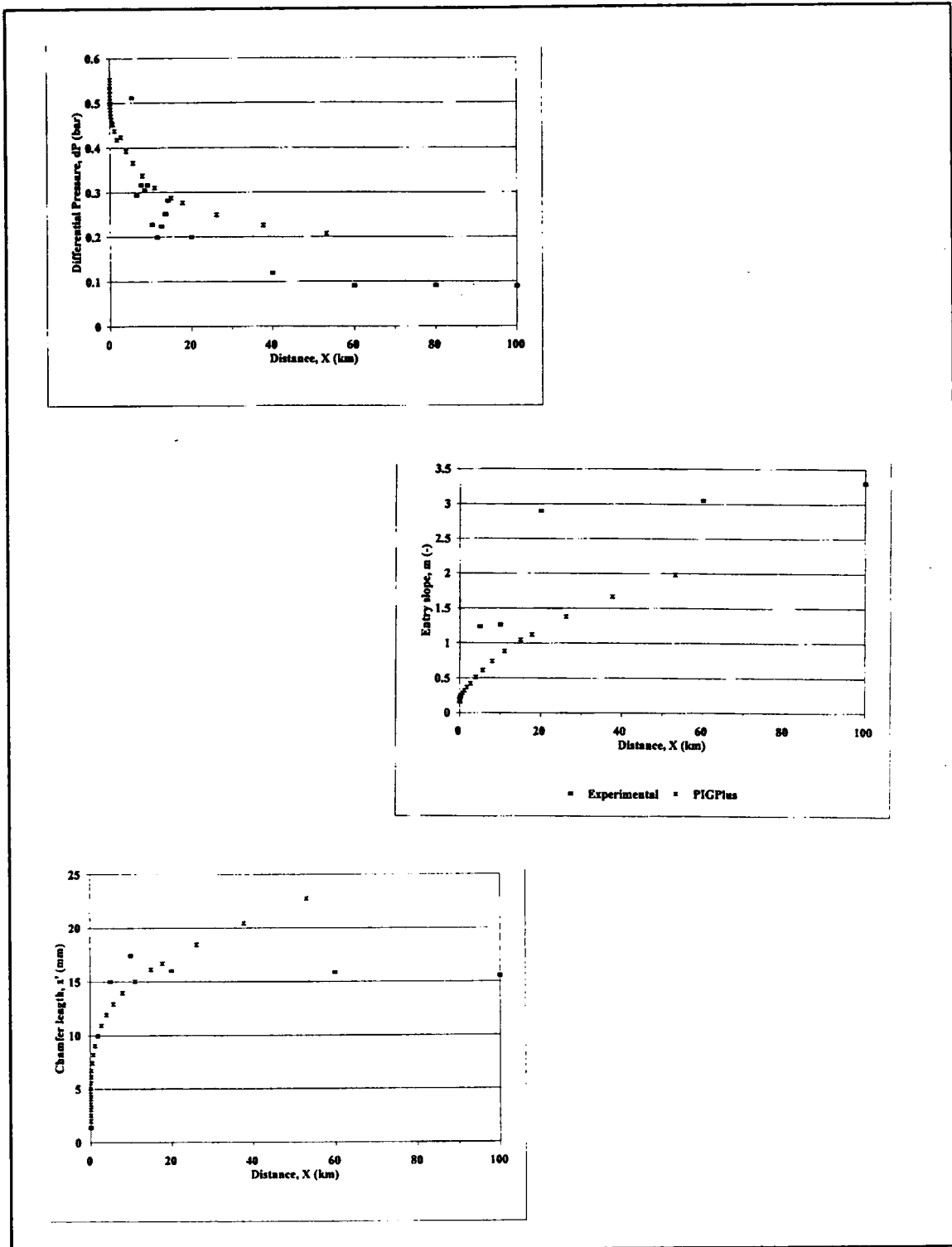


Figure 6.20 Wear test 8, 100km, Shore 65, 1.4m/s

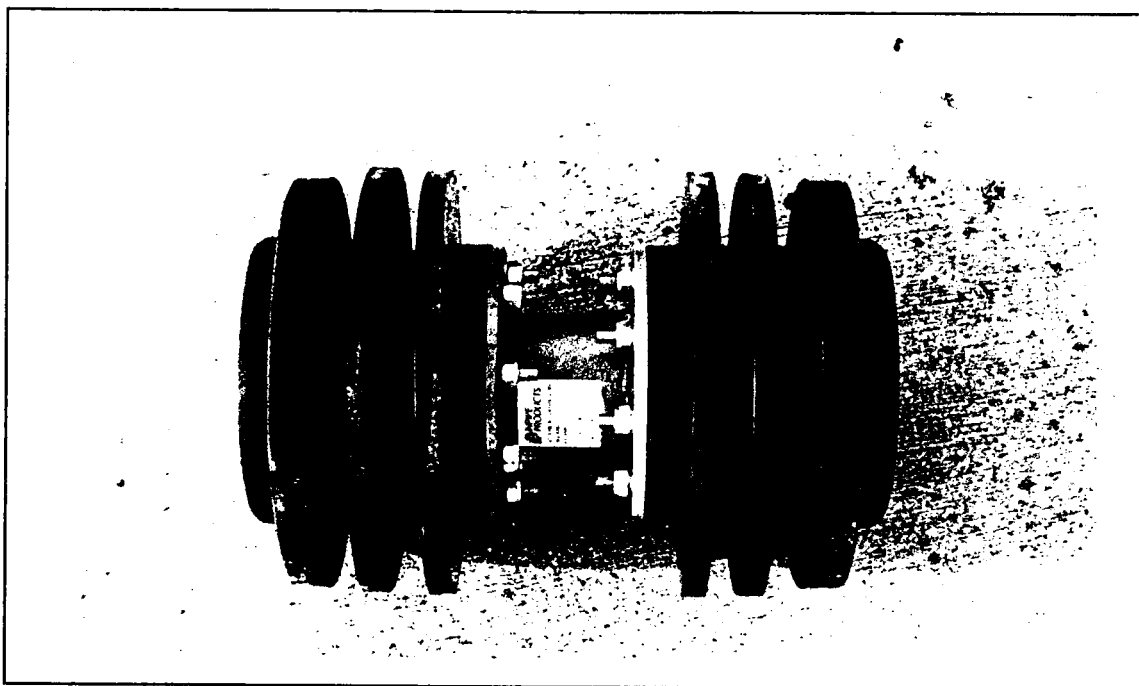


Figure 6.21 Photograph of bidirectional pig tested

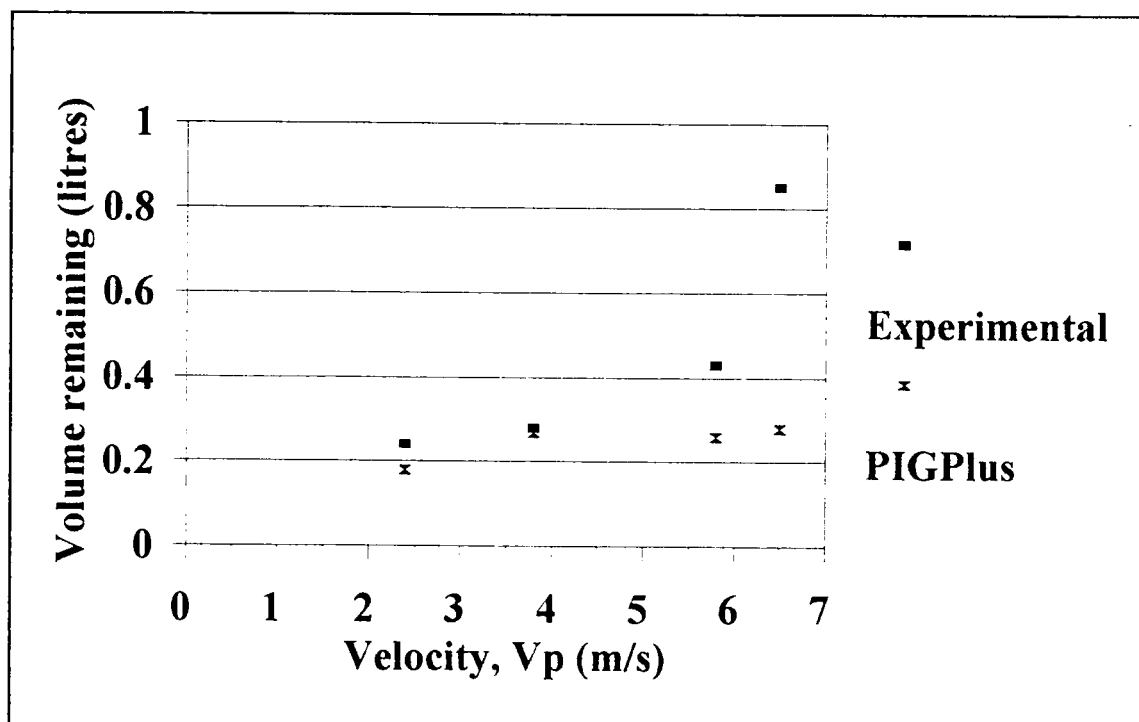


Figure 6.22 Swabbing trial, No. 9

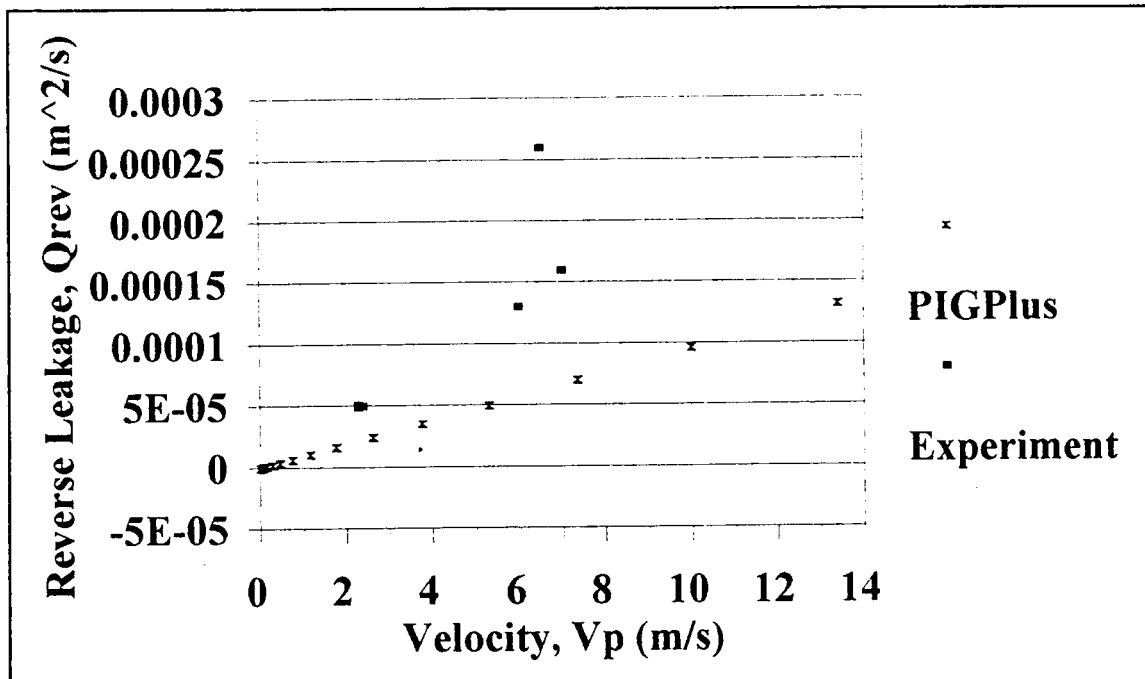


Figure 6.23 Swabbing trial, No. 10

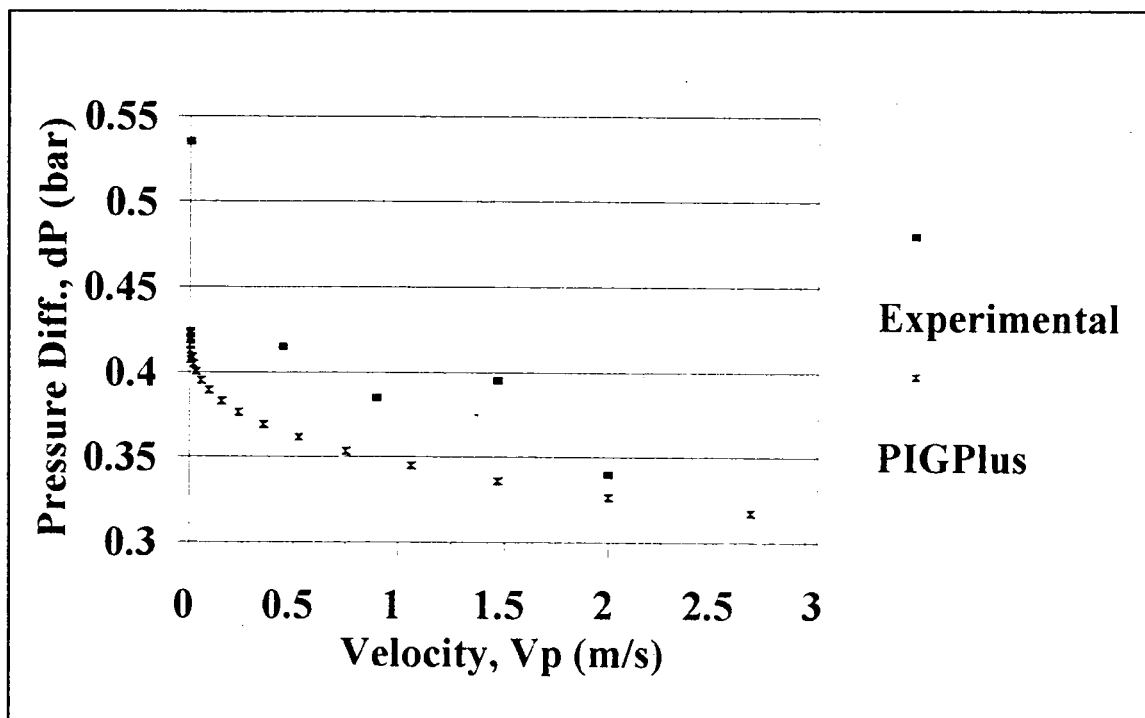


Figure 6.24 Cleaning trial, No. 11

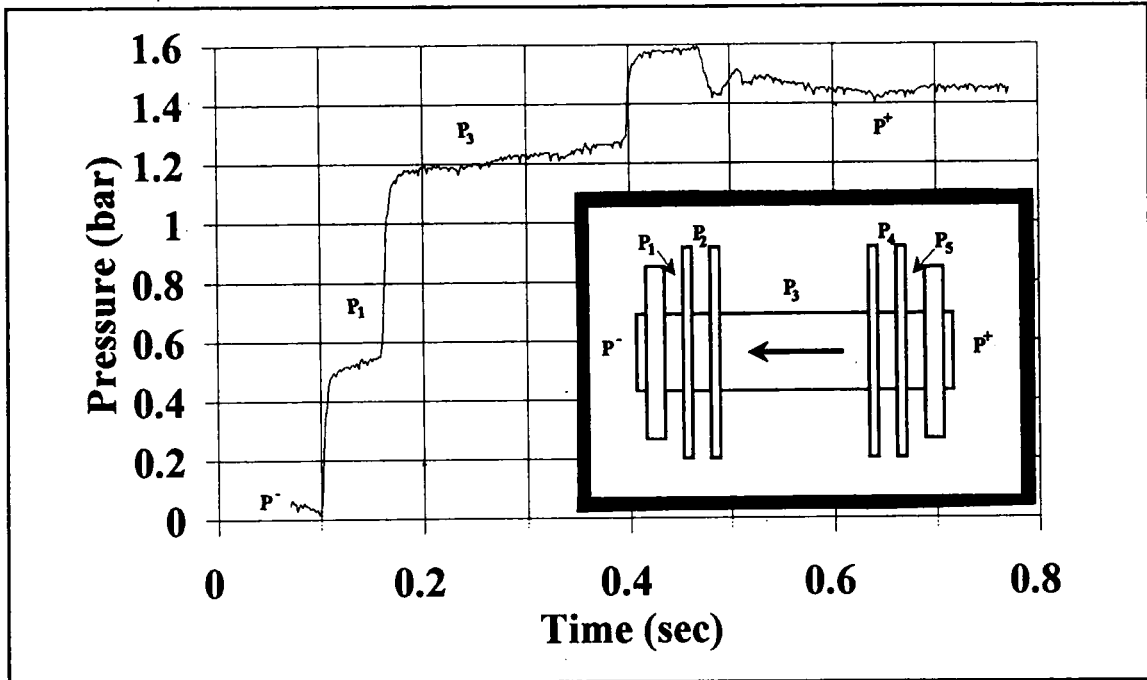


Figure 6.25 Internal pressure level measurement

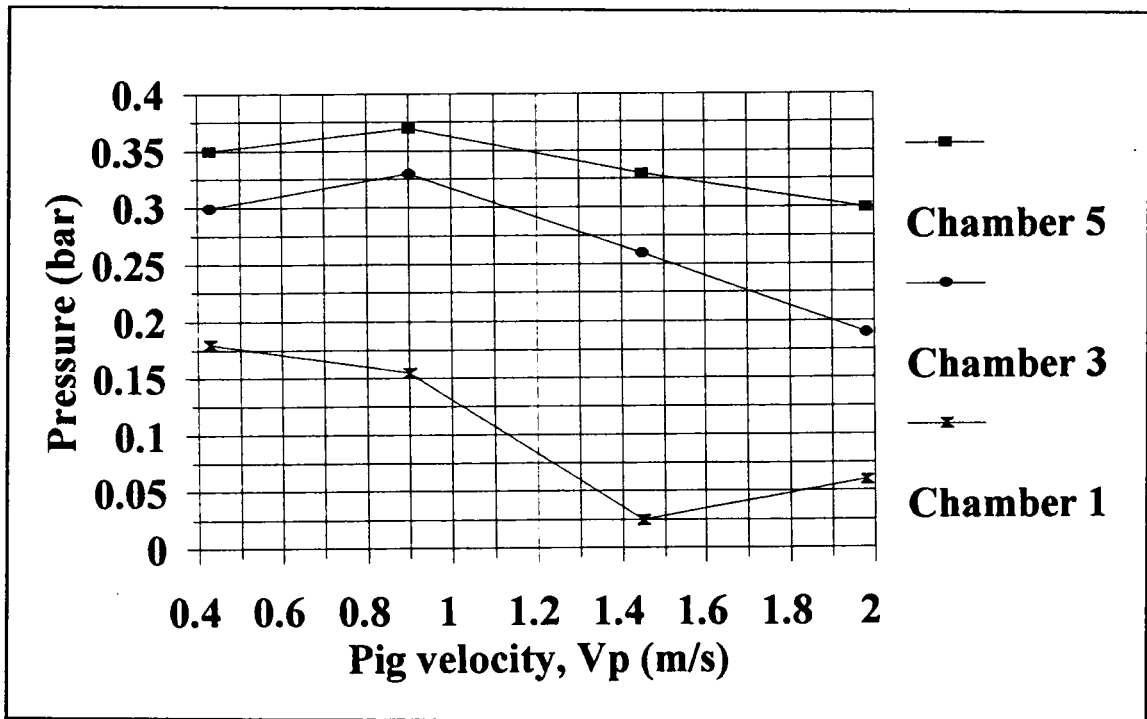


Figure 6.26 Variation in internal pressure against velocity

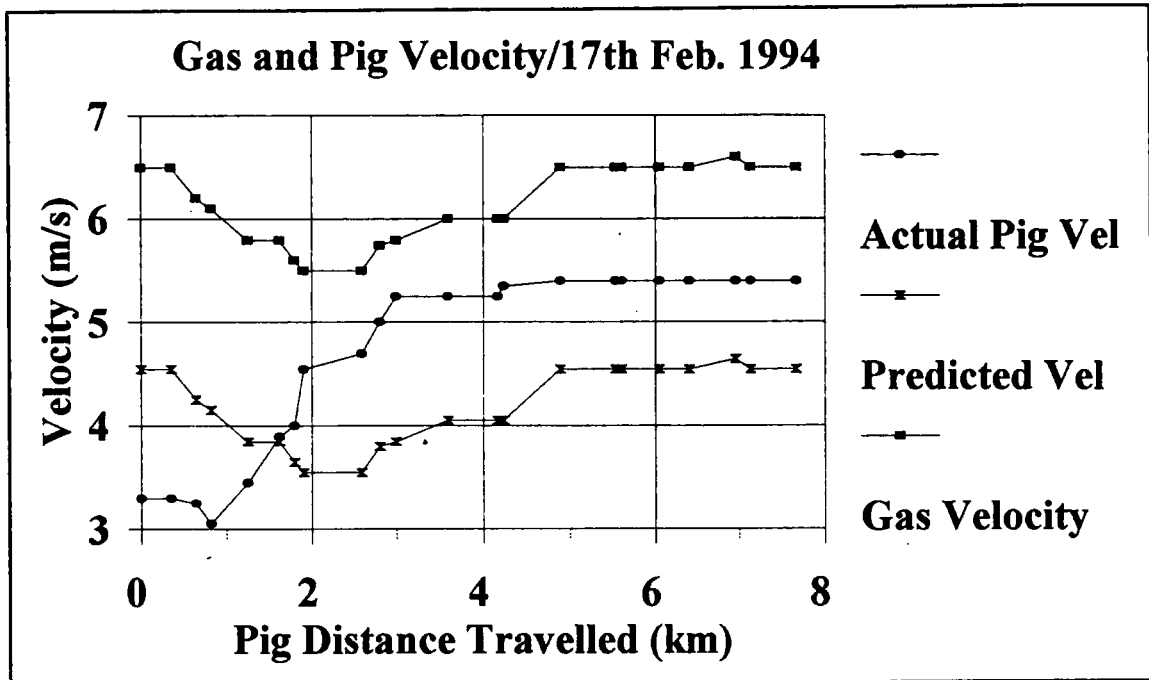


Figure 6.27 Increase in bypass pig velocity with increasing distance as described by Wu et al

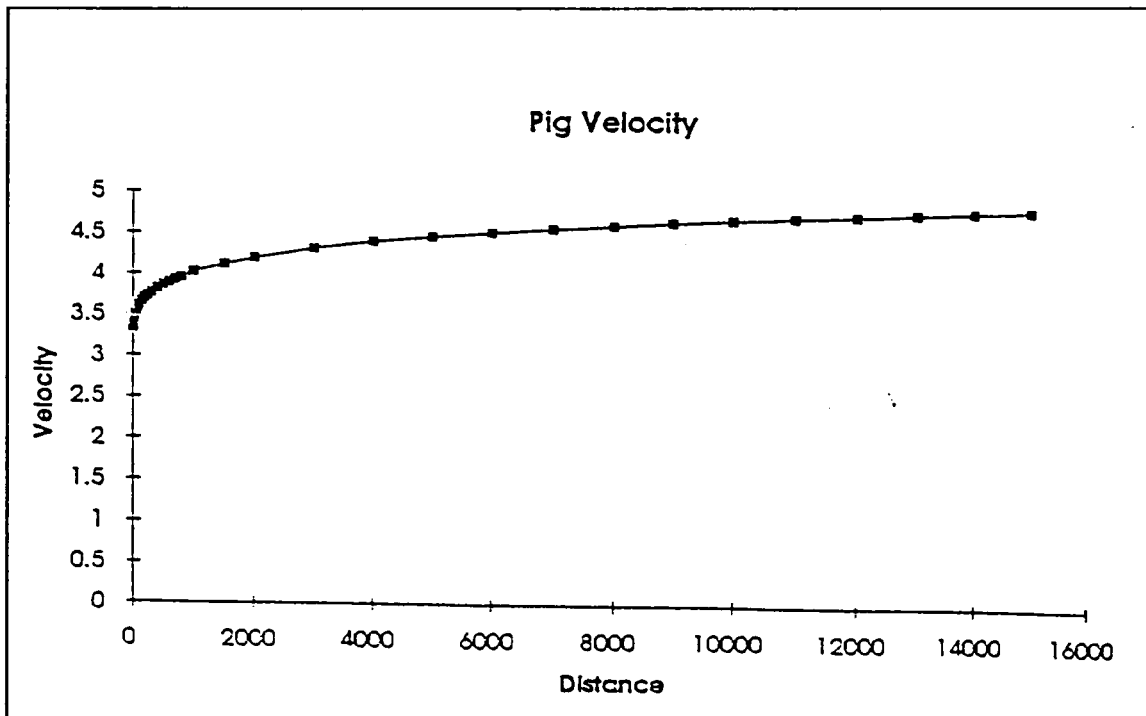


Figure 6.28 Model of high bypass pig showing increasing velocity with distance

CHAPTER 7

DISCUSSION AND CONCLUSION

7. DISCUSSION AND CONCLUSION

In general the *mechanical* description of the pig appears to be satisfactory - that is, the wall force calculation and the contact analysis components of the analysis. Wall force calculation and subsequent wear predictions appear to give reasonable chamfer length and seal entry slope estimations. The trends in differential pressure are correct although the magnitude is smaller than observed values. Similarly with the *fluid* side of the problem in the prediction of leakage for instance, the trends appear correct, but the magnitude is wrong. The description of the pipeline surface also needs more attention as the exponential distribution of asperity heights is inaccurate at high loads.

This chapter discusses the results of the Pigging Technology Project in the light of the *PIGPlus* analysis. Major discrepancies are pointed out and an explanation given. This leads to a discussion of the limitations of the model as presented in this work. Finally, a list of conclusions are given summarising the main findings of the research work.

7.1 Discussion

The main success of the pig steady state motion modelling is the mechanical description of the pig and the subsequent wear and differential pressure trend predictions. The general, the differential pressures calculated are representative. The main criticism that could be levelled here is that they are approximately a factor of two too low in each case. This is possibly because:-

- (I) The Finite Element Analysis shows that for very large and very small deflections the equilibrium wall force model is always lower.
- (ii) The material properties were found from handbooks and as such may have seen higher for the actual polyurethanes used. Experimentation with material properties shows that the observed results are modelled better with higher elastic moduli values - except for the first kilometre or so.

Looking at figures 6.13 to 6.20, the wear trials have been modelled fairly well. As the pig velocity increases however, the difference between the results becomes more obvious. This may be due to the insufficient lubrication model as discussed below. However, a number of points about the tests themselves must be made. On launching the pig when it was new, it was exceedingly difficult to keep the pig at a constant velocity. This was only possible once the seals had worn sufficiently for the centrifugal pump to see a steadier pressure drop in the line. Hence at bends and flange joints the differential pressure to move the pig was initially very high. For this reason the raw data velocity traces could vary from the required velocity for the first kilometre or so, by as much as $\pm 50\%$.

The tests were stopped every 5km in order to inspect the pig and take measurements. On relaunch, every attempt was made to mimic the conditions just prior to taking the pig out. This was not always and in certain cases, the velocity was slightly different. Finally, due to the time required for testing, some tests were terminated and resumed the next day (the pig was taken out of the line and relaunched in the morning to avoid compression set, or permanent deformation of the seals due to the time dependency of the material) - thus allowing the materials to relax back to the unstressed state.

Hence, the *PIGPlus* output represents a more steady state scenario than the actual physical tests. Such transient effects are not modelled by *PIGPlus*. However, the results are still encouraging with the steady state differential pressures, after say 10km, similar in all cases as in the 10" experimental work. This suggests that hardness and velocity only vary the path to this final steady state. Harder seals and slower speeds mean that the pig reaches the final differential pressure sooner. For this particular design of seal, this pressure is in the order of 0.3 to 0.5 bar.

For the 100km test, *PIGPlus* failed after about 50km, figure 6.20. It is interesting

to note that in the real pig test, the pig seals all went below line six at about 50km. Calculation of the wall force is not possible once the seal diameter is less than the pipeline internal diameter, using the method detailed in chapter 3, the equilibrium wall force model. However, it would be easy to include a routine in the model to avoid the program crashing at this point. Chamfer length of these test is matched until the seal goes under line size. This is because there is no limit to how large the chamfer can get in the *PIGPlus* model. However, this could be rectified using a separate routine.

Seal entry slopes trends are matched well again at lower velocities. However, as the speed increases they begin to diverge even more. This is possibly due to the fact that in reality, the whole changed length does not stay in contact with the pipe wall, and the leading edge lifts off as it wears out. It has been observed that the chamfers are slightly rounded rather than flat in general. It is important to note that the chamfer lengths taken from the experiments are averaged over the front three sealing discs. The rear seal is ignored since this was trapped over the rear guide-disc when the pig was new, and as such it suffered excessive wear. This effect was not modelled. The front guide-disc also showed signs of severe nosing down due to overturning moment. Hence, wear is unevenly distributed around the guide-discs and to a lesser extent around the seals.

What is also encouraging is that the model is independent of distance step size, as long as they are small to begin with then progressively larger. Figure 6.20 matches figure 6.16, test 4, for the first 15km. Test 4 makes up the first 15km of test 8, the 100km test. Both are modelled using 20 distance increments.

Application of the technique to the bypass pig as described by Wu et al (1995) also shows general agreement. Wu measured an initial velocity of about 3.25m/s for the pig. Initially, the increase in velocity is rapid, rising to about 5.5m/s after about

2km. This distance is calculated using the average velocity of the pig and the lapsed time, see figure 6.27. Using a simplified version of the *PIGPlus* program, in order to include gas dynamics and bypass effects, the initial velocity calculated was about 3.25m/s again and which would account for more wear of the seals and hence final higher velocities once the gas rate increased again. Again the initial rapid increase in velocity is modelled and the subsequent steady state once the seals have worn in.

The main problems with *PIGPlus* and the model in general appears to be with the description of fluid pressure in the seal and subsequent leakage rates. Unlike previous applications of the Inverse Hydrodynamic Lubrication theory, the fluid pressure does not match the total seal pressure since the surface is so rough (Kantars, A, 1990). For this reason a simplified pressure profile has been taken whose magnitude can be easily calculated. However, there are a number of problems with the whole method:-

- (i) Conservation of fluid flow is not obeyed in the seal area. This was in order to simplify the film thickness calculations.
- (ii) At high loads, the seal total pressure is so high that the seal sits below the rough surface datum line. The exponential distribution of asperity summit heights is not valid under such circumstances.

The pig is analysed as an axi-symmetric problem. Nose-down, as a result of moments on the pig body, would lead to non-uniform film thicknesses. Since leakage is proportional to the cube of the film thickness, this will lead to much larger leakage values, as observed. In test 9, since the pig was new, the WEARS module was used to model the volume of liquid remaining in the pipeline of the 90km test section. This means that the seal was wearing as the test took place and as such it was not a steady state test.

A number of points must be made about these test, which used a gas drive to propel the pig with a column of water in front. Since the new pig was initially pushed to the test section, see figure 6.6, using air in a dry pipeline, the wear is thought to be substantial for the new bidi. However, there is no way of knowing what the chamfer length was at this stage as the pig is in the pipeline. Unfortunately, measurements of the chamfer lengths were not taken when the pig was removed from the pipe for each of the 4 runs. Measurement of the volume of liquid remaining in the line was performed using foam swabbing pigs to push out and soak up the remaining volume of liquid. This was checked using a video crawler pig which showed that the excess water was removed from the line when two such swabs were used, but the line was still damp. Finally, since the pig was gas driven, the velocity would not have been entirely steady. Pigs driven by gas pressure tend to experience “Velocity Excursions”, or high accelerations and velocities as a result of sudden gas expansion. Steps were taken to avoid velocity excursions - including “packing” the line with gas at 12 bar to dampen velocity and using a sonic nozzle to keep volumetric flow rate independent of pressure. This worked well, but some smaller accelerations were recorded, though their magnitude is unknown. Such acceleration will affect reverse leakage since the liquid in front of the pig will exert an inertial pressure on the front of the pig. For example, an acceleration of 1m/s^2 of 20m of water in the 10" line would have caused an instantaneous inertial pressure in front of the pig of about 3 bar.

However, the output from the experiments is important showing an increase in reverse leakage with increasing velocity. In addition the effect of wear on the leakage rate is marked - the worn seal allow much more liquid to bypass the seals, see figure 6.23. This makes sense from the model point-of-view. An increase in chamfer length will increase the film thickness since fluid pressure will have more of an impact on performance. This is borne out by the output from *PIGPlus*, but the magnitudes are not correct.

Differential pressure against velocity of the 15km worn-in bidi from the cleaning trials is considered in figure 6.24. Again the PIGPlus output is about a factor of two less than observed. The cleaning trials also indicate that the assumption that the pressure drop across the pig is distributed evenly across all seals, and not the guidediscs, is incorrect. It appears that the guidediscs do have a pressure drop associated.

An important point to note in the lubrication analysis is the arbitrary selection of the datum level. Initially, for a new pig seal, the static film height can be below this datum level. For this reason, the additional fluid lift is assumed to be additive. If the film was not allowed to drop below the datum then:-

- (i) At high loads the surface roughness could not support the load and this would be supported by the fluid. This is since the extremely small resultant film thickness would generate relatively high fluid pressures. This is unrealistic.
- (ii) Because of this frictional trends at low velocity and high load would be incorrect.

A better roughness model is required. One possible method of correcting this is to specify a cut-off point where boundary lubrication stops (no fluid effects) and mixed lubrication starts (fluid effects). In the boundary lubrication case, all the load is taken by the roughness and no leakage could be assumed due to the lack of a fluid path.

This discussion of the results and the model analysis leads to a number of important conclusions which are now presented.

7.2 Conclusions

The following conclusions regarding the model and the work presented above are

made:-

- (I) The equilibrium wall force model calculates the pig seal wall force successfully. More specific input for the materials used, in terms of elastic moduli would be welcomed however. Calculation of the seal entry slope is satisfactory.
- (ii) The contact model is adequate. Although it was felt that it would not model the sharp seal contact well, this is not the case since, due to wear a chamfer length is worn onto the disc quickly. Modelling of the worn chamfer length has been achieved.
- (iii) The lubrication analysis is representative in terms of trends but from an absolute magnitude point of view, it is insufficient. This is a result of:-
 - Assumed fluid pressure distribution is incorrect and does not conserve continuity of flow in the seal.
 - The roughness model fails at high loads, as the exponential approximation of the Gaussian distribution of summit heights is invalid.

In general, since the lubrication of pig seals is so bad, the problem with the lubrication analysis does not show up until leakage is calculated. It is possible that the wear analysis could have been performed equally well without recourse to a lubrication analysis in the first instance.

Despite the limitations, *PIGPlus* has been used and accepted on a number of commercial projects, more to *optimise* than to *predict* for the reasons given above.

For example:-

- (i) Reduction of leakage past an intelligent pig batching train. Many of the seal

parameters were varied until minimum leakage was attained, both in terms of distance and velocity in this particular case for the Lille-Frigg pipeline.

- (ii) Estimation of final velocity for High Bypass Pig. An additional gas dynamics module was added to this version of the software in order to limit the velocity of Shells' High Bypass Pig. This was achieved by altering bypass size and disc properties.
- (iii) Reduction of seal wear for development of long distance bidirectional pig. Due to the interaction of all the variables *PIGPlus* was used to determine the optimum seal design for this pig in terms of minimisation of wear (eg seal diameter change, differential pressure, etc).
- (iv) Provision of frictional data for velocity control of pig train. In order to determine the velocity variation of a pig train in a gas pipeline, the variation of friction with velocity is required. *PIGPlus* provided the frictional data while further work assessed the subsequent pig motion.

CHAPTER 8

RECOMMENDATIONS FOR FUTURE WORK

8. RECOMMENDATIONS

Whereas it is clear that a combination of an accurate stress analysis of the pig sealing disc to calculate wall force and contact parameters, and a lubrication analysis can be used to model the motion of the pig, a number of improvements can be made. This chapter sets out recommendations for future work to build on the model detailed in this thesis. These recommendations fall into three categories:-

- (i) Improvements to modelling pig motion
- (ii) Linking the characteristics of the pig to its intended function
- (iii) Standards for pipeline pigging

The remainder of this thesis discusses these recommendations and how they might be actioned.

Improvements to modelling pig motion

Several aspects of the pig motion need to be understood more fully. A more detailed study of the steady state motion of the pipeline pig should be undertaken, using the information detailed in this work as a starting point. A number of aspects should be addressed:-

- (i) A complete three dimensional model of the pig would more accurately model the nose down effect. To achieve this wall force would have to be calculated as a function of circumferential position, although it may be possible to describe the disc in a number of discrete segments, with accuracy dependant on the angle of each segment. The mass of the pig, and its length would play an important role - mass will cause a higher friction along the bottom of the pig, thus causing an overturn moment. Length and position of the seals will influence the degree of nose down.

It is expected that this three dimensional nature will influence the pig

characteristics in a number of different ways. Nosing down is surely the cause of uneven wear on the discs. The high levels of forward leakage found in trials on the 10" loop could be influenced by this effect. In addition, the internal pressure levels will have to be looked at in detail, as the assumption that pressure drop across each of the seals is the same has been shown by experiment to be false. Calculation of internal pressure levels would be based on continuity of flow through the pig.

- (ii) An improvement to the lubrication analysis is required. A better description of $P(x)$, the fluid pressure in the seal is required. This analysis has assumed a pressure distribution which does not conserve continuity in the seal area. Work should be done to rectify this essential aspect. This would involve a proper EHL analysis at the seal contact, although the IHL method is still worth pursuing. Although the seal is apparently badly lubricated, work could be undertaken to investigate methods of improving the seal lubrication to limit wear or reduce leakage by investigating wall force and seal shapes.
- (iii) The guide-discs have not been modelled in the analysis presented in this work. This was difficult due to the axisymmetrical nature of the work. It is clear from experimental work that the guide-discs wear as well, especially the front guide along the bottom, due to nose-down. A shape could be assumed for the guide disc contact. Such a shape could be taken from experimental evidence.
- (iv) A better description of the roughness of the pipewall is required. The current model allows the film thickness to go negative especially when the seals are new. This calls into question the use of an exponential distribution of asperity summits. In addition, the effect of roughness on the lubrication itself has not been modelled - work detailed by Patir and Cheng (1978, 1979) could be used to model this aspect. Roughness undoubtedly influences the lubrication process and directional effects such as longitudinal scraping on the pipe wall should be investigated.

-
- (v) More information is required about leakage, especially the forward leakage rates. Experimentation into forward leakage should be done in tandem with more accurate modelling of the phenomenon. A major part of this problem would be to develop a technique for measurement of forward leakage. It should be remembered that some of the fluid which leaks forward, is returned as reverse leakage!
 - (vi) The model should be adapted to other situations besides steady state motion of bidirectional pigs. A more generalised model could look at other seal designs, and in gas pipelines or indeed multiphase pipelines. A gas lubrication analysis of the seal could aid in modelling this difficult frictional problem. Two phase calculations would need to look at the inertial effects of the liquid in front of the pig. A more accurate description of the forces acting on the pig would lead to better understanding of the motion and performance of the pig.
 - (vii) A number of "transient" aspects of steady state motion require investigation. These include the effects of bends and pipe features such as weld intrusions. It is also suspected that pigs turn slightly in negotiating bends, thus helping to even out the wear of the seals. Certain types of drive, such as that supplied by a centrifugal pump make the pigs run unsteadily when wearing in. This makes it difficult to track due to their unsteady speed. A stick-slip analysis is possibly required, but this is known to be difficult.

Linking the characteristics of the pig to its intended function

Work is on going at CALtec on this aspect of pigging. Pipeline pigs are launched for an intended purpose, for example cleaning wax from a pipeline. CALtec are attempting to understand the link between performance and characteristics outlined in this work. However, more investigation could be done. The wax example could be studied as a non-Newtonian lubrication problem. Any debris build-up will cause a force on the seals or the guide discs and this could be modelled. Wax could build-

up in front of the pig until the back-force on the discs was large enough the bend them and cause ride over.

In addition to this, much more work needs to be done on bypass systems to aid in the cleaning process. A differential pressure of about 1 bar across a pig represents much energy that could be put to useful work in cleaning or jetting. However, most of the pig bypass systems available today involve removal of a bolt from the pig - correct directing of the bypass jets has not been investigated.

Standards for pipeline pigging

It has been noticed over the course of this investigation that a number of definitions used in conventional pipeline pigging are ambiguous. For example, oversize is frequently quoted as the percentage difference between the pig disc diameter and the pipeline internal diameter. However if a chamfer has been machined or worn onto the disc then this definition fails to describe the pig correctly. For this reason, it is recommended that correct and unequivocal descriptions of all aspects of pigging be prepared to avoid confusion. Another good example is bypass expressed as a percentage of pipe area, although this has not been dealt with in this work. This tells the engineer nothing about the relationship between fluid flow and pressure drop across the pig, not to talk about direction of the bypass jets.

Finally since many of the variables used in this work are difficult to measure, a test house should be set up to measure material properties and to give advice on pipeline roughness parameters. Information on material properties could also be useful in setting minimum standards for pigs for certain duties. For example, a simple abrasion test could be linked to pig tests to tell if a seals' maximum diameter will remain over line size for a 100km run, for instance. Extension and compression tests could lead to more accurate descriptions of wall force and allow use of rubber models such as Mooney-Rivlin or Neo-Hookean in calculation of wall force.

Although it is unlikely that funding will be found for all this work, certain aspects should be seriously considered by the likes of operators in the Oil and Gas industry if pipeline pigging is to emerge from its dark days as a black art, and allow engineers to understand exactly what a pig is doing when it is launched.

REFERENCES

REFERENCES

- Azevedo L.F., Gomes G. 1995
Simple hydrodynamic models for the prediction of pig motion in pipelines, *Pontificia Universidade Católica do Rio de Janeiro* 1995
- Barrett M.L. 1959
Using expandable spheroids for batch separation, *Pipeline Industry*, June 1959
- Blok H. 1963
Inverse problems in Hydrodynamic lubrication and design directives for lubricated flexible surfaces, *Symposium on Lubrication and Wear, Houston, Texas, 1963*
- Bush A.W., Gibson R.D. 1980
The effect of surface roughness and elastic deformation in HDL - a perturbation approach, *Surface roughness effects in Hydrodynamic and mixed lubrication symposium, ASME, Chicago, Nov 16-21, 1980*
- BRMA (British Rubber Manuf. Ass.)
Guide book on Polyurethane
- Cameron A. 1987
Basic Lubrication Theory, 3rd Ed., Ellis Horwood Ltd
- Chatfield C., 1983
Statistics for technology, 3Ed, Chapman & Hall, NY, 1983
- Cheng H.S., Dyson A. 1976
Elastohydrodynamic lubrication of

-
- circumferentially ground rough discs, *ASLE Transactions Oct 1976 Vol 21, pp25-50*
- Cordell J.L. 1988 Pipeline pigging - an industry overview, *Pipes and Pipelines International, May/June 1988*
- Cordell J.L., Saunders P. 1991 Shell visits report, 1991
- Cordell J.L., Russell D.A., Short G.C. 1991 Pigging Technology Project, Phase 1 - State of the art review, *Final report, Vol 1, CALtec, August 1991 (Confidential)*
- Cordell J.L. 1991 Pigging research, *Pipeline Pigging and Inspection Technology Conference, Houston TX, Feb 1991*
- Cordell J.L., Gorzeman G. 1991 Visit report, *Pigging Technology Project, Phase 1, April 1991 (Confidential)*
- Cordell J.L. 1992 Conventional pigs - what to use and why, *Pipeline Pigging and Inspection Technology Conference, Houston TX, Feb 1992*
- Dowson D., Higginson G.R. 1966 *Elastohydrodynamic lubrication, 1st ed, 1996, Pergamon Press*
- Gohar, R. 1988 *Elastohydrodynamics, 1st ed, Ellis Horwood Ltd, UK*

-
- Greenwood J.A., Williamson J.B. 1966 *Contact of nominally flat surfaces, Royal Society Proceedings, A295, 1966*
- Halling J. 1978 *Principles of Tribology, Macmillian Press Ltd, London, 1978*
- Hara A., Hayashi H., Tsuchiya M. 1979 *Sphere separation systems aids long haul oil-product transport, the Oil & Gas Journal, January 22, 1979*
- Inpipe products, 1995 *Product review lecture held at CALtec, Aberdeen, August 1995*
- Johnson K.L. 1987 *Contact Mechanics, 2nd ed, Cambridge University Press*
- Juvinal, R.C. 1983 *Fundamentals of machine component design, Wiley, US*
- Kanters A.F.C. 1990 *On the calculation of leakage and friction of reciprocating elastomeric seals, Thesis, Technische Universiteit Eindhoven, 1990*
- Kennard M.A. 1993 *Pigging Technology Project, Phase II - The wear project, Final Report, Dec 1993 (Confidential)*
- Kennard, M.A. 1995 *Pigging Technology Project, Phase 2 - Swabbing Report, Draft Report, CALtec,*

September 1995

- Kershaw C. 1991 *Specialist Pigging Techniques, Pipes and Pipelines International, May/June 1991*
- Kershaw C., Cordell J.C. Private communication
- Landes, M. 1983 A pig for every pipeline, *Pipeline Digest*, July 4th
- Lochte G.E., Kozel T. 1995 How pigging operations impact deepwater production economics, *Offshore, April 1995*
- Massey B.S. 1979 *Mechanics of fluids*, 4th ed, Von Nostrand Reinhold (UK) Ltd
- Mathews L., Rendle M. 1994 CALTEC proves the viability of North Sea pigging operation, *Pipeline pigging and Integrity Monitoring Conference, Amsterdam, April 1994*
- McNulty J.G., Short G.C., Russell D. 1992 Predicting the performance of conventional pigs, *Pipeline Pigging and Inspection Technology Conference, Houston TX., Feb 1992*
- MICROSOFT, 1990 *Microsoft QuickBASIC™*, 2nd ed, Microsoft
- Moore D.F. 1972 *The friction and lubrication of elastomers*, 1st

-
- ed, Pergamon Press, Oxford
- O'Donoghue, A.F.A. 1993 Pigging Technology Project, Phase 2 - Cleaning Report, *Final Report, CALtec, Aug (Confidential)*
- O'Donoghue, A.F. 1993 Characteristics and performance of conventional cleaning pigs, *Pipes and pipelines international, Sept/Oct 1993*
- O'Donoghue A.F., Russell D.A. 1992 On the dynamics of pipeline pigs and plugs, CALtec, August 1992 (Confidential)
- Out J.M.M. 1993 On the dynamics of pig-slug trains in gas pipelines, *Pipeline Technology, 1993*
- Patir N., Cheng H.S. 1978 An average flow model for determining effects of three dimensional roughness on partial hydrodynamic lubrication, *Trans of the ASME, Vol 100, Jan 1978*
- Patir N., Cheng H.S. 1979 Application of average flow model to lubrication between rough sliding surfaces, *Trans of the ASME, Vol 101, April 1979*
- Peppiatt N. Private communication
- Perkins A. 1994 Private communication

-
- Rhode S.M. 1980
A mixed friction model for dynamically loaded contacts with application to piston ring lubrication, *Surface roughness effects in Hydrodynamic and mixed lubrication symposium, ASME, Chicago, Nov 16-21, 1980*
- Romagnoli R., Varvelli R. 1991
FEM approach to the deformation study of pig cups, *Proc. 1st International Offshore and Polar Engineering Conference, Edinburgh, Aug 1991*
- Rosen H. 1995
Mechanical Pipeline Pigs, Company Brochure, Offshore Europe '95, Aberdeen
- Saevik S., Soreide T.H. 1988
The finite element method in deformation analysis of pig cups, *Proc 7th International Conference on Offshore Mechanics and Arctic Engineering (OMAE), Houston TX, Feb 1988*
- Smith G.L. 1992
Pigging velocities and the variable speed pig, *Pipeline Pigging and Inspection Technology Conference, Houston TX., Feb 1992*
- Smith G. 1992
The scientific art of pipeline pigging, *Pipeline and Gas Journal, August, 1992*
- Szeri A.Z. 1987
Some extensions of the lubrication theory of

-
- Osbourne Reynolds, *Journal of Tribology*,
Jan 1987, Vol 109, p21
- TDWilliamsons Ltd, 1993 Private communication, *Oct 1993*
- Tiratsoo, J. 1989 The British pipeline picture - on and
offshore, *Pipeline Digest, Oct*
- Webb S., Rogucz E., Larg E. 1987 Evacuation of a residual Oil pipeline by inert
gas, *SPE Production Engineering, Vol 2,*
Feb 1987
- Weingarten J.S., et al 1984 Analysis of the motion of pigs through gas
pipelines, *Journal of Fluid Engineering, 106,*
4 Dec, 1984
- Wu H.L., Van Spronsen G. et al Bypass pigs for two phase flow pipelines,
Multiphase flow confernce BHRGroup,
Cannes, 1995

APPENDIX A

THE EQUILIBRIUM WALL FORCE MODEL

A. THE EQUILIBRIUM WALL FORCE MODEL

Figure A.1 shows the forces involved in the wall force calculation. In cross section, five forces and/or stresses act on the disc segment:-

- (i) Wall force, w (N/m)
- (ii) Friction, f (N/m)
- (iii) Differential pressure, ΔP (N/m²)
- (iv) Hoop stress, σ_θ (N/m²)
- (v) Radial stress, σ_r (N/m²)

These stresses and forces are all in equilibrium. All can be estimated - if f and ΔP are assumed (and later estimated from steady state motion model). A shape is assumed for the disc, then w , the wall force can be estimated by taking moments.

The geometry is shown in figure A.2. Assume the final shape of the deflected seal is an arc of a circle of angle β and radius R . Then

$$l = R \beta$$

Also

$$\frac{l'}{R} = \sin \beta$$

Therefore

$$\frac{l}{R} = \frac{l'}{\sin \beta}$$

From this expression, β and R can be calculated. Where, from geometry:-

$$l = \frac{D - \phi}{2}$$

And

$$l' = \frac{d - \phi}{2} - \frac{t \sin \beta}{2} + \delta_o$$

Positive moments due to wall force and friction

Figure A.3 shows the wall force and frictional forces acting on the pig seal.

Taking moments about A:-

$$M_w^* = w r_o R (1 - \cos \beta) d\theta$$

$$M_f^* = f r_o (r_o - r_i) d\theta$$

where $r_o = d/2$, and $r_i = \phi/2$.

Negative moment due to differential pressure

Figure A.4. shows the differential pressure acting on the seal. Over a small angle $d\alpha$, the force $dF_{\Delta P}$ acts. This can be resolved into two components. The resulting moment due to these two forces is:-

$$\begin{aligned} dM_{\Delta P}^- &= \Delta P R d\alpha (r_i + R \sin \alpha) R \cos \alpha \sin \alpha d\theta \\ &+ \Delta P R d\alpha (r_i + R \sin \alpha) (R + R \cos \alpha) \sin \alpha d\theta \end{aligned}$$

$$= \Delta P R^2 d\theta \sin \alpha (r_i + R \sin \alpha) d\alpha$$

Integrating to determine the total moment:-

$$M_{\Delta P} = \Delta P R^2 d\theta \int_0^{\beta} r_i \sin \alpha + R \sin^2 \alpha d\alpha$$

$$= \Delta P R^2 \left(\frac{R \beta}{2} - \frac{R \sin 2\beta}{4} + r_i - r_o \sin \beta \right)$$

Negative moment due to radial stress

Figure A.5 shows the calculation method for the negative moment due to radial stress in the seal. Working on the compressive side, the strain is:-

$$\epsilon_r = \frac{\text{Change in length}}{\text{Original length}}$$

$$= \frac{\beta R - \beta (R - y)}{\beta R}$$

$$= \frac{y}{R}$$

Stress is given by:-

$$\sigma_r = E_c \frac{y}{R}$$

at A therefore, the force is:-

$$dF_r = E_c \frac{y}{R} r_i d\theta dy$$

therefore the moment due to this force is:-

$$dM_r = E_c \frac{y}{R} r_i d\theta dy y$$

Integrating this to get the entire compressive moment:-

$$M_{\sigma_c} = \frac{E_c d\theta r_i t^3}{24 R}$$

Similarly for the tensile moment:-

$$M_{\sigma_t} = \frac{E_t d\theta r_i t^3}{24 R}$$

Negative moment due to hoop stress

Figure A.6 shows the compressive hoop stress component acting on the seal.

The strain is again given by:-

$$\epsilon_{\theta} = \frac{\text{Change in circumference}}{\text{Original circumference}}$$

$$= \frac{2 \pi (\alpha R + r_i) - 2 \pi (R \sin \alpha + r_i)}{2 \pi (\alpha R + r_i)}$$

$$= \frac{\alpha - \sin \alpha}{\alpha + \frac{r_i}{R}}$$

The stress can be now taken as:-

$$\sigma_{\theta} = \frac{E_c}{(1 - \nu^2)} (\epsilon_{\theta} + \nu \epsilon_r)$$

The radial stress is now removed for clarity as it would later cancel in the integration operation. Therefore the force acting on the thin strip is:-

$$dF_{\sigma_{\theta}} = \frac{E_c R t d\theta}{(1 - \nu^2)} \frac{\alpha - \sin \alpha}{\alpha + \frac{r_i}{R}} d\alpha$$

Now the moment due to this small force alone is:-

$$dM_{\sigma_{\theta}} = \frac{E_c R^2 t d\theta}{(1 - \nu^2)} \frac{\alpha - \sin \alpha}{\alpha + \frac{r_i}{R}} (1 - \cos \alpha) d\alpha$$

Integrating to determine the total moment:-

$$M_{\sigma_0} = \frac{E_c R^2 t d\theta}{(1 - \nu^2)} \int_0^{\beta} \frac{(\alpha - \sin \alpha) (1 - \cos \alpha)}{\alpha + \frac{r_i}{R}} d\alpha$$

The addition of all these moments equals zero. Since w is the only unknown it is possible to estimate the wall force.

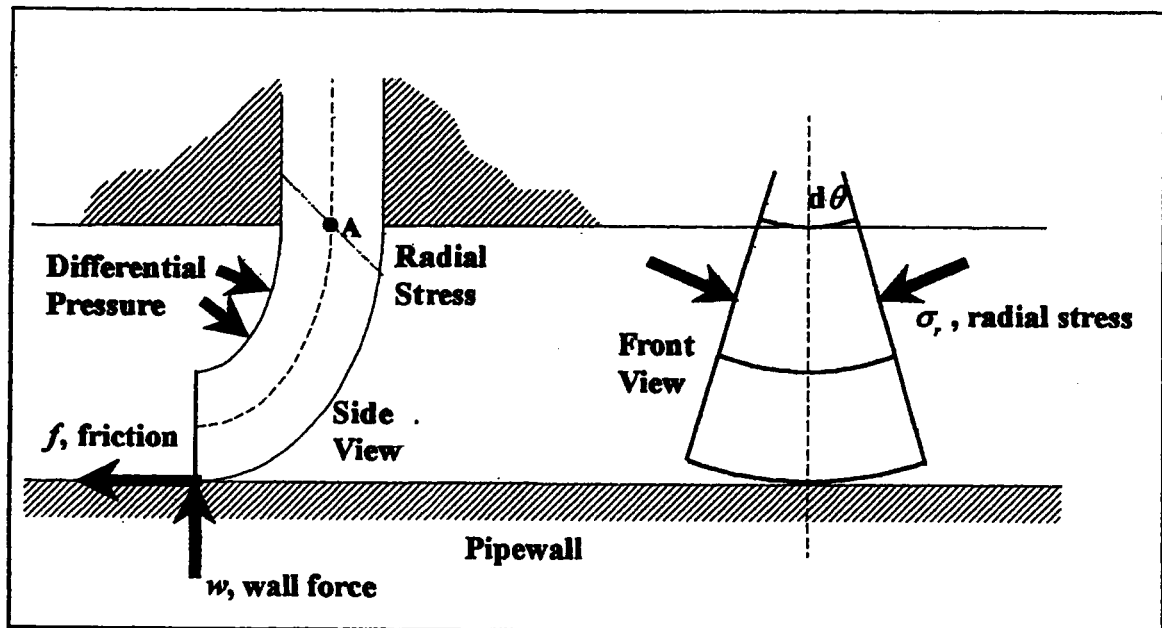


Figure A.1 Basic of wall force calculation

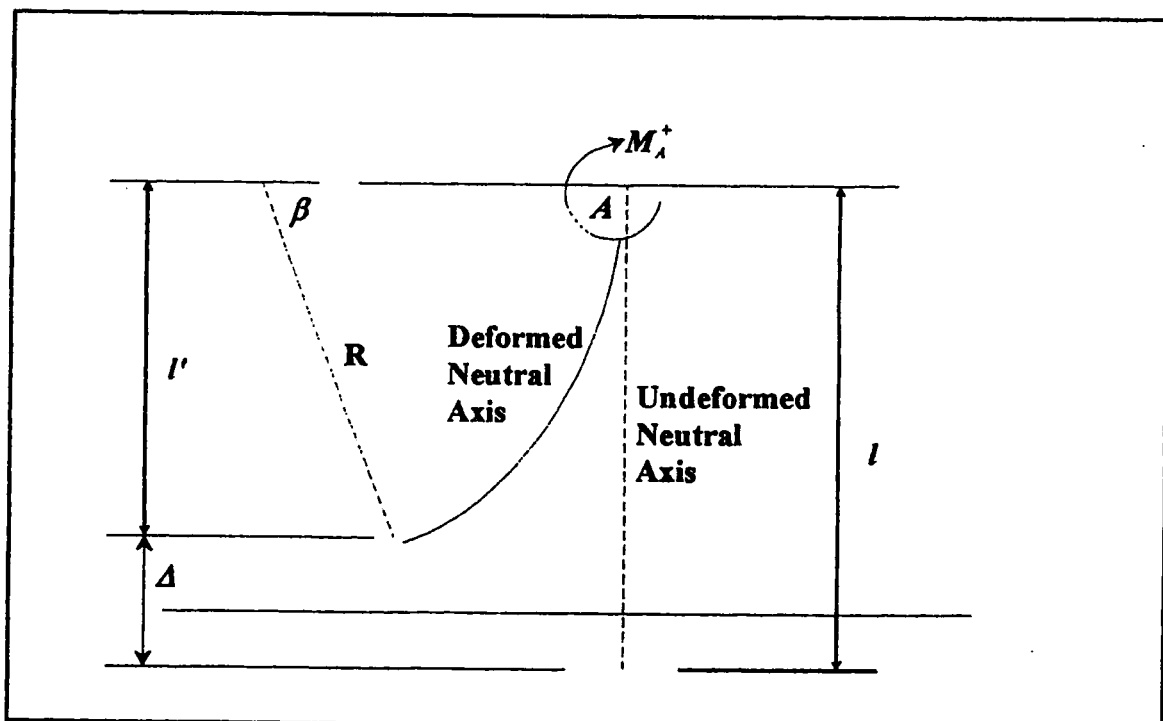


Figure A.2 Geometry of stressed pig sealing disc

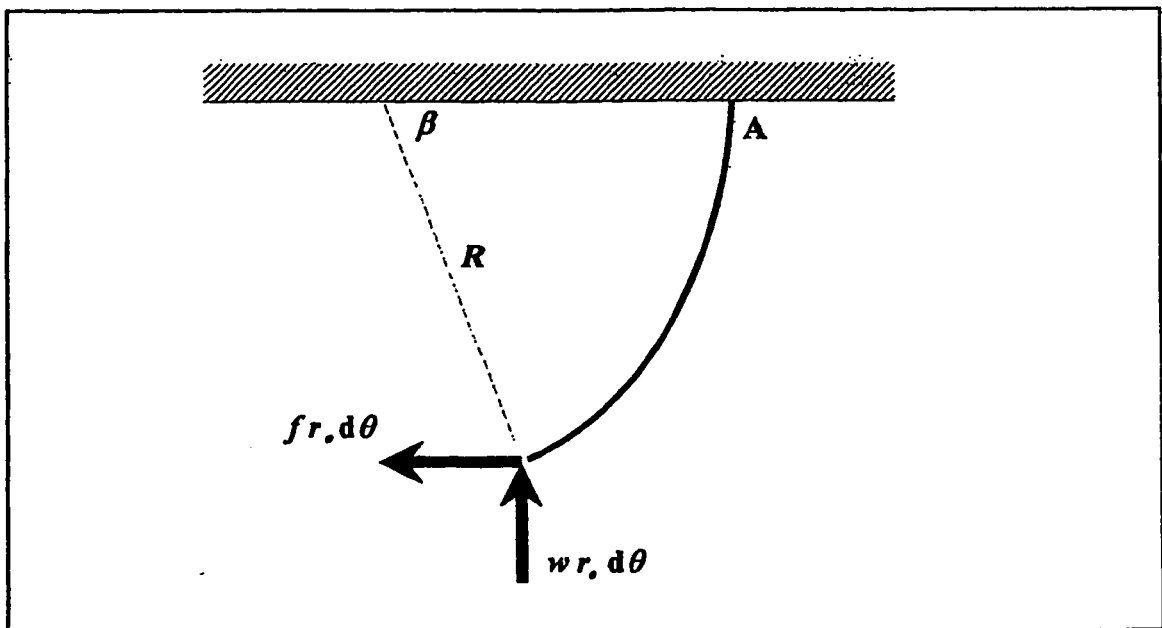


Figure A.3 Positive moments due to wall force and friction

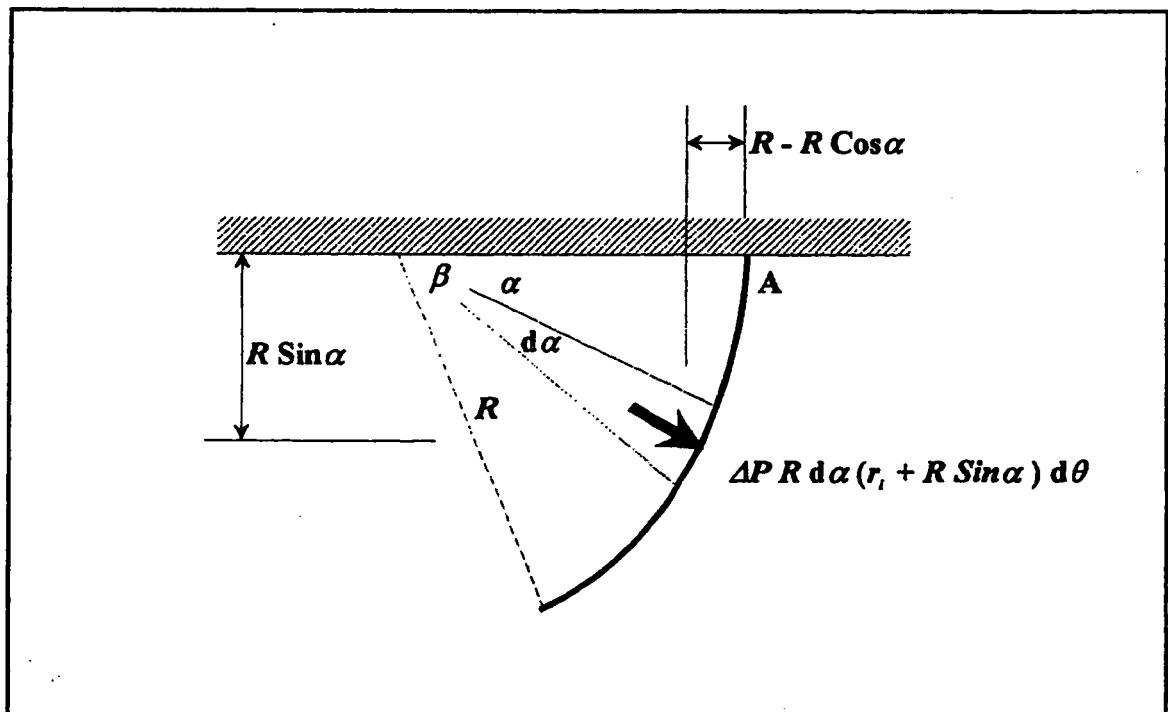


Figure A.4 Negative moment due to differential pressure

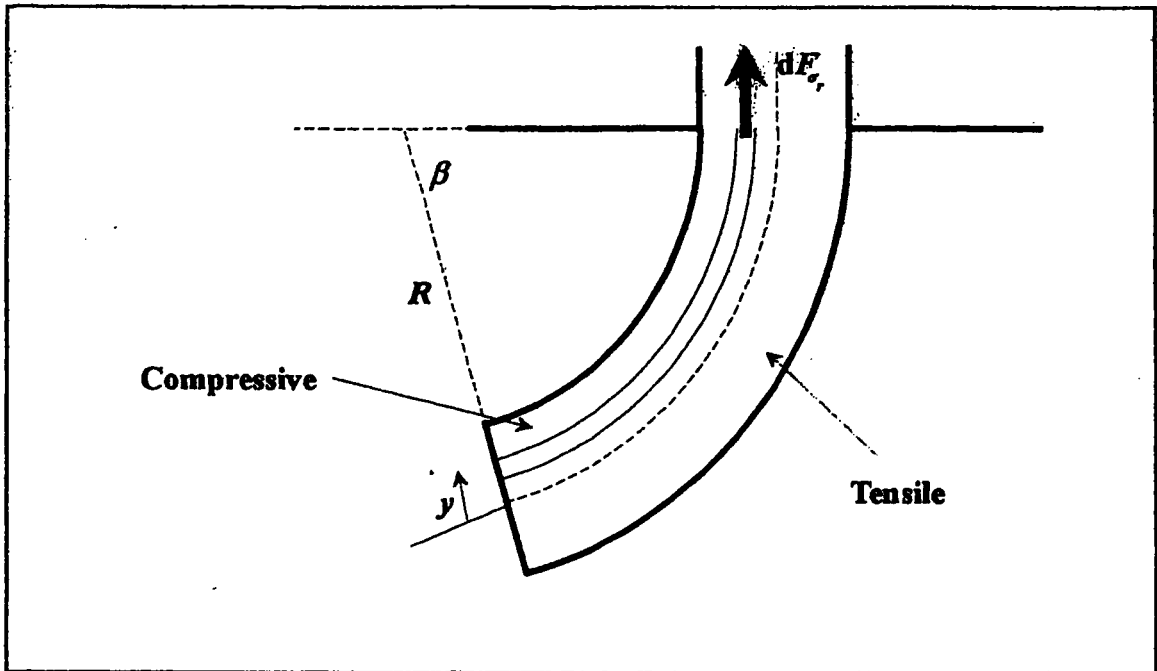


Figure A.5 Negative moment due to radial stress

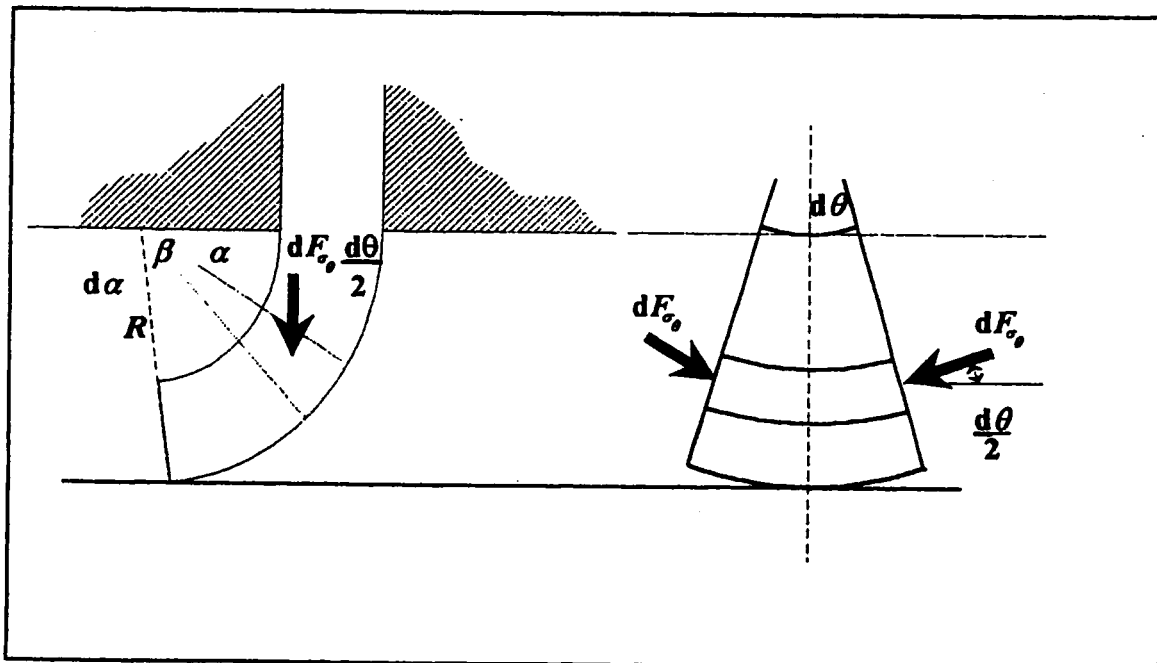


Figure A.6 Negative moment due to hoop stress component

APPENDIX B

FINITE ELEMENT ANALYSIS OF PIG SEALING DISC

Analysis of Pig Cup Disc

Presented to

Aidan O'Donoghue
of

CALtec

A subsidiary of the British Hydromechanics Research Group
bH^{Group}

9th October 1995

Presented by

Stephen Hodbod M.Eng
Laurence Marks B.Eng(Hons) C.Eng. M.I.Mech.E

Summary

This report details the work carried out by Desktop Engineering on the Finite Element Analysis of the Pig Cup Disc during the 2nd quarter of 1995. The results given are the product of extensive testing into the solution method and the models used have been checked for convergence. All models were solved using the Non-linear module of Cosmos/m.

Introduction

The Pig Cup Disc (described in the CALtec faxes of the 28th April 1995 and the 17th May 1995) acts to stop a flow of fluid from passing down a pipe, a static equilibrium is reached with the external forces such as the wall friction, wall reaction, clamping, differential pressure and stresses in the disc.

The Finite Element Model

Discretisation of Component Geometry

The finite element model is an axisymmetric representation of the Pig Cup Disc. The structure is constrained rigidly at its internal diameter and has a pressure applied to its lower face. The frictional force is simulated by two coupled forces applied to one corner in the relationship of $F_y = 0.8F_x$. The final model uses a mesh of 4x2 higher order HO plane2d elements. This mesh has been checked for convergence against a model of 10x4 HO plane2d elements, with values for the wall force changing by no more than 1%. (Note, the finer meshed model requires the addition of stiff struss elements around the position of the wall forces, to prevent some of the elements collapsing during the analysis).

Non-linear Solution Method

The analysis is a non-linear large strain, large displacement problem utilising a linear material model. The plane2d element formulation uses the Total Lagrangian (TL) option for large displacements with the full integration of terms.

Force control with the Newton Raphson NR iteration scheme is used to apply the pressure and wall forces under the control of two time curves. The opposing pressure and wall shear force are almost identical, therefore require careful control to achieve the desired loading path. Deformation dependent loading is not used since the wall forces act only in the X and Y directions, whereas the pressure loading is applied normal to the element faces and remains so during the analysis.

Material Properties

Three values of material have been used and are as follows: 3.5, 4.8, 6.2×10^6 N/m²

Results

The results presented below give values for the normal wall force for three values of material properties for a fixed displacement of 15×10^{-3} m at the mid plane edge of the Pig Cup Disc. The normal wall force w and differential pressure ΔP are then varied and the displacements given where the disc deformed within reasonable limits.

Elastic Modulus	$\text{N/m}^2 \times 10^6$	3.5	4.8	6.2
Normal Wall Force per Radian w	N	162.35	211.37	264.5
Normal Circumferencial Force	N/m	1292	1682	2104
Angle at Wall	Degrees	31.7	29.6	30.5

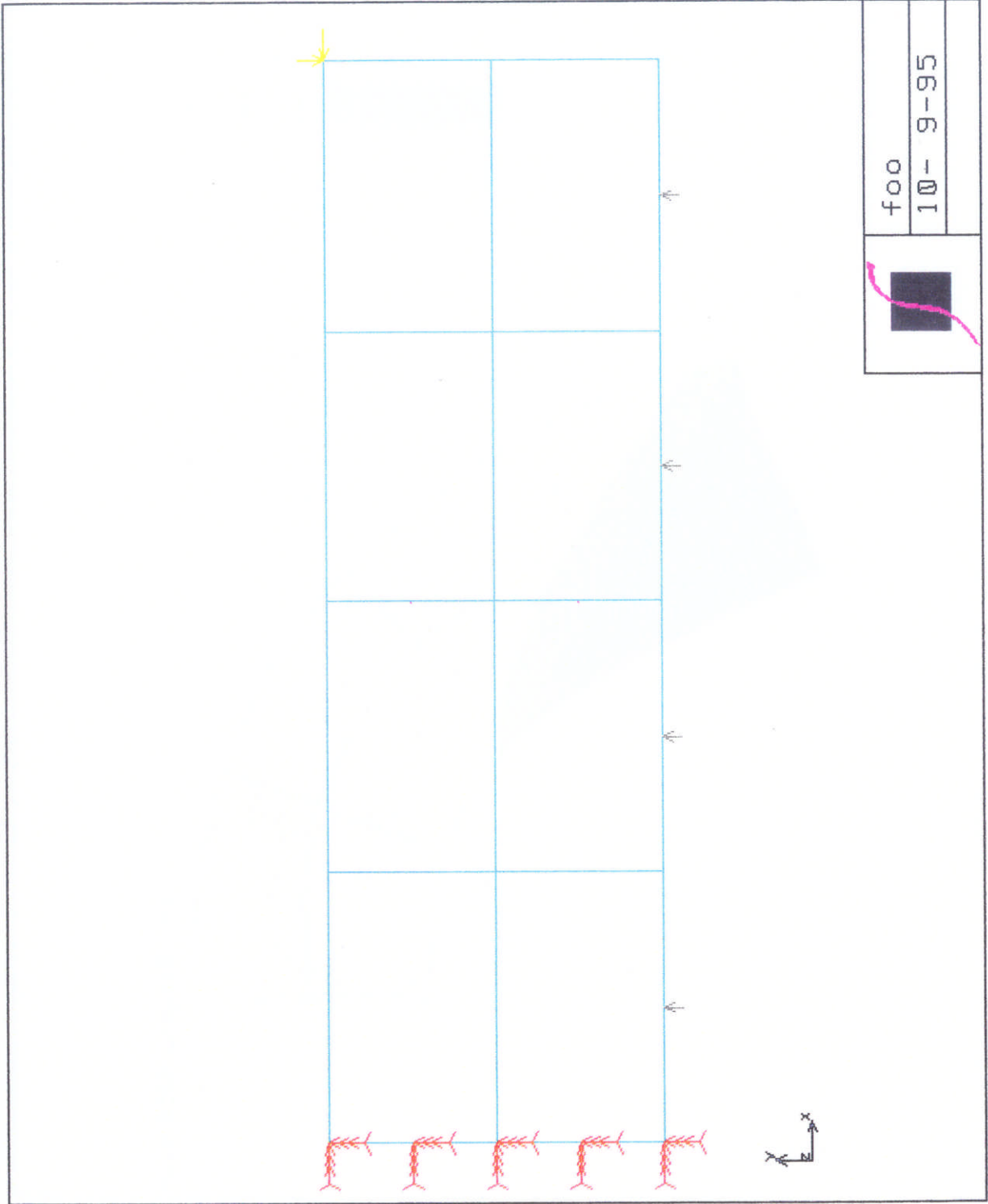
ΔP Pa $\times 10^5$	Friction Coefficient μ	Normal Wall Force	Displacement at mid plane edge of disc $\times 10^{-3}$ m		
0.1	0.8	$w/2$	-2.39	-2.52	-2.59
0.1		w	-21.2	-19.33	-18.3
0.5		$w/2$	+	+	+
0.5		w	-15.0	-15.0	-15.0
0.5		$2w$	-	-	-
1		w	+	+	+
1		$2w$	+	+	+
2		$2w$	+	+	+

Discussion

The disc is a very compliant structure with virtually identical loading applied to both sides and an end load which may cause the structure to deform in either direction. The rate of loading is crucial to the end state and can only be found by careful trial and error. In addition, the flexural weakness allows the disc to deform beyond allowable limits if either the pressure or the wall force is increased significantly in the solution method. The quoted angles for the disc at the wall are calculated from the nodal positions and are only approximate due to the discretisation of the mesh.

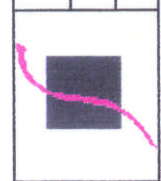
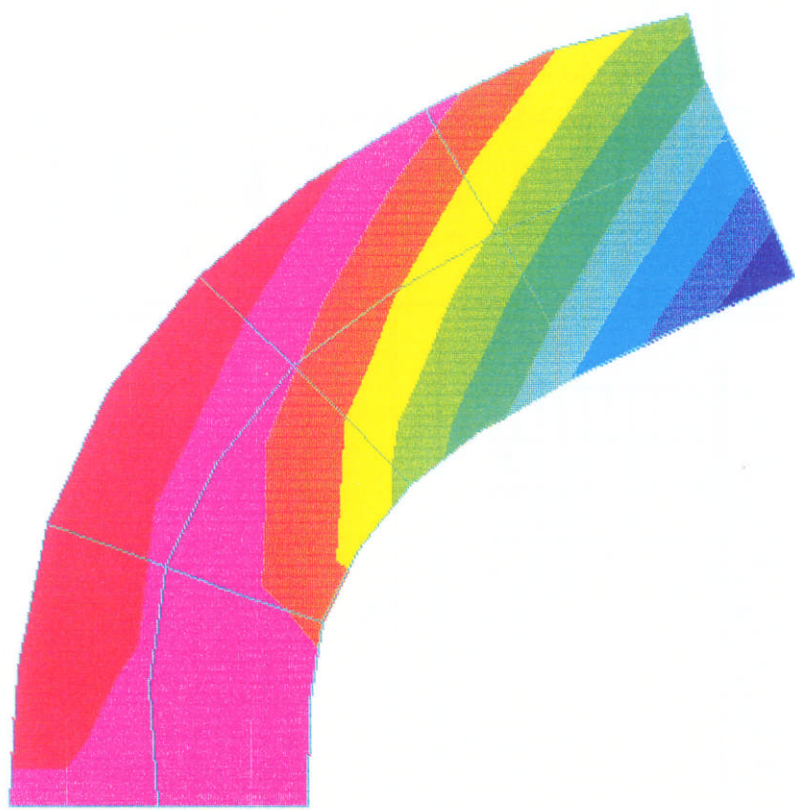
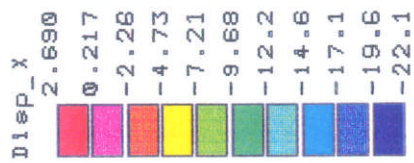
Conclusion

The values given for the normal wall force represent this type of solution method. A more accurate analysis may be possible from a sliding contact analysis.



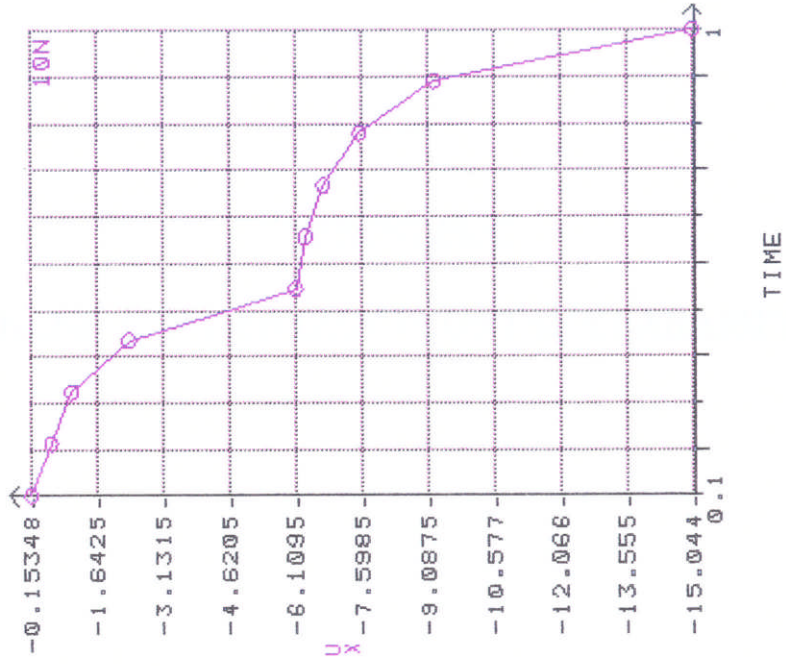
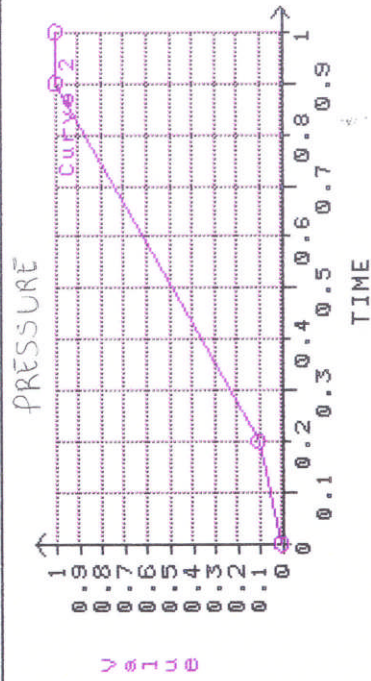
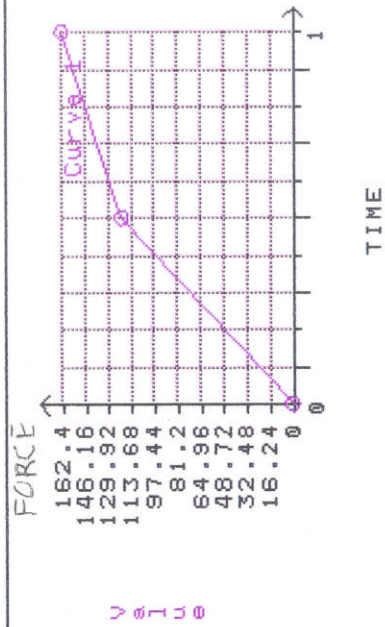
foo
10- 9-95

NL1n DISP Step:10 =1



foo

10- 9-95



foo

10- 9-95

APPENDIX C

WINKLER AND HERTZIAN CONTACT PARAMETERS

C. WINKLER AND HERTZIAN CONTACT PARAMETERS

C.1. Winkler analysis

Figure C.1 shows the assumed deformation of the parabolic punch according to a Winkler analysis. The positive footprint extreme is:-

$$a^+ = \sqrt{2 R \delta_o}$$

Since a^- is merely $-a^+$, then the half footprint length is:-

$$a = \sqrt{2 R \delta_o}$$

The total pressure is directly proportional to the deformation, or:-

$$P_t(x) = \frac{C E_c}{(1 - \nu^2) a} \left(\delta_o - \frac{x^2}{2 R} \right)$$

The point of maximum pressure is at $x = 0$, so:-

$$P_{t_o} = \frac{C E_c \delta_o}{(1 - \nu^2) a}$$

now, the total load w is equal to the integral of the pressure, i.e.:-

$$w = \int_{a^-}^{a^+} P_t(x) dx$$

$$= \frac{2 C E_c}{(1 - \nu^2) a} \int_0^{\sqrt{2 R \delta_o}} \delta_o - \frac{x^2}{2 R} dx$$

$$= \frac{2 C E_c \delta_o}{3 (1 - \nu^2)}$$

Therefore, the deformation is:-

$$\delta_o = \frac{3 (1 - \nu^2) w}{2 C E_c}$$

Substituting this into the expressions for a and P_{to} :-

$$a = \sqrt{\frac{3}{2 C}} \sqrt{\frac{(1 - \nu^2) R w}{E_c}}$$

$$P_{to} = \sqrt{\frac{3 C}{8}} \sqrt{\frac{E_c w}{(1 - \nu^2) R}}$$

$$= \frac{2 C E_c \delta_o}{3 (1 - \nu^2)}$$

C.2 Hertzian contact analysis

According to the Hertzian contact analysis, the deformation inside the contact is:-

$$\delta = \delta - \frac{x^2}{2R}$$

Therefore, the surface gradient is:-

$$\frac{d\delta}{dx} = -\frac{x}{R}$$

According to Johnson (1987), the surface gradient can also be expressed as:-

$$\frac{d\delta}{dx} = -\frac{2(1-\nu^2)}{\pi E_c} \int_{-a}^a \frac{P_f(s)}{x-s} ds$$

Combining the above, Johnson solves for $P_f(x)$:-

$$P_f(x) = -\frac{\pi E_c}{2(1-\nu^2)R} \frac{x^2 - a^2/2}{\pi \sqrt{a^2 - x^2}} + \frac{w}{\pi \sqrt{a^2 - x^2}}$$

now, $P_f(x) > 0$ for all x . Therefore,

$$w \geq \frac{\pi a^2 E_c}{4(1-\nu^2)R}$$

If w is greater than this expression, then $P_i(x)$ goes to infinity at the extremes of the contact footprint. Therefore:-

$$w = \frac{\pi a^2 E_c}{4 (1 - \nu^2) R}$$

Rearranging, this leads to the half footprint length:-

$$a = \sqrt{\frac{4}{\pi}} \sqrt{\frac{w R (1 - \nu^2)}{E_c}}$$

Since the pressure distribution is assumed to be elliptical, the peak pressure is estimated at:-

$$P_{t_0} = \sqrt{\frac{1}{\pi}} \sqrt{\frac{w E_c}{(1 - \nu^2) R}}$$

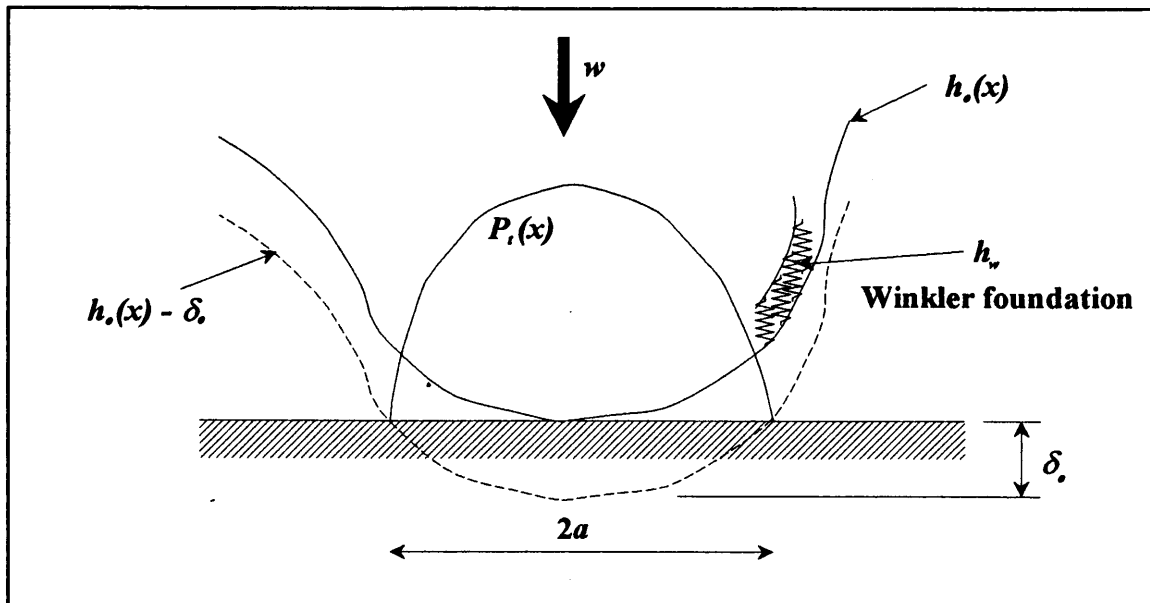


Figure C.1 Typical deformation of the punch

APPENDIX D

ASPERITY CONTACT PRESSURE

D. ASPERITY CONTACT PRESSURE

Figure D.1 shows the rough surface model. From Greenwood et al, (1966),

$$P_a(x) = \frac{4}{3} \frac{E_c}{(1 - \nu^2)} R_s^{\frac{1}{2}} \eta_s \int_h^{\infty} (z_s - h)^{\frac{3}{2}} e^{-\frac{z_s}{\sigma_s}} \phi(z_s) dz_s$$

Assuming a negative exponential distribution,

$$\phi(z_s) = \frac{e^{-\frac{z_s}{\sigma_s}}}{\sigma_s \sqrt{2\pi}}$$

And so:-

$$P_a(x) = \frac{4}{3} \frac{E_c}{(1 - \nu^2)} \frac{R_s^{\frac{1}{2}} \eta_s}{\sigma_s \sqrt{2\pi}} \int_h^{\infty} (z_s - h)^{\frac{3}{2}} e^{-\frac{z_s}{\sigma_s}} dz_s$$

Evaluating the integral:-

$$I_n = \int_h^{\infty} (z_s - h)^{n-1} e^{-\frac{z_s}{\sigma_s}} dz_s$$

Let

$$u = z_s - h$$

Differentiating:-

$$\frac{du}{dz_s} = 1$$

$$\rightarrow du = dz_s$$

Therefore:-

$$I_n = \int_0^{\infty} u^{n-1} e^{-\frac{u+h}{\sigma_s}} du$$

$$= e^{-\frac{h}{\sigma_s}} \int_0^{\infty} u^{n-1} e^{-\frac{u}{\sigma_s}} du$$

$$= \sigma_s^n e^{-\frac{h}{\sigma_s}} \int_0^{\infty} \left(\frac{u}{\sigma_s}\right)^{n-1} e^{-\frac{u}{\sigma_s}} d\left(\frac{u}{\sigma_s}\right)$$

$$= \sigma_s^n e^{-\frac{h}{\sigma_s}} \Gamma(n)$$

where Γ is the gamma function. Letting $n = 2.5$, then $\Gamma(1.5) = 1.33$ approximately.

Therefore, the asperity contact pressure is

$$P_a = 0.707 \frac{E_c}{(1 - \nu^2)} R_s^{1/2} \eta_s \sigma_s^{3/2} e^{-\frac{h}{\sigma_s}}$$

APPENDIX E

ITERATIVE ELASTOHYDRODYNAMIC PROGRAM

E. ELASTOHYDRODYNAMIC ANALYSIS PROGRAM

```
DECLARE SUB PROFILE (SIGS#, KS!, S!, DELO#, A#, X#(), XDASH#, H#(),  
    EC!, NU!, AN#, PPLUS!, M!, AP#, HO#, HSTAR#)  
DECLARE SUB SCALC (SIGS#, KS!, DELO#, A#, EC!, M!, NU!, PPLUS!,  
    ETA!, VP!, XDASH#, AN#, AP#, S!, HSTAR#, HO#)  
DECLARE SUB CONTACT (XDASH#, M!, W!, EC!, NU!, DELO#, A#, AP#,  
    AN#)  
DECLARE SUB PITIN (W!, XDASH#, M!, E!, NU!, KS!, SIGS#, PP!, VP!,  
    ETA!)
```

```
***** Comparison between EHL and IHL *****
```

```
***** Input *****
```

```
DIM XX#(100), HH#(100)  
CALL PITIN(W, XDASH#, M, E, NU, KS, SIGS#, PP, VP, ETA)  
  
CALL CONTACT(XDASH#, M, W, E, NU, DELO#, A#, AP#, AN#)  
  
CALL SCALC(SIGS#, KS, DELO#, A#, E, M, NU, PPLUS, ETA, VP, XDASH#,  
    AN#, AP#, S, HSTAR#, HO#)  
  
CALL PROFILE(SIGS#, KS, S, DELO#, A#, XX#(), XDASH#, HH#(), E, NU,  
    AN#, PPLUS, M, AP#, HO#, HSTAR#)
```

```
HIHL = HH#(30) / SIGS#
```

```
***** EHL PROGRAM *****
```

```
***** Dimension arrays *****
```

```
DIM X#(80), X(80), H(80), H#(80), HO#(80), PT(80), PA(80), PF1(80), PF2(80),  
    DEL#(80)
```

```
***** Initial calculations *****
```

```
HO# = SIGS#  
RELAX = 200  
X#(0) = AN#  
H#(0) = HO#  
HO#(0) = 0  
PT(0) = 1.013 * E * (DELO# + X#(0) / M + H#(0)) / ((1 - NU ^ 2) * A#)  
PA(0) = .707 * E * KS * EXP(-(H#(0) / SIGS#)) / (1 - NU ^ 2)  
PF1(0) = PP
```

```
FOR I = 1 TO 19
  X#(I) = X#(I - 1) + ABS(AN#) / 20
  HO#(I) = -X#(I) / M - DELO#
  H#(I) = HO#
  PT(I) = 1.013 * E * (H#(I) - HO#(I)) / ((1 - NU ^ 2) * A#)
  PA(I) = .707 * E * KS * EXP(-(H#(I) / SIGS#)) / (1 - NU ^ 2)
  PF1(I) = 0
NEXT
FOR I = 20 TO 39
  X#(I) = X#(I - 1) + XDASH# / 20
  H#(I) = HO#
  HO#(I) = -DELO#
  PT(I) = 1.013 * E * (H#(I) - HO#(I)) / ((1 - NU ^ 2) * A#)
  PA(I) = .707 * E * KS * EXP(-(H#(I) / SIGS#)) / (1 - NU ^ 2)
  PF1(I) = 0
NEXT
FOR I = 40 TO 59
  X#(I) = X#(I - 1) + ABS(XDASH# - AP#) / 20
  H#(I) = HO#
  HO#(I) = M * (X#(I) - XDASH#) - DELO#
  PT(I) = 1.013 * E * (H#(I) - HO#(I)) / ((1 - NU ^ 2) * A#)
  PA(I) = .707 * E * KS * EXP(-(H#(I) / SIGS#)) / (1 - NU ^ 2)
  PF1(I) = 0
NEXT
FOR I = 60 TO 80
  X#(I) = X#(I - 1) + ABS(XDASH# - AP#) / 2
  HO#(I) = M * (X#(I) - XDASH#) - DELO#
  H#(I) = HO#(I)
  PT(I) = 1.013 * E * (H#(I) - HO#(I)) / ((1 - NU ^ 2) * A#)
  PA(I) = .707 * E * KS * EXP(-(H#(I) / SIGS#)) / (1 - NU ^ 2)
  PF1(I) = 0
NEXT

***** Calculate CONV1 *****

S = 0
FOR I = 0 TO 80
  IF ABS(PA(I) + PF1(I) - PT(I)) < 5 THEN
    C = 0
  ELSE
    C = 1
  END IF
S = S + C
```

```

NEXT
CONV1 = S

***** The crux of the program *****

DO UNTIL CONV1 = 0
  RELAX = 200
  CLS
  PRINT "Outer loop, CONV1 = ", CONV1, CONV2, H#(30) / SIGS#

  ***** Calculate Fluid Pressure *****

  CONV2 = 80
  DO UNTIL CONV2 = 0
    PRINT "Inner loop, CONV2 = ", CONV2, CONV1, H#(30) /
    SIGS#
    FOR I = 1 TO 79
      PF2(I) = ((H#(I) ^ 3) * (PF1(I + 1) + PF1(I - 1)) + 3 *
      (H#(I) ^ 2) * (H#(I + 1) - H#(I)) * PF1(I + 1) + 6 * VP *
      ETA * (H#(I + 1) - H#(I)) * (X#(I + 1) - X#(I))) / ((H#(I)
      ^ 2) * (3 * H#(I + 1) - H#(I)))
    NEXT
    S = 0
    FOR I = 1 TO 79
      IF ABS(PF1(I) - PF2(I)) < 5 THEN
        C = 0
      ELSE
        C = 1
      END IF
      S = S + C
    NEXT
    CONV2 = S
    FOR I = 1 TO 79
      PF1(I) = PF2(I)
    NEXT
  LOOP
  S = 0
  FOR I = 0 TO 80
    DEL#(I) = (PF1(I) + PA(I) - PT(I)) * (1 - NU ^ 2) * A# / (1.013 *
    RELAX * E)
    H#(I) = H#(I) + DEL#(I)
    PT(I) = 1.013 * E * (H#(I) - HO#(I)) / ((1 - NU ^ 2) * A#)
    PA(I) = .707 * E * KS * EXP(-(H#(I) / SIGS#)) / (1 - NU ^ 2)
  
```

```

        IF ABS(PF1(I) + PA(I) - PT(I)) < 5 THEN
            C = 0
        ELSE
            C = 1
        END IF
        S = S + C
    NEXT

    '   OPEN "A:\EHL\OUT.DAT" FOR OUTPUT AS #1
    '   FOR I = 0 TO 80
    '       WRITE #1, X#(I), H#(I), PT(I), PA(I), PF1(I)
    '   NEXT
    '   CLOSE #1 .
    CONV1 = S
LOOP
OPEN "A:\EHL\OUT.DAT" FOR OUTPUT AS #1
FOR I = 0 TO 80
    X(I) = X#(I)
    H(I) = H#(I)
    WRITE #1, X(I), H(I), PT(I), PA(I), PF1(I)
NEXT
CLOSE #1

***** Screen Output *****

FOR I = 0 TO 59
    TA = TA + (PA(I + 1) + PA(I)) * (X#(I + 1) - X#(I)) / 2
    TT = TT + (PT(I + 1) + PT(I)) * (X#(I + 1) - X#(I)) / 2
NEXT
S = 1 - TA / TT
FA = .7 * TA * .254 * 3.14
FOR I = 0 TO 79
    TF = TF + ((PF1(I + 1) - PF1(I)) * H#(I) / ((X#(I + 1) - X#(I)) * 2) - VP *
    ETA / H#(I)) * .254 * 3.14 * (X#(I + 1) - X#(I))
NEXT
FF = TF
DP = 4 * (4 * (FA - FF) + .7 * 20 * 9.81) / (3.14 * .254 ^ 2)
FT = FA - FF
FOR I = 20 TO 39
    TOT = H#(I) + TOT
NEXT
HAVG = TOT / (20 * SIGS#)
MIN# = H#(20)

```

```

FOR I = 21 TO 40
  IF H#(I) < MIN# THEN
    MIN# = H#(I)
  END IF
NEXT
HMIN = MIN# / SIGS#
MAX# = H#(20)
FOR I = 21 TO 40
  IF H#(I) > MAX# THEN
    MAX# = H#(I)
  END IF
NEXT
HMAX = MAX# / SIGS#
CLS
BEEP
BEEP
PRINT
PRINT "***** Elastohydrodynamic Analysis Output *****"
PRINT
PRINT "Minimum film thickness, hmin = ", HMIN
PRINT "Average film thickness, havg = ", HAVG
PRINT "Maximum film thickness, hmax = ", HMAX
PRINT "IHL film thickness, hihl = ", HIHL
PRINT
PRINT "Pressure fraction, s = ", S
PRINT "Pig differential pressure, dP = ", DP
PRINT "Disk fluid friction, FF = ", FF
PRINT "Disk asperity friction FA = ", FA
PRINT "Total disk friction, FTOT = ", FT
END

```

E.1 Subroutine CONTACT()

```
SUB CONTACT (XDASH#, M, W, E, NU, DELO#, A#, AP#, AN#)
```

```
***** Calculate contact parameters *****
```

```

DELO1# = .000001 'Calculate local deformation
DELO2# = .0000001
CONV5 = 0
DO UNTIL CONV5 > .99
  A1# = ((M ^ 2) * DELO1# + XDASH# * M + DELO1#) / (2 * M)
  A2# = ((M ^ 2) * DELO2# + XDASH# * M + DELO2#) / (2 * M)

```



```

F1 = W - 1.013 * E * (M * (DELO1# ^ 2) / 2 + DELO1# * XDASH# +
(DELO1# ^ 2) / (2 * M)) / (A1# * (1 - NU ^ 2))
F2 = W - 1.013 * E * (M * (DELO2# ^ 2) / 2 + DELO2# * XDASH# +
(DELO2# ^ 2) / (2 * M)) / (A2# * (1 - NU ^ 2))
DTEMP# = DELO1# - F1 * (DELO2# - DELO1#) / (F2 - F1)
IF DELO1# > DTEMP# THEN
    CONV5 = ABS(DTEMP# / DELO1#)
ELSE
    CONV5 = ABS(DELO1# / DTEMP#)
END IF
DELO1# = DTEMP#
DELO2# = DELO1# + 1E-09
LOOP
DELO# = DELO1#

AN# = -DELO# * M           'Other contact parameters
AP# = XDASH# + DELO# / M
A# = (AP# - AN#) / 2

END SUB

```

E.2 Subroutine PUTIN()

```
SUB PUTIN (W, XDASH#, M, E, NU, KS, SIGS#, PP, VP, ETA)
```

```

OPEN "C:\PIGGING\SELECT\EHLIN.DAT" FOR INPUT AS #1
INPUT #1, W, XDASH#, M, E, NU, KS, SIGS#, PP, VP, ETA
CLOSE #1
DO
CLS
PRINT "Input:"
PRINT
PRINT "1. Wall force, w = "; W
PRINT "2. Chamfer length, x' = "; XDASH#
PRINT "3. Entry slope, m = "; M
PRINT "4. Elastic modulus, E = "; E
PRINT "5. Poissons ratio, v = "; NU
PRINT "6. Surface parameter, Ks = "; KS
PRINT "7. Surface roughness, os = "; SIGS#
PRINT "8. Pressure drop, dP = "; PP
PRINT "9. Pig velocity, Vp = "; VP
PRINT "10. Viscosity, u = "; ETA
PRINT

```

```
INPUT "Enter case to change, 0 to exit "; X
SELECT CASE X
  CASE 0
    EXIT DO
  CASE 1
    INPUT "Enter wall force, w = "; W
  CASE 2
    INPUT "Enter chamfer length, x' = "; XDASH#
  CASE 3
    INPUT "Enter entry slope, m = "; M
  CASE 4
    INPUT "Enter Elastic Modulus, E = "; E
  CASE 5
    INPUT "Enter Poissons ratio, v = "; NU
  CASE 6
    INPUT "Enter surface parameter, Ks = "; KS
  CASE 7
    INPUT "Enter surface roughness, os = "; SIGS#
  CASE 8
    INPUT "Enter pressure drop, dP = "; PP
  CASE 9
    INPUT "Enter pig velocity, Vp = "; VP
  CASE 10
    INPUT "Enter viscosity, u ="; ETA
  CASE ELSE
    BEEP
END SELECT
LOOP

OPEN "C:\PIGGING\SELECT\EHLIN.DAT" FOR OUTPUT AS #1
WRITE #1, W, XDASH#, M, E, NU, KS, SIGS#, PP, VP, ETA
CLOSE #1

END SUB
```

E.4 Subroutine PROFILE()

```
SUB PROFILE (SIGS#, KS, S, DELO#, A#, X#(), XDASH#, H#(), EC, NU, AN#,
  PPLUS, M, AP#, HO#, HSTAR#)
```

```
***** Calculate the film profile in the seal *****
```

```
***** Zone 2 *****
```

```

X#(20) = 0
DX2# = XDASH# / 20

FOR I = 21 TO 40
  H#(I) = HO# + 1.5 * HSTAR#
  X#(I) = X#(I - 1) + DX2#
NEXT

***** Zone 3 *****

DX3# = (AP# - XDASH#) / 20

FOR I = 41 TO 59
  X#(I) = X#(I - 1) + DX3#
  H1# = H#(I - 1)
  H2# = H1# * 1.1
  CONVP = 0
  DO UNTIL CONVP > .99
    F1 = .707 * KS * EXP(-H1# / SIGS#) - 1.013 * (1 - S) * (DELO#
      - M * (X#(I) - XDASH#) + H1#) / A#
    F2 = .707 * KS * EXP(-H2# / SIGS#) - 1.013 * (1 - S) * (DELO#
      - M * (X#(I) - XDASH#) + H2#) / A#
    HTEMP# = H1# - F1 * (H2# - H1#) / (F2 - F1)
    IF HTEMP# > H1# THEN
      CONVP = ABS(H1# / HTEMP#)
    ELSE
      CONVP = ABS(HTEMP# / H1#)
    END IF
    H1# = HTEMP#
    H2# = H1# * 1.1
  LOOP
  H#(I) = HTEMP#
NEXT
H#(60) = H#(59)           'For simplicity

END SUB

```

E.5 Subroutine SCALC()

```

SUB SCALC (SIGS#, KS, DELO#, A#, E, M, NU, PPLUS, ETA, VP, XDASH#,
  AN#, AP#, S, HSTAR#, HO#)

```

```

***** Calculate s, the pressure factor *****

```

```
HO# = -SIGS# * LOG(1.013 * DELO# / (.707 * KS * A#))
S = .0000001#
DS = .1
DO UNTIL DS < 1E-08
    DPFDX = 1.013 * E * S * (DELO# + 1.5 * HSTAR#) / ((1 - NU ^ 2) * A#
        *(AP# - XDASH#))
    HSTAR# = SQR(8 * ETA * VP / (9 * DPFDX))
    FUNC = .707 * KS * EXP(-(HO# + 1.5 * HSTAR#) / SIGS#) - 1.013 * (1
        - S)*(DELO# + 1.5 * HSTAR#) / A#
    IF FUNC < 0 THEN
        S = S + DS
    ELSE
        S = S - DS
        DS = DS / 10
    END IF
LOOP

END SUB
```

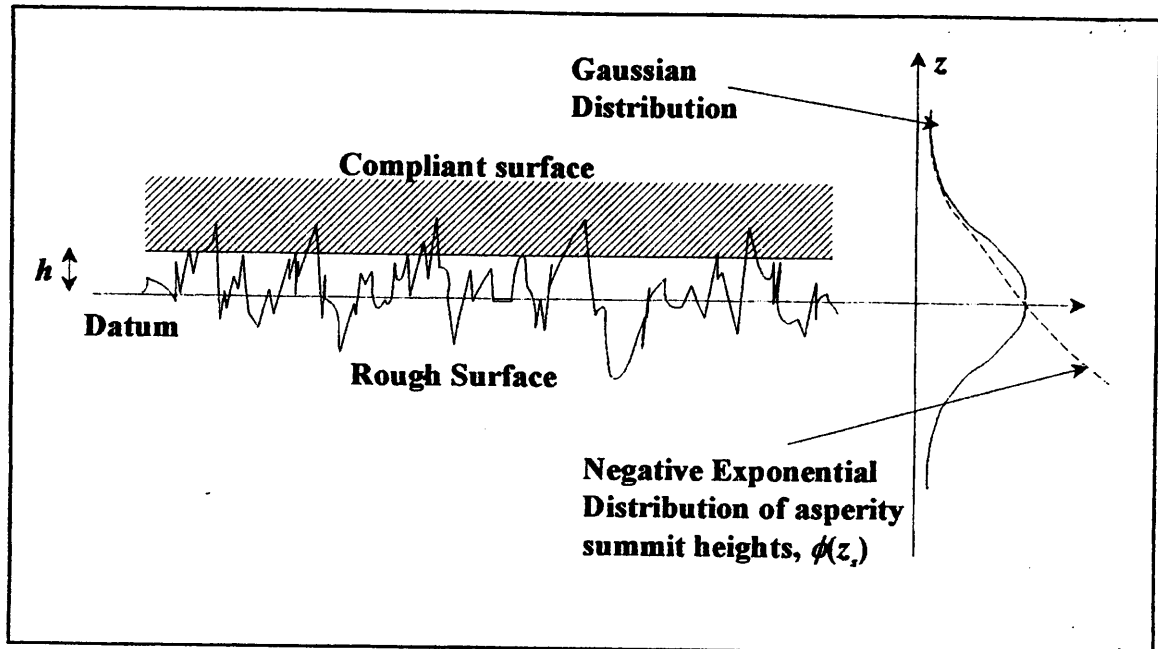


Figure D.1 Rough surface model

APPENDIX F

PIG*Plus* PROGRAM LISTING

F. PIGPlus PROGRAM LISTING

F.1. PIGPlus main program listing

***** PIGPlus Ver 1.0 *****

***** (c)Aidan O'Donoghue, 1995 *****

***** Declare subroutines *****

```
DECLARE SUB DRAW2 (X!)
DECLARE SUB DRAW1 (I!, DP!(), X!(), L!, M, XDASH#, T)
DECLARE SUB RESETER (FILE$())
DECLARE SUB LEAKAGE (VP, ETA, A#, H#(), PPLUS, CD, PI, D, QTOT,
    QREV, QFOR, SIGS#, VOL, NODE())
DECLARE SUB STORE2 (FILE$(), I, J, VPIG(), DP, QTOT, QFOR, QREV)
DECLARE SUB STORE1 (I, DP, QTOT, QFOR, QREV, XDASH#, WEAR(), S,
    W, M, H#(), FA, FF, L, LDASH)
DECLARE SUB REMOVE (I, SIGS#, A#, M, KWEAR, WA, NODE(), XDASH#)
DECLARE SUB CONVGT (DP!, FRICT!, DP1!, FRICT1!, CONV!)
DECLARE SUB PRESSURE (W, HO#, HSTAR#, DELO#, M, WA, PI, F, D, EC,
    KS,H#(), SIGS#, X#(), NU, PPLUS, ETA, VP, S, A#, FRICT, MASS, G,
    DP, N, FA, FF, XDASH#, AP#)
DECLARE SUB PROFILE (SIGS#, KS, S, DELO#, A#, X#(), XDASH#, H#(),
    EC, NU,AN#, PPLUS, M, AP#, HO#, HSTAR#)
DECLARE SUB CONTACT (XDASH#, M!, W!, EC!, NU!, DELO#, A#, AP#,
    AN#)
DECLARE SUB SCALC (SIGS#, KS, DELO#, A#, EC, M, NU, PPLUS, ETA,
    VP,XDASH#, AN#, AP#, S, HSTAR#, HO#)
DECLARE SUB FORCE (PI, DD, DELO#, XDASH#, M, EC, ET, D, PHI, B, R,
    FRICT, PPLUS, T, NU, W, HSTAR#, HO#, L, LDASH1)
DECLARE SUB MAINS (PI, DD, XDASH#, EC, ET, D, PHI, T, NU, SIGS#, KS,
    ETA, X#(), H#(), VPIG(), F, MASS, G, CD, FILE$(), I, N, DP2())
DECLARE SUB INIT (DP1!, FRICT!)
DECLARE SUB WEARS (XDASH#, N, PI, DD, EC, ET, D, PHI, T, NU, SIGS#,
    KS,ETA, VP, X#(), H#(), F, MASS, G, CD, I, WEAR(), NODE(),
    KWEAR, DP())
DECLARE SUB FILER (FILE$())
DECLARE SUB SAMPLE (VMAX!, L!, WEAR!(), NODE!(), VPIG!(), MAIN!())
DECLARE SUB PUTIN (L, D, KS, SIGS#, EC, ET, F, KWEAR, MASS, N,
    XDASHO#, NU, PHI, DD, T, CD, VP, ETA, G, PI, VMAX)
DECLARE SUB WIND (X!)
DECLARE SUB TITLE (X!)
```

***** Show title on screen *****

```
CLS
SCREEN 12
CALL TITLE(X)
```

***** Setup window *****

```
CALL WIND(X)
```

***** Dimension arrays *****

```
DIM WEAR(20), NODE(20), VPIG(20), MAIN(20), FILE$(20)
DIM QTOT(20), QFOR(20), QREV(20), DP(20), DP2(20), XDASH#(20)
DIM X$(60), H$(60)
```

***** Accept input into programme *****

```
CALL PUTIN(L, D, KS, SIGS#, EC, ET, F, KWEAR, MASS, N, XDASHO#, NU,
          PHI, DD, T, CD, VP, ETA, G, PI, VMAX)
```

***** Setup sampling points *****

```
CALL SAMPLE(VMAX, L, WEAR(), NODE(), VPIG(), MAIN())
```

***** Setup files for storage *****

```
CALL FILER(FILE$())
```

***** Reset storage files *****

```
CALL RESETTER(FILE$())
```

***** PIGPlus calculations *****

```
XDASH# = XDASHO#           'Set chamfer length to initial length
FOR I = 0 TO 20           'Start pig motion through pipeline
    IF MAIN(I) = 1 THEN   'If MAIN(I) = 1 then branch to MAINS
        CALL MAINS(PI, DD, XDASH#, EC, ET, D, PHI, T, NU, SIGS#,
                  KS, ETA, X#(), H#(), VPIG(), F, MASS, G, CD, FILE$(), I, N,
                  DP2())
    END IF
```



```

CALL WEARS(XDASH#, N, PI, DD, EC, ET, D, PHI, T, NU, SIGS#, KS,
ETA, VP, X#(), H#(), F, MASS, G, CD, I, WEAR(), NODE(),
KWEAR, DP())
NEXT
***** The End *****
END

```

The following subroutines are listed in alphabetical order.

F.2. Subroutine CONTACT()

```
SUB CONTACT (XDASH#, M, W, EC, NU, DELO#, A#, AP#, AN#)
```

```
***** Calculate contact parameters *****
```

```

DELO1# = .000001      'Calculate local deformation
DELO2# = .0000001
CONV5 = 0
DO UNTIL CONV5 > .99
  A1# = ((M ^ 2) * DELO1# + XDASH# * M + DELO1#) / (2 * M)
  A2# = ((M ^ 2) * DELO2# + XDASH# * M + DELO2#) / (2 * M)
  F1 = W - 1.013 * EC * (M * (DELO1# ^ 2) / 2 + DELO1# * XDASH# +
    (DELO1# ^ 2) / (2 * M)) / (A1# * (1 - NU ^ 2))
  F2 = W - 1.013 * EC * (M * (DELO2# ^ 2) / 2 + DELO2# * XDASH# +
    (DELO2# ^ 2) / (2 * M)) / (A2# * (1 - NU ^ 2))
  DTEMP# = DELO1# - F1 * (DELO2# - DELO1#) / (F2 - F1)
  IF DELO1# > DTEMP# THEN
    CONV5 = ABS(DTEMP# / DELO1#)
  ELSE
    CONV5 = ABS(DELO1# / DTEMP#)
  END IF
  DELO1# = DTEMP#
  DELO2# = DELO1# + 1E-09
LOOP
DELO# = DELO1#

AN# = -DELO# * M      'Other contact parameters
AP# = XDASH# + DELO# / M
A# = (AP# - AN#) / 2

```

'Where:

```
' DELO# = Local deformation
' AN# = Negative seal footprint extreme
' AP# = Positive seal footprint extreme
' A# = Half footprint length

***** Return to WEARS or MAINS routine *****

END SUB
```

F.3. Subroutine CONVGTO

```
SUB CONVGTO (DP, FRICT, DP1, FRICT1, CONV)
```

```
***** Test for convergence on WEARS routine *****

IF DP > DP1 THEN
    CONV = ABS(DP1 / DP)
ELSE
    CONV = ABS(DP / DP1)
END IF
DP1 = (DP1 + DP) / 2
FRICT1 = (FRICT1 + FRICT) / 2

***** Return to WEARS or MAINS routine *****

END SUB
```

F.4 Subroutine DRAW()

```
SUB DRAW1 (I, P(), X(), L, M, XDASH#, T)
```

```
***** Subroutine for drawing current situation *****

CLS 2

***** Setup axis *****

LINE (50, 300)-(570, 300)
LINE (100, 325)-(100, 50)
LINE (570, 295)-(580, 300)
LINE (580, 300)-(570, 305)
LINE (570, 305)-(570, 295)
LINE (100, 40)-(105, 50)
```

LINE (105, 50)-(95, 50)
LINE (95, 50)-(100, 40)

***** Titles *****

```
PRINT "                PIGPlus - WEARS Module"
PRINT
PRINT
PRINT
PRINT " D"
PRINT " i"
PRINT " f P"
PRINT " f r"
PRINT " e e"
PRINT " r s"
PRINT " e s"
PRINT " n u"
PRINT " t r"
PRINT " i e"
PRINT " a"
PRINT " l"
PRINT
PRINT
PRINT
PRINT
PRINT "                Distance "
```

***** Pipewall *****

```
LINE (300, 100)-(500, 100)
LINE (325, 100)-(300, 125)
LINE (350, 100)-(325, 125)
LINE (375, 100)-(350, 125)
LINE (400, 100)-(375, 125)
LINE (425, 100)-(400, 125)
LINE (450, 100)-(425, 125)
LINE (475, 100)-(450, 125)
LINE (500, 100)-(475, 125)
```

***** Seal and chamfer *****

```
A = CINT(100 * XDASH# / T)
B = CINT(50 / M)
```

```
LINE (350, 100)-(350 + A, 100), 4
LINE (350 + A, 100)-(B + 350 + A, 50), 4
LINE (350, 100)-(325, 50), 4
```

```
END SUB
```

F.5 Subroutine DRAW2()

```
SUB DRAW2 (X)
```

```
'***** Subroutine for drawing current situation *****
```

```
CLS 2
```

```
'***** Setup axis *****
```

```
LINE (50, 300)-(570, 300)
LINE (100, 325)-(100, 50)
LINE (570, 295)-(580, 300)
LINE (580, 300)-(570, 305)
LINE (570, 305)-(570, 295)
LINE (100, 40)-(105, 50)
LINE (105, 50)-(95, 50)
LINE (95, 50)-(100, 40)
```

```
'***** Titles *****
```

```
PRINT "                PIGPlus - MAINS Module"
PRINT
PRINT
PRINT
PRINT " D"
PRINT " i"
PRINT " f P"
PRINT " f r"
PRINT " e e"
PRINT " r s"
PRINT " e s"
PRINT " n u"
PRINT " t r"
PRINT " I e"
PRINT " a"
```

```

PRINT " 1"
PRINT
PRINT
PRINT
PRINT
PRINT "
                                Velocity"

END SUB

```

F.6 Subroutine FILER()
SUB FILER (FILE\$(I))

```

***** Setup Storage Files *****

OPEN "C:\PIGGING\PROGRAMFILES.DAT" FOR INPUT AS #1
FOR I = 0 TO 20
    INPUT #1, FILE$(I) 'Storage files for MAINS output
NEXT
CLOSE #1

***** Return to main routine *****

END SUB

```

F.7 Subroutine FORCE()
SUB FORCE (PI, DD, DELO#, XDASH#, M, EC, ET, D, PHI, B, R, FRICT1,
PPLUS,T, NU, W, HSTAR#, HO#, L, LDASH1)

```

***** Calculate shape *****

L = (DD - PHI) / 2
B1 = .1
B2 = .2
CONV3 = 0 'Calculate angle, B
DO UNTIL CONV3 > .99
    LDASH1 = (D - PHI) / 2 - (T * SIN(B1)) / 2 - HSTAR# - HO# + DELO#
              + XDASH# * SIN(PI / 2 - B1) * COS(PI / 2 - B1)
    LDASH2 = (D - PHI) / 2 - (T * SIN(B2)) / 2 - HSTAR# - HO# + DELO#
              + XDASH# * SIN(PI / 2 - B2) * COS(PI / 2 - B2)
    F1 = L / B1 - LDASH1 / SIN(B1)
    F2 = L / B2 - LDASH1 / SIN(B2)

```

```

      BTEMP = B1 - F1 * (B2 - B1) / (F2 - F1)
      IF B1 > BTEMP THEN
        CONV3 = ABS(BTEMP / B1)
      ELSE
        CONV3 = ABS(B1 / BTEMP)
      END IF
      B1 = BTEMP
      B2 = B1 + .001

LOOP
B = B1
R = L / B
M = TAN(PI / 2 - B)

'Where:
'   L = Seal unstressed length
'   B = Seal axial angle
'   R = Seal axial radius
'   LDASH = Seal stressed radial length
'   M = Inlet slope into seal

***** Calculate wall force *****

RO = D / 2           'Geometry considerations
RI = PHI / 2
MF = FRICT1 * RO * (RO - RI)  'Calculate moments
MDP = PPLUS * (R ^ 2) * (RI - RI * COS(B) + R * B / 2 - R * (SIN(2 * B)) / 4)
MRT = ET * RI * (T ^ 3) / (24 * R)
MRC = EC * RI * (T ^ 3) / (24 * R)

INTEG = 0           'Hoop moment calculation
ALPHA = 0
DALPHA = B / 20
FOR I = 1 TO 20
  ALPHA = ALPHA + DALPHA
  INTEG = INTEG + (ALPHA - SIN(ALPHA)) * (1 - COS(ALPHA)) *
    DALPHA / (ALPHA + RI / R)
NEXT
MH = EC * (R ^ 2) * T * INTEG / (1 - NU ^ 2)

W = (MDP + MRT + MRC + MH - MF) / (RO * R * (1 - COS(B)))  'Wall force
IF W < 0 THEN
  W = 50
  'Precaution in case of negative wall
  force

```

END IF

'Where:

' RO = Half pipe diameter/pipe radius
 ' RI = Half pig hub diameter
 ' MF = Moment due to friction
 ' MDP = Moment due to differential pressure
 ' MRT = Moment due to radial tensile stress
 ' MRC = Moment due to radial compressive stress
 ' MH = Moment due to hoop stress
 ' W = Wall force

'***** Return to WEARS or MAINS routine *****

END SUB

F.8 Subroutine INIT()
 SUB INIT (DP1, FRICT1)

'***** Sets up initial conditions for iterative solution *****

DP1 = 0
 FRICT1 = 0

'Where:

' DP1 = Differential pressure across the pig
 ' FRICT1 = Friction per unit length at seal tip

'***** Return to WEAR or MAINS routine *****

END SUB

F.9. Subroutine LEAKAGE()
 SUB LEAKAGE (VP, ETA, A#, H#(), PPLUS, CD, PI, D, QTOT, QREV, QFOR,
 SIGS#, VOL, NODE())

'***** Subroutine for calculation of leakage past the seals *****

'***** Mid-film height *****

HHAT# = H#(30) + 2.5 * SIGS#

***** Calculate leakage *****

IF HHAT# < 0 THEN

 QFOR = 0

 QREV = 0

 QTOT = 0

ELSE

 DIM Z#(50), U(50)

 ***** Setup velocity profile, u(z) *****

 Z#(0) = 0

 DZ# = HHAT# / .50

 U(0) = 0

 Z#(0) = 0

 FOR I = 1 TO 50

 Z#(I) = Z#(I - 1) + DZ#

 U(I) = PPLUS * (Z#(I) ^ 2 - HHAT# * Z#(I)) / (2 * ETA * 2 * A#)
 + VP * Z#(I) / HHAT#

 NEXT

 ***** Total leakage *****

 QTOT = 0

 FOR I = 1 TO 50

 QTOT = QTOT + (U(I - 1) + U(I)) * DZ# / 2

 NEXT

 ***** Reverse and forward leakage *****

 QREV = 0

 QFOR = 0

 FOR I = 1 TO 50

 IF U(I) < VP THEN

 QREV = QREV + (U(I - 1) + U(I)) * DZ# / 2

 ELSE

 QFOR = QFOR + (U(I - 1) + U(I)) * DZ# / 2

 END IF

 NEXT

END IF

'Where:


```
' QTOT = Total leakage
' QREV = Reverse leakage
' QFOR = Forward leakage
' U() = Velocity profile
' Z() = Radial axis
```

```
***** Return to WEARS or MAINS routine *****
```

```
END SUB
```

F.10 Subroutine MAINS()

```
SUB MAINS (PI, DD, XDASH#, EC, ET, D, PHI, T, NU, SIGS#, KS, ETA, X#(),
          H#(), VPIG(), F, MASS, G, CD, FILE$, I, N, DP2())
```

```
***** Pig characteristic against velocity *****
```

```
DIM NODE(20)
FOR J = 0 TO 20
```

```
***** Setup MAINS window *****
```

```
VPIG = VPIG(J)
```

```
***** Setup initial conditions *****
```

```
CALL INIT(DP1, FRICT1)
```

```
***** Convergence loop *****
```

```
CONV2 = 0
DO UNTIL CONV2 > .99
```

```
***** Set up loop initial conditions *****
```

```
PPLUS = DP1 / N
```

```
***** Calculate wall force *****
```

```
CALL FORCE(PI, DD, DELO#, XDASH#, M, EC, ET, D, PHI, B,
          R, FRICT1, PPLUS, T, NU, W, HSTAR#, HO#, L,
          LDASH1)
```

***** Calculate contact parameters *****

CALL CONTACT(XDASH#, M, W, EC, NU, DELO#, A#, AP#, AN#)

***** Calculate pressure factor *****

CALL SCALC(SIGS#, KS, DELO#, A#, EC, M, NU, PPLUS, ETA, VPIG, XDASH#, AN#, AP#, S, HSTAR#, HO#)

***** Setup film profile *****

CALL PROFILE(SIGS#, KS, S, DELO#, A#, X#(), XDASH#, H#(), EC, NU, AN#, PPLUS, M, AP#, HO#, HSTAR#)

***** Calculate differential pressure *****

CALL PRESSURE(W, HO#, HSTAR#, DELO#, M, WA, PI, F, D, EC, KS, H#(), SIGS#, X#(), NU, PPLUS, ETA, VPIG, S, A#, FRICT, MASS, G, DP, N, FA, FF, XDASH#, AP#)

***** Convergence? *****

CALL CONVGT(DP, FRICT, DP1, FRICT1, CONV2)

LOOP

***** Calculate leakage *****

CALL LEAKAGE(VPIG, ETA, A#, H#(), PPLUS, CD, PI, D, QTOT, QREV, QFOR, SIGS#, VOL, NODE())

***** Store data to file *****

CALL STORE2(FILE\$, I, J, VPIG(), DP, QTOT, QFOR, QREV)

DP2(J) = DP

CALL DRAW2(X)

PRINT "Node "; J

IF J > 0 THEN

FOR K = 1 TO J

X1 = CINT(100 + 470 * VPIG(K) / VPIG(20))

X2 = CINT(100 + 470 * VPIG(K - 1) / VPIG(20))

```

        Y1 = CINT(300 - 250 * (DP2(K)) / (DP2(0)))
        Y2 = CINT(300 - 250 * (DP2(K - 1)) / (DP2(0)))
        LINE (X1, Y1)-(X2, Y2), 10
    NEXT
END IF

NEXT

***** Return to main routine *****

END SUB

```

F.11 Subroutine PRESSURE()

```

SUB PRESSURE (W, HO#, HSTAR#, DELO#, M, WA, PI, F, D, EC, KS, H#(),
SIGS#, X#(), NU, PPLUS, ETA, VP, S, A#, FRICT, MASS, G, DP, N, FA,
FF, XDASH#, AP#)

```

```

***** Calculation of pig differential pressure *****

```

```

WA = (1 - S) * W           'Asperity load
FA = F * WA                'Asperity friction
FF = 0

```

```

***** Zone 2 fluid priction *****

```

```

FOR I = 21 TO 40
    FF = FF + (-ETA * VP / H#(I)) * (X#(I) - X#(I - 1))
NEXT

```

```

***** Zone 3 fluid priction *****

```

```

DPFDX3 = -1.013 * EC * (DELO# + 1.5 * HSTAR#) / ((1 - NU ^ 2) * (AP# -
XDASH#))

FOR I = 41 TO 60
    FF = FF + (DPFDX3 * H#(I) / 2 - VP * ETA / H#(I)) * (X#(I) - X#(I - 1))
NEXT
FTOT = N * PI * D * (FA - FF) + F * MASS * G
FRICT = FA - FF
DP = 4 * FTOT / (PI * D ^ 2)

```

'Where:

' FA = Asperity friction
 ' FF = Fluid friction
 ' FTOT = Total friction
 ' FRICT = Friction on seal tip
 ' DP = Current differential across pig

'***** Return to MAIN or WEARS routine *****

END SUB

F.12 Subroutine PROFILE()

SUB PROFILE (SIGS#, KS, S, DELO#, A#, X#(), XDASH#, H#(), EC, NU, AN#,
 PPLUS, M, AP#, HO#, HSTAR#)

'***** Calculate the film profile in the seal *****

'***** Zone 2 *****

X#(20) = 0
 DX2# = XDASH# / 20

FOR I = 21 TO 40
 H#(I) = HO# + 1.5 * HSTAR#
 X#(I) = X#(I - 1) + DX2#
 NEXT

'***** Zone 3 *****

DX3# = (AP# - XDASH#) / 20

FOR I = 41 TO 59
 X#(I) = X#(I - 1) + DX3#
 H1# = H#(I - 1)
 H2# = H1# * 1.1
 CONV# = 0
 DO UNTIL CONV# > .99
 F1 = .707 * KS * EXP(-H1# / SIGS#) - 1.013 * (1 - S) * (DELO#
 - M * (X#(I) - XDASH#) + H1#) / A#
 F2 = .707 * KS * EXP(-H2# / SIGS#) - 1.013 * (1 - S) * (DELO#
 - M * (X#(I) - XDASH#) + H2#) / A#
 HTEMP# = H1# - F1 * (H2# - H1#) / (F2 - F1)

```

        IF HTEMP# > H1# THEN
            CONV# = ABS(H1# / HTEMP#)
        ELSE
            CONV# = ABS(HTEMP# / H1#)
        END IF
        H1# = HTEMP#
        H2# = H1# * 1.1
    LOOP
    H#(I) = HTEMP#
NEXT
H#(60) = H#(59)           'For simplicity

```

'Where:

' H#() = Film profile
' X#() = X-axis

***** Return to WEARS or MAINS routine *****

END SUB

F.13 Subroutine PUTIN()

```

SUB PUTIN (L, D, KS, SIGS#, EC, ET, F, KWEAR, MASS, N, XDASHO#, NU,
          PHI, DD, T, CD, VP, ETA, G, PI, VPMAX)

```

***** Input data into programme *****

```

OPEN "C:\PIGGING\PROGRAM\PIPELINE.DAT" FOR INPUT AS #1 'Pipeline
data input
INPUT #1, L, D, KS, SIGS#
CLOSE #1
DO
    CLS 1
    PRINT "Pipeline data:"
    PRINT
    PRINT "1. Pipeline length, L =           ", L; "m"
    PRINT "2. Pipeline diameter, d =           ", D; "m"
    PRINT "3. Roughness parameter, Ks =           ", KS
    PRINT "4. Std deviation of roughness height, os = ", SIGS#; "m"
    PRINT
    PRINT
    PRINT
    PRINT

```

```
PRINT
PRINT
PRINT
PRINT
PRINT
PRINT
PRINT
PRINT
PRINT
PRINT
PRINT
INPUT "Enter case number to change (0 to quit) ", X
SELECT CASE X
    CASE 1
        INPUT "Enter new pipeline length, L ", L
    CASE 2
        INPUT "Enter new pipeline diameter, d ", D
    CASE 3
        INPUT "Enter roughness parameter, Ks ", KS
    CASE 4
        INPUT "Enter Std deviation of roughness, os ", SIGS#
    CASE 0
        EXIT DO
    CASE ELSE
        BEEP
END SELECT
LOOP
OPEN "C:\PIGGING\PROGRAM\PIPELINE.DAT" FOR OUTPUT AS #1
WRITE #1, L, D, KS, SIGS#
CLOSE #1

'Where:
' L = Length of Pipeline (meters)
' D = Internal Diameter of Pipeline (meters)
' KS = Surface Parameter (-), see explanation in Chapter 4
' SIGS = Standard deviation of asperity heights (m)

OPEN "C:\PIGGING\PROGRAM\PIG.DAT" FOR INPUT AS #1      'Pig data
input
INPUT #1, EC, ET, F, KWEAR, MASS, N, XDASHO#, NU, PHI, DD, T, CD
CLOSE #1
DO
    CLS 1
    PRINT "Pig Data:"
```

```
PRINT
PRINT "1. Compressive Youngs Modulus, Ec = ", EC; "Pa"
PRINT "2. Tensile Youngs Modulus, Et = ", ET; "Pa"
PRINT "3. Dynamic coefficient of friction, f = ", F
PRINT "4. Wear coefficient, Kwear = ", KWEAR
PRINT "5. Mass of pig, M = ", MASS; "kg"
PRINT "6. Number of sealing disks, n = ", N
PRINT "7. Initial champhor length, x'o = ", XDASHO#; "m"
PRINT "8. Poissons ratio, v = ", NU
PRINT "9. Pig body hub diameter, O = ", PHI; "m"
PRINT "10. Sealing disk diameter, D = ", DD; "m"
PRINT "11. Sealing disk thickness, t = ", T; "m"
PRINT "12. Coefficient of discharge, Cd = ", CD
PRINT
PRINT
PRINT
PRINT
PRINT
PRINT
INPUT "Enter case to change (0 to exit) ", X
SELECT CASE X
CASE 1
    INPUT "Enter Compressive Youngs Modulus, Ec ", EC
CASE 2
    INPUT "Enter Tensile Youngs Modulus, Et ", ET
CASE 3
    INPUT "Enter Dynamic coefficient of friction, f ", F
CASE 4
    INPUT "Enter Coefficient of wear, Kwear ", KWEAR
CASE 5
    INPUT "Enter pig mass, M ", MASS
CASE 6
    INPUT "Enter number of sealing disks, n ", N
CASE 7
    INPUT "Enter initial champhor length, x'o ", XDASHO#
CASE 8
    INPUT "Enter Poissons ratio, v ", NU
CASE 9
    INPUT "Enter pig bdy hub diameter, O ", PHI
CASE 10
    INPUT "Enter Sealing disk diameter, D ", DD
CASE 11
    INPUT "Enter Sealing disk thickness, t ", T
```

```

CASE 12
    INPUT "Enter coefficient of discharge, Cd ", CD
CASE 0
    EXIT DO
CASE ELSE
    BEEP
END SELECT
LOOP
OPEN "C:\PIGGING\PROGRAMPIG.DAT" FOR OUTPUT AS #1
WRITE #1, EC, ET, F, KWEAR, MASS, N, XDASHO#, NU, PHI, DD, T, CD
CLOSE #1

```

'Where:

```

' EC = Compressive Youngs Modulus, (Pascals)
' EC = Tensile Youngs Modulus, (Pascals)
' F = Coefficient of Static Friction (-)
' KWEAR = Wear Coefficient (-)
' MASS = Mass of pig (kg)
' N = Number of seals (-)
' XDASHO# = Initial champhor on seal (m)
' NU = Poissons Ratio (-)
' PHI = Diameter of pig central shaft (m)
' DD = Diameter of pig disk seal (m)
' T = Thickness of pig disk seal (m)
' CD = Discharge coefficient through seal (-)

```

```

OPEN "C:\PIGGING\PROGRAMOPER.DAT" FOR INPUT AS #1 'Operation
data input
INPUT #1, VP, ETA
CLOSE #1
DO
    CLS 1
    PRINT "Operational data:"
    PRINT
    PRINT "1. Pig velocity, Vp = ", VP; "m/s"
    PRINT "2. Fluid viscosity, eta = ", ETA; "Pa.s"
    PRINT
    PRINT
    PRINT
    PRINT
    PRINT
    PRINT
    PRINT
    PRINT

```



```
PRINT
PRINT
PRINT
PRINT
PRINT
PRINT
PRINT
PRINT
PRINT
PRINT
INPUT "Enter case to change (0 to exit) ", X
SELECT CASE X
  CASE 1
    INPUT "Enter pig velocity, Vp ", VP
  CASE 2
    INPUT "Enter fluid viscosity, eta ", ETA
  CASE 0
    EXIT DO
  CASE ELSE
    BEEP
END SELECT
LOOP
OPEN "C:\PIGGING\PROGRAM\OPER.DAT" FOR OUTPUT AS #1
WRITE #1, VP, ETA
CLOSE #1

'Where:
'  VP = Operating Velocity of Pig (m/s)
'  ETA = Dynamic Viscosity of Fluid (Pa.s)

OPEN "C:\PIGGING\PROGRAM\CONTROL.DAT" FOR INPUT AS #1 'Control
  inputs
INPUT #1, VPMAX
CLOSE #1
DO
  CLS 1
  PRINT "Contol data:"
  PRINT
  PRINT "1. Maximum velocity, Vmax = ", VPMAX; "m/s"
  PRINT
  PRINT
  PRINT
  PRINT
  PRINT
```

```
PRINT
PRINT
PRINT
PRINT
PRINT
PRINT
PRINT
PRINT
PRINT
PRINT
PRINT
PRINT
PRINT
INPUT "Enter case to change (0 to quit) ", X
SELECT CASE X
    CASE 1
        INPUT "Enter maximum velocity, Vmax ", VPMAX
    CASE 0
        EXIT DO
    CASE ELSE
        BEEP
END SELECT
LOOP
OPEN "C:\PIGGING\PROGRAM\CONTROL.DAT" FOR OUTPUT AS #1
WRITE #1, VPMAX
CLOSE #1

'Where:
'   VPMAX = Maximum velocity for pig main characteristic (m/s)

***** Constants *****

G = 9.81
PI = 4 * ATN(1)

'Where:
'   G = Acceleration due to gravity
'   PI = pi, 3.14 etc

***** Return to main programme *****

END SUB
```

F.14 Subroutine REMOVE()

```
SUB REMOVE (I, SIGS#, A#, M, KWEAR, WA, NODE(), XDASH#)
```

```
***** Subroutine for estimating new chamfer and loss of material *****
```

```
IF I < 20 THEN
```

```
  A1# = (M + 1 / M) / 2
```

```
  B1# = 2 * A#
```

```
  C1# = -KWEAR * WA * NODE(I + 1)
```

```
  DELW# = (-B1# + SQR(B1# ^ 2 - 4 * A1# * C1#)) / (2 * A1#)
```

```
END IF
```

```
***** New chamfer length *****
```

```
XDASH# = 2 * A# + DELW# * (M + 1 / M)
```

```
***** Return to WEARS routine *****
```

```
'Where:
```

```
'  XDASH# = Chamfer length
```

```
'  DELW# = Worn depth
```

```
END SUB
```

F.15 Subroutine RESETTER()

```
SUB RESETTER (FILES$())
```

```
***** Subroutine to empty all storage files *****
```

```
FOR I = 0 TO 20
```

```
  OPEN FILES$(I) FOR OUTPUT AS #1
```

```
  CLOSE #1
```

```
  KILL FILES$(I)          'Empties old information
```

```
NEXT
```

```
OPEN "C:\PIGGING\PROGRAM\WEARS.DAT" FOR OUTPUT AS #1
```

```
CLOSE #1
```

```
KILL "C:\PIGGING\PROGRAM\WEARS.DAT"  'WEARS output file clearance
```

```
***** Return to main routine *****
```

```
END SUB
```

F.16 Subroutine SAMPLE()

```
SUB SAMPLE (VPMAX, L, WEAR(), NODE(), VPIG(), MAIN())
```

```
***** Sampling points in WEARS and MAINS routines *****
```

```
***** Wear sampling points *****
```

```
CLS 1          'Clear and define view port
VIEW PRINT 3 TO 25
NODE(0) = 0
FOR I = 0 TO 20      'Location of each distance step
    WEAR(I) = L * (I / 20) ^ 6
NEXT
FOR I = 1 TO 20      'Distance steps
    NODE(I) = WEAR(I) - WEAR(I - 1)
NEXT
```

```
***** Main Characteristic velocities *****
```

```
FOR I = 0 TO 20      'MAINS velocity sample points
    VPIG(I) = VPMAX * ((I + 1) / 20) ^ 6
NEXT
```

```
***** Main Characteristic Sampling Points *****
```

```
FOR I = 1 TO 20      'Initial settings
    MAIN(I) = 0
NEXT
DO                  'Select MAINS sample points
    PRINT "Sampling Points: "
    PRINT "Node", "Distance", "1/0"
    FOR I = 1 TO 20
        PRINT I, WEAR(I), MAIN(I)
    NEXT
    INPUT "Enter node for main characteristic, (0 to Quit)", X
    LINE (1, 400)-(620, 400), 10
    MAIN(X) = 1
    IF X = 0 THEN
        EXIT DO
    END IF
LOOP
MAIN(0) = 1          '1st point is MAINS sample point
```

```
CLS 1
```

```
'***** Return to main routine *****
```

```
END SUB
```

F.17 Subroutine SCALC()

```
SUB SCALC (SIGS#, KS, DELO#, A#, EC, M, NU, PPLUS, ETA, VP, XDASH#,  
          AN#, AP#, S, HSTAR#, HO#)
```

```
'***** Calculate s, the pressure factor *****
```

```
HO# = -SIGS# * LOG(1.013 * DELO# / (.707 * KS * A#))
```

```
S = .0000001#
```

```
DS = .1
```

```
DO UNTIL DS < 1E-08
```

```
    DPFDX = 1.013 * EC * S * (DELO# + 1.5 * HSTAR#) / ((1 - NU ^ 2) *  
    A# * (AP# - XDASH#))
```

```
    HSTAR# = SQR(8 * ETA * VP / (9 * DPFDX))
```

```
    FUNC = .707 * KS * EXP(-(HO# + 1.5 * HSTAR#) / SIGS#) - 1.013 * (1  
    - S) * (DELO# + 1.5 * HSTAR#) / A#
```

```
    IF FUNC < 0 THEN
```

```
        S = S + DS
```

```
    ELSE
```

```
        S = S - DS
```

```
        DS = DS / 10
```

```
    END IF
```

```
LOOP
```

```
'Where:
```

```
' HO# = Static film height on rough surface
```

```
' S = Pressure factor
```

```
' HSTAR# = Additional film height due to motion
```

```
' DPFDX = Pressure gradient at seal inlet
```

```
'***** Return to WEARS or MAINS routine *****
```

```
END SUB
```

F.18 Subroutine STORE1()

```
SUB STORE1 (I, DP, QTOT, QFOR, QREV, XDASH#, WEAR(), S, W, M, H#(),  
FA, FF, L, LDASH)
```

```
'***** Subroutine for adding data to WEAR.DAT output file *****
```

```
OPEN "C:\PIGGING\PROGRAM\WEARS.DAT" FOR APPEND AS #1  
XDASH = XDASH#  
H = H#(30)  
WRITE #1, I, WEAR(I), DP, QTOT, QFOR, QREV, XDASH, M, L - LDASH  
CLOSE #1
```

```
'***** Return to WEARS routine *****
```

```
END SUB
```

F.19 Subroutine STORE2()

```
SUB STORE2 (FILE$, I, J, VPIG(), DP, QTOT, QFOR, QREV)
```

```
'***** Store data from MAINS routine *****
```

```
'***** Select appropriate file *****
```

```
OPEN FILE$(I) FOR APPEND AS #1
```

```
'***** Store data from this run *****
```

```
WRITE #1, J, VPIG(J), DP, QTOT, QFOR, QREV  
CLOSE #1
```

```
'***** Return to MAINS routine *****
```

```
END SUB
```

F.20 Subroutine TITLE()

```
SUB TITLE (X)
```

```
'***** Subroutine for showing title and initial screen graphics *****
```

```
SCREEN 12          'Screen resolution setting
```



```

CIRCLE (64, 64), 15, , .75, 4
CIRCLE (110, 90), 20, , 5.4, 2.6, 1.7
CIRCLE (90, 90), 20, , .7, 4, 1.7
CIRCLE (110, 90), 5
CIRCLE (90, 90), 5

```

```

***** Clearing the screen to continue *****

```

```

INPUT "Press RETURN to continue", X
DO
    SELECT CASE X
        CASE 0
            EXIT DO
    END SELECT
LOOP
VIEW
CLS

```

```

***** Return to main routine *****

```

```

END SUB

```

F.21 Subroutine WEARS()

```

SUB WEARS (XDASH#, N, PI, DD, EC, ET, D, PHI, T, NU, SIGS#, KS, ETA,
    VP,X#(), H#(), F, MASS, G, CD, I, WEAR(), NODE(), KWEAR, DP())

```

```

***** Pig characteristic against distance *****

```

```

***** Setup initial conditions *****

```

```

CALL INIT(DP1, FRICT1)

```

```

***** Convergence loop *****

```

```

CONV1 = 0          'Convergence for start of distance step
DO UNTIL CONV1 > .99

```

```

    ***** Initial loop conditions *****

```

```

    PPLUS = DP1 / N      'dP across seal is pig dP over number of seals

```

```

    ***** Calculate wall force *****

```

```
CALL FORCE(PI, DD, DELO#, XDASH#, M, EC, ET, D, PHI, B, R,
          FRICT1,PPLUS, T, NU, W, HSTAR#, HO#, L, LDASH1)

***** Calculate contact parameters *****

CALL CONTACT(XDASH#, M, W, EC, NU, DELO#, A#, AP#, AN#)

***** Calculate pressure factor *****

CALL SCALC(SIGS#, KS, DELO#, A#, EC, M, NU, PPLUS, ETA, VP,
          XDASH#, AN#, AP#, S, HSTAR#, HO#)

***** Setup film profile *****

CALL PROFILE(SIGS#, KS, S, DELO#, A#, X#(), XDASH#, H#(), EC,
          NU,AN#, PPLUS, M, AP#, HO#, HSTAR#)

***** Calculate differential pressure *****

CALL PRESSURE(W, HO#, HSTAR#, DELO#, M, WA, PI, F, D, EC, KS,
          H#(), SIGS#, X#(), NU, PPLUS, ETA, VP, S, A#, FRICT, MASS,
          G, DP, N, FA, FF, XDASH#, AP#)

***** Convergence? *****

CALL CONVG(T, DP, FRICT, DP1, FRICT1, CONV1)

LOOP

***** Calculate leakage *****

CALL LEAKAGE(VP, ETA, A#, H#(), PPLUS, CD, PI, D, QTOT, QREV, QFOR,
          SIGS#, VOL, NODE())

***** Store data to file *****

CALL STORE1(I, DP, QTOT, QFOR, QREV, XDASH#, WEAR(), S, W, M,
          H#(), FA, FF, L, LDASH1)

***** Remove material by abrasion *****
```

```
CALL REMOVE(I, SIGS#, A#, M, KWEAR, WA, NODE(), XDASH#)
```

```
***** Draw current situation *****
```

```
DP(I) = DP
```

```
VOL = VOL + QREV * NODE(I) / VP
```

```
CALL DRAW1(I, DP(), WEAR(), L, M, XDASH#, T)
```

```
IF I > 0 THEN
```

```
  FOR K = 1 TO I
```

```
    X1 = CINT(100 + 470 * WEAR(K) / WEAR(20))
```

```
    X2 = CINT(100 + 470 * WEAR(K - 1) / WEAR(20))
```

```
    Y1 = CINT(300 - 250 * (DP(K) / DP(0)))
```

```
    Y2 = CINT(300 - 250 * (DP(K - 1) / DP(0)))
```

```
    LINE (X1, Y1)-(X2, Y2), 10
```

```
  NEXT
```

```
END IF
```

```
PRINT VOL, XDASH#
```

```
***** Return to main routine *****
```

```
END SUB
```

F.22 Subroutine WINDOW()

```
SUB WIND (X)
```

```
***** Subroutine for defining a graphics view port *****
```

```
CLS 'Clear screen and set title
```

```
SCREEN 12
```

```
PRINT "PIGPlus Version 1.0"
```

```
LINE (1, 20)-(620, 20), 10
```

```
LINE (1, 400)-(620, 400), 10
```

```
VIEW (1, 25)-(620, 395)
```

```
PRINT
```

```
PRINT
```

```
PRINT
```

```
PRINT
```

```
PRINT
```

```
PRINT
```

```
PRINT
```

```
PRINT
```

```
PRINT
PRINT
PRINT
PRINT
PRINT
PRINT
PRINT
PRINT
PRINT
PRINT
PRINT
PRINT
PRINT
PRINT
PRINT
PRINT
PRINT
PRINT
PRINT
PRINT "(c) CALtec, 1996"      'Set view port
VIEW PRINT 4 TO 24

***** Return to main routine *****

END SUB
```